Developing an effective and economical bacterial expression system for the production of animal vaccines in Thailand and South East Asia

Amber Rose Peswani

A thesis submitted for the degree of

Doctor of Philosophy in Biochemistry

University of Kent

Department of Natural Sciences

October 2021

Table of contents

Declaration

The work presented in this thesis is original, and was conducted myself (unless stated otherwise) under the supervision of Professor Colin Robinson. All sources of information have been acknowledged by means of references. None of this work has been used in any previous application for a degree.

For the assistance in collecting the data for this thesis, I would like to acknowledge Dr. Peera Jaru-Ampornpan and Jaraspim Narkpuk for collecting and processing cell-based virus neutralization assay and mouse trial data; Dr. Anja Krueger for collecting and processing mass spectrometry data; Prof. Tanja Opriessnig for collecting and processing pig challenge trial data; and Dr. Ian Brown for performing transmission electron microscopy.

Some of the results presented in this thesis have been submitted for publication, and a patent application under the same name:

Peswani, A. R., Narkpuk, J., Krueger, A., Bracewell, D. G., Lekcharoensuk, P., Haslam, S. M., Dell, A., Jaru-Ampornpan, P., Robinson, C. Novel constructs and 1-step purification protocols for the production of Porcine Circovirus 2d (PCV2d) and Circovirus 3 (PCV3) subunit vaccine candidates. Food and Bioproducts Processing.

This research was funded by the BBSRC Global Challenges Research Fund.

Acknowledgements

First thank you must go to the boss, Colin Robinson. You were an excellent supervisor to me during my time at the University, I have gained so much independence and confidence through being in your lab and it will always be one of the best choices I've made in life to join the CR group. Thanks for your generosity in biscuits, Colin Caterpillar cakes and working hard to give us all lots of opportunities.

Much love to CR lab members past and present for all the fun times: Kelly Walker, Jo Roobol, Andrew Dean, Isabel Guerrero-Montero, Daphne Mermans, Julie Zedler, Doris Gangl, Wayne Miller, Serena Lima, Sarah Bischoff, Chi Jawara, Hollie Scarsbrook, Charlotte Bilsby. My gratitude in particular to Kirsty Bellchambers, who taught me mostly everything I knew initially when I was just a small-time tech, without your intuitive and gentle encouragement I don't think I would have had the confidence to do a PhD. Special thanks to Conner Webb and Alex Jones who have been with me throughout almost the entirety of my PhD and given me invaluable technical and intellectual support with their insightful perspectives, as well as being reliable coffee time buddies. Thanks to Ally Walters for your advice and keeping us on track! Many thanks also to my little lab lass's Emi Nemoto-Smith and Kelly Frain for our chats and laughs especially in difficult times! Can't wait for a CR reunion.

A big acknowledgement to the GCRF consortium, in particular Peera Jaru-Ampornpan, Lalintip Hocharoen, Jaraspim Narkpuk, Anja Krueger, Mark Smales, James Budge, Lina Mikaliunaite, Stephanie Frank, Sarah Slack, Stuart Haslam, Anne Dell, Barbara Mulloy. We've been an excellent team and I have enjoyed multiple great trips to Thailand with you all!

Finally, thanks to my family Diana Sherwood Peswani, Prakash Peswani, Lana Peswani and Cherry Simmonds for believing in my abilities, supporting my goals and being proud of me no matter what!

List of tables

List of figures

Abbreviations

APS	Ammonium persulphate
BSA	Bovine serum albumin
CAB	Sodium cacodylate buffer
CHO	Chinese hamster ovary
CIEX	Cation exchange chromatography
CTL	Cytotoxic T lymphocyte
CPP	Cell-penetrating peptide
CV	Column volumes
DTT	1,4-Dithiothreitol
EDTA	Ethylenediaminetetraacetic acid
ELISA	Enzyme-linked immunosorbent assay
ESI-LC-MS	Electrospray ionization - liquid chromatography - mass spectrometry
FBS	Foetal bovine serum
ffu	Fluorescent focus units
FPLC	Fast protein liquid chromatography
FMD	Food and mouth disease
HPV	Human papilloma virus
HRP	Horseradish peroxidase
IAM	Iodoacetamide
IAV-S	Influenza A virus in swine
IEX	Ion exchange chromatography
IMAC	Immobilized metal ion affinity chromatography

IPTG	Isopropyl β-D-1-thiogalactopyranoside
KLH	Keyhole limpet haemocyanin
LB	Luria broth
mAU	Milli-absorbance unit
MEM	Minimum essential medium
MHC	Major histocompatibility complex
MLP	3-O-desacyl-4'-monophosphoryl lipid A
mQ	Milli-Q
NLS	Nuclear localisation signal
OD_{600}	Optical density at 600 nm
OmpA	Outer membrane protein A
PAGE	Polyacrylamide gel electrophoresis
PBS	Phosphate-buffered saline
PBST	Phosphate-buffered saline, 0.1% tween20
PCR	Polymerase chain reaction
PCVD	Porcine circovirus associated diseases
PDNS	Porcine dermatitis and nephropathy syndrome
PEDV	Porcine epidemic diarrhoea virus
pO_2	Dissolved oxygen partial pressure
PRRS	Porcine reproductive and respiratory syndrome
PRRSV	Porcine reproductive and respiratory syndrome virus
PWMS	Post-weaning multi-systemic wasting syndrome
scFv	Single-chain variable-fragment from an antibody
SDS	Sodium dodecyl sulphate
Sec	General secretory pathway

SLA	Swine leukocyte antigen
SM6	Synthetic medium 6
TB	Terrific broth
TBST	Tris-buffered saline, 0.1% tween20
$TCID_{50}$	Median tissue culture infectious dose
TEM	Transmission electron microscopy
TEMED	Tetramethylethylenediamine
TLR	Toll-like receptor
TMB	Tetramethylbenzidine
Tris	Tris (hydroxymethyl) aminomethane
Tween20	Polyoxyethylenesorbitan monolaurate
VLP	Virus like particle
VNT	Virus neutralisation titre
v/v	Volume per volume
w/c/w	Wet cell weight
W/O	Water in oil
W/O/W	Water in oil in water
WT	Wild type
w/w	Weight per weight
Δ (Delta)	Gene deletion

Abstract

The lack of capacity to produce animal vaccines within low and middle income countries in South East Asia poses a significant risk to their food security and economic stability; Thailand's economy relies heavily on their production of pork, however viral diseases have spread within livestock populations to endemic levels. In the last few decades, porcine circoviruses have become ubiquitous almost worldwide, with developing countries like Thailand needing to rely on expensive, imported vaccine technology to combat the risk of economic losses caused by livestock diseases. Current imported vaccines against PCV2 are mismatched to the local strains in circulation, and due to the high rate of genetic shift occurring among viruses, the effectiveness of the imported vaccines is limited. This research set out to develop a low cost recombinant expression system in *E. coli* to generate subunit vaccines to protect against porcine circovirus 2 (PCV2) and porcine circovirus 3 (PCV3) strains circulating locally in Thailand, with the wider goal to establish production capacity within Thailand to allow for local production of vaccines for appropriate circulating strains. Through optimising expression of PCV2d and PCV3 capsid (Cap) genes in *E. coli* to generate high protein yields at 1.5 L fed-batch fermentation and purify using a single-step cation exchange purification, we were able to achieve high purity (>95%) PCV2d proteins capable of inducing neutralising antibody responses in rabbits and mice as demonstrated by PK-15 cell-based virus neutralisation assays. Purified PCV2d protein was also developed into an adjuvanted vaccine candidate, showing an immunological response in a pig viral challenge trial. In addition, promising steps were made towards developing a chimeric PCV2d-PCV3 dual vaccine candidate for protection against both viruses in a single vaccine. We have established a minimal step, low-cost, laboratory-scale vaccine production process that is able to generate a virus-neutralising subunit vaccine against PCV2d, with the potential for scale-up, to contribute towards facilitating vaccine production capabilities locally within Thailand.

Chapter 1: Introduction

1.1 Background

1.1.1 Widespread effects of livestock disease on Thai swine farming industry

Livestock production is an essential contributor to both the Thai economy and in maintenance of domestic food security. According to the Department of Livestock Development 2014 report, Thailand's swine farming industry produced more than 9 million pigs, 95 % of which were used for domestic consumption supplying an estimated 200,000 households. The value of the remaining exported goods was estimated at £82 million. However, disease control is a persistent problem in livestock farming, with a number of severe epidemics in recent years. Diseases of continuing concern causing economic losses for the Thai swine industry include foot-and-mouth disease virus (FMDV), several porcine circoviruses and coronaviruses, and porcine epidemic diarrhoea virus (PEDV). In 2009, an epidemic of PEDV killed 3 million piglets, losing £94.8 million and causing panic over domestic food security (Song et al., 2015; Thornton, 2010). Further PEDV outbreaks since then have exhibited mortality rates of up to 90% while FMD continues to cause an estimated 25 % loss in pigs each year (Helke et al., 2015). Porcine circovirus 2 (PCV2) meanwhile, has over the past 20 years been increasingly correlated with the exhibition of post-weaning multi-systemic wasting syndrome (PMWS), porcine dermatitis and nephropathy syndrome (PDNS), respiratory and reproductive failure and other associated diseases, controversially being implicated as the cause of such disease deaths (Segalés, 2012). The disease mortality rate reportedly varies between 3-10 % but with an estimated incidence rate of 60% within the global swine herd population, the virtually ubiquitous virus has posed a growing threat due to its rapidly shifting genetic diversity (Afolabi et al., 2017).

Currently, Thai farmers combat these viruses with vaccination but most vaccines must be imported at high cost due to the lack of capacity and economy to produce them within the country. Critically, many of these imported vaccines have reduced effectiveness due to mismatches between the imported vaccine and the local circulating strain. Thus the need is clear to develop more effective vaccines that are suitable for the local market, and can be established with a production capacity within Thailand – this will reduce costs by eliminating export costs and allow for local production of vaccines for appropriate circulating strains when required.

The wider goal of the project is to provide a progression in developing a vaccine production system that will in the future help to reduce poverty, hunger and to promote wellbeing and a sustainable economy in low and middle income countries in South East Asia.

1.1.2 Evolution and pathogenicity of porcine circoviruses

The first reported case of pathogenic PCV infection associated with symptoms of PMWS was described in 1998, which differentiated this PCV species from the previously identified non-pathogenic species of PCV, with only 68 % homology between the two species (Hamel et al., 1998). These viruses were classified as non-pathogenic PCV1 and disease-causing PCV2. In 2008, the EU Consortium on Porcine Circoviruses proposed a new naming system to classify globally identified strains; thus the first strains of subtypes PCV2a, PCV2b and PCV2c were categorized (Thangthamniyom et al., 2017; Guo et al., 2010). A further study of isolates from symptomatic pigs in China collected between 2004-2008 showed further variation, and led to the classification of PCV2d and PCV2e subtypes (Wang et al., 2009). In Korea between 2009 and 2016, samples isolated from farmed pigs showed over half were infected with PCV2, and evidence of a genotypic shift from PCV2b to PCV2d was visible prior to 2012. In 2016, analysis of samples collected across Korea showed 50/69 farms contained PCV2d infected pigs, but 21/69 farms showed multiple PCV2 subtypes still in circulation (Kwon, Lee, et al., 2017). Meanwhile in Thailand, the strain shift since 2009 saw the most prevalent subtype, PCV2d, become the only identified subtype in 2015 (Thangthamniyom et al., 2017). While the genetic diversity has continued to increase among PCV strains infecting swine since the introduction of vaccines, it is clear that the genotypic shift and increasing prevalence of PCV2d strains is mirrored by neighbouring countries.

Since the initial link was made between PMWS and PCV2 infection, a number of other diseases such as PDNS and porcine reproductive and respiratory syndrome (PRRS) have been subsequently linked. The collection of these diseases have since been grouped under the term porcine circovirus associated diseases (PCVD) (Segalés, 2012). Although not necessary to produce symptoms, infection with PCV2 is often also seen with co-infection of another pathogen (Genzow et al., 2009). Co-infection significantly worsens the severity of symptoms and clinical outcome of PCV2 associated diseases. Porcine reproductive and respiratory syndrome virus (PRRSV) is a common co-infective virus with PCV2, has been shown to induce similar symptoms of PRRS and this may be a result of a high level of co-infection, however the interaction between the two viruses in worsening the clinical state has not been elucidated (Lunney et al., 2016).

Although the mechanism of pathogenicity is not clear, porcine circoviruses rely heavily on utilizing the host machinery for their own replication, due to small genome size and thus few encoded proteins. These interactions stimulate the host immune system resulting in cytokine imbalance and immunosuppression leading to the observed disease symptoms. That said, there is evidence of asymptomatic infection with PCV2 and phylogenetic analysis has traced PCV2 back to at least 1973 where it was discovered in Northern Ireland, 25 years prior to the first report of PMWS

symptoms. The various subtypes of PCV2 isolated from pigs worldwide themselves also demonstrate differences in symptom severity; for example, PCV2c has only been identified in pigs in Danish farms, displaying no disease symptoms. Furthermore, up until 2003, PCVD-associated PCV2a and PCV2b strains were both highly prevalent strains worldwide but following 2003, there was a clear genotypic shift to PCV2b as the most prevalent strain, accompanied by increasing severity of the associated disease symptoms (Meng, 2013). More recently, as the incidence of PCV2d infections rose, cases were reported to display an earlier onset of viremia as well as increased virulence in comparison to PCV2b (Guo et al., 2012; Opriessnig et al., 2014). Evidence over the past few years has begun to suggest that porcine and other avian circoviruses also exhibit cross-species transmission, with viruses almost identical to PCV2 being isolated from beef in the last 10 years (Li et al., 2010, 2011).

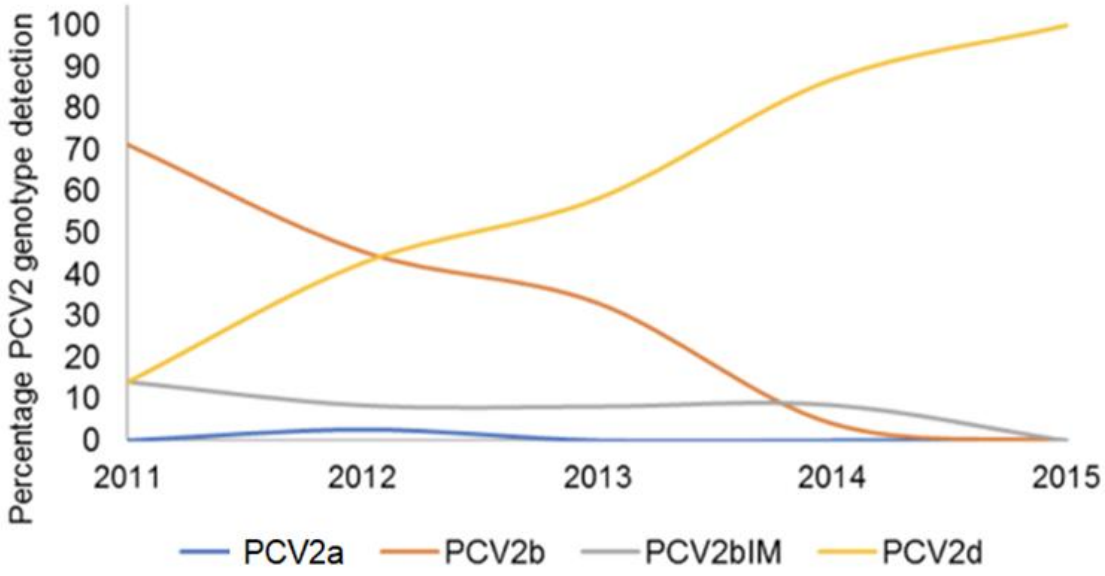

Figure 1. Genetic diversity of PCV2 in Thailand between 2011 and 2015. A total of 694 serum samples from 70 farms from different geographical areas of Thailand were submitted for PCV2 PCR diagnosis during 2009–2015. PCV2 genotypes were classified by the signature motifs and topology of ORF2. Those classified included PCV2a, PCV2b, intermediate group of PCV2b (PCV2b_IM1) and PCV2d. PCV2c was not found in Thailand. The PCV2b_IM1 was a new actively growing clade separated from the classical PCV2b (Xiao et al., 2015)(Thangthamniyom et al., 2017).

PCV3 on the other hand, was only identified as a new species in 2016 when it appeared in diseased pigs in the United States exhibiting acute symptoms of PDNS. Since then, the virus has emerged in nearby Brazil in addition to further reaching countries such as Poland, China and Korea (Kwon, Yoo, et al., 2017; Stadejek et al., 2017; Tochetto et al., 2018; Varela et al., 2021; J. Zhang et al., 2018). However, phylogenetic analysis suggests this newly discovered species did not

evolve recently or from the previously known circoviruses PCV1 or PCV2 (Saraiva et al., 2018); in fact, research suggests that PCV3 shows only 37 % sequence identity with PCV2 (Palinski et al., 2017) and that that its origin may more likely have been through a recombination event with bat circoviruses around 50 years ago (Saraiva et al., 2018). PCV3 has also been detected in other mammalian animals including wild boar (Klaumann et al., 2019), mice (S. Jiang et al., 2019), cattle (W. Wang et al., 2019), dogs (J. Zhang et al., 2018) and chamois (Vargas-Bermudez et al., 2019), as well as in ticks (Franzo et al., 2019) which could serve as potential reservoirs for PCV3 infection and circulation (Ouyang et al., 2019).

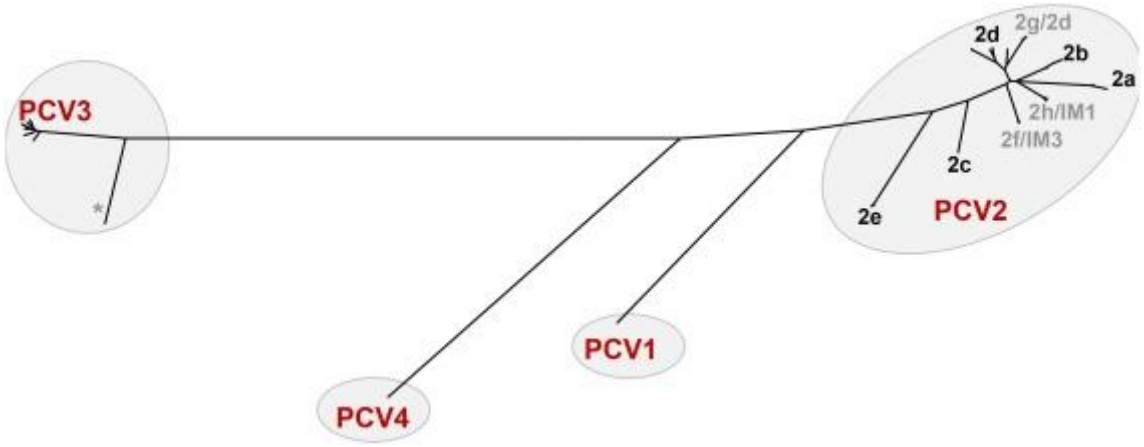

Figure 2. Overview and relationship of known porcine circoviruses. Phylogenetic analysis based on the complete open reading frame 2 (ORF2) gene sequences of selected representative strains of PCV1, PCV2, PCV3 and PCV4 obtained from GenBank. The evolutionary tree was constructed by anaylsis of 626 positions in the final dataset using MEGA7 software (Kumar et al., 2016). PCV2 genogroups are specified by 2a, 2b, 2c, 2d, and 2e. The classification of intermediate clades IM1 and IM3 was described previously (Xiao et al., 2015). PCV2g, (Huynh et al., 2014), PCV2h and PCV2f HM776452 (Bao et al., 2018) all denote the earliest genotype members identified of these prospective genogroups. * indicates a single PCV3 sequence distant from all other sequences (Opriessnig et al., 2020).

In the past two years, reports of a new PCV4 species have emerged. First identified in pigs with serious PDNS-like symptoms in China in 2019, studies of a sample of 257 viral isolates from pigs in Guangxi Province, China, collected between 2015 and 2019, discovered that 5.1 % were in fact positive for PCV4 (Sun et al., 2021). Of these PCV4-positive samples, 69.2 % were also found to be co-infected with PCV2 or PCV3, and one PCV4-positive sample was co-infected with both PCV2 and PCV3. Sequenced PCV4 genomes so far indicate 36.9-73.8 % nucleotide similarity with other

representative circovirus genomes, while phylogenetic analysis indicates that PCV4 is most closely related to bat-associated circovirus and mink circovirus, displaying 66.9 % genomic identity to mink circovirus and identities of 43.2%–51.5% to the other PCV genomes (Sun et al., 2021; H. H. Zhang et al., 2020).

1.1.3 Structure and immunogenicity of PCV2

Porcine circoviruses are non-enveloped, T= 1 icosahedral viruses with their genetic information encoded within a small circular genome of single-stranded DNA, only 1.7kb in size for PCV1 and PCV2 viruses (Meng, 2013; Khayat et al., 2011) . Within this small genome is encoded three open reading frames (ORFs): ORF1 translates Rep proteins required for viral replication, ORF2 translates the viral capsid protein, Cap, while ORF3 expression product modulates cell signalling pathways to induce apoptosis of infected cells (Jue Liu et al., 2005; Mankertz & Hillenbrand, 2001). Molecular modelling predicts the PCV2 capsid structure to be a canonical viral jelly roll with eight β-strands organized in two sheets (Gava et al., 2018). The Cap protein includes an N-terminal nuclear localisation signal (NLS) peptide functioning to direct the virus particle to the host cell nucleus for replication (Trundova & Celer, 2007; Xiao et al., 2018). The NLS of PCV2 consists of a 41 amino acid sequence at the N-terminus of the Cap protein, and the presence of basic amino acids residues between regions 12-18 and 34-41 are reported to be essential for its nuclear targeting ability (Q. Liu et al., 2001). The NLS region also contains a high concentration of arginine residues in what resembles a poly-arginine cell-penetrating peptide (CPP), suggesting a mechanism of PCV2 entry into host cells through CPP-mediated binding via heparan sulphate proteoglycan and chondroitin sulphate B sites (Khayat et al., 2011; Misinzo et al., 2006; N. Wang et al., 2016; Wittrup et al., 2011).

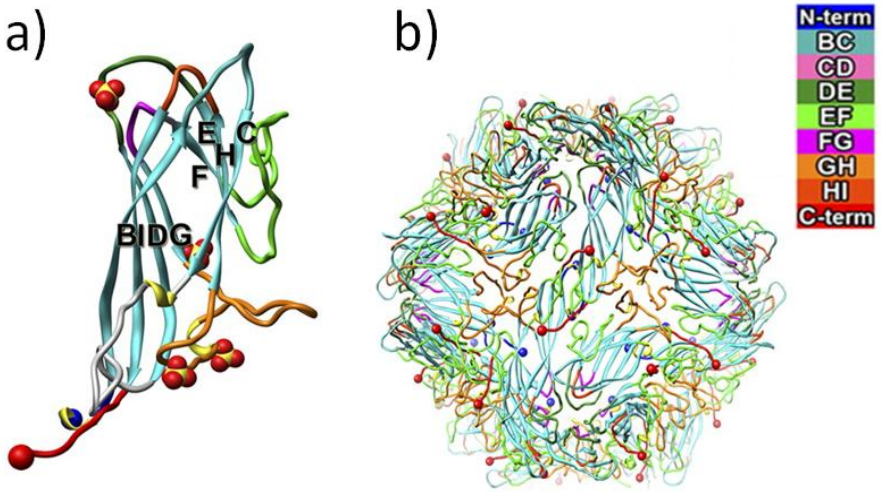

Figure 3. Crystal structure of PCV2 VLP. a) Ribbon diagram of the PCV2 capsid protein with the secondary structural regions labelled: B, C, D, E, F, G, H, I. The N- and C -termini are labelled using blue and red spheres, respectively. b) Stereoscopic representation of a ribbon diagram of the PCV2 VLP. The loops connecting the different strands have been colour coded according to the bar diagram at the top right. N-term: N termini; C-term: C-termini (Khayat et al., 2011).

Amino acid sequence comparison of the complete ORF2 sequences of forty-three Belgian PCV2 isolates collected between 2009 – 2013 revealed 88.5–100 % identity between isolated strains of PCV2a, PCV2b and PCV2d, but showed that a greater sequence diversity was observed within certain regions, generally corresponding to the location of immunorelevant epitopes, suggesting altered host antibody binding during an immune response (Wei et al., 2019). While PCV2a and PCV2b strains consist of 233 amino acid residues, PCV2d was the first strain to contain 234 amino acids, due to an additional lysine residue on its C-terminus, which has been attributed to the earlier onset of viremia and increased virulence of this particular subtype (Guo et al., 2012; Opriessnig et al., 2014). Lys234 along with Phe8, Ile53, Lys59 and Asn68 are considered PCV2d -specific amino acids (Xiao et al., 2016). Although their roles in PCV2d virulence and differentiation from previous PCV2 strains are not yet known, a study of Korean pig herds identified that seven sites on the capsid protein of Korean PCV2 were identified as having evolved under positive selection pressure and all of these were found to be related to the generation of an antibody response in the host, specifically within epitope regions potentially capable of inducing a neutralising antibody response (Kwon et al., 2017).

In the early 2000s, the first commercial PCV2a vaccines Circovac® from Merial and Fostera™ PCV from Pfizer were introduced and their use became widespread across the world within the next few years, proving successful. However, in recent years, systemic PCV2 infection has returned as a

problem. One study sequenced the genomes of PCV2 virus isolated from infected pigs in Brazil and identified A190T amino acid substitution in the Cap gene (Gava et al., 2018). Six predicted PCV2 epitopes were identified by this study to be important for antibody recognition, referred to as A, B, C, D, E and F. Residue 190 was found to be situated on the external capsid structure, adjacent to epitope E, an important predicted region for antibody recognition; A190T mutations, present in 100% of isolates, were discovered which would cause a local physical–chemical change from a non-polar, hydrophobic side chain to a forked, polar side chain; this was hypothesized to alter the antigen-antibody interaction. It was concluded that substitutions leading to changes in the viral protein conformation may cause antibodies raised by the current PCV2 vaccine to have reduced binding efficiency. Further evidence suggests residues 190, 191, 206 and 210 to be signature motifs in differentiating between PCV2a and PCV2b subtypes (N. Wang et al., 2016), while other evidence suggest motifs in the region 86-91 can be used as genetic markers to distinguish between PCV2a, PCV2b and PCV2d subtypes (Cheung et al., 2007; Wei et al., 2019).

In another study, the Cap gene from a PCV2a vaccine strain, along with a classical PCV2b strain and a newly discovered “mPCV2b” isolate were sequenced to reveal antigenic differences between the strains, characterized by a range of amino acid substitutions, including differences at positions 190 and 210. Using immunoinformatic analysis to predict potential epitope regions, critical differences between the immunogenicity of the strains were identified. The mPCV2b isolate was also characterised by the addition of Lys234 residue now known to identify the PCV2d strain. In regions of the protein previously predicted as binders of swine leukocyte antigen (SLA) class-I molecules, antigen presenting molecules crucial in generating specific cellular immune responses in swine, as a result of the identified substitutions in the Cap protein these regions were predicted to retain weak or no binding capacity by SLA class-I molecules (Constans et al., 2015). Of predicted B-cell epitopes, both classical PCV2b and mPCV2b isolates showed variation to the PCV2a vaccine strain, but none of these differences were conserved, suggesting immunity against a circulating PCV2b strain cannot guarantee any protection against PCV2d strains.

While structurally the NLS region of PCV2 Cap is not predicted to be involved in antibody binding (Lekcharoensuk et al., 2004), previous studies have indicated that loop structures on the surface of PCV2 capsid could form conformational epitopes recognized by several neutralising antibodies (Huang et al., 2011; Lekcharoensuk et al., 2004; Jianbo Liu et al., 2013; Shang et al., 2009) while three residues in particular at positions 59, 131 and 190, located each in separate loop structures, have been identified to be important in raising a neutralising antibody response (Huang et al., 2011; Saha et al., 2012). Additional epitope regions have been discovered containing a rich number of antibody binding residues at region 70-78 and between residues 203-207 (Khayat et

al., 2011). However one major difference between PCV2d and previous subtypes is the addition of Lys234 residue; it is thought this may be important in PCV2d evasion of immune recognition conferred by exposure to previous PCV2 subtypes (Zhan et al., 2016). A "decoy" epitope region is also hypothesized to exist within PCV2 Cap. This region is highly immunogenic but results in the production of non-neutralising antibodies, and functions as a tactic evolved by the pathogen to evade the host immune responses (Jin et al., 2018). Although there are discrepancies over the exact location, residues 169-180 are consistently considered to be included in this region (Khayat et al., 2011; Mahé et al., 2000; Trible et al., 2012; N. Wang et al., 2016). Monomeric subunits of the viral capsid proteins when expressed recombinantly in the absence of the viral genomic DNA can self-assemble to form structures that closely resemble the outer structure of the actual virion. These structures are known as virus like particles (VLPs). Evidence suggests a conserved loop region exists in PCV2 Cap wherein there is a unique cysteine residue located. This cysteine residue has been identified as a critical component in the integrity of PCV2 VLPs through stabilization of monomers in the structure via a disulphide bonding (Wu et al., 2012).

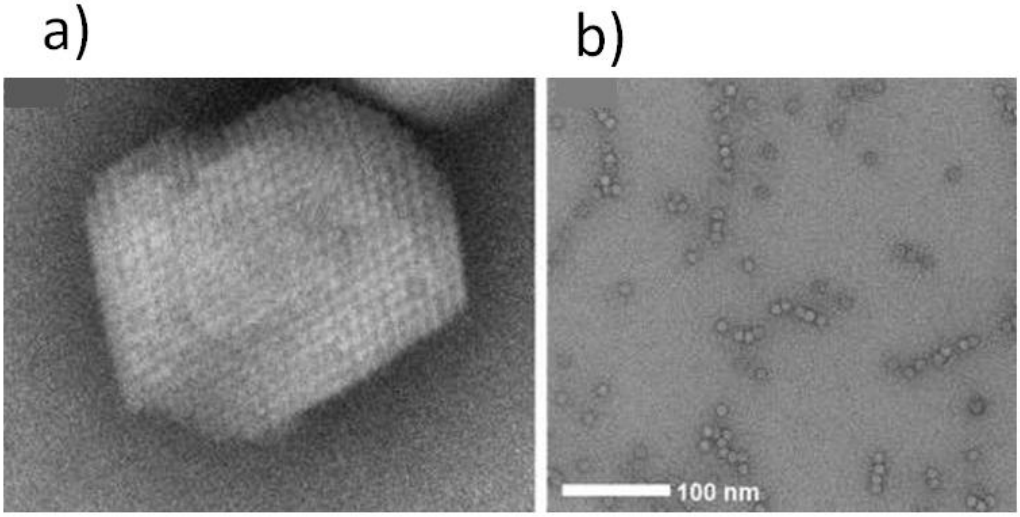

Figure 4. PCV2 VLP assembly visualized by electron microscopy. a) Electron micrograph of a crushed PCV2 crystal negative stained with 2 % (w/v) uranyl acetate. b) The condition was optimised to produce VLPs without crystal growth (Khayat et al., 2011).

Evidence has also shown in crystal structure that PCV2 VLPs derived from NLS-truncated capsid proteins form unstable VLPs that are easily disassembled by changes in redox state. Cryo-electron microscopy of PCV2 VLPs formed from full length capsid proteins showed interaction between NLS structural regions stabilizes the assembled PCV2 VLP in solution, where the interaction between the arginine-rich residues in the NLS of one capsid protein and the adjacent NLS regions from another capsid protein stabilizes the VLP (Mingfang et al 2020).

1.1.4 Structure and immunogenicity of PCV3

The novel PCV3 species with a 2 kb genome was first identified in 2015 on farms in North Carolina, USA, in sows that died with clinical signs of porcine dermatitis and nephropathy syndrome (PDNS) and reproductive failure. The capsid and replicase proteins of this new virus displayed only 37 % and 55 % sequence identity to PCV2 (Palinski et al., 2017). Even lower sequence identities of 27 % have been reported between PCV3 Cap protein and strains belonging to other PCV subtypes, and as such, there is no cross-protection against PCV3 infection conferred by PCV2 vaccination and indeed no cross-reactivity of PCV3 anti-sera with either PCV1 and PCV2 viruses (Deng et al., 2017). That said, while the PCV3 Cap protein is significantly shorter than the PCV2 Cap at only 214 amino acids in length, the capsid structure of PCV3 is morphologically similar to that of native PCV2 virions and overall shows significant structural conservation among different types of PCVs (Mingfang et al., 2020).

The most significant structural differences between PCV2 and PCV3 capsids are reported among the surface-exposed loops referred to as BC-loop (51-59 residues), CD-loop (72-79) and EF-loop (109-131) (Mingfang et al., 2020). In particular, sequence alignment and structural comparison suggests that the PCV3 CD-loop is shorter than PCV2 CD-loop, at 8 residues compared to 16 residues in PCV2, while residues located on PCV3 CD-loop are less conserved than those in the core β-strands and other loop regions. Moreover, the conformation of the N-terminal region of PCV3 capsid protein appears to be different from that of PCV2 capsid protein.

A major PCV3-specific epitope has so far been identified in the CD-loop region of PCV3 Cap between residues 72-79 existing on the exterior surface of the capsid (Mingfang et al., 2020). Three B-cell epitope sequence motifs have also been identified: NKPWH located between resides 57-61, KHSRYFT between residues 140-146, and QSLFFF between residues 161-166, and showing a high level of conservation among different PCV3 strains. The motif between 140-146 in fact appears highly conserved in all four reported species of PCVs (M. Jiang et al., 2020).

With the widespread reach of PCV2 infection, rapid strain shift and outdated vaccine technology combined with the emerging threat of PCV3 virus, there is a necessity to combat both of these viruses. In particular, for low-middle income countries in Thailand and South East Asia who rely on livestock farming as an important basis for their economy, protection of swine livestock against PCV viral infection by cost-effective methods such as vaccines that are able to protect against multiple viral diseases in one product would be ideal. With this in mind, in this project we aimed to investigate the potential to develop not only single but also dual vaccine designs that would protect against PCV2 and PCV3 simultaneously.

1.2 Introduction to vaccines

1.2.1 Considerations in vaccine design

Vaccines belong predominantly to one of two groups, between which there is an important distinction: live and non-live vaccines. Live vaccines are designed to replicate sufficiently in the host so as to produce a strong immune response, but not enough to cause significant disease manifestations or adverse reactions; for example, some vaccines using live attenuated pathogens such as the widely used measles, mumps and rubella vaccine have been reported to cause mild disease symptoms following immunisation (Sukumaran et al., 2015). As such, there is a balance to be determined between raising a strong immune response versus avoiding symptomatic disease. Because of this, many live attenuated vaccines require multiple doses and induce relatively short-term immunity. Live vaccines are also restricted in their usability due to the potential of the administered live organism to replicate in an uncontrolled manner, making them inappropriate for immunocompromised individuals (Rubin et al., 2014). Non-live vaccines on the other hand may contain a killed whole organism or only an antigenic component of a pathogen such as subunit or toxoid vaccines. Subunit vaccines contain recombinant proteins or polysaccharides from the target pathogen, while toxoid vaccines use formaldehyde-inactivated protein toxins that have been purified from the pathogen. Several other non-live vaccine platforms have been developed within the past few decades, including viral vectors, nucleic acid-based RNA and DNA vaccines, and virus like particles (VLPs).

Infection by a virulent pathogen provides the necessary signals to induce the correct type of immune response. Live vaccines are able to provide these signals by mimicking the virulent pathogen. However, when vaccines are administered by unnatural routes of exposure such as injection, they may not provide the necessary signals to induce protective immunity. As a result, the route of administration of a vaccine can have a profound effect on the immunity it can induce. For example, the live attenuated influenza A virus in swine (IAV-S) vaccine is administered intranasally to neonatal pigs to circumvent passively acquired immunity. Reportedly, vaccination through this route is able to induce a broader protective immune response in young pigs when compared to inactivated vaccines given intramuscularly (Eichmeyer et al., 2018).

The antigenic contents of a vaccine are also widely variable in their ability to generate an effective immune response. Purified subunit vaccines used to elicit an immune response may lack molecular structures called pathogen-associated molecular patterns which are common to a class of pathogen. These structures can be identified by immune cells and recognised as danger signals, thus their absence may result in a weaker immune response (Demento et al., 2011). Also, because the antigens do not infect cells, subunit vaccines mainly only trigger antibody-mediated immune

responses. For this reason, adjuvants are used to provide artificial signals to the immune system to initiate the immune response, functioning to minimize the number of immunisations required for a sufficient immune response. This also decreases the amount of antigen needed, providing a cost-effective solution. The two main types of PCV2 vaccines currently commercially available are subunit and attenuated/killed whole viral vaccines. Examples of current subunit vaccines are Porcilis® PCV (Schering-Plough/Merck), Ingelvac CircoFLEX® (Boehringer Ingelheim) and Circumvent® (Intervet/Merck) which are all generated using baculovirus/insect expression systems. Attenuated or killed PCV viral vaccines include Circovac® (Merial) and Fostera™ PCV (Pfizer).

1.2.2 Role of adjuvants in immunogenicity

Vaccine adjuvants are substances that increase the intensity of the immune response after co-administration with an antigen. They are useful for enabling vaccines to induce strong and persistent immune responses, while reducing the vaccine dose and number of injections, and increasing the vaccine's stability.

Adjuvants are widely used in the formulation of human and veterinary vaccines. In human vaccination, only few adjuvant technologies are used in the formulation of vaccines currently on the market, however veterinary vaccination uses a greater variety of adjuvant technologies; nevertheless, all vaccine adjuvants function by one of two mechanisms of action: firstly, by simulating the presence of an infectious agent; these promote recruitment of immune cells and effectively present antigens to generate an immune response. This is especially so with aluminium salts (Danielsson & Eriksson, 2021), which have been used for over a century, and oil emulsions. Secondly, they may function as immunostimulants that specifically interact with receptors located on immune cells. For example, this is the mechanism of action in Toll-Like Receptor (TLR) ligands such as 3-O-desacyl-4'-monophosphoryl lipid A (MLP). Some adjuvant technologies combine these two mechanisms to potentiate their effectiveness (Didierlaurent et al., 2009).

Current veterinary adjuvants most commonly use technologies such as aluminium salts, polymer dispersions, *Quillaja saponaria* saponins (Kensil et al., 1991), as well as other naturally occurring immunostimulants. New technologies have been developed in recent decades, such as squalene-type emulsions in water. These squalene-type emulsions are derived from shark liver oil (Bastola et al., 2019) and include SEPPIC's range of ISA adjuvants consisting of purified mineral or squalene oil and mannitol esters as emulsifiers (Iyer et al., 2001). Examples of newer adjuvant technologies currently approved for human vaccination include the oil-in-water emulsion MF59, which is used in some influenza vaccines (Wilkins et al., 2017); AS01, an aluminium salt, which is used in one existing shingles vaccine as well as the licensed malaria vaccine (Kaslow & Biernaux, 2015); and

AS04, a combined MLP and saponin type adjuvant, which is currently used in formulation of a human papillomavirus (HPV) vaccine (Pedersen et al., 2007).

There are many mechanisms by which adjuvants can impact the immune response; during an immune response, vaccine antigens must reach secondary lymphoid tissues, usually the lymph nodes. Most of these antigens are carried to lymph nodes by dendritic cells. These antigen-presenting cells (APCs), as well as macrophages and B cells, process the antigens and present the epitopes via major histocompatibility complex (MHC) molecules. The porcine MHC is made up of the highly polymorphic swine leukocyte antigen (SLA) class-I, II and III gene clusters (Renard et al., 2006). SLA class-I and class-II proteins are involved in the adaptive immune response through presentations of endogenous and exogenous antigenic peptides to circulating T cells (Neefjes et al., 2011). There are two arms of T cell stimulation, wherein class-I molecules present antigenic peptides on infected cells to CD8+ cytotoxic T cells while APCs present these to CD4+ helper T cells via class-II molecules (Figure 4). Both stimulate T cell responses causing naive T cells to undergo clonal expansion and differentiate into antigen-specific effector and memory cells. SLA class-III cluster encodes many genes important in immune defence, such as the tumour necrosis factor gene families and components of the complement cascade (Lunney et al., 2009).

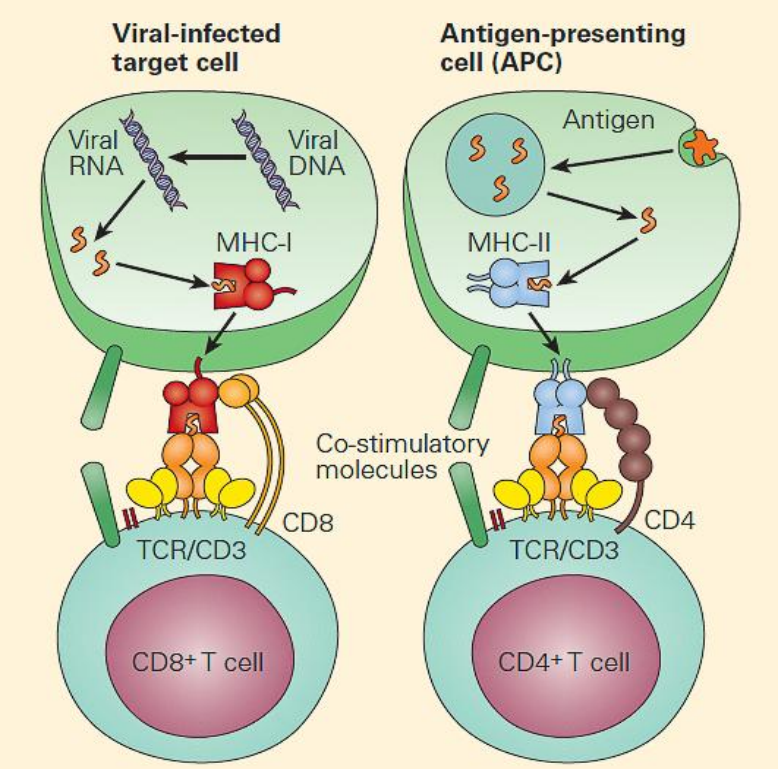

Figure 5. Antigen presentation to T cells by MHC molecules. Endogenous antigens are presented to CD8+ cytotoxic T cells (left panel), and exogenous antigens are presented to CD4+ helper T cells (right panel) (Stiehm, 2012).

Dendritic cells, macrophages, and B cells also provide signalling required to initiate immunity. Some adjuvants function by improving antigen uptake by these cells, by increasing co-stimulatory or MHC molecules for immune cell activation, or by enhancing migration to the lymph nodes (Yang et al., 2018). On the other hand, some adjuvants appear to work by exhibiting a "depot effect", trapping the antigen close to the site of administration to provide a continuing supply of antigen to the local APCs. Reportedly, this effect may slow down the rate elimination of the antigen (Cox & Coulter, 1997). Oil emulsions such as Freund's adjuvants can form short-term depots, lasting for approximately 8 to 10 days, which are sufficient to enhance immunity (Cox & Coulter, 1997) while microparticle adjuvants has been shown to form long-term depots that last for between 1 and 6 months and may be able to deliver pulsed doses of the antigen (Cox & Coulter, 1997; Morein et al., 1996). Similarly, carrier proteins such as bovine serum albumin, keyhole limpet hemocyanin (KLH), and diphtheria or tetanus toxoids in a vaccine can aid in raising an immune response by recruiting helper T cells. Some adjuvants such as liposomes also appear to deliver antigens to pathways that lead to the presentation in MHC-I molecules and the induction of a cytotoxic T cell response (Vogel, 2000; Cox & Coulter, 1997; Alving, 1995).

Alternatively, some adjuvants are hypothesised to function by saturating liver-localized macrophages known as Kupffer cells, thus reducing hepatic uptake and elimination of the antigen (Cox & Coulter, 1997). Other mechanisms by particulate adjuvants such as aluminium salts (alum) promote formation of aggregates along with the administered antigen, which is thought to make them more easily phagocytosed (Cox & Coulter, 1997), however modern vaccine technology is moving away from this due to debate over detrimental pathophysiological effects of long-term aluminium tissue deposits and associated macrophagic myofasciitis (Gherardi et al., 2019).

Selecting an appropriate vaccine adjuvant is important to guarantee the effectiveness of the vaccine and the duration of the immunity conferred, and are particularly useful in increasing the immunogenicity of non-live vaccines including subunit, toxoid and killed whole organism vaccines (Pulendran & Ahmed, 2011). It is also essential to consider adjuvant suitability based on the mode of vaccine administration, the duration and type of immunity sought and the target animal species. As such, the chosen adjuvant must be: effective and capable of inducing a strong immune response, in combination with the selected antigen; well-tolerated so as not to cause an adverse local or systemic reaction; compatible with the antigen to allow the formulation of a stable vaccine that preserves the antigen's structure; reproducible in order to guarantee the same performance independently of the batch, and consistently capable of being produced to the necessary quality benchmarks; and easy to use, both for formulation and for administration.

1.3 Designing a platform for subunit vaccine production

1.3.1 Current PCV2 vaccine platforms

As outlined previously in the chapter, there are a range of PCV2 subunit vaccine types currently in use in livestock; a subunit vaccine contains an isolated fragment of a pathogen, purified and selected for their ability to stimulate an immune response. These fragments are often polysaccharides or proteins located on the pathogen's surface, such as PCV2 Cap protein located on the viral capsid surface.

All currently licensed PCV2 subunit vaccines are generated using a baculovirus expression system in insect cell hosts. Baculoviruses are insect-specific pathogens that are able to infect in vivo tissues and insect cell cultures, allowing them to be propagated in cell culture. Baculovirus vectors are particularly advantageous in vaccine design as they can be engineered to express recombinant antigens within the insect host cells then display the foreign proteins on the surface of virions or in nucleocapsid structures, or to assemble expressed proteins to form VLPs (Fabre et al., 2020; Lu et al., 2012). However, insect cell culture is expensive and time consuming compared to prokaryotic expression systems.

In recent years, multiple groups have been able to successfully generate PCV2 capsid proteins and virus like particle structures with potential to be used as vaccine candidates using prokaryotic, *E. coli* expression systems. These systems have proved to be simple, inexpensive tools that can provide high yields of PCV2 Cap proteins (Wu et al., 2016; Yin et al., 2010).

1.3.2 Bacterial expression systems as a platform for biopharmaceuticals and therapeutics

Following the emergence of the biopharmaceutical industry in the 1980's, *E. coli* dominated as the most widely used production organism, in >60% of cases for biopharmaceutical protein production (Huang, Lin and Yan 2012). This was due to a combination of a short doubling time, ability to grow to high cell densities and the relatively simple scale-up procedure. Nowadays, mammalian cell lines, most notably CHO (Chinese Hamster Ovary) cells are the most popular option for protein production platforms, due their suitability for generating more complex, glycosylated proteins. However, *E. coli* is still the organism of choice to express heterologous proteins for therapeutic use, with approximately 30% of approved therapeutic proteins currently generated by overexpression in *E. coli* (Walsh, 2014).

Some of the main challenges of *E. coli* include host cell-derived impurities, such as dsDNA contamination and the presence of endotoxins consisting of components of the Gram-negative bacterial cell wall along with difficulty completely removing other host cell proteins. These impurities have to be removed within subsequent downstream processing steps in order to meet distinct quality standards that are defined by regulatory bodies if they are to succeed as biopharmaceuticals, as they are related to severe health risks in patients (HHS Food and Drug Association, 2012).

Functionally, the cell envelope of the prokaryotic cell is a major line of defence against environmental challenges. In Gram-negative bacteria such as *E. coli* the cell envelope consists of the inner membrane, the outer membrane and the peptidoglycan cell wall. The aqueous compartment existing between inner and outer membranes, known as the periplasmic space, is the main site for the maturation of proteins transported from the cytoplasm through stabilization by disulphide bond formation, which can occur in this cellular compartment due to the oxidizing environment and the overall lower abundance of proteases in the periplasm than the cytoplasm (Ryan & Henehan, 2013). The cell envelope is also the barrier which allows secretion of proteins through the outer membrane and into the external environment. Approximately 300 native *E. coli* proteins are predicted to be stabilized by one or more disulphide bonds (Dutton et al., 2008). One way in which the bacterial compartmentalisation has been exploited for use as an effective recombinant expression system is by utilizing native signal sequence tags to direct non-native proteins to cellular compartments as desired (Freudl, 2018). Two major protein transport systems

in *E. coli* are the secretory (Sec) and twin-arginine translocase (Tat) pathways which direct cytoplasmic proteins to the periplasmic space through specific recognition of such signal sequences. These can be invaluable tools in ensuring proper protein folding of recombinant targets by relocation to the periplasmic space where disulphide bonding can take place, while the Tat pathway is thought to play an important role in protein proofreading and quality control (Robinson et al., 2011). Extraction of proteins from the periplasmic space can also be advantageous in downstream processing as it contains fewer impurities such as host cell proteins or DNA compared to whole cell extracts (Balasundaram et al., 2009).

As recombinant expression systems, bacterial are widely known to have some limitations in expressing more complex proteins especially those of eukaryotic origin due to the lack of sophisticated machinery to perform post-translational modifications, which can result in poor solubility of the protein of interest and formation of inclusion bodies (Demain & Vaishnav, 2009; Kamionka, 2011). In addition to this, the naturally reducing environment of the *E. coli* cytosol prevents formation of disulphide bonds, which can be necessary for stability of heterologous proteins; meanwhile the absence of some chaperones for protein folding and mismatches in codon usage between the host cell and the protein of interest can further contribute to this problem (Demain & Vaishnav, 2009; Pacheco et al., 2012; Terpe, 2006).

However, over the many years of research into *E. coli* as an expression system, many adaptations and modifications have been employed in order to develop the organism into a superior host to generate high quality heterologous protein products. A huge variety of modified *E. coli* expression strains have come about and are readily available commercially, combating almost any imaginable downfall of the prokaryotic expression system through precise engineering. Such engineered strains can be utilised to enhance both the quantity and quality of therapeutic products. *E. coli* K-12 strain derivatives such as W3110 are most widely used in the biotechnology industry, however, modified BL21 strains lacking functional proteases have been shown to be more effective in high-density fermentation techniques due to their low acetate accumulation (Sørensen & Mortensen, 2005) and are also a popular choice. Due to the relative ease of genetic engineering in bacteria, a large range of modified cell lines have been developed to work around all sorts of the organism's limitations; some examples include SHuffle (NEB) cells which are a modified K-12 strain engineered to promote disulphide bond formation in the cytoplasm, through addition of a disulphide bond isomerase. ArcticExpress (Agilent) BL21-derived strain can be used to express heterologous proteins that tend to be insoluble under standard conditions, engineered to use cold-adapted chaperonins that retain high protein folding capabilities at growth temperatures as low as 4 °C (Ferrer et al., 2003). Meanwhile, Rosetta BL21-derivatives are designed to enhance the

expression of eukaryotic proteins that contain codons rarely used in *E. coli* by supplying rare tRNAs.

While such useful cell lines are widely available, the additional costs of licensing agreements with respect to intellectual property must be taken into consideration. In development of technology intended for use in low income countries, such costs would pose a great hurdle in industrialisation and commercialisation of the technology.

1.4 Aims

The aims of the project were to develop a recombinant bacterial expression system using *E. coli* as a host organism to express viral capsid proteins from PCV2d and PCV3 viruses, with the end goal of optimizing both upstream and downstream steps to obtain a product of sufficient quality, quantity and purity to formulate into a vaccine candidate. Upstream process development was to be achieved by optimisation of vector constructions and expression conditions to provide a high yield of soluble protein. Downstream steps aimed to determine the most suitable purification technique for isolation of the soluble protein targets that ideally would attain a high level of purity in a single purification step. End goals of the project were to formulate a vaccine candidate against PCV2d and potentially also PCV2d-PCV3 as a dual vaccine candidate, and to test these vaccine candidates in a live pig trial for efficacy. Considerations throughout the project centred on developing a low cost system with minimal processing steps.

Chapter 2: Materials and Methods

2.1 Suppliers of chemicals, reagents and equipment used

Reagents, materials and equipment were obtained from the companies detailed below, unless otherwise specified.

Centrifuge equipment was obtained from Beckman Coulter Inc (USA) and Thermo Fisher Scientific Inc (USA). PCR, electrophoresis and western blotting machines and reagents were obtained from Bio-Rad (USA). Consumable plastic-ware was obtained from Eppendorf, Thermo Fisher Scientific Inc (USA), WVR, Greiner, Starstedt and Starlabs. Gene fragments and oligonucleotides (primers) were sourced primarily from IDT DNA. DNA polymerase, restriction enzymes and competent cells were obtained from New England Biolabs (NEB; UK). Other reagents were sourced primarily from Thermo Fisher Scientific Inc (USA), Oxoid and Melford. Sequencing was performed by Eurofins Genomics or Genewiz.

2.2 DNA techniques

2.2.1 Preparation of Plasmid DNA

Plasmids were purified using a QIAprep Spin Miniprep Kit (QIAGEN) as per the manufacturer's instructions. Plasmids were eluted in 50 µL elution buffer (10 mM Tris-HCl pH 8.5). DNA concentrations were determined using a NanoDrop 2000 (Thermo Fisher Scientific Inc).

2.2.2 Phosphorylation of primers

For amplifications of primers for overlap or mutagenesis, in order to allow direct ligation of the amplified DNA fragment, primers were 5' phosphorylated prior to PCR amplification using T4 polynucleotide kinase.

Reagent	Volume
100 µM primer stock	1 µL
10X T4 DNA ligase buffer	1 µL
T4 Polynucleotide Kinase	0.5 µL (5 U)
Water	7.5 µL

Table 1. 5' Phosphorylation of primers.

After PCR amplification, the DNA was purified before ligation.

2.2.3 DNA amplification by Polymerase Chain Reaction (PCR)

DNA fragments were amplified using a BioRad T100TM Thermal Cycler machine. Each reaction contained the following reaction mix:

Reagent	Volume
5X Phusion HF buffer	10 µL
10mM dNTPs	1 µL
10uM forward primer	2.5 µL
10uM reverse primer	2.5 µL
Vector DNA (50-150 ng)	X µL
DMSO (3%)	1.5 µL
Phusion polymerase	0.5 µL
Water	to 50 µL

Table 2. Reagents for DNA amplification by PCR.

The general protocol for PCR cycles is shown below. Annealing temperatures were determined based on primer pair Tm and the specified DMSO concentration added.

Step	Temperature	Time	Cycles
Initial denaturation	98 ˚C	*0:30 sec*	
Denaturation	98 ˚C	*0:10 sec*	
Annealing	X ˚C	*0:30 sec*	X30
Elongation	72 ˚C	*30 sec/kbp + 30 sec*	
Final elongation	72 ˚C	*5:00 min*	
Pause	4 ˚C	∞	

Table 3. Thermocycler steps for DNA amplification by PCR.

Following PCR amplification, 1 µL Dpn1 enzyme was added per 50 µL reaction and incubated for 16 hours at 37 °C followed by 20 minutes at 80 °C, to digest vector DNA.

2.2.4 Agarose gel electrophoresis

Samples were prepared using 1X SybrGreen and 6X Purple Loading Dye (NEB).

DNA was separated by horizontal electrophoresis in a Bio-Rad Mini-Sub® DNA electrophoresis chamber using gels formulated using 1 % molecular biology grade agarose (Melford) in TAE buffer. Gels were run for 40 minutes at 120 V.

2.2.5 Purification of DNA from agarose gels

DNA was visualised under UV light and the desired band excised as a gel slice. Gel slices were processed and DNA extracted using a QIAquick Gel Extraction Kit (QIAGEN) according to the manufacturer's instructions.

2.2.6 Restriction digests of DNA

Restriction digests were carried out using a combination of XbaI, NdeI and SpeI restriction enzymes from NEB along with the supplied 10X Cutsmart buffer.

Reagent	Volume
DNA	1 µg
10X CutSmart buffer	5 µL
Enzyme 1	1 µL (10 U)
Enzyme 2	1 µL (10 U)
Water	to 50 µL

Table 4. Reagents for restriction digests of DNA.

Mixtures were incubated at 37 ˚C in water bath for 1 hour then heat inactivated at 80 ˚C for 20 minutes. Digested DNA was then purified using a Monarch® PCR & DNA Cleanup Kit (NEB) according to the manufacturer's instructions.

2.2.7 Ligation of DNA fragments into plasmid vector backbone

If ligating a single fragment of DNA amplified using 5' phosphorylated primers, the ligation mixture was as follows:

Reagent	Volume
10x T4 DNA ligase buffer	2 µL
Vector DNA	10 µL
T4 DNA ligase	1 µL
Water	7 µL

Table 5. Reagents for ligation of a single DNA fragment.

If ligating multiple fragments of DNA following restriction digest, the volume of vector and insert DNA was calculated based on the molar concentration of each fragment, where a standard amount of vector DNA was added to the ligation mixture along with a 3:1 molar excess of insert DNA to vector DNA. The ligation mixture was as follows:

Reagent	Volume
10x T4 DNA ligase buffer	2 µL
Vector DNA (50 ng)	X µL
Insert DNA (3:1 molar excess)	X µL
T4 DNA ligase	1 µL
Water	to 20 µL

Table 6. Reagents for ligation of multiple DNA fragments.

Ligation reaction mixtures were incubated for 3 hours at room temperature before transformation into *E. coli* cells.

2.2.8 Transformation of competent *E. coli* cloning cell lines and sequencing of plasmid DNA

Following ligation, the DNA was transformed into *E. coli* NEB Turbo cloning cell line by mixing 10 µL of ligation mix with 100 µL cells, incubating on ice for 20 minutes followed by a 45 second thermal shock in a 42 °C water bath, incubation on ice for a further 30 minutes before adding 100 µL LB medium and incubating for 1 hour at 37 °C, 200 rpm in a shaking incubator. Cell suspensions were spread onto LB agar medium containing antibiotic and incubated overnight for typically 16 hours at 37 °C in a static incubator.

Grown colonies were picked and a single colony inoculated into 5 mL LB medium containing antibiotic then incubated overnight for typically 16 hours at 37 °C, 200 rpm in a shaking incubator. The following day, the plasmid DNA was isolated from the NEB Turbo cells using a QIAprep Spin Miniprep Kit (QIAGEN) and the concentration of isolated DNA determined using a Nanodrop 2000. Plasmid DNA was prepared for sequencing by mixing 5 µL of an appropriate 5 mM concentrated sequencing primer with 5 µL of plasmid DNA at a concentration between 80-100 ng/µL.

2.2.9 Constructs used in this study

Name	Vector type	Details	Source
pARP2	pBAD24	pBAD modified cloning plasmid	This study
pARP3	pET23/*ptac*	pYU49 modified cloning plasmid	This study
pARP5	pBAD24	OmpA-PCV2d-H6	This study
pARP6	pBAD24	OmpA-PCV3-H6	This study
pARP7	pBAD24	OmpA-PCV2d-GSGSG-PCV3-H6	This study
pARP8	pBAD24	OmpA-PCV2d-GSGSGSGSGS-PCV3-H6	This study
pARP9	pET23/*ptac*	OmpA-PCV2d-H6	This study

pARP10	pET23/*ptac*	OmpA-PCV3-H6	This study
pARP11	pET23/*ptac*	OmpA-PCV2d-GSGSG-PCV3-H6	This study
pARP12	pET23/*ptac*	OmpA-PCV2d-GSGSGSGSGS-PCV3-H6	This study
pARP13	pBAD24	PCV2d-H6	This study
pARP14	pBAD24	PCV3-H6	This study
pARP15	pBAD24	PCV2d-GSGSG-PCV3-H6	This study
pARP16	pBAD24	PCV2d-GSGSGSGSGS-PCV3-H6	This study
pARP17	pET23/*ptac*	PCV2d-H6	This study
pARP18	pET23/*ptac*	PCV3-H6	This study
pARP19	pET23/*ptac*	PCV2d-GSGSG-PCV3-H6	This study
pARP20	pET23/*ptac*	PCV2d-GSGSGSGSGS-PCV3-H6	This study
pARP21	pBAD24	*Δ2-40* PCV2d-H6	This study
pARP22	pBAD24	*Δ2-34* PCV3-H6	This study
pARP23	pBAD24	*Δ2-40* PCV2d-GSGSG-*Δ2-34* PCV3-H6	This study
pARP24	pBAD24	*Δ2-40* PCV2d-GSGSGSGSGS-*Δ2-34* PCV3-H6	This study
pARP25	pET23/*ptac*	*Δ2-40* PCV2d-H6	This study
pARP26	pET23/*ptac*	*Δ2-34* PCV3-H6	This study
pARP27	pET23/*ptac*	*Δ2-40* PCV2d-GSGSG-*Δ2-34* PCV3-H6	This study
pARP28	pET23/*ptac*	*Δ2-40* PCV2d-GSGSGSGSGS-*Δ2-34* PCV3-H6	This study
pARP29	pET23/*ptac*	*Δ2-34, Δ195-214*PCV3-H6	This study
pARP30	pET23/*ptac*	*Δ2-40* PCV2d-GSGSG-*Δ2-34, Δ195-214*PCV3-H6	This study
pARP31	pET23/*ptac*	*Δ2-40* PCV2d-GSGSG-*Δ1-34, Δ195-214*PCV3-H6 (PCV3 start codon removed)	This study
pARP34	pET23/*ptac*	*Δ2-40* PCV2d-GGGGS-*35-194* PCV3-H6	This study
pARP35	pET23/*ptac*	*Δ2-40* PCV2d-EAAAK-*35-194* PCV3-H6	This study
pARP36	pET23/*ptac*	*Δ2-40* PCV2d-AEAAAKALEAEAAAKA-*35-194* PCV3-H6	This study
pARP37	pET23/*ptac*	*Δ2-40* PCV2d-EPEPEP-*35-194* PCV3-H6	This study
pARP38	pET23/*ptac*	*Δ2-40* PCV2d - *35-194* PCV3-H6	This study
pARP39	pET23/*ptac*	*Δ2-40* PCV2d(C108S)-H6 (Cys > Ser mutant)	This study
pARP40	pET23/*ptac*	*Δ2-40* PCV2d(C108A)-H6 (Cys > Ala mutant)	This study
pARP41	pET23/*ptac*	*Δ2-40* PCV2d(C108S)-GSGSG-*Δ1-34, Δ195-214*PCV3-H6 (Cys > Ser mutant)	This study
pARP42	pET23/*ptac*	*Δ2-40* PCV2d(C108A)-GSGSG-*Δ1-34, Δ195-214*PCV3-H6 (Cys > Ala mutant)	This study

Table 7. Constructs used in this study.

2.2.10 Primers used in this study

Primer name	5' PHO	Sequence 5' - 3'	Purpose
13_Chimera_PCV3_seq_F		CAGGACTACAACATCCGCATTACCATGT	Sequencing
HIS pKRAP F primer		GAGCTCCACCATCACCATCAC	Sequencing
19 ptac SEQ P F		ACTCCCGTTCTGGATAAT	Sequencing
1_pKRK39_F_RBS		TCTAGAGGTTCTATGTGACTAGACCACAGAGGA TCATATG	RBS pARP2 creation
2_pKRK39_R_RBS		CATATGATCCTCTGTGGTCTAGTCACATAGAACC TCTAGA	RBS pARP2 creation
3_CRP01_R_RBS	✓	CACCTAAACGGACTGGCTG	PHO pARP3 creation
4_CRP01_F_RBS	✓	TCTAGACACAGAGGATCATATGACTAGTGATCCG GCTGCTAACAAAGC	PHO pARP3 creation
14_ΔompA/NLS_pBAD_R	✓	CATTCATATGATCCTCTGTGGTCTAGTC	pBAD ompA/NLS removal
15_ΔompA/NLS_pET_R	✓	CATTCATATGATCCTCTGTGTCTAGACAC	pET23/*ptac* ompA/NLS removal
16_ΔompA_PCV2_F	✓	ACCTATCCGCGTCGTCGTT	PCV2 ompA removal
17_ ΔompA_PCV3_F	✓	CGTCATCGTGCAATTTTTCG	PCV3 ompA removal
18_ΔNLS_PCV2_F	✓	AAAAATGGTATCTTTAATACCCGTCTGAG	PCV2 NLS removal
19_ ΔNLS_PCV3_F	✓	GCAGGCACCTATTATACCAAAAAATACA	PCV3 NLS removal
20_5xChimera_ΔNLS_PCV3_R	✓	CATACCACTACCGCTACCTTTCGGA	GSGSG constructs NLS removal
21_10xChimera_ΔNLS_PCV3_R	✓	CATGCTACCACTACCAGAACCG	GSGSGSGSGS constructs NLS removal
22_PCV3_C-term_R	✓	GGTTTTTTCCGGAACATAAATTG	PCV3 C-term truncation

23_PCV3_HIS_F	✓	CATCATCACCACCATCACTAAAC	PCV3 C-term truncation
24_PCV3_M-Rem_R	✓	ACCACTACCGCTACCTTTCGGA	PCV3 start codon removal
36_pARP31Linker_R	✓	TTTCGGATTCAGAGGCG	PHO overlap
37_Linker_overlap_F	✓	GGTGGTGGTGGTTCTGCAGGCACCTATTATACCA	PHO overlap
38_Linker_overlap_F	✓	GAAGCTGCTGCTAAAGCAGGCACCTATTATACCA	PHO overlap
39_Linker_overlap_F	✓	GCTGAAGCTGCTGCTAAAGCTCTGGAAGCTGAAGCT GC TGCTAAAGCTGCAGGCACCTATTATACCA	PHO overlap
40_Linker_overlap_F	✓	GAACCGGAACCGGAACCGGCAGGCACCTATTATAC CA	PHO overlap
41_NoLinker_F	✓	GCAGGCACCTATTATACCA	PHO overlap
42_PCV2Cys_R	✓	CACCTTCACTTTGCGAATACGAT	Quick-change
43_PCV2Cys-Ser_F	✓	GAATTTTGGCCGAGCAGCCCGATTAC	Quick-change
44_PCV2Cys-Ala_F	✓	GAATTTTGGCCGGCAAGCCCGATTAC	Quick-change

Table 8. Primers used in this study. 5' PHO = 5' phosphorylation.

2.3 Maintenance of *E. coli* cultures

Name	Genotype	Source
NEB Turbo	*E. coli* K-12 strain. *F' proA B lacIq ΔlacZM15 / /fhuA2 Δ(lac-proAB) glnV galK16 galE15 R(zgb-210::Tn10)TetS endA1 thi-1 Δ(hsdS-mcrB)5*	NEB
DH5α	*E. coli* K-12 strain. *dlacZ Delta M15 Delta(lacZYA-argF) U169 recA1 endA1 hsdR17(rK-mK+) supE44 thi-1 gyrA96 relA1*	ThermoFisher
BL21	*E. coli* B strain. *F– ompT gal dcm lon hsdSB(rB–mB–) [malB+]K-12(λS)*	ATCC
W3110	*E. coli* K-12 strain. *F- λ- rph-1 INV(rrnD, rrnE)*	ATCC

Table 9. *E. coli* strains used in this study.

2.3.1 Media and supplements

Cultures were grown in the medium specified. For colony growth, LB agar (LB recipe as below with the addition of 10 g/L bacto-agar) was used. All were supplemented with an appropriate antibiotic as determined by plasmid vector: ampicillin at a working concentration of 100 µg/mL or kanamycin at a working concentration of 50 µg/mL.

Media	Components
Luria Broth (LB) medium	10 g/L sodium chloride, 10 g/L tryptone, 5 g/L yeast extract
Terrific Broth (TB) medium	24 g/L yeast extract, 12 g/L tryptone, 4 mL/L glycerol Potassium phosphate buffer: 125.4 g/L K_2HPO_4, 23.2 g/L KH_2PO_4
SM6Gc medium	10 mL 10X SM6 trace elements, 95 g/L glycerol, 5.2 g/L $(NH_4)SO_4$, 3.83 g/L NaH_2PO_4, 4.16 g/L citric acid, 4.03 g/L KCl, 1.04 g/L $MgSO_4.7H_2O$, 0.25 g/L $CaCl_2.H_2O$
10X SM6 trace elements	104 g/L citric acid, 10.06 g/L $FeCl_3.6H_2O$, 5.22 g/L $CaCl_2.H_2O$, 2.72 g/L $MnSO_4.4H_2O$, 2.06 g/L $ZnSO_4.7H_2O$, 0.81 g/L $CuSO_4.5H_2O$, 0.42 g/L $CoSO_4.7H_2O$, 0.03 g/L H_3BO_3, 0.02 g/L $Na_2MoO_4.2H_2O$

Table 10. Media and supplements.

2.3.2 Transformation of competent *E. coli* expression cell lines

Plasmid DNA from a clone identified as positive by sequencing was isolated from NEB Turbo cells using a QIAprep Spin Miniprep Kit (QIAGEN). The isolated DNA was transformed into competent BL21 *E. coli* cells. For transformation into W3110 *E. coli* cells, DNA isolated from NEB Turbo cells was first passaged through DH5α *E. coli* cells. Transformation was achieved by mixing 2 µL of plasmid DNA with 50 µL cells, incubating on ice for 10 minutes followed by a 45 second thermal shock in a 42 °C water bath, incubation on ice for a further 10 minutes before adding 100 µL LB medium and incubating for 1 hour at 37 °C, 200 rpm in a shaking incubator. Cell suspensions were spread onto LB agar medium containing antibiotic and incubated overnight for typically 16 hours at 37 °C.

2.3.3 Storage of *E. coli* cells

One colony of transformed *E.coli* was inoculated into 5 mL LB media with appropriate antibiotic and grown overnight at 37 °C in a shaking incubator. The next morning, 500 µL of cell culture was mixed with an equal volume of 50 % (v/v) glycerol in a 2 mL cryovial, vortexed briefly, and transferred to -80°C for long term storage.

2.4 Protein production and *E. coli* cell fractionation

2.4.1 Cell culture and induction of plasmids

For shake flask screening experiments of gene expression, a 5 mL overnight culture of LB medium with antibiotic was inoculated with a single colony from a freshly streaked LB agar plate or glycerol stock and grown at 30 °C, 200 rpm in a 50 mL falcon tube. The following morning, a 50 mL LB culture in a 250 mL Erlenmeyer flask was inoculated with the overnight culture, to an OD_{600} of 0.05 and grown at 30 °C, 200 rpm until it reached OD_{600} 0.5. Once reached, gene expression was

induced by adding 100 µM IPTG to the culture and continued to grow, harvesting samples at 3 hours and 21 hours following induction.

2.4.2 *E. coli* isolation of soluble and insoluble proteins from shake flask cultures

At the specified timepoints, the OD_{600} of the shake flask culture was determined and a volume of culture equivalent to 10 OD_{600} was harvested by centrifugation at 3000 rpm for 10 minutes at 4 °C. The cell pellet was resuspended in 1 mL resuspension buffer (50 mM Tris-acetate, 2.5 mM EDTA pH 7.0) then lysed by sonication in ice at all times, using amplitude 8.0 for 4-6 rounds consisting of 10 seconds sonicating, alternated with 10 seconds resting. Lysed suspensions were centrifuged at 14,000 rpm for 15 minutes at 4 °C and the supernatant kept as "Soluble" cell fraction, while the pellet was resuspended in a further 1 mL resuspension buffer and kept as "Insoluble" cell fraction.

2.4.3 *E. coli* fed-batch fermentation

The day prior to beginning fermentation, a pre-inoculant culture was prepared by inoculating a single colony taken from a freshly streaked *E. coli* LB agar plate into 5 mL TB media with antibiotic and grown for 6-8 hours 37°C, 250 rpm. Following this, 1 mL of the pre-inoculant was transferred to a 1 L baffled flask containing 200 mL SM6Gc media with antibiotic and grown overnight at 30 °C, 250 rpm. The next day, 300 OD_{600}/L of the overnight culture were inoculated into 500 mL SM6Gc medium into a Minifors 2 1.5 L fermenter, to a total volume of 500 mL. Antibiotic and 1 mL/L PPG 2000 were injected and the fermenter parameters were set to pH 7.0, 40 % pO_2, total flow 1.5-2.0 L/min and stirrer speed 800-1600 rpm, where total flow and stirrer speed are regulated by pO_2. The cultures were grown at 30 °C until the total flow and stirrer speed had reached maximum capacity and pO_2 is below 40%, then the growth temperature lowered to 25 °C. Once the culture had reached OD_{600} 38-42, an 8 mL/L shot of 1 M $MgSO_4 \cdot 7H_2O$ was injected. At OD_{600} 54-58, a 5 mL/L shot of 1.687 M NaH_2PO_4 was added, followed by a further shot of 7 mL/L of 1.687 M NaH_2PO_4 at OD_{600} 66-70, and a glycerol feed (80 % w/v glycerol) was set at a rate of 0.7 % pump capacity (equates to approximately 0.025 mL/min). Once the culture had reached OD_{600} 75, protein expression was induced by addition of 9 mL/L 0.0181 M IPTG, and grown for the remainder of the experiment taking regular OD_{600} measurements and harvesting cell samples to monitor protein expression and solubility.

2.4.4 *E. coli* isolation of soluble and insoluble proteins from fed-batch fermentation cultures

As per optimised protocol for soluble and insoluble protein isolation from fed-batch fermentation cultures, at the end of the fermentation time, the 500 mL culture was harvested by centrifugation in 250 mL bottles at 4000 rpm for 40 minutes at 4 °C then the supernatant discarded and cell pellets stored at -20 °C for later use. For processing, the cell pellet was resuspended in

resuspension buffer (50 mM Tris-acetate pH 7.0) at a concentration of 15% w/v and lysed using a Gaulin style homogeniser at 500 bar for 4 passages. Alternatively, a sonication cell lysis method was used by resuspending 10g of the cell pellet in 20 mL reuspension buffer and sonicating for 3 seconds followed by 7 seconds rest on ice, for 5 minutes, then repeating this cycle twice more with 2 minute 30 second breaks resting samples on ice in between cycles. Lysates were centrifuged at 15,000 rpm for 30 minutes at 4 °C to separate insoluble material. The supernatant containing soluble cell proteins was aspirated and taken forward for purification.

2.4.5 Preparation and denaturation of inclusion body proteins

For denaturation of inclusion bodies on a small scale for later purification, 10 OD units of cells were harvested from a shake flask culture of transformed W3110 cells, induced with 100 µM IPTG then grown at 30 °C for 3 hours post-induction in LB with antibiotic and lysed by sonication as described in chapter 2.4.2. Insoluble proteins were separated from soluble proteins by centrifugation in a chilled centrifuge for 15 minutes at 14,000 rpm, 4 °C. Supernatant was aspirated and the pellet was subjected to three washing steps by resuspending in 1 mL 50 mM Tris-acetate, 1 % triton X-100, 4 M urea, pH 7.0 and centrifuging at 20 °C, then repeating this process two more times, finally the pelleted material was washed once more with 1 mL dH2O. The washed inclusion body pellet was resuspended in 1 mL 50 mM sodium phosphate dibasic heptahydrate, 5 mM DTT buffer containing between 0-8 M urea at variable pH as specified in text, and agitated using a magnetic stirrer for 16 hours at room temperature. After this time, the solution was centrifuged at 14,000 rpm for 15 minutes at 20 °C and the resulting supernatant containing solubilised, denatured inclusion body proteins taken forward for analysis.

2.4.6 Larger scale shake flask preparation and denaturation of inclusion body proteins for rabbit immunisation

A pre-inoculate culture containing a single colony from the transformed plate inoculated into 5 mL LB medium with antibiotic was set up and for 16 hours at 30 °C, 200 rpm in a shaking incubator. The following day, two baffled flasks containing a total of 500 mL LB medium containing 100 µg/mL ampicillin were inoculated with the pre-inoculate culture to an OD_{600} of 0.05, then grown at 30 °C, 200 rpm for approximately 3 hours until the OD_{600} of the culture reached 0.4-0.6. Once reached, expression was induced by adding 100 µM IPTG to the culture, then the cultures continued to grow at 30 °C, 200 rpm. After 21 hours following induction, a volume of culture equivalent to 300 OD_{600} was harvested by centrifugation at 4000 rpm for 40 minutes at 4 °C. The cell pellet was resuspended in 30 mL resuspension buffer (50 mM Tris-acetate pH 7.0) then lysed by sonication in ice at all times, using amplitude 8.0 for 3 cycles of lysis. Each cycle of lysis consisted of 3 seconds sonicating, alternated by 7 seconds resting, for 5

minutes, with 2 minutes 30 seconds of resting in between each cycle. Lysed suspensions were then centrifuged at 15,000 rpm for 30 minutes at 20 °C and the supernatant removed. The insoluble pellet material was resuspended by brief sonication in 30 mL resuspension buffer and centrifuged again. The supernatant was removed and the pellet subjected to three washing steps by resuspending in 30 mL 50 mM Tris-acetate, 1 % triton X-100, 4 M urea, pH 7.0 and centrifuging, then repeating this process two more times, finally the pelleted material was washed once more with 30 mL dH_2O. The washed inclusion body pellet was resuspended in 30 mL 50 mM sodium phosphate dibasic heptahydrate, 6 M urea, 5 mM DTT, pH 12.0 and agitated using a magnetic stirrer for 16 hours at room temperature. After this time, the solution was centrifuged at 15,000 rpm for 30 minutes at 20 °C and the resulting supernatant filtered using a 0.45 µm syringe filter for purification.

2.5 Protein purification and quantification

2.5.1 Nickel affinity purification of soluble proteins

Following protein expression in *E. coli* cells for 3 hours post-induction, cells were harvested by centrifugation at 3000 rpm for 20 minutes at 4 °C. The cell pellet was resuspended in 2 mL/g (w/c/w) of 50 mM Tris-HCl, 1 % Triton X-100 pH 8.0 then sonicated as described in chapter 2.4.2. Lysates were centrifuged at 15,000 rpm for 30 minutes at 4 °C and the supernatant aspirated then filter sterilised using a 0.45 µm syringe filter. A GE LifeSciences 5 mL HisTrap HP pre-packed column was set up in an ÄKTA Pure refrigerated system and equilibrated with 50 mM Tris-HCl, 20 mM imidazole, 150 mM NaCl pH 8.0. The filtered supernatant was applied to the column then the column was washed with 50 mM Tris-HCl, 30 mM imidazole, pH 8.0 until the A_{280} peak descended and plateaued. Bound protein was eluted with 50 mM Tris-HCl, 300 mM imidazole, 150 mM NaCl pH 8.0 and samples collected as A_{280} peaks appeared. Elutions were ceased once the A_{280} had continued to plateau for 50 mL of elution buffer. The quantity of the purified protein was obtained by measuring samples at A_{280} on a spectrophotometer in a 1 mL quartz cuvette using milliQ water as a blank, and calculated using the specific extinction coefficient and molecular weight of the protein.

2.5.2 Nickel affinity purification of insoluble proteins

For purification of His-tagged inclusion body proteins prepared in 6 M urea, a GE LifeSciences 5 mL HisTrap HP pre-packed column was set up in an ÄKTA Start system at room temperature. All steps were run at a flow rate of 5 mL/min and DTT was added fresh upon use. The column was equilibrated with 5 CV Binding buffer (50 mM sodium phosphate dibasic heptahydrate, 500 mM NaCl, 6 M urea, 5 mM DTT, 20 mM imidazole pH 12.0. The inclusion body sample, prepared by filtering with a 0.45 µm syringe filter and adding 5 mM DTT fresh, was applied to the column then

washed with 5 CV Binding buffer. Bound proteins were eluted with 5 CV Elution buffer (50 mM sodium phosphate dibasic heptahydrate, 500 mM NaCl, 6 M urea, 5 mM DTT, 500 mM imidazole pH 12.0. Eluted samples were analysed by SDS PAGE and the protein content of determined by Bradford Assay.

2.5.3 Cation exchange purification using bench-top system

Bench-top cation exchange purification was carried out on ice using 13 mL column packed with 5 mL SP Sepharose FF resin and syringe system to regulate flow rate. Purifications were run with the addition of DTT to sample and buffers, added fresh upon use, unless otherwise specified. The column was first equilibrated with 2 CV Binding buffer (50 mM Tris-HCl, 0.1 mM DTT, pH 7.0) and the sample, with 0.1 mM DTT added, was applied the column. The column was washed with 2 CV Binding buffer, then an elution gradient applied in stepwise increments of 50 mM increasing salt concentration over 20 CV, using a combination of Binding buffer and Elution buffer (50 mM Tris-HCl, 1 M NaCl, 0.1 mM DTT, pH 7.0) to elute bound proteins. A further 2 CV of Elution buffer was washed through the column to remove any residual proteins. Elution samples were analysed by SDS PAGE and the protein content of peak elution fractions was determined by Bradford Assay.

2.5.4 Cation exchange purification using ÄKTA Pure system

Cation exchange purification was carried out using a GE LifeSciences HiTrap SP 5 mL column in an ÄKTA Pure refrigerated system. Purifications were run with the addition of DTT to sample and buffers unless otherwise specified. All steps were run at a flow rate of 5 mL/min and DTT was added fresh upon use. The column was first equilibrated with 5 CV Binding buffer (50 mM Tris-HCl, 0.1 mM DTT, pH 7.0) and the sample, with 0.1 mM DTT added, was applied the column. The column was washed with 5 CV Binding buffer, then an elution gradient applied in stepwise increments of 50 mM increasing salt concentration over 20 CV, using a combination of Binding buffer and Elution buffer (50 mM Tris-HCl, 1 M NaCl, 0.1 mM DTT, pH 7.0) to elute bound proteins. A further 5 CV of Elution buffer was washed through the column to remove any residual proteins. Elution samples were analysed by SDS PAGE and the protein content of peak elution fractions was determined by Bradford Assay.

2.5.5 Desalting

To buffer exchange protein samples following cation exchange purification, five GE LifeSciences 5 mL Desalting columns were attached and prepared in an ÄKTA Pure refrigerated system, creating an equivalent column volume of 25 mL. All steps were run at a flow rate of 8 mL/min and DTT was added fresh upon use. The columns were equilibrated with 5 CV Loading buffer (50 mM Tris-HCl, 900 mM NaCl, 0.1 mM DTT, pH 7.0), the same buffer composition as the protein sample to be applied. The first protein sample of 7.5 mL was applied to the column and the first 7.5 mL void

volume collected. To elute into the new desired buffer, 1 CV Desalting buffer (50mM sodium phosphate, 100mM NaCl pH 7.0) was washed through the column and collected in 5 mL fractions. A further 1 CV Desalting buffer was washed through the column to remove residual contaminants, before applying the next sample and repeating the process. Protein content of elution fractions was determined by Bradford Assay.

2.5.6 Gel-filtration chromatography

Purification by gel-filtration for analysis of VLP formation was carried out using a GE LifeSciences Superdex 200 Increase 10/300 column in an ÄKTA Pure refrigerated system. Samples used had been previously purified by cation exchange without DTT. Protein samples with concentrations between 0.25-0.5 mg/mL were carried forward for gel filtration, preparing 500 µL of each sample by centrifuging at 60,000 rpm for 20 minutes, 4 °C to pellet any insoluble material. Supernatants were aspirated and carefully prepared into a 1 mL syringe, removing any air bubbles. The column was washed with 2 CV filtered and degassed H_2O at flow rate 0.4 mL/min, then equilibrated with 2 CV Gel filtration buffer (50 mM sodium phosphate, 100 mM NaCl, pH 7.0) at flow rate 0.5 mL/min. Through a 1 mL capillary loop, 500 µL of sample was loaded onto the column, and Gel filtration buffer run through the column (flow rate 0.5 mL/min) until no more protein peaks could be seen on the UV trace. Elutions were collected in 1 mL fractions and their molecular weights determined using a calibration curve created with GE LifeSciences Gel Filtration Calibration HMW and LMW kits, according to the manufacturer's instructions.

2.5.7 Protein quantification by Bradford Assay

Elution fractions collected following purification were quantified using Thermo Scientific™ Pierce™ Coomassie (Bradford) Protein Assay Kit. A standard curve was first created according to the manufacturer's instructions. Protein samples were analysed by adding 1 mL of reagent to a 1 mL cuvette and adding 20 µL of protein sample. Cuvettes were covered and inverted 4-6 times to mix, then incubated at room temperature for 15 minutes before measuring at A_{595} in a spectrophotometer.

2.6 Protein electrophoresis

2.6.1 SDS poly-acrylamide gel electrophoresis (SDS PAGE)

Gel preparation and resolution of protein samples was performed using vertical PAGE apparatus from Bio-Rad Mini-PROTEAN¤ Tetra System. Gels were prepared according to the manufacturer's instructions to a thickness of 0.75 mm, consisting of a resolving gel section composed of 15 % acrylamide, 0.3 % bis-acrylamide (37:5:1), 375 mM Tris-HCl pH 8.85, 0.1 % SDS, 0.1 % APS and 0.06 % TEMED, layered with a stacking gel section composed of 5 % acrylamide, 0.0375 % bis-

acrylamide, 125 mM Tris-HCl pH 6.8, 0.001 % SDS, 0.6 % APS and 0.06 % TEMED. Before loading, protein samples were mixed with protein gel loading buffer (125 mM Tris-HCl pH 6.8, 20 % glycerol, 4 % SDS, 0.02 % bromophenol blue). For non-reducing SDS PAGE, samples were loaded into the stacking gel at this stage; for reducing SDS PAGE, samples were further mixed with 5 % β-mercaptoethanol and heated for 10 minutes at 90 °C before loading. Vertical electrophoresis was typically performed at 40 mA for 35 minutes in protein gel running buffer (25 mM Tris, 192 mM glycine, 0.1 % SDS, pH 8.3).

2.6.2 Native PAGE

Gel preparation and resolution of protein samples was performed using vertical PAGE apparatus from Bio-Rad Mini-PROTEAN¤ Tetra System. Gels were prepared according to the manufacturer's instructions to a thickness of 0.75 mm, consisting of a resolving gel section composed of 15 % acrylamide, 0.3 % bis-acrylamide (37:5:1), 375 mM Tris-HCl pH 8.85, 0.1 % APS and 0.06 % TEMED, layered with a stacking gel section composed of 5 % acrylamide, 0.0375 % bis-acrylamide, 125 mM Tris-HCl pH 6.8, 0.6 % APS and 0.06 % TEMED. Before loading, protein samples were mixed with native protein gel loading buffer (125 mM Tris-HCl pH 6.8, 20 % glycerol, 0.02 % bromophenol blue). Vertical electrophoresis was typically performed at 40 mA for 35 minutes in native protein gel running buffer (25 mM Tris, 192 mM glycine, pH 8.3).

2.6.3 Coomassie Brilliant Blue staining

Proteins were visualised on SDS PAGE gels by incubating with 50 mL Coomassie Brilliant Blue stain (10 % acetic acid, 40 % methanol, 1 g/L Coomassie Brilliant Blue) for 1 hour at room temperature on an orbital rocker. Following this, excess stain was removed by replacing the Coomassie stain with Destaining solution (5 % ethanol, 7.5 % acetic acid) and incubating for at least 2 hours at room temperature on an orbital rocker.

2.7 Protein detection

2.7.1 Western-blotting

Following vertical PAGE, proteins were transferred onto PVDF membrane by activating the membrane using 100 % methanol then placing the PAGE gel on top. This was then sandwiched between two sheets of Whatman paper and two sponges, all pre-soaked in Western blot transfer buffer (192 mM glycine, 25 mM Tris and 10 % ethanol). The sandwich was placed in a cassette between electrodes in the vertical PAGE system and submerged with Western blot transfer buffer. A current of 55 V was applied to the system and proteins left to transfer under the current for 1 hour. Once transfer was complete, the PVDF membrane was blocked overnight at 4 °C in a solution containing 2.5 % skimmed milk powder in 1X PBS-tween (1X PBS, 0.1 % tween 20), then

with each of the following steps carried out on an orbital shaker, the membrane was washed three times for 5 minutes each in PBS-tween before the incubation of primary antibody (Anti-HIS 1 in 10,000 concentration; or anti-PCV2d 1 in 2,000,000 concentration) for 1 hour. The membrane was washed again three times for 5 minutes each in PBS-tween before incubation with the appropriate secondary antibody (Anti-mouse 1 in 10,000 concentration; anti-rabbit 1 in 10,000 concentration) for 1 hour. Finally, the membrane was washed eight times for 5 minutes each before imaging. Immunoreactive bands were detected using the ECLTM kit according to the manufactures instructions and visualised using Bio-Rad Gel-doc XR+ chemiluminescence imager with associated software.

2.7.2 Antibodies used in this study

Antibody	Usage concentration	Source
Anti-His (C-terminal), mouse monoclonal	1:10,000	Invitrogen
Anti-Mouse HRP conjugate, goat polyclonal	1:10,000	Promega
Anti-PCV2d, rabbit polyclonal	1:2,000,000	This study
Anti-PCV3, rabbit polyclonal	1:10,000	This study
Anti-Rabbit HRP conjugate, goat polyclonal	1:10,000	Promega

Table 11. Antibodies used in this study. Usage concentrations indicated as a ratio of antibody to PBS-tween by volume.

2.7.3 PCV3 antibody purification by protein affinity chromatography

A preparation of CIEX purified PCV2d protein was supplied to Cambridge Research Biochemicals to generate a PCV2d bound-NHS activated sepharose column with a 5 mL bed volume. The bench-top purification was carried out on ice. First, the column was equilibrated with 10 CV Binding buffer (20 mM sodium phosphate, 150 mM NaCl, pH 7.0). Harvest bleed serum from rabbit immunized with chimera protein was diluted in binding buffer to reduce viscosity then filtered using a 0.45 µm syringe filter. The serum was applied to the column and the flow through containing polyclonal PCV3 antibodies was collected. The column was washed with 5-10 CV Binding buffer until no material appeared in wash fractions. Elution tubes were prepared containing 5 mL Collection buffer (1 M sodium phosphate pH 7.0) to collect elution fractions containing polyclonal PCV2d antibodies. Elution was carried out in two steps; first, 3 CV of Glycine elution buffer (100 mM glycine-HCl pH 2.0) was applied to the column and collected into tubes

containing Collection buffer. Secondly, 3 CV of TEA elution buffer (100 mM triethylamine pH 10.5) was applied to the column and collected as previously. The column was swiftly washed and stored in phosphate-buffered saline (PBS), 0.05 % sodium azide, pH 7.2 at -20 °C.

2.8 Cell-based PCV2d virus neutralization assay

Neutralisation assay based on fluorescent foci reduction was performed by collaborators at Biotec, Thailand according to (Worsfold et al., 2015) with some modifications. Briefly, 50 µL of 2-fold serial dilutions of rabbit antisera (Bleed 3) in minimum essential medium (MEM) were incubated with 50 µL containing 1000 PCV2d virus particles (BDH strain; Genbank no. HM038017) at 37 °C for 1 hour. The undiluted pre-immunisation sera were used as a control. After incubation, the mixtures were used to inoculate fresh PK-15 cells in a 96-well plate (15,000 cells per well) at 37 °C for 3 hours. After two PBS washes, 200 µL of MEM supplemented with 5 % foetal bovine serum (FBS) was added to each well, and the plate was incubated at 37 °C for 48 hours. PCV2d infection was later detected by immunofluorescence. After two PBS washes, cells were fixed with 80 % acetone for 15 minutes at room temperatures. With PBS washes in between, rabbit-anti-PCV2d capsid antibody (or mouse-anti-PCV2d in mouse study) was used as a primary antibody and Alexa488-labeled goat-anti-rabbit IgG (or goat-anti-mouse in mouse study) was used as a secondary antibody. DAPI was used to identify cell nuclei, and the numbers of infected cells (concurrence of DAPI- and Alexa488-positive nuclei) were scored on a high-content screening system (Opera Phenix). Virus neutralisation titres (VNT) were defined as the serum dilutions at which 50 % inhibition of PCV2d infection occurred. Values were reported as average±SE from two independent experiments.

2.9 TEM

2.9.1 Immunogold labelling

Carbon/formvar-coated 400-mesh gold grids were placed onto a layer of parafilm which had been stretched over dental wax. In a humid chamber at room temperature, 2 µL of protein sample which had been purified by CIEX and diluted to 0.125 mg/mL in 50 mM Tris-HCl, 150 mM NaCl pH 7.0 was applied to the grid in a droplet and incubated for 5 minutes. The sample was then fixed on the grid by applying a 20 µL droplet of freshly prepared 2 % formaldehyde, 0.5 % glutaraldehyde in sodium cacodylate buffer (CAB) pH 7.2 and incubating for 5 minutes. The grid was then moved into another 20 µL drop of the same fixative for 15 minutes. Grids were washed by passing through 6 drops (20 µL per drop) of CAB followed by 6 drops of TBST (20 mM Tris, 500 mM NaCl, 0.1 % BSA, 0.05 % Tween 20 pH 7.4). After this, grids were blocked by incubating in a drop of 2 % BSA in TBST for 30 minutes. They were carefully dabbed dry and placed in a 20 µL drop of primary antibody (Rabbit polyclonal anti-PCV2d) diluted at 1:200, 1:2000, 1:20,000 and

1:200,000 in TBST and incubated for 1 hour. A negative control consisting of a drop of TBST was also used. Grids were washed with 6 drops of TBST as previously, before being placed in a 20 µL drop of gold-conjugated second antibody (Goat anti-rabbit IgG, 5 nm gold; British Biocell International) diluted 1:50 in TBST, then immediately placed into another drop of the same, and left to incubate for 30 minutes. After this time, grids were washed through 6 drops of TBST followed by 6 drops of mQ water. Grids were air dried and then negative stained.

2.9.2 Negative staining

A 2 µL droplet of sample was placed on a carbon/formvar-coated 600-mesh copper grid and left for 5 minutes. Excess liquid was then removed with a drawn out pipette, before applying a drop of 2 % uranyl acetate in water to the grid. This was immediately aspirated with the drawn out pipette. The grid was then air dried for 10 minutes and viewed in a Jeol 1230 transmission electron microscope operating at an accelerating voltage of 80 kV. Images were recorded with a Gatan One view digital camera in 4kx4k mode with automatic drift correction.

2.10 Mouse vaccination study

2.10.1 Mouse vaccination with purified PCV2d protein

Four groups of 6 mice were used for the experiment. Group 1 contained a PBS control; Group 2 contained PCV2d purified protein derived from OT yeast (*Ogataea thermomethanolica*); Group 3 contained *Δ2-40* PCV2d purified protein derived from *E. coli*; Group 4 contained *Δ2-40* PCV2d(C108S) mutant purified protein derived from *E.coli*. Immunization was performed on day 0 of the experiment by intraperitoneal injection of a preparation containing 30 µg of the purified protein and Freund's complete adjuvant. A second immunization was performed on day 14 by intraperitoneal injection of a preparation containing 30 µg of the purified protein and Freund's incomplete adjuvant. A pre-immunization serum sample was taken at day 0 of the experiment, along with Bleed 1 on day 28 and Bleed 2 on day 35. Cell-based PCV2d virus neutralization assays were carried out using antibodies from each of the bleeds, with pre-immune serum as a control.

2.10.2 Enzyme-linked immunosorbent assay (ELISA)

ELISA plates were coated with 500 ng recombinant PCV2d-dN capsid protein or 500 ffu (fluorescent focus units) of PCV2d virus in 100 µL carbonate buffer (pH 9.6) at 4 °C overnight. The plates were washed with PBS, 0.1 % tween-20 (PBST) and blocked with 100 µL 2 % BSA in PBST for 1 hour at room temperature. The plates were washed twice with 200 µL PBST. Mouse sera diluted in 0.5 % BSA in PBST (1:5000 for recombinant protein or 1:200 for virus) were incubated in the plates for 2 hours at room temperature. The plates were then washed three times with 200 µL PBST and incubated with 100 µL HRP-conjugated Goat pAb Ms IgG (abcam) diluted at 1:5000 in

0.5 % BSA in PBST for 1 hour at room temperature. Following three washes with PBST, the plates were incubated with 3,3',5,5'- Tetramethylbenzidine (TMB) substrate for 5 minutes at room temperature. The reactions were stopped with 100 µL $2NH_2SO_4$. Absorbance at 450 nm was measured with an ELISA plate reader (Synergy HTX Multi-Mode Reader). Plots are generated and data were analyzed with Prism Graphpad.

2.11 Preparation of PCV2d vaccine candidates

2.11.1 Preparation of adjuvant emulsions

PCV2d protein was purified by CIEX by applying the soluble cell lysates of W3110 pARP31 or W3110 pARP25 peak fractions to a 5 mL HiTrap SP™ column in an ÄKTA Pure system. Peak elution fractions were pooled and then diluted down to a final, standardized concentration of 150 mM NaCl using 50 mM Tris-HCl pH 7.0 buffer. These were then further diluted to give a stock concentration of 125 µg/mL protein in 50 mM Tris-HCl, 150 mM NaCl, pH 7.0 buffer and filter sterilized using a 0.2 µm syringe filter in a laminar flow hood. Gel adjuvants were sterilised by autoclaving, while oil-containing adjuvants were sterilised by autoclaving for trial 1 and filter sterilisation for trial 2.

Adjuvant	Type	Ratio Adj/Aqu phase (v/v)
Montanide™ Gel 01 PR 36067D	Gel	55/45
Montanide™ Gel 02 PR 36084X	Gel	54/46
Montanide™ ISA 201 VG 36075M	W/O/W	55/45
Montanide™ ISA 206 VG 36022E	W/O/W	54/46
Montanide™ ISA 660 VG 80274Q	W/O	64/36

Table 12. Preparation of adjuvant emulsions. Adj/Aqu = adjuvant to aqueous.

The aqueous phase, consisting of purified PCV2d protein plus buffer to give the appropriate final concentration, and adjuvant phases were emulsified using two Braun 2 piece luer lock syringes with luer lock femelle connectors according to preparation guidelines supplied by SEPPIC. Emulsification was performed using cycles where one cycle indicates the emptying the phase in one syringe into the other; the aqueous phase was always emptied into the adjuvant phase for the first cycle. Gel formulations were emulsified in a single emulsification step consisting of 20 quick cycles (<1 sec/cycle). For trial 1, emulsions contained 50 % gel adjuvant, while for trial 2, emulsions contained 10 % gel adjuvant. For W/O/W emulsions, both aqueous and adjuvant

phases were pre-warmed in a water bath to 35 °C until immediately before emulsification to ensure both phases were at 31 °C at the time of mixing. These were mixed using an emulsification step of 10 quick cycles (<1 sec/cycle) followed by cooling for 1 hour at room temperature with minimal transport or agitation. For W/O emulsions, a pre-emulsification step of 20 slow back and forth cycles (~4 sec/cycle) was required, followed by an emulsification step of 60 quick cycles (<1 sec/cycle).

Three technical repeats of each condition were prepared to a final protein concentration of 40 µg/mL, and stored in 4 mL aliquots. Samples were stored at either 4 °C or 22 °C (room temperature) in 4 mL glass vials with butane screw lids resistant to oil degradation. Emulsions were prepared on day 0 of the trial then left to settle without disturbing for at least one day before the first analysis was performed.

2.11.2 Antigen extraction from a W/O/W vaccine emulsion

A sample of the formulated ISA 201 PCV2d vaccine was removed from storage following 105 days at 4 °C and equilibrated to room temperature for at least 15 minutes. A solution of 5 % acetic acid was added to the sample at a 1:1 ratio and vortexed to mix. The mixture was centrifuged at 20,000 rpm for 10 minutes and following this, the oily white top layer carefully decanted by pipetting. Centrifugation and decanting was repeated until the sample was clear of oily contaminants and all possible white top layer had been removed. The sample was then prepared for SDS PAGE.

2.12 Pig viral challenge trial using experimental PCV2d vaccine

2.12.1 Preparation of live PCV2d virus

The PCV2 isolate used in this study was field isolate ISU-40895 (Genbank AF264042).The virus preparation was generated in PK-15 cells free of PCV1 and PCV2. PK-15 cells were cultivated at Biotec, Thailand, in T-25 culture flasks and transfected with the PCV2-infectious DNA clone. The transfected cells were harvested at 3 days post-transfection by freezing and thawing at −80 C three times. The infectious titer of the inoculum was determined by immunofluorescence assay. The virus inoculum was stored at −80 °C until use.

2.12.2 Pig vaccination and viral challenge

Pigs were purchased at weaning (3.5 weeks of age) from a high health pig farm in Minnesota, USA, with low levels of PCV2 antibodies and no breeding herd PCV2 vaccination and were transferred to the livestock infectious disease isolation facility at Iowa State University, USA where the trial took place. The pigs were assigned randomly to rooms and pens and were housed in four rooms. Serum samples taken from pigs at arrival were screened by PCR for the presence of

PCV2 viral DNA and were deemed free of PCV2 DNA. Serum samples were also serologically screened by assay ELISA and contained low levels of maternally derived antibodies against PCV2. The experiment contained four groups of 10 pigs each; Group 1 was an unvaccinated negative control group (no viral challenge); Group 2 was an unvaccinated positive control group (with viral challenge); Group 3 was the experimental PCV2d vaccinated group; and Group 4 was a commercial PCV2a vaccinated group. The experimental PCV2d vaccine was prepared at the University of Kent (UK) then transferred to Iowa State University (USA) for the trial to be performed, where it was stored at 4 °C until usage at day 117 and day 131 following preparation. The experimental PCV2d vaccine was administered intramuscularly to Group 3 pigs in two 2 mL doses, once at 5 weeks of age in the right neck and once at 7 weeks of age in the left neck. The commercial PCV2a vaccine (Ingelvac CircoFLEX®, Boehringer Ingelheim, Lot# 309144A, Exp. Date: 06 Aug 2022) was administered to Group 4 pigs intramuscularly in a single 1 mL dose at 5 weeks of age in the right neck. At 9 weeks of age, Groups 2, 3 and 4 were challenged with a live PCV2d virus administered intranasally via a viral suspension of 2.5 mL into each nostril, standardized to contain a viral titer of 3.16×10^6 $TCID_{50}$ per mL. At 12 weeks of age, necropsy analysis was performed.

2.12.3 Viral challenge disease monitoring

Throughout the study, clinical signs of infection and weight gain were monitored. Pigs were observed at 24 hours, 48 hours and 72 hours post-vaccination for signs of vaccine reaction by monitoring redness, swelling, pain and rectal temperature. Serology was measured at time intervals of 3.5 weeks, 5 weeks (first vaccination), 9 weeks (viral challenge), 10 weeks (7 days post-challenge), 11 weeks (14 days post-challenge) and 12 weeks (20 days post-challenge). Serology for detection of PCV2-specific antibodies was performed using an Ingezim Circo IgG commercial ELISA kit (R.11.PCV.K1) (Eurofins, Ingenasa) coated with PCV2b ORF2 monoclonal antibodies. Samples with a sample to positive ratio value higher than the positive cut off were considered positive while samples with a sample to positive ratio value lower than or equal to the negative cut off were considered negative. Samples with sample to positive ratio values higher than the negative cut off but lower than the positive cut off were considered suspect.

Viremia was also monitored in serum samples over time by isolating viral DNA using KingFisher extraction system and MagMAX Pathogen RNA/DNA Kit (ThermoFisher Scientific) and amplifying PCV2 viral DNA by real time PCR using an Applied Biosystems 7500 Fast Dx Real-Time PCR machine for 37 cycles with a primer and probe targeting ORF1 (Opriessnig et al., 2003). In addition, nasal shedding was monitored over time by performing two repeat nasal swabs where

both were used to sample both nostrils, before placing swabs into 1 mL of saline solution and processing immediately by PCR amplification as previously.

Chapter 3: Expression of PCV2d and PCV2d-PCV3 chimera

3.1 Introduction

In initial stages of process development, the first step is to achieve a suitable level of expression. The main consideration in achieving a successful recombinant expression system for this project was high level expression of soluble target protein. There were two pathogens we aimed to develop vaccines against, PCV2d and PCV3. Whilst a number of researchers have achieved satisfactory expression of PCV2 capsid proteins in a variety of expression systems including *E. coli* (Khayat et al., 2011; Wu et al., 2016; Yin et al., 2010), this project aimed to do this in a more simple, more streamlined, and lower cost process than had been done before, using a low maintenance bacterial expression system and to a quality standard that could be formulated with into a subunit vaccine with few additional steps. Better yet, production of a dual subunit vaccine candidate protecting against both PCV2d and PCV3 pathogens would effectively halve the processing costs.

Choosing an appropriate expression vector is one of the major ways of meeting the expression goals. Too low an expression level will result in poor expression yields, while too high may cause overexpression of the target gene leading to overwhelm of the cell; inclusion body formation of the product may occur as the cellular machinery struggles to correctly process the product, or it may result in lysis of the cell especially in fermentation under high stress (Liu et al., 2016). One consideration in moderating expression level is the replicon of the vector, containing the origin of replication, which determines the number of plasmid copies to be replicated per cell. Another is the promoter type, responsible for the binding of RNA polymerase and initiation of transcription. A staple in prokaryotic promoter research is undoubtedly the lac promoter, key component of the lac operon (Müller-Hill, 1996). However, lac promoters can suffer from the disadvantage of sometimes having unacceptably high levels of expression in the absence of inducer, termed “leakiness”. In the presence of a toxic gene product requiring tightly controlled expression, this can be problematic. One such range of expression vectors utilizing the lac promoter is pET vectors. More than 40 different pET plasmids are commercially available. Expression requires a host strain lysogenized by a DE3 phage fragment, encoding the T7 RNA polymerase under an inducible lacUV5 promoter, a mutated version of the lac promoter boasting less sensitivity to catabolite repression and less leaky expression. Upon induction, T7 RNA polymerase binding of the plasmid’s lac promoter is able to offer five times faster transcription rate than *E. coli* RNA polymerase and offers precise control of target protein expression (Sørensen & Mortensen,

2005). Synthetic hybrids combining the strength of other promoters and the advantages of lac promoters are also available, for example, the tac promoter consisting regions of the trp promoter and the lac promoter is commonly employed to tackle this issue, and is approximately 10 times stronger than lacUV5 (Boer et al., 1983). Meanwhile, expression plasmids based on the araBAD promoter are designed for tight control of background expression and L-arabinose-dependent graded expression of the target protein by positive control (Guzman et al., 1995). The latter property is in contrast to the "on" or "off" induction offered by most other bacterial expression systems such as those relying on IPTG induction. The araBAD system offers tunable gene expression where increasing inducer concentration correlates with a linear increase in expression (Morgan-Kiss et al., 2002).

Next, it is necessary to monitor the success of vector designs by detecting expression level of the target gene. Simple tags expressed at the termini of the gene are often utilized in engineered recombinant expression systems, with tags such as poly histidine, FLAG, Myc or other short, linear recognition motifs commonly used (Kimple et al., 2013). Commercial antibodies specific to these tags are readily available to be used in expression analysis. Many of these tags also have dual functions particularly as solubility aids or affinity tags for protein purification.

Once achieving a desirable level of protein quantity, the next steps are to extract and purify the product. In this project it was essential to keep the process low cost by using techniques and resources that were cost-effective and by reducing downstream processing steps. Poly histidine tags, also known as HIS tag or His6, usually consist of six consecutive histidine residues and exhibit strong binding to a variety of metallic cations, but Ni^{2+} is most commonly used in purification of His6-tagged proteins by immobilized metal ion chromatography (IMAC). Resins for this purpose are available through many commercial companies, and present advantages in being unaffected by protease or nuclease activity, tolerant to denaturing agents such as 8 M urea, 6 M guanidine HCl, detergents and low concentrations of reducing agents making the technique suitable for the purification of insoluble or membrane-bound proteins as well as soluble crude cell lysates. Most of these resins can also be regenerated and reused indefinitely. Affinity-tagged protein purities can achieve up to 95 % purity by IMAC in high yields and can be used for a variety of expression systems including *E. coli, S. cerevisiae*, mammalian cells, and baculovirus-infected insect cells (Bornhorst & Falke, 2000). Another popular purification technique requiring readily available resins and resources is ion exchange chromatography (IEX), which involves the separation of ionizable molecules based on their total charge. This technique enables the separation of similar types of molecules that would be difficult to separate by other techniques, through manipulating the charge carried by the molecule of interest by simply changing buffer pH. Although this

technique does not offer the same breadth of chemical tolerance as with other resins, this can be an extremely useful and low cost method, requiring simple, cheap buffer components and relying on elution by an increasing salt gradient only. From *E. coli,* recombinant products have been reported of up to 90 % purity using a single step of IEX (Kuo et al., 2016).

In this chapter, the initial stages of vector and strategy development are presented for high level expression of recombinant PCV2d and PCV3 capsid proteins in *E. coli* at shake flask and fed-batch fermentation, working towards a single step purification method with analysis of protein purity, quality and efficacy as measures of technique suitability.

3.2 Results

3.2.1 Expression of full length PCV genes and investigation of production capability

The first generation of constructs consisting of full length PCV2d ORF2 genes included a HIS tag and an N-terminal *E. coli*-derived OmpA signal peptide for direction of the expressed protein to the periplasmic space via the Sec pathway, designed as such for ease of downstream processing. Chimeric constructs containing both PCV2d and PCV3 ORF2 Cap genes were also generated, connected by either a long or short flexible glycine-serine linker. All designs were initially tested in a modified pET23/*ptac* vector replacing T7 promoter with *ptac* promoter, or pBAD24 vector.

Construct	Backbone	Details
pARP5	pBAD24	OmpA-PCV2d-H6
pARP6	pBAD24	OmpA-PCV3-H6
pARP7	pBAD24	OmpA-PCV2d-GSGSG-PCV3-H6
pARP8	pBAD24	OmpA-PCV2d-GSGSGSGSGS-PCV3-H6
pARP9	pET23/*ptac*	OmpA-PCV2d-H6
pARP10	pET23/*ptac*	OmpA-PCV3-H6
pARP11	pET23/*ptac*	OmpA-PCV2d-GSGSG-PCV3-H6
pARP12	pET23/*ptac*	OmpA-PCV2d-GSGSGSGSGS-PCV3-H6

Table 13. First generation of PCV constructs. H6 = HIS tag.

Following initial culture in W3110 cells to exponential growth phase, expression was induced by adding 100 µM arabinose to cell cultures containing vectors with a pBAD24 backbone or 10 µM IPTG to cell cultures containing vectors with a pET23/*ptac* backbone. Cells were harvested following 3 hours of protein expression and cell extracts prepared for PAGE, to visualise the expression capacity of each of the constructs.

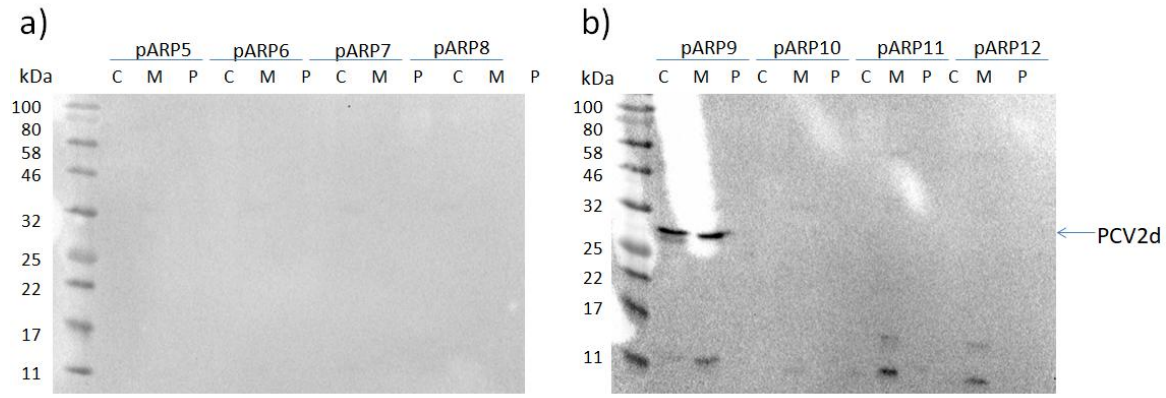

Figure 6. Anti-HIS western blots of cell fractions from BL21 cells expressing PCV constructs harvested following 3 hours growth post-induction in TB media. Cells expressing PCV constructs in either a) pBAD24 or b) pET23/*ptac* vectors were fractionated into cytoplasm (C), membrane (M) and periplasm (P). Fractions were separated by SDS PAGE before transfer to western blot. Arrows denote PCV2d species.

When PCV genes were expressed from pBAD24 vectors in *E. coli,* no proteins were detected in any cell fractions after immunoblotting. For most of the genes, it was a similar situation when expressed from pET23/*ptac* vectors, however OmpA-PCV2d-H6 protein was detected in both cytoplasm and membrane fractions at 30.8 kDa when expressed in a pET23/*ptac* vector. Despite this, there was no indication that any of the protein was being exported to the periplasmic space.

Following evidence of PCV2d expression, the next consideration was to determine whether the full length protein retained the capacity to oligomerise into VLPs. To analyse this, whole cell extracts from shake flask cultures expressing each construct were prepared and separated by either reducing SDS or native PAGE, then transferred to western blot and visualised by immunoblotting, with the aim of determining whether the protein was able to oligomerise through non-covalent bonds in the absence of a reducing agent.

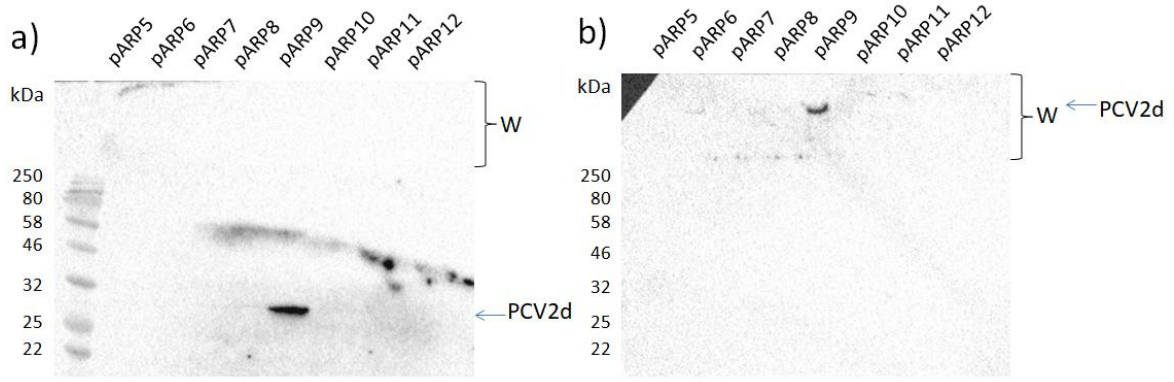

Figure 7. Anti-HIS western blots of whole cell extracts from BL21 cells expressing PCV constructs harvested following 3 hours growth post-induction in TB media. Cell extracts were separated by a) SDS PAGE and b) native PAGE before transfer to western blot. W: wells. Arrows denote PCV2d species.

Immunoblotting of samples separated by SDS PAGE showed detection of OmpA-PCV2d-H6 protein at monomeric size (30.8 kDa). The protein was also detected when immunoblotted following native PAGE, however under native conditions the protein did not migrate further than the wells of the SDS PAGE gel, indicating potentially an oligomer with a molecular weight of >250 kDa or aggregation.

As it had been shown that the expressed proteins were not able to be exported to the periplasmic space via the Sec pathway despite the addition of an OmpA signal peptide, the signal peptide sequence was removed from each construct so as to turn focus to maximizing the yield of protein that could be obtained from the cytoplasm.

Construct	**Backbone**	**Details**
pARP13	pBAD24	PCV2d-H6
pARP14	pBAD24	PCV3-H6
pARP15	pBAD24	PCV2d-GSGSG-PCV3-H6
pARP16	pBAD24	PCV2d-GSGSGSGSGS-PCV3-H6
pARP17	pET23/*ptac*	PCV2d-H6
pARP18	pET23/*ptac*	PCV3-H6
pARP19	pET23/*ptac*	PCV2d-GSGSG-PCV3-H6
pARP20	pET23/*ptac*	PCV2d-GSGSGSGSGS-PCV3-H6

Table 14. Second generation of PCV constructs.

Again, to analyze the tendency of the expressed Cap proteins to oligomerise into VLPs, whole cell extracts from shake flask cultures were prepared and separated by either reducing SDS or native PAGE, then transferred to western blot and visualised by immunoblotting.

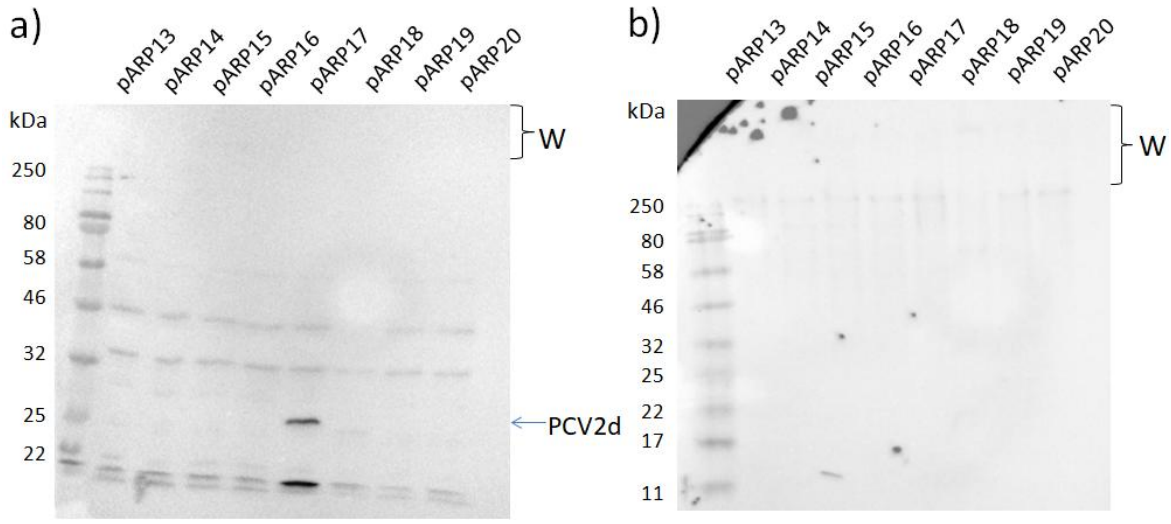

Figure 8. Anti-HIS western blots of whole cell extracts from BL21 cells expressing PCV constructs harvested following 3 hours growth post-induction in LB media. Cell extracts were separated by a) SDS PAGE and b) native PAGE before transfer to western blot. W: wells. Arrows denote PCV2d species.

With the OmpA signal peptide removed, it remained that the only construct to show detectable expression was PCV2d-H6, the product of which could be detected at monomeric size (28.8 kDa) by immunoblotting following SDS PAGE, as well as evidence of lower molecular weight bands within the sample also detected by the anti-HIS antibody (Fig. 8a). However, no trace of the protein could be detected when the same sample was separated under the conditions of native PAGE.

3.2.2 Truncation of the NLS region from PCV genes

A new generation of constructs were created with a truncation to the N-termini of both PCV genes, to remove the protein's NLS region but retain immunogenic epitopes. The 2-40 amino acid region of PCV2d sequence was removed based on reports in literature that this region may cause difficulty for heterologous expression in an *E. coli* host (Khayat et al., 2011), while the PCV3 amino acid sequence was aligned to PCV2d sequence to determine the position of the truncation.

Construct	Backbone	Details
pARP21	pBAD24	*Δ2-40* PCV2d-H6
pARP22	pBAD24	*Δ2-34* PCV3-H6
pARP23	pBAD24	*Δ2-40* PCV2d-GSGSG-*Δ2-34* PCV3-H6
pARP24	pBAD24	*Δ2-40* PCV2d-GSGSGSGSGS-*Δ2-34* PCV3-H6
pARP25	pET23/*ptac*	*Δ2-40* PCV2d-H6
pARP26	pET23/*ptac*	*Δ2-34* PCV3-H6
pARP27	pET23/*ptac*	*Δ2-40* PCV2d-GSGSG-*Δ2-34* PCV3-H6
pARP28	pET23/*ptac*	*Δ2-40* PCV2d-GSGSGSGSGS-*Δ2-34* PCV3-H6

Table 15. Third generation of PCV constructs.

The new constructs were expressed in BL21 cells in shake flask cultures and whole cell extracts separated by reducing SDS or native PAGE. Proteins were visualised by immunoblotting.

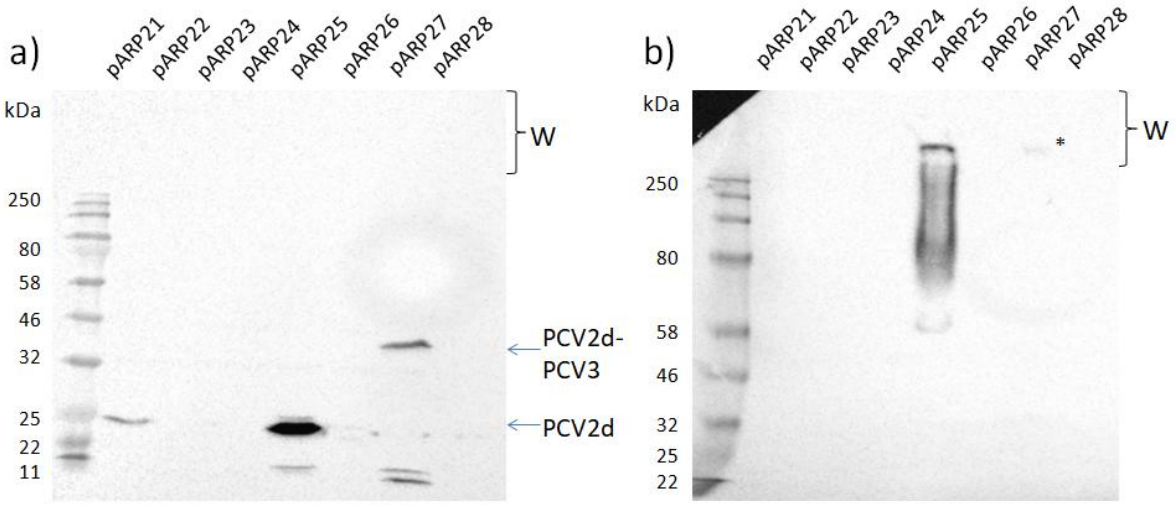

Figure 9. Anti-HIS western blots of whole cell extracts from BL21 cells expressing PCV constructs harvested following 3 hours growth post-induction in LB media. Cell extracts were separated by a) SDS PAGE and b) native PAGE before transfer to western blot. W: wells. Arrows denote PCV2d and PCV2d-PCV3. * denotes PCV2d-PCV3.

Immunoblotting data following SDS and native PAGE showed the first visible expression of PCV2d in the pBAD24 backbone vector as a result of the N-terminal 2-40 amino acid truncation (Fig. 9a); meanwhile, expression of PCV2d derived from the pET23/*ptac* backbone vector increased significantly as a result of the same truncation, but continued to show higher molecular weight oligomers when separated by native PAGE. Furthermore, the first visible expression of a PCV2d-

PCV3 chimera protein was also seen from the double NLS-truncated pARP27 construct (Fig. 9b, indicated by *). In addition to visualisation following SDS PAGE at its expected monomeric size, 44.6 kDa, lower molecular weight bands were also detected, whilst by native PAGE, the protein could only be detected in low amounts and at a high molecular weight of >250 kDa (Fig. 3.4b).

3.2.3 Investigating the effect of N-terminal truncation on protein solubility

Following successful expression of PCV2d and a PCV2d-PCV3 chimera, the next step was to investigate the solubility state of each of the products. The aim of this was two-fold: firstly, to determine which would be most suitable design to go forward with considering the ease of downstream processing; a soluble protein that was stable in conditions broadly representing the physiological state was desired, to minimise the processing steps in between protein extraction and administration to an animal as a finished vaccine. Secondly, whilst some of the expressed proteins had appeared at high molecular weights on native PAGE, the question still remained whether these oligomers were VLPs – consisting of soluble proteins – or protein aggregates consisting of insoluble proteins.

As such, all constructs that had successfully demonstrated visible protein production were again expressed at shake flask in BL21 cells. This time after the induction period, whole cell protein contents were harvested and then further separated into soluble and insoluble fractions and analysed by SDS PAGE.

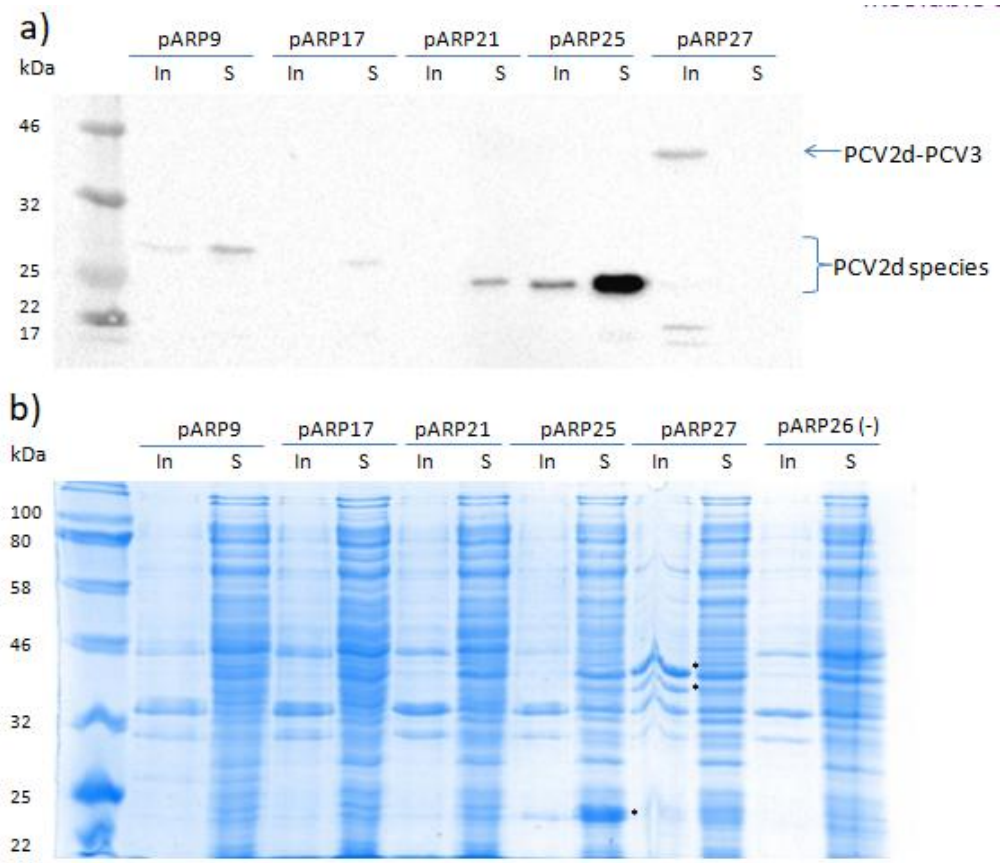

Figure 10. Visualisation of cell extracts from BL21 cells expressing PCV constructs harvested following 3 hours growth post-induction in LB media. Soluble and insoluble cell fractions were isolated and separated by SDS PAGE. Following this, they were visualised by a) Anti-HIS western blot and b) Coomassie Brilliant Blue. In: Insoluble; S: Soluble. Arrows denote PCV2d and PCV2d-PCV3 species. * indicates predicted species of PCV2d and PCV2d-PCV3. Extracts of cells expressing pARP26 plasmid were used as negative controls for the Coomassie stain (b) lanes 12-13.

Of the cells expressing PCV2d protein, the N-terminally-truncated construct pARP25 showed very high expression. The majority of the protein expressed solubly, with only a small proportion of insoluble protein (Fig. 10a). Meanwhile, the first expression of a PCV2d-PCV3 chimera was seen from pARP27 construct, although the product was entirely insoluble protein when visualised by anti-HIS immunoblot, and the full length protein was accompanied by an assortment of lower molecular weight peptides. The Coomassie stain gave further insights into pARP27 expression, visibly demonstrating at least two unique insoluble protein species not visible in the negative control, yet only one of these species was detectable by immunoblotting.

3.2.4 Improving PCV3 expression

Following on from the success of PCV2d expression and the first visible expression of a PCV2d-PCV3 chimera protein, attention was shifted to improving the expression of PCV3, which had so far been elusive. A further modification was made to the N-terminally truncated PCV3 and PCV2d-

PCV3 short linker constructs, truncating 20 amino acids from the C-termini of the PCV3 sequences.

Construct	Backbone	Details
pARP29	pET23/*ptac*	*Δ2-34, Δ195-214*PCV3-H6
pARP30	pET23/*ptac*	*Δ2-40* PCV2d-GSGSG-*Δ2-34, Δ195-214*PCV3-H6

Table 16. Double truncated PCV3 constructs.

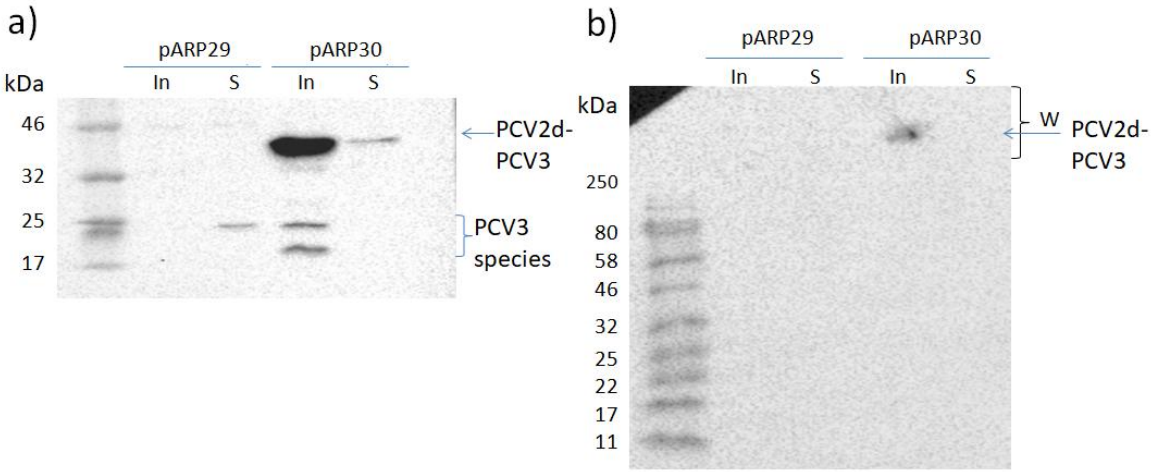

Figure 11. Anti-HIS western blots of cell extracts from BL21 cells expressing PCV constructs harvested following 3 hours growth post-induction in LB media. Soluble and insoluble cell fractions were isolated and separated by a) SDS PAGE and b) native PAGE then visualised by anti-HIS western blot. In: Insoluble; S: Soluble. W: wells. Arrows denote PCV species.

Immunoblotting of cell fractions from BL21 cells expressing the double truncated PCV3 gene showed the first visible detection of PCV3 protein by SDS PAGE (Fig. 11a, pARP29, S) at 19.4 kDa but was not visible on native PAGE. Likewise, the double truncated PCV2d-PCV3 chimera also showed a much higher level of detectable protein compared to previous versions of the chimera constructs and was visualised in large amounts in the insoluble cell fraction at 42.3 kDa by immunoblot following reducing SDS PAGE, with some protein also visible in the soluble cell fraction. The majority of the protein remained nonetheless insoluble, and appeared at a large molecular weight of >250 kDa when run by native PAGE (Fig. 11b) suggesting aggregation.

The PCV3 protein with genotype Δ2-34, Δ195-214PCV3-H6 (pARP29) would herein be referred to simply as PCV3, while Δ2-40 PCV2d-GSGSG-Δ2-34, Δ195-214PCV3-H6 chimera (pARP30) would be referred to simply as PCV2d-PCV3. An additional chimeric construct, pARP31, with the genotype Δ2-40 PCV2d-GSGSG-1-34, Δ195-214PCV3-H6 was also developed from PCV2d-PCV3, wherein the PCV3 starting methionine residue was removed in order to increase expression efficiency. This

construct would herein be referred to as PCV2d-ΔMetPCV3. Likewise, the PCV2d construct with genotype Δ2-40 PCV2d-H6 (pARP25) would be referred to simply as PCV2d.

3.2.5 Development of a fed-batch fermentation and purification process for PCV2d and PCV2d-PCV3 proteins

Now that an optimal PCV2d construct and expression system had been determined at shake flask level, showing a good level of expression and protein yield, the next step was to investigate whether this would translate to a larger scale expression system such as fed-batch fermentation, which would be the culturing method used for commercial production of the vaccine candidate.

The chosen pARP25 plasmid expressing PCV2d was transformed into BL21 or W3110 cells for fermentation and inoculated into 500 mL SM6 defined media in 1.5 L Minifors bioreactors.

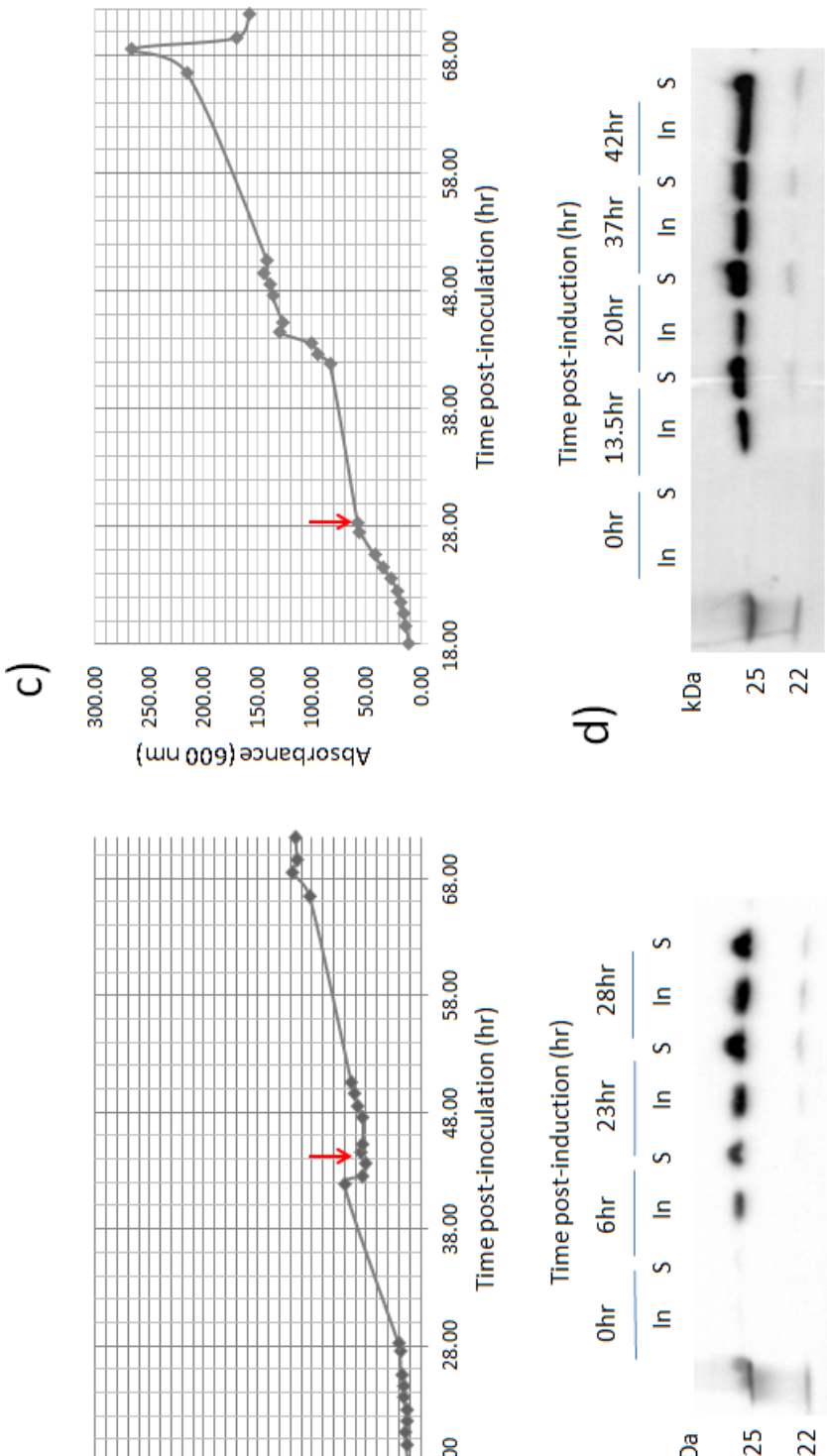

Figure 12. Fed-batch fermentation of *E. coli* BL21 and W3110 cell lines expressing PCV2d in SM6 media. After inoculation into the bioreactor, cells were cultured at 30 °C until shortly before induction when growth temperature was reduced to 25 °C. The pO_2 parameter was set at 30 % and the glycerol feed rate was set to 0.35 % of pump capacity using 80 % (w/w) glycerol. a) Growth curve of BL21 cells expressing PCV2d. At 28.25 hours following inoculation, airflow and stirring speed were manually increased to maximum. At 41.75 hours, glycerol feed was increased to 1 % of pump capacity. Cells were induced 44.5 hours following inoculation (0 hr P/I). b) Anti-HIS blot of W3110 cell samples taken at various timepoints during fed-batch fermentation. c) Growth curve of W3110 cells expressing PCV2d. Cells were induced 28.25 hours following inoculation (0 hr P/I) and were harvested 42 hours post-induction. To prepare samples for western blotting, cells were separated into insoluble and soluble fractions. Insoluble; S: Soluble. Red arrow indicates induction time.

Fed-batch fermentation of BL21 cells expressing PCV2d demonstrated a number of difficulties; growth of the cells began to stagnate on the second day after inoculation allthough it appeared to maintain a high dissolved oxygen concentration, and it was necessary to manually increase stirrer speed and airflow to increase oxygenation and continue growth. Despite this, the growth rate was very slow and was not at a suitable cell density to induce expression until 44.5 hours post-inoculation. Following induction, a reduction in optical density was observed so the glycerol feed rate was increased to 1 %. This was able to sustain slow growth for the remainder of the experiment but only reached a maximum culture OD_{600} of 119 at 39 hours post-induction (68 hours post-inoculation). On the other hand, the growth curve data indicated that the W3110 cells had responded very well to the culturing conditions used and the parameters in place, and the maximum culture OD_{600} reached 268 at 39 hours post-induction (68 hours post-inoculation), after which point the optical density began to drop rapidly indicating death phase so was harvested at a final culture OD_{600} of 158 at 42 hours post-induction. Based on this, the W3110 cell line was considered a more suitable choice for fed-batch fermentation experiments moving forward. Immunoblotting data from both cell lines indicated that whilst in shake flask culture the PCV2d protein expressed was almost entirely soluble, fractions from cells cultured in fed-batch fermentation showed that over 50 % of PCV2d protein was insoluble at all timepoints following induction (Fig. 12b, d).

The remaining proportion of soluble protein needed to be quantified, so a sample of the harvested W3110 fermentation culture was taken forward for purification by immobilized metal ion affinity chromatography (IMAC) using nickel-sepharose resin.

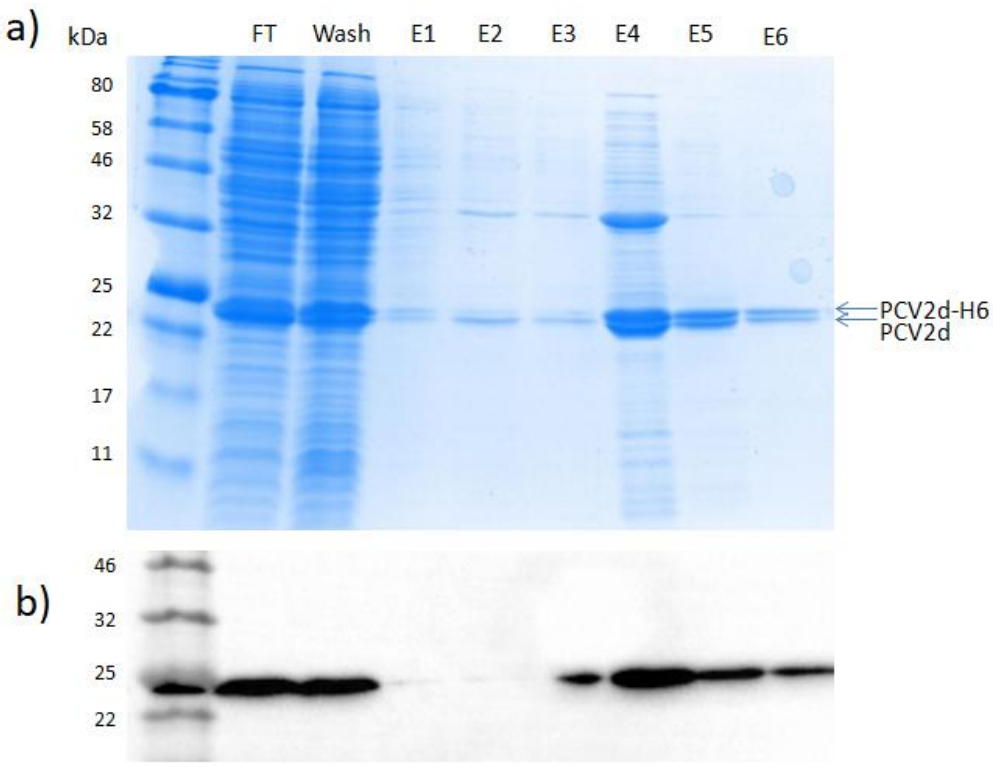

Figure 13. Purification of cell lysates from W3110 cells expressing PCV2d at fed-batch fermentation by IMAC. Following cell harvest at 42 hours post-induction, soluble cell proteins from 10 mL of culture were isolated by centrifugation and the supernatant applied to a 5 mL HisTrap™ column and the flow through collected (FT). The column was washed with buffer containing 20 mM imidazole (Wash) to remove impurities. After washing, proteins were eluted using a buffer containing 500 mM imidazole and collected by peak fractionation (E1-6). Following this, purified fractions were separated by SDS PAGE and visualised by a) Coomassie Brilliant Blue and b) anti-HIS western blot.

The results from IMAC showed the majority of PCV2d protein was eluted in fraction E4, although impure. A large amount of protein was also eluted in surrounding fractions, where E5 and E6 showed comparatively high purity. Calculation of the protein content in elution fractions using the equation [Concentration (M) = A280/ε], where the extinction coefficient for PCV2d protein was 34380 M/cm, indicated E4 fraction contained 2.06 mg/mL of protein where approximately 50 % was estimated to be PCV2d, and E5 fraction contained 0.99 mg/mL where approximately 95 % was estimated to be PCV2d. Interestingly, SDS PAGE showed a doublet of bands at around 23.4 kDa, the expected size for PCV2d (Fig. 13a, indicated by arrows) which appeared in equal proportion to each other, while immunoblotting with an anti-HIS antibody only displayed detection of one of these bands; at this stage, it was unclear whether this was a co-purifying

contaminant or an alternate species of PCV2d unrecognized by the antibody, although it was suspected to be a cleaved PCV2d species (this was later confirmed to be the case by mass spectrometry).

One major issue with this purification technique was that the peak elution fractions showed contamination with a very abundant higher molecular weight protein, along with an array of less abundant cellular proteins – it would require at least a second step of purification to obtain a sufficiently pure product to take forward for vaccine formulation. There was also some PCV2d protein lost in the flow through in the presence of a low concentration of imidazole, suggesting inefficient protein binding. In order to maintain a low processing cost especially at a large enough scale for commercial production, it was essential that purification of the PCV2d protein was kept to a minimum, ideally a single step, and that this purification method was inexpensive. For this reason, ion exchange was investigated as an alternative method to IMAC. Conveniently, the isoelectric point (pI) of the PCV2d protein including HIS tag was starkly different from the majority of native *E. coli* proteins, with a pI of 9.49, making cation exchange a very promising potential purification method.

Initially, a bench-top cation exchange (CIEX) method was trialled using an inexpensive resin packed into a homemade column. Soluble cell lysate from fed-batch fermentation cells expressing PCV2d was applied to the column under pH 7.0 conditions and following washing, proteins were eluted using a simple combination of buffers by a salt gradient increasing in 50 mM NaCl steps up to 1 M NaCl, over 20 column volumes.

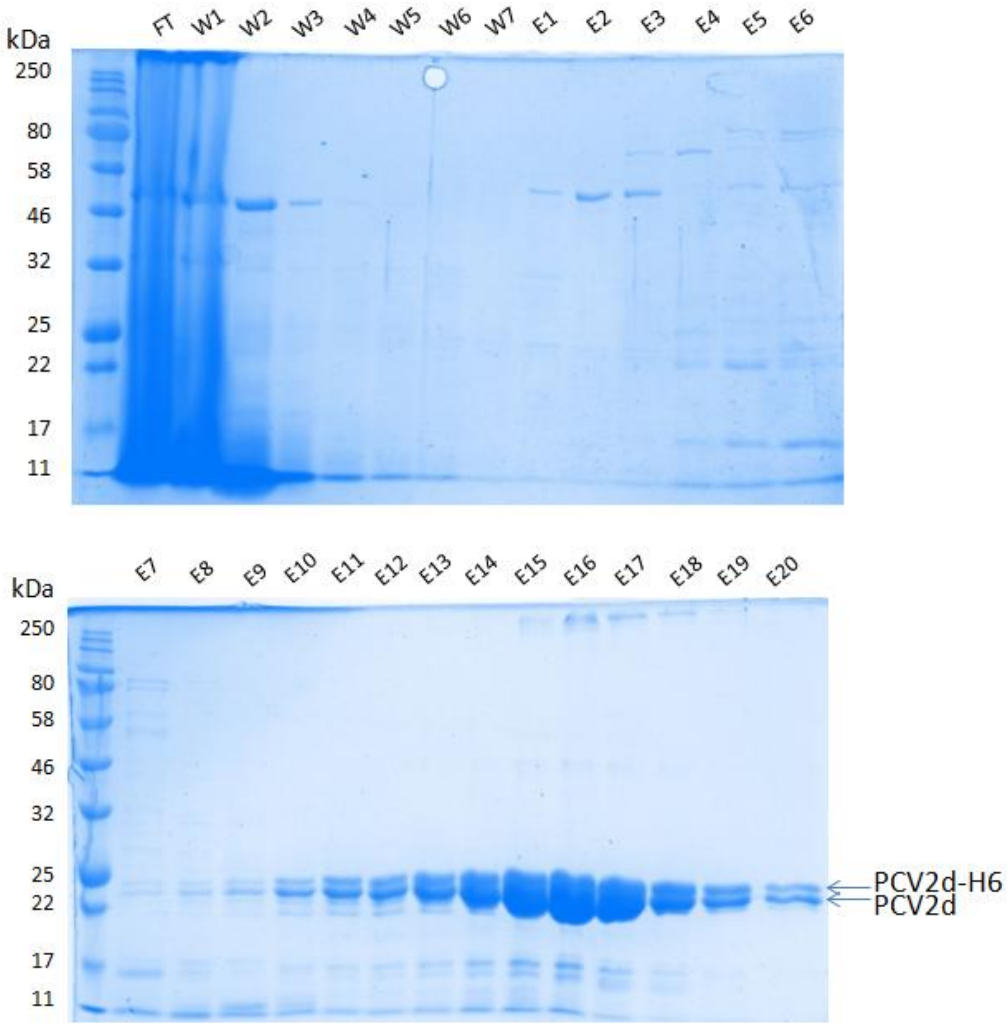

Figure 14. Purification of cell lysates from W3110 cells expressing PCV2d at fed-batch fermentation by bench-top CIEX. Following cell harvest at 42 hours post-induction, soluble cell proteins from 10 mL of culture were isolated by centrifugation and the supernatant applied to a bench-top column packed with SP Sepharose FF™ resin and the flow through collected (FT). The column was washed and fractions collected (W1-7). After washing, bound proteins were eluted using an increasing salt gradient at pH 7.0 and fractions collected (E1-20). Fractions were separated by SDS PAGE then visualised with Coomassie Brilliant Blue. Arrows denote PCV2d species.

SDS PAGE of fractions following bench-top CIEX demonstrated the vast majority of cellular proteins were removed in the flow through and early washes. Bands corresponding to PCV2d molecular weight (23.4 kDa) eluted in a large peak spanning E8 (400 mM NaCl) to E20 (1 M NaCl) where the largest concentration of protein appeared to be in E15 – E17. Elution fractions were analysed for protein content by Bradford Assay, and peak fractions E15 and E16 contained 1.466 mg/mL and 1.904 mg/mL of high purity PCV2d respectively. The overall yield of PCV2d protein

was estimated at 0.7 g/L of culture when combining this fermentation method and purification technique.

It was however noted that peak elution samples in a buffer containing over 500 mM NaCl particularly those with a protein concentration over 1 mg/mL tended to form protein precipitates that could not be resolubilised by mixing, especially if the sample had undergone a freeze-thaw cycle or been stored at 4 °C for longer than 24 hours. For this reason, it was necessary to either snap freeze highly concentrated protein samples quickly after collection or dilute them to a lower salt concentration prior to storage. A salt concentration of 150 mM was deemed optimal for these protein samples to prevent precipitation.

As observed previously when purifying by IMAC, a doublet of bands, or possibly more, consistently appeared closely around the expected size of PCV2d. A few lower molecular weight bands were also visualised consistently in peak elution fractions from CIEX, meanwhile later peak elution fractions E15 – E18 also showed a small amount of very high molecular weight protein at >250 kDa; it would require further investigation to determine whether these were impurities or PCV2d species. The first bench-top CIEX experiment had shown a large number of peak fractions containing PCV2d protein when eluting over 20 column volumes, and had yielded a relatively diluted product. In order to use for further analysis, a more concentrated product was necessary, so a two-step elution over a smaller volume was instead trialled. This time, following application of the sample and washing steps, a moderately concentrated salt buffer was applied to remove weakly bound contaminants from the column before applying a high salt buffer to elute PCV2d proteins into three 5 mL fractions. An elution sample was then analysed by mass spectrometry.

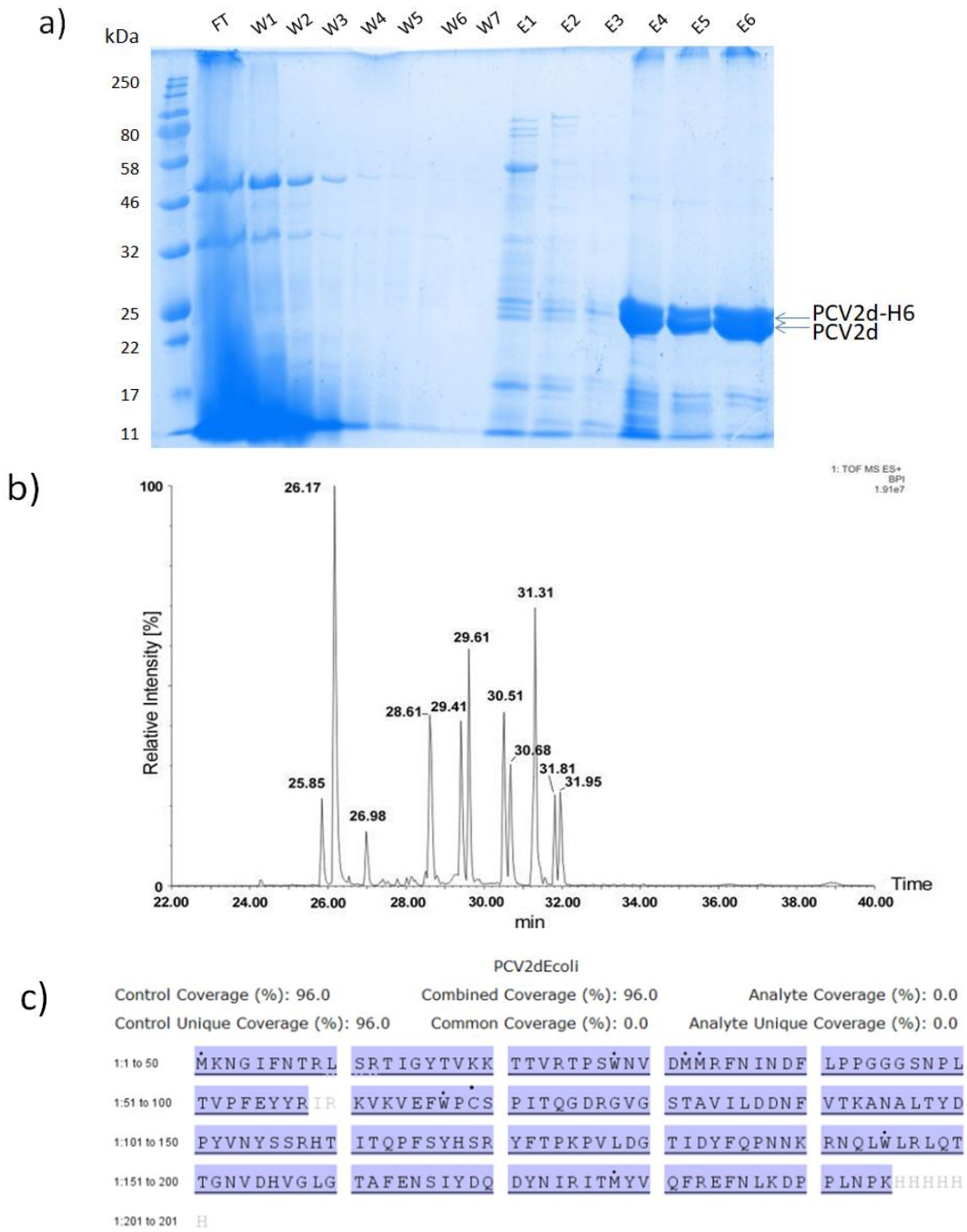

Figure 15. MALDI-TOF MS analysis of CIEX purified soluble cell contents isolated from W3110 cells expressing PCV2d protein in fed-batch fermentation. a) Purified fractions from bench-top CIEX were separated by SDS PAGE and visualised with Coomassie Brilliant Blue. Arrows denote PCV2d species. Following cell harvest, soluble cell proteins from 10 mL of culture were isolated by centrifugation and the supernatant applied to a column packed with SP Sepharose FF™ resin and the flow through collected (FT). The column was washed and fractions collected (W1-7). The column was washed using a 400 mM NaCl buffer (E1-3) at pH 7.0 then bound proteins eluted using a 950 mM NaCl buffer (E4-6) at pH 7.0. b) Electrospray ionization - liquid chromatography - mass spectrometry (ESI-LC-MS) chromatogram (base peak intensity) for CIEX fraction E6 after an

in-solution protease trypsin digestion with 1,4-Dithiothreitol and Iodoacetamide (DTT/IAM) for 12 hours. c) Peptide mapping of PCV2d protein in CIEX fraction E6.

Mass spectrometry of E6 elution fraction detected pure PCV2d protein in the sample and no native *E. coli* proteins were found to be present. Various sized peptides of PCV2d were detected but the predominant two species corresponded to a HIS-tagged and HIS-tag-cleaved PCV2d protein, which correlated with the SDS PAGE data where doublet bands were consistently visualised around PCV2d size in CIEX purified elution samples (Fig. 15a, indicated by arrows). Nevertheless, this data confirmed that CIEX was the best choice of purification technique to go forward with.

As this fed-batch fermentation and CIEX purification system had shown success for obtaining a good yield of pure PCV2d protein, the same techniques were applied to culture the PCV2d-PCV3 chimera protein. The pARP30 plasmid expressing PCV2d-PCV3 was transformed into W3110 cells for fermentation, again using SM6 defined media in a 1.5 L Minifors 2 bioreactor.

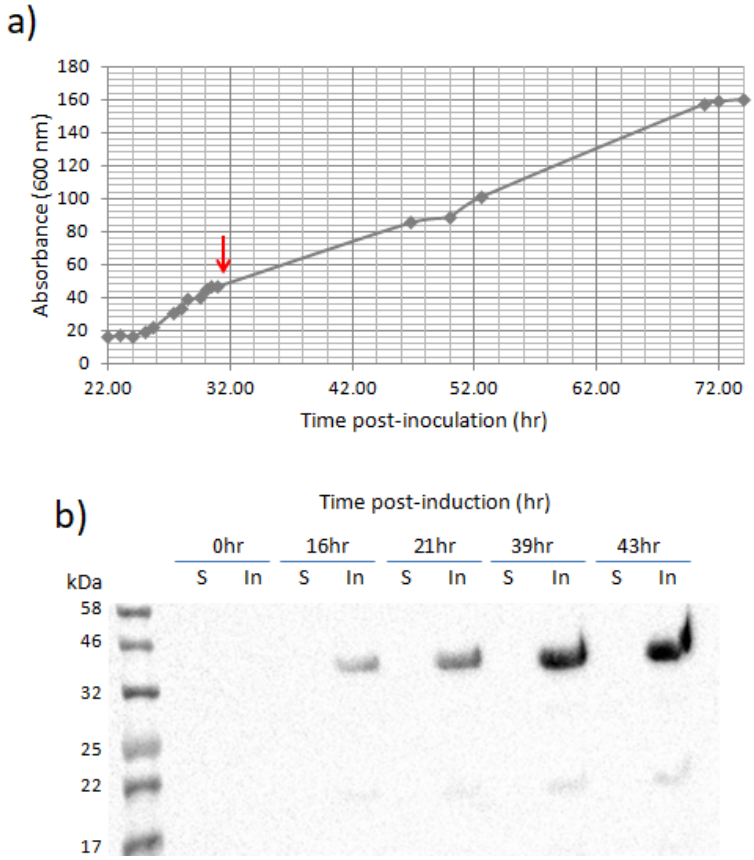

Figure 16. Growth data of W3110 cells expressing PCV2d-PCV3 protein in pET23/*ptac* vector at fed-batch fermentation. (a). Growth curve; after inoculation into the bioreactor, cells were cultured at 30 °C until shortly before induction when growth temperature was reduced to 25 °C. Cells were induced 31 hours following inoculation (0 hr P/I) and were harvested 43 hours post-induction. The pO_2 parameter was set at 30 % and the glycerol feed rate was set to 0.35 % of pump capacity using 80 % (w/w) glycerol. b) Anti-HIS blot of samples taken at various timepoints during fed-batch fermentation where cells were lysed by sonication then centrifuged at 14,000 rpm to separate insoluble and soluble proteins. In: Insoluble; S: Soluble. Red arrow indicates induction time.

Growth curve data from fed-batch fermentation of cells expressing PCV2d-PCV3 protein showed a slower growth rate compared to cells expressing PCV2d in the previous experiment and the maximum OD_{600} of the culture reached 160, in comparison to the maximum OD_{600} of 268 when expressing PCV2d protein alone. That said, the growth rate was steady throughout the experiment and did not indicate any signs of toxicity conferred by expression of the protein.

Immunoblotting using anti-HIS antibody demonstrated that all PCV2d-PCV3 protein (42.3 kDa) was detected in the insoluble cell fraction. Curiously however, there was an additional band in the insoluble cell fraction between 17-22 kDa detected by the anti-HIS antibody. This suggested the possibility of proteolytic cleavage of the chimera protein.

To elucidate the presence of possible protein cleavage species from the chimera protein, the soluble cell fraction isolated from 10 mL of W3110 cells expressing PCV2d-PCV3 in fed-batch fermentation was applied to a bench-top CIEX to investigate the contents.

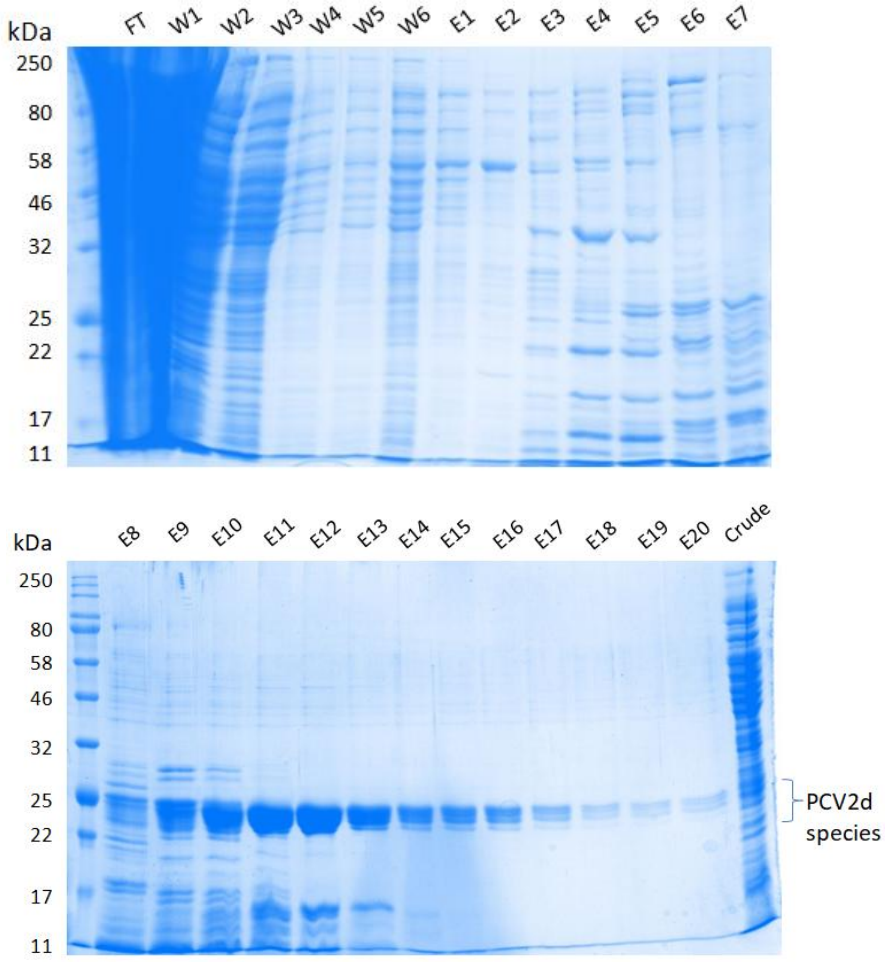

Figure 17. Purification of cell lysates from W3110 cells expressing PCV2d-PCV3 at fed-batch fermentation by CIEX. Following cell harvest, soluble cell proteins from 10 mL of culture were isolated by centrifugation and the supernatant applied to a column packed with SP Sepharose FF™ resin and the flow through collected (FT). The column was washed and fractions collected (W1-6). After washing, bound proteins were eluted using an increasing salt gradient at pH 7.0 and fractions collected (E1-20). A sample of the crude soluble cell lysate was used as a control. Proteins were separated by SDS PAGE and visualised with Coomassie Brilliant Blue. Bracket denotes protein species predicted to be PCV2d.

After purifying the soluble fraction from cells grown in fed-batch fermentation, SDS PAGE of CIEX elutions showed a large number of proteins of varying sizes removed using a low concentration salt buffer in E1-E7 (50-350 mM NaCl). A significant amount of protein corresponding to the size of PCV2d (22.6 kDa) eluted between E8 (400 mM NaCl) and E17 (850 mM NaCl) with numerous species around similar size, co-purifying along with a few smaller molecular weight proteins (Fig. 17, indicated by bracket). It was unclear from SDS PAGE whether any PCV3 protein (18.6 kDa) was present in the elutions. Nevertheless, although no full length PCV2d-PCV3 chimera protein could be visualised from the soluble cell lysate following CIEX purification, this suggested a novel potential method for generating soluble PCV2d protein, and could be advantageous as a dual vaccine candidate if PCV3 peptides could also be detected in eluted fractions.

To investigate what regions of the protein were susceptible to proteolytic digestion and to determine whether any PCV3 peptides were present following purification, two of the elution fractions from CIEX were sent to Anja Krueger at Imperial College London for mass spectrometry analysis.

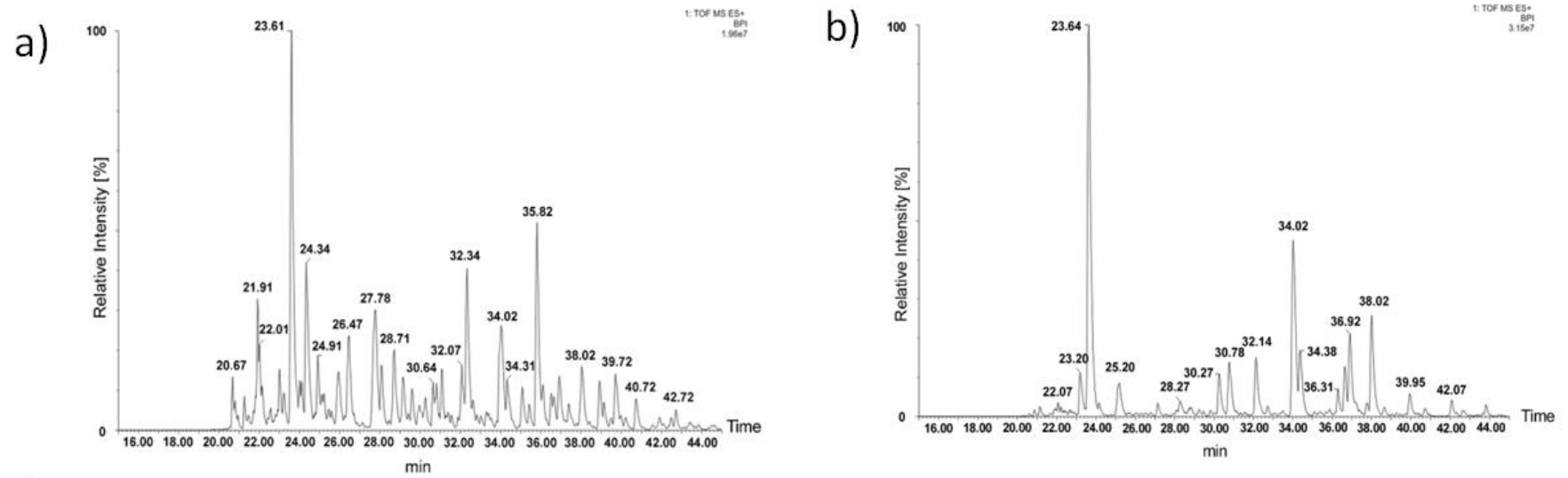

Figure 18. MALDI-TOF MS analysis of CIEX purified soluble cell contents isolated from W3110 cells expressing PCV2d-PCV3 protein in fed-batch fermentation. Following purification using a bench-top column packed with SP Sepharose FF™ resin, elution fractions E8 and E10 were analysed by mass spectrometry. a) ESI-LC-MS chromatogram (base peak intensity) for CIEX fraction E8 after an in-solution protease trypsin digestion (DTT/IAM, for 12 hours). b) ESI-LC-MS chromatogram (base peak intensity) for CIEX fraction E10 after an in-solution protease trypsin digestion (DTT/IAM, for 12 hours). c) Peptide mapping of PCV2d protein sample E8. d) Peptide mapping of PCV2d protein sample E10.

Mass spectrometry of cation exchange purification elution fractions from cells expressing PCV2d-PCV3 showed co-elution with a range of *E. coli* ribosomal proteins, which have a similar pI to the PCV proteins. Peptide mapping was able to demonstrate that the majority of the full length chimera protein was being cleaved around or shortly after the linker region; analysis of CIEX fractions E8 and E10 both showed clear detection of peptides up until K208 residue of the chimeric protein, early within the PCV3 protein sequence, but peptides detected after this point were distinctly absent. This cleavage appeared to liberate a large amount of PCV2d protein as seen in CIEX elution fractions by SDS PAGE. Three peptides of PCV3 were identified by mass spectrometry, namely the peptide -MAGTTYK located up to residue 208 of the chimera protein (peptide A), VMTSK peptide at position 301-305 (peptide B), and VTLSPVISPAQQTK peptide between residues 255-268 (peptide C) which was detected in fraction E8 but not E10, likely due to its pI. It is interesting to note that all three of these cleaved peptides contained a K residue immediately before the cleavage site, while peptides B and C both contained a K residue immediately after the cleavage site. Despite this, the intact PCV3 amino acid sequence as expressed in the chimera protein was not detectable in any soluble cell fractions analysed by mass spectrometry following fed batch fermentation.

3.2.6 Generation of a specific PCV2d antibody

Experiments to detect expression of PCV2d-PCV3 chimera protein using a HIS tag-specific antibody had so far indicated that there may be a number of cleavage peptides present, suggesting the protein was potentially unstable and susceptible to degradation. To detect these peptides, PCV2d and PCV3-specific antibodies would be required for immunoblotting.

Thus, a commercial PCV2a antibody was sourced from Biorbyt (Cambridge, UK) and used to probe western blots containing samples of lysates from cells expressing pARP25, pARP27, pARP29 and pARP30 constructs to test the antibodies' capability to detect the PCV2d protein at varying expression levels.

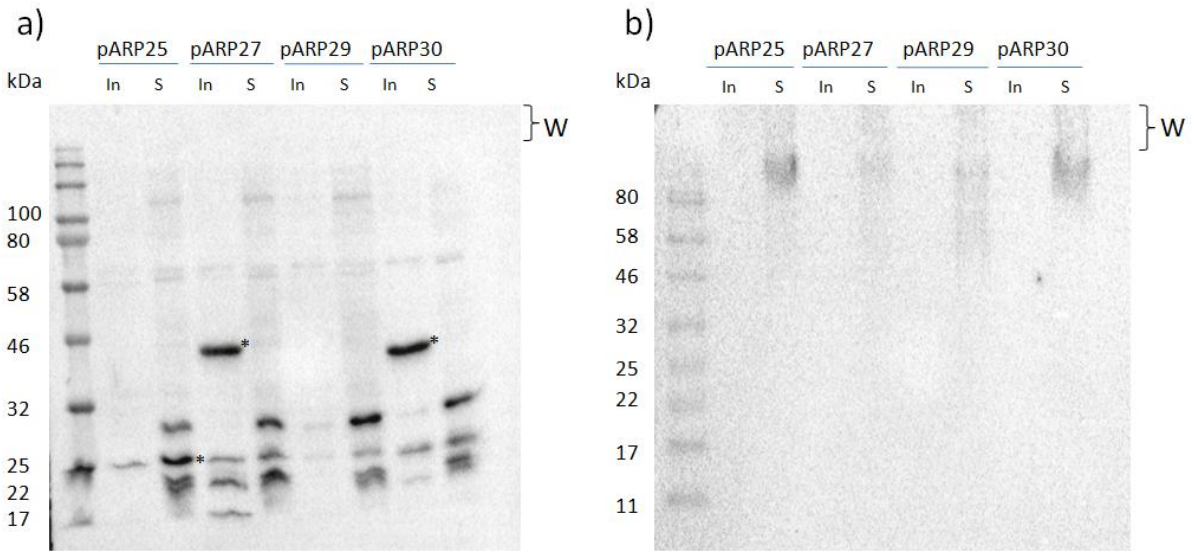

Figure 19. Anti-PCV2a western blot using commercial antibody. Following 3 hours growth post-induction in LB media, soluble and insoluble cell extracts from BL21 cells were harvested and separated by a) SDS PAGE and b) native PAGE then immunoblotted using Biorbyt anti-PCV2a antibody. In: Insoluble; S: Soluble. * indicate predicted PCV2d and PCV2d-PCV3 species.

PCV2d protein was detected in both soluble and insoluble cell fractions at 23.4 kDa following reducing SDS PAGE when expressed in pARP25 construct. PCV2d-PCV3 proteins expressed from pARP27 and pARP30 constructs were visualised in the insoluble cell fractions at 44.6 kDa in pARP27 insoluble fraction, and 42.3 kDa in pARP30 insoluble fraction by SDS PAGE. Proteins could only be detected in the soluble cell fractions following native PAGE, and all appeared at a large molecular weight of >80 kDa. Immunoblotting using the commercial PCV2a antibody showed detection of a larger range of protein bands following SDS PAGE in comparison to the HIS antibody. However, the majority of the soluble cell lysates showed a remarkably similar banding pattern, including in the PCV3 only samples (Fig 19a, pARP29 In; S). A significant number of less intense proteins bands were also detected in all cell lysate samples following SDS PAGE.

As the commercial antibody had not showed the desired level of protein specificity, a preparation of purified soluble PCV2d protein was transferred to Cambridge Research Biochemicals in order to raise a specific antibody. To achieve this, two rabbits, CRB393 and CRB392, were each immunised with 0.1 mg of the PCV2d antigen at weeks 1, 3, 5, 7 and 9. Blood samples were taken at weeks 4, 6 and 8 (test bleeds 1, 2 and 3 respectively) and the final harvest bleed was obtained at week 10. Samples of test bleeds were transferred periodically for antibody specificity testing by western

blotting using a range of test samples and controls. As a starting point, all serum samples were used at a dilution of 1 in 10,000 in *PBST* (PBST) for immunoblotting.

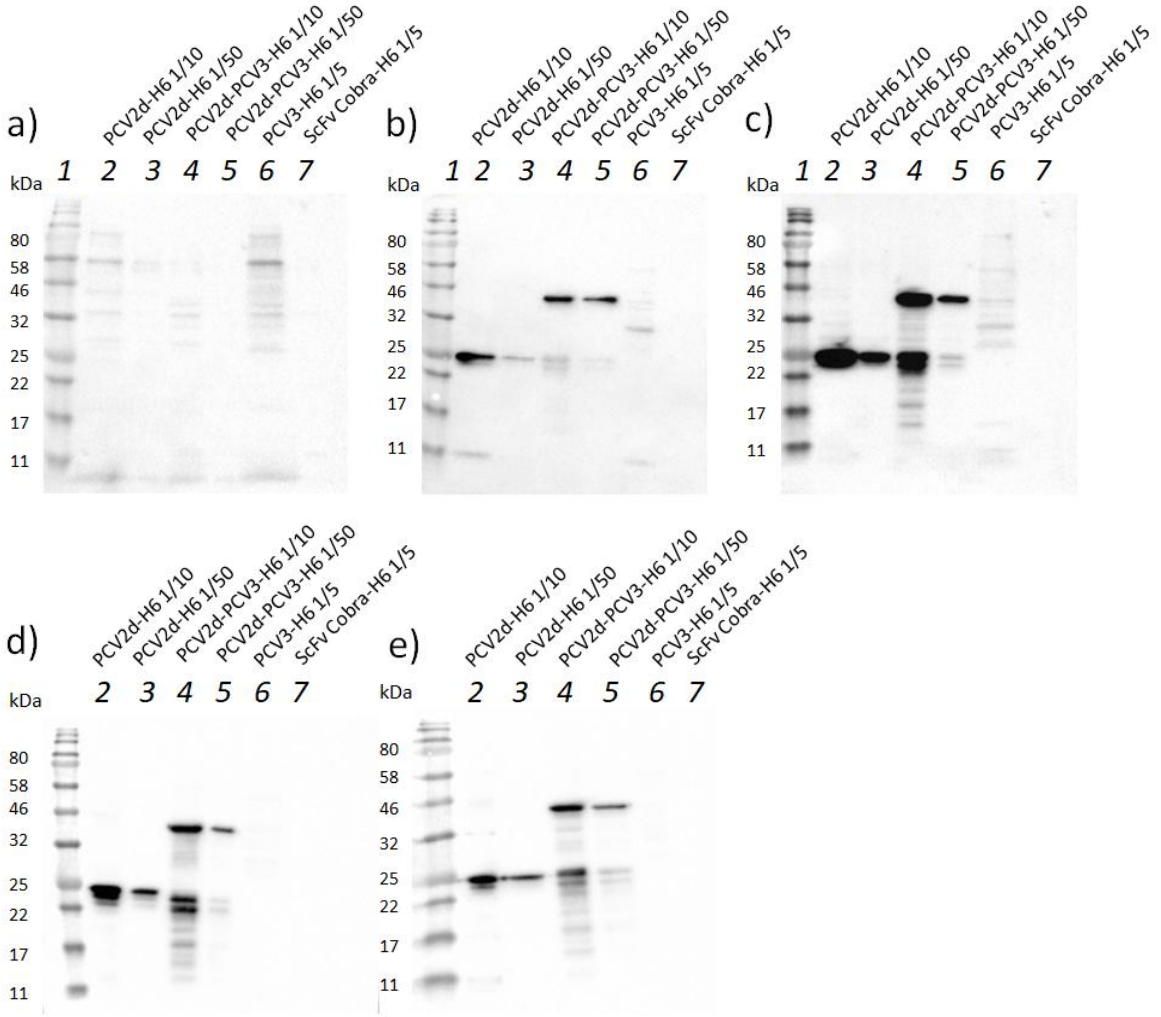

Figure 20. Western blots using test serum from CRB393 rabbit immunised with PCV2d protein. After blocking in 5 % milk with PBST, blots were incubated in a) pre-immune serum; b) test bleed 1; c) test bleed 2; d) test bleed 3; e) harvest bleed. Following this, blots were incubated in anti-rabbit secondary antibody. Lane 1: Protein marker; lane 2: Soluble fraction from *E. coli* cells expressing PCV2d-H6, 1/10 dilution; lane 3: As lane 2, 1/50 dilution; lane 4: Insoluble fraction from *E. coli* cells expressing PCV2d-PCV3-H6, 1/10 dilution; lane 5: As lane 4, 1/50 dilution; lane 6: Soluble fraction from *E. coli* cells expressing PCV3-H6, 1/5 dilution; lane 7: Periplasmic fraction from *E. coli* cells expressing ScFv-Cobra-H6, 1/5 dilution (negative control).

Per-immune serum from rabbit CRB393 showed no detection of PCV peptides and only a small amount of non-specific binding when used for immunoblotting. Test bleed serum from this rabbit

began to show high specificity for PCV2d peptides as early as test bleed 1, taken at 4 weeks after immunisation with the PCV2d antigen, which was evidenced by its detection of PCV2d proteins in by immunoblotting (Fig. 20b, lanes 2-5). Serum from test bleed 3 and the harvest bleed showed a very high degree of specificity and affinity, with virtually no background protein detection. None of the test bleed sera showed any non-specific binding to an unrelated HIS-tagged protein, ScFv-Cobra. This indicated the PCV2d antigen used for immunisation had been very successful in raising a strong antibody response.

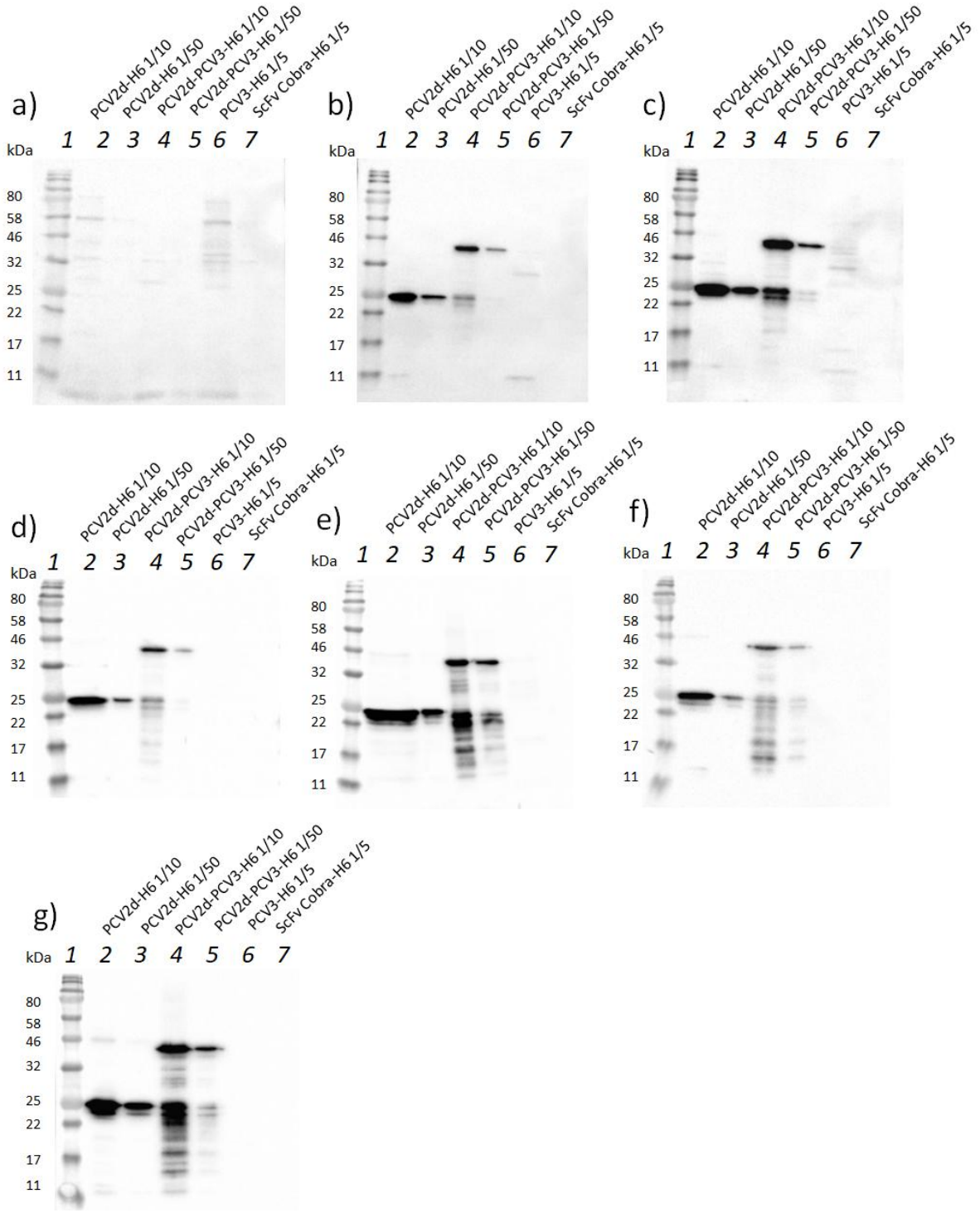

Figure 21. Western blots using test serum from CRB392 rabbit immunised with PCV2d protein. After blocking in 5 % milk with PBST, blots were incubated in a) pre-immune serum; b) test bleed 1; c) test bleed 2; d) test bleed 3; e) harvest bleed; f) purified antibody eluate 1; g) purified antibody eluate 2. Following this, blots were incubated in anti-rabbit secondary antibody. Lane 1: Protein marker; lane 2: Soluble fraction from *E. coli* cells expressing PCV2d-H6, 1/10 dilution; lane 3: As lane 2, 1/50 dilution; lane 4: Insoluble fraction from *E. coli* cells expressing PCV2d-PCV3-H6, 1/10 dilution; lane 5: As lane 4, 1/50 dilution; lane 6: Soluble fraction from *E. coli* cells expressing PCV3-H6, 1/5 dilution; lane 7: Periplasmic fraction from *E. coli* cells expressing ScFv-Cobra-H6, 1/5 dilution (negative control).

Similarly to CRB 393, serum from CRB 392 rabbit also showed high specificity for PCV2d proteins when used for immunoblotting as early as tests bleed 1, and there was also no non-specific binding to unrelated HIS-tagged protein, ScFv-Cobra. Following comparison of test bleeds 1, 2 and 3 from both rabbits, CRB 392 rabbit was determined to have the highest titre of specific antibody and the harvest bleed taken forward for antibody purification by PCV2d-coupled NHS-activated sepharose affinity chromatography. Of the two elution steps, eluate 2 which used a pH 10.5 glycine buffer to elute, contained a significantly higher concentration of antibody, at 2.48 mg/mL, compared with eluate 1 which used a pH 2 TEA buffer to elute, and contained only 0.31 mg/mL antibody concentration. Upon imaging western blots probed using a 1 in 10,000 dilution of eluate 2 in PBST, bands appeared saturated after only a few seconds exposure following application of chemiluminescence solution. Further optimization experiments were performed to investigate the most appropriate concentration of purified eluate 2 for immunoblotting.

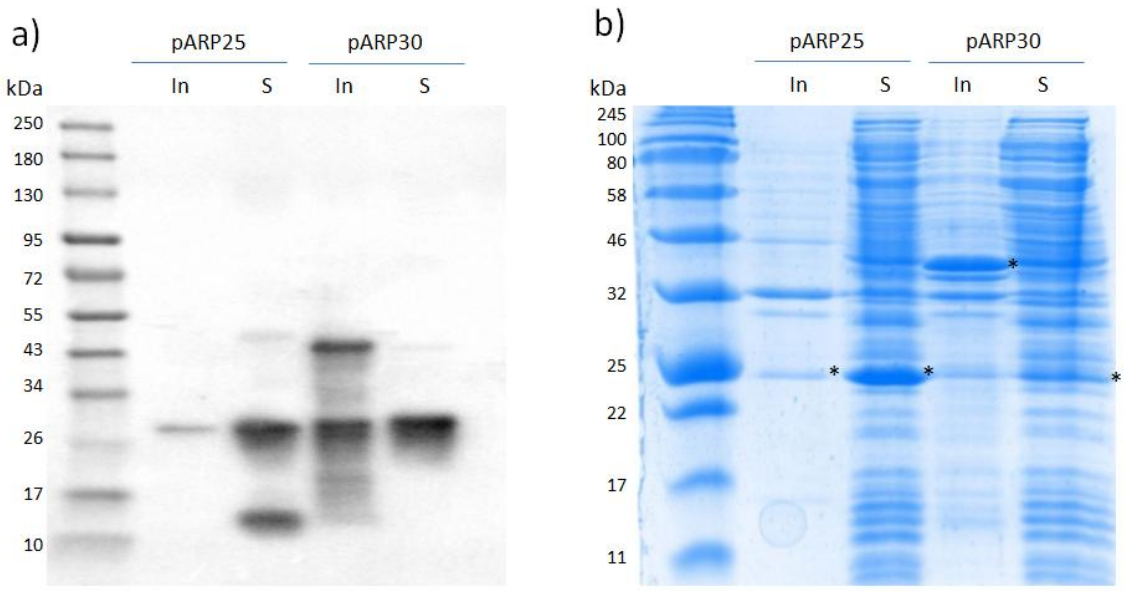

Figure 22. Anti-PCV2d western blot using purified antibodies from rabbit CRB 392. Soluble and insoluble cell fractions were isolated from BL21 cells expressing PCV2d and PCV2d-PCV3 chimera proteins and were harvested following 3 hours growth post-induction at shake flask level in LB media. Proteins were then separated by SDS PAGE and visualised by anti-PCV2d western blot at 1/2,000,000 dilution in PBST. For comparison of specificity, an SDS PAGE gel containing the same samples was stained with Coomassie Brilliant Blue to visualise native *E.coli* proteins present in the samples. In: Insoluble; S: Soluble.

When immunoblotting using a 1 in 2,000,000 dilution of purified anti-PCV2d eluate 2 as primary antibody, it was able to detect a range of bands in the insoluble fraction from cells expressing PCV2d-PCV3 chimera protein (Fig. 3.17a. pARP30, In) and a very small amount of full-length chimeric protein in the soluble fraction (Fig. 22a. pARP30, S) without causing overexposure of the blot. Overall, it was determined that a dilution of 1 in 2,000,000 purified eluate 2 in PBST was the most effective working concentration for detection of PCV2d proteins in cell lysates.

3.2.7 Testing the capability of recombinant truncated PCV2d to raise neutralising antibodies

While it was evidenced by western blotting data that PCV2d antigen was able to raise a strong antibody response when immunised into rabbits, it was necessary to investigate whether the serum also contained neutralising antibodies, capable of neutralising the live PCV2d virus in order to protect cells from infection in the porcine host. Successful virus neutralising activity would be essential in order for this design to be considered for use as a vaccine.

Serum from CRB 392 and CRB 393 rabbits before immunization with the PCV2d antigen (pre-immune serum) and following all four immunisations with the antigen over the 10 week period (test bleed 1, test bleed 2 and harvest bleed) were transferred to Biotec (Thailand) to test for the presence of antibodies with PCV2d virus-neutralising capacity in an *in vitro* cultured porcine kidney (PK-15) cell line by cell-based virus neutralisation assay. As detailed in chapter 2, DAPI stain was used to identify cell nuclei and the numbers of infected cells identified by concurrence of DAPI- and Alexa488-positive nuclei were scored on a high-content screening system. Fluorescent background signal (green) that does not coincide with DAPI staining (blue) was not counted as infected cells. Using the scored number of infected cells, percent infection was then plotted.

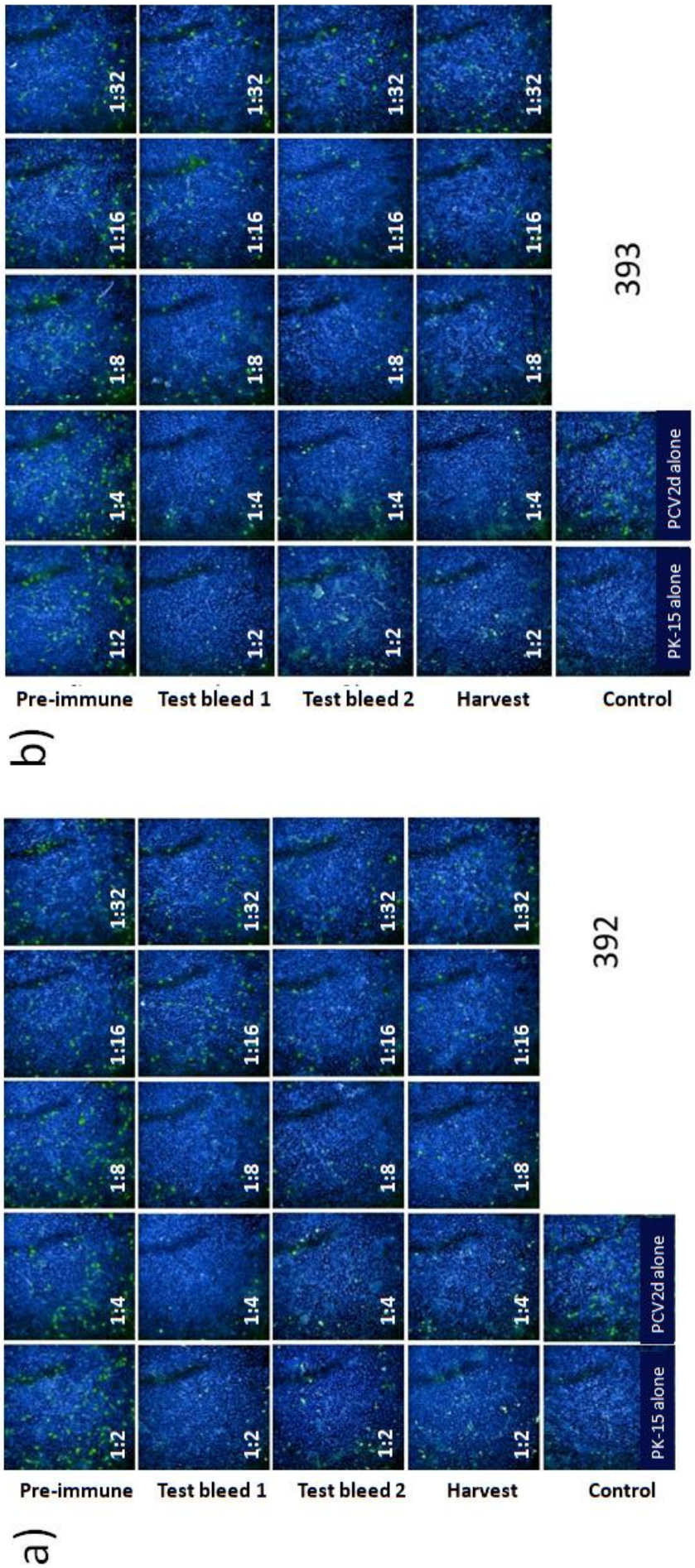

Figure 23. Immunofluorescence viral neutralisation assay using PK-15 cells with PCV2d-immunised rabbit serum. Serum taken from a) CRB 392 or b) CRB 393 rabbit was mixed with PCV2d virus particles, using undiluted serum or serum diluted to a ratio of 1:2, 1:4, 1:8, 1:16 or 1:32, then infected into PK-15 cells. Following incubation, PK-15 cell cultures were probed with immunofluorescent Alexa488-labelled anti-rabbit antibody to detect PCV2d infected cells indicated by green fluorescent foci. Controls were performed using uninfected PK-15 cells (PK-15 alone), by mixing pre-immune rabbit serum with PCV2d virus particles prior to PK-15 cell infection (Pre-immune) and by infecting PK-15 cells with PCV2d virus particles not mixed with rabbit serum (PCV2d alone).

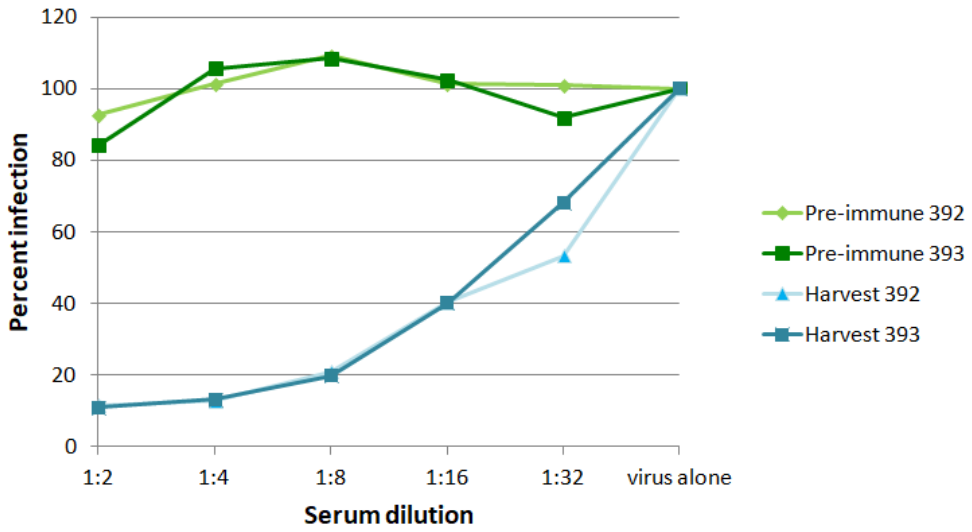

Figure 24. Percentage infection of PK-15 cells with PCV2d virus following incubation with rabbit serum. Immunofluorescence data from cell-based virus neutralisation assay testing pre-immune, test bleed 1, test bleed 2 and harvest bleed serum from both rabbits CRB 392 and CRB 393 were plotted. Where PK-15 cells had been infected with PCV2d virus particles not mixed with rabbit serum (virus alone), this was used as the value for 100 % infection.

Serum from rabbit CRB 392 showed a strong protective effect against PCV2d virus in the immunofluorescent virus neutralisation assay (Fig. 23a); test bleed 1 taken following only 2 immunisations with PCV2d antigen began to show a strong protective effect against PCV2d viral infection conferred to the treated PK-15 cells, where dilutions of 1:2, 1:4 and 1:8 showed a very low number of infected cells (green foci). Test bleed 2, taken after 3 immunisations with PCV2d antigen, showed a protective effect at all dilutions tested. Treatment with harvest bleed serum showed a comparable number of infected cells to test bleed 2 serum. Meanwhile, immunofluorescence data generated using serum from rabbit CRB 393 showed less protection against PCV2d virus compared to equivalent CRB 392 serum samples, showing a slightly higher number of infected cells when test bleeds were used at 1:32 dilution (Fig. 23b). Graphical representation of percentage infection showed a clear virus neutralising effect conferred by harvest bleed serum from both rabbits (Fig. 24). Overall these results were incredibly promising and demonstrated that immunisation with the purified PCV2d antigen was able to induce a strong neutralising response.

3.3 Conclusions

Construct optimization experiments testing multiple generations of vector designs discovered that pET23/*ptac* medium copy vector was able to provide a high expression level of codon optimized, truncated PCV genes. Truncation of the NLS region proved to make a significant improvement to

the expression capacity of both PCV2d and PCV3 genes and expression experiments showed the optimized genes could be expressed consistently in large amounts in BL21 cell line at shake flask level.

Initial culture showed that when PCV2d was expressed in a pET23/*ptac* vector in BL21 cell line at shake flask, large amounts of soluble PCV2d expression could be achieved when using complex media, LB. The PCV2d protein showed little evidence of instability or degradation but the protein showed a tendency to oligomerise into structures exceeding 250 kDa in weight, which was reliably demonstrated by native PAGE data. In fed-batch fermentation when using SM6 minimal defined medium, the high expression level had no apparent detrimental effect on W3110 cell viability and it was possible to obtain an OD_{600} of 268 corresponding to approximately 180 g/L of wet biomass after 42 hours cultivation in a 1.5L Minifors 2 fermenter with continuous glycerol feed rate. Upon purification by CIEX, a total of 0.7 g of highly pure PCV2d protein per litre of culture was obtained. PCV2d protein purified by CIEX demonstrated the capability to raise a specific immunoglobulin in rabbits with very high affinity and neutralising activity in a PK-15 cell-based assay. It was decided a good option to take forward for downstream processing optimization as the first viable vaccine candidate.

Expression of optimized PCV2d-PCV3 in a pET23/*ptac* vector in BL21 cell line at shake flask also showed a high expression level. However, the chimeric protein was for the most part insoluble; native PAGE data detected structures exceeding 250 kDa in weight in these samples, suggested these proteins may form aggregates or inclusion bodies when expressed to a high level. Although expression of the chimeric proteins at fed-batch fermentation did slow the growth rate of W3110 cells compared to those expressing PCV2d alone, there appeared to be no detrimental effect on viability. Purification of the soluble extract from cells expressing PCV2d-PCV3 chimera proteins by CIEX provided a novel method of purifying high yields of PCV2d protein with peptides of PCV3 present.

Chapter 4: Development of a dual-protective PCV2d-PCV3 vaccine candidate

4.1 Introduction

In chapter 3, it was demonstrated that truncation of both PCV2d and PCV3 Cap N-termini in a chimeric protein was able to facilitate expression of a chimeric protein with flexible 60 % Gly glycine–serine linker containing 5 residues (-GSGSG-), but not a 50 % Gly glycine-serine linker containing 10 residues (-GSGSGSGSGS-). However, the PCV2d-PCV3 chimera was highly insoluble, probably forming inclusion bodies. The linker region could be playing an important role in the folding capacity of the two proteins and thus the chimera's solubility potential, but the functional properties facilitating this needed to be investigated. Some studies have found small, polar amino acids such as glycine (G), serine (S) and threonine (T) can provide good flexibility when the joined domains require a certain degree of movement or interaction; inclusion of these residues can maintain the protein's stability in aqueous solutions by forming hydrogen bonds with water molecules, reducing unfavourable interactions between the linker and the protein moieties (Argos, 1990; George & Heringa, 2002). However, there are examples in the literature where the use of flexible linkers resulted in poor expression yields or loss of biological activity, which was attributed to an inefficient separation of the protein domains to minimize their interference with each other (Amet et al., 2008). Rigid linkers have been utilized to solve this problem as a fixed distance between the domains can help to maintain their independent functions, typically containing proline (P) and glutamic acid (E) residues. Linkers containing proline residues have a very restricted conformation due to proline's cyclic side chain and its lack of amide hydrogen group may prevent the formation of hydrogen bonds with other amino acids therefore reducing the interaction between the linker and the protein domains (Williamson, 1994); meanwhile, polar glutamic acid residues may help to aid solubility through formation of salt bridges (Argos, 1990). Alternatively, alpha helix-forming linkers have been found to separate functional domains more effectively than non-helical linkers due to their low flexibility (Arai et al., 2001) and are frequently present in naturally occurring proteins (George & Heringa, 2002), suggesting they are relatively stable structures. The degree of separation between domains can be modulated by inclusion of regions containing repeating glutamic acid and lysine (K) residues to promote the formation of salt bridges, stabilizing the alpha helical conformation.

In this chapter, the functional properties of the chimeric protein linker were investigated as a potential way to increase soluble expression of a chimeric PCV2d-PCV3 protein for formulation as a dual vaccine candidate. The effect of growth temperature on solubility was also investigated for this purpose. Alternate methods of processing an inclusion body protein are also presented, yielding a denatured, solubilised PCV2d-PCV3 protein for downstream processing to raise a PCV3-specific antibody.

4.2 Results

4.2.1 Designing an optimal linker region for expression of full length PCV2d-PCV3 chimeric protein

Since the utilisation of anti-PCV2d serum for immunoblotting in Chapter 3, it had become clear that the PCV2d-PCV3 chimeric proteins had been subject to a large amount of proteolytic cleavage particularly within the linker region, resulting in the majority of the protein existing as smaller peptide species. It was also suspected the proteins were aggregating to form insoluble inclusion bodies which would be difficult to process downstream. The construct design of the chimera protein was reassessed, with the aim to increase stability and solubility of the resulting protein product by altering the level of folding interactions between the two proteins.

Using pARP31 as a template, which contained a short and flexible 60% Gly linker (-GSGSG-), a range of five new constructs was designed with variations in the properties of their linker regions. The first new construct pARP34 contained a short 80% Gly linker (-GGGGS-). The pARP35 construct was designed to use a short, rigid non-helical linker (-EPEPEP-); pARP36 contained a short, rigid alpha helical linker (-EAAAK-), whilst pARP37 used a longer variation of the rigid alpha helical linker (-AEAAAKALEAEAAAKA-). Finally, for pARP38 construct the linker peptide was removed altogether, fusing the PCV2d and PCV3 proteins together directly.

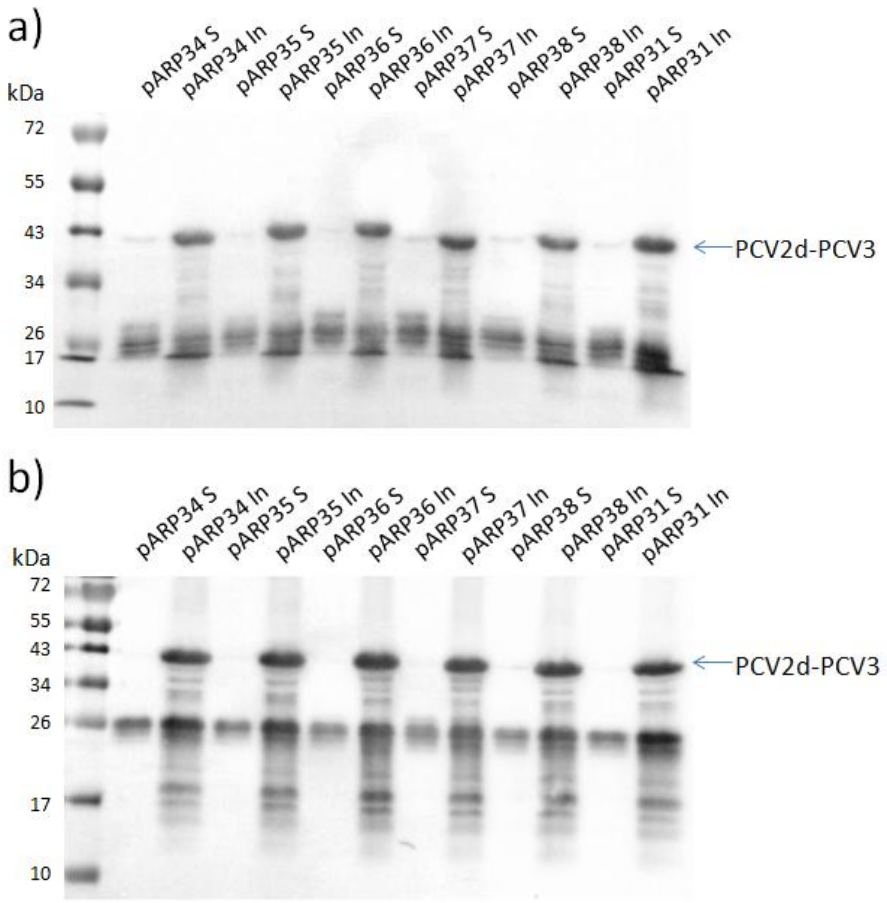

Figure 25. Anti-PCV2d western blots of cell fractions from BL21 cells expressing PCV2d-PCV3 constructs. Five new PCV2d-PCV3 chimeric constructs with differing linker regions (pARP34 – pARP38) alongside the original control construct pARP31 were expressed in LB media then cells were harvested after a) 3 hours and b) 21 hours growth post-induction in LB media. Soluble and insoluble cell fractions were isolated and separated by SDS PAGE before transferring to western blot. In: Insoluble; S: Soluble.

Immunoblotting using anti-PCV2d antibody showed a small amount of soluble full length protein was visible in all constructs after 3 hours expression, but the majority of protein remained insoluble or had been degraded to yield smaller PCV2d peptides. There was no increase in soluble product in constructs pARP34-pARP38 compared to pARP31 containing the original linker (Fig. 25a). After 21 hours expression, a larger yield of protein had been obtained but almost entirely existing in insoluble form for all constructs (Fig. 25b). A large amount of cleaved peptides smaller than the full length protein were still detected in all constructs and this was particularly noticeable after 21 hours expression.

4.2.2 Solubilisation and denaturation of PCV2d-PCV3 chimeric protein inclusion bodies

A range of angles to optimise the gene and vector constructions of PCV2d-PCV3 had now been tested in the interests of producing a soluble, full length chimeric protein product, but these had so far yielded few promising results. It was strongly suspected that the chimeric protein was aggregating into inclusion bodies quickly following translation.

It was decided that optimisations to growth protocols may be more effective and so attention was turned to culturing conditions as a starting point. Returning to shake flask experiments, the PCV2d-PCV3 chimera was expressed under the standard growth temperature in addition to two lower temperatures to facilitate slower rates of expression and protein folding. To the insoluble cell contents, a series of washing steps using a non-ionic surfactant and a chaotropic denaturant were employed to look for liberation of soluble proteins that may have become trapped within the inclusion body aggregate or for any protein that could be solubilised by relatively mild treatment, and whether growth temperature had any effect on this.

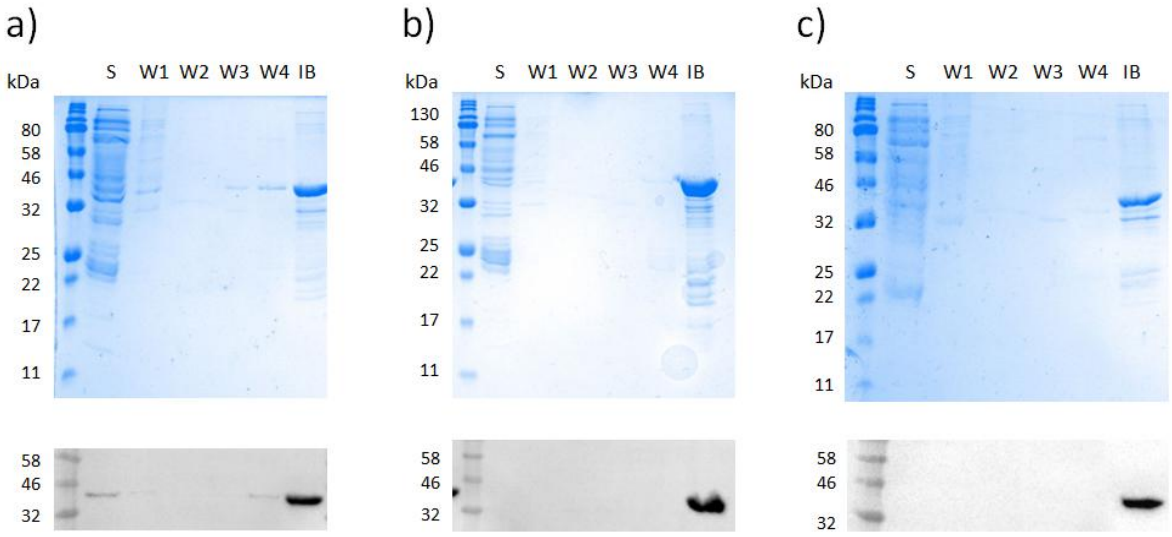

Figure 26. Isolation of PCV2d-PCV3 inclusion bodies from W3110 cells grown at shake flask. Cells were expressed for 3 hours post-induction in LB media at temperatures of a) 18 °C, b) 22 °C or c) 30 °C. Cells were lysed and insoluble cell fraction isolated from the soluble cell fraction (S). Insoluble proteins were washed stepwise in four 50 mM Tris-acetate, 2.5 mM EDTA, pH 7.0 buffers containing 0.5 % Triton X-100 (W1), 5 % Triton X-100 (W2), 1 M urea (W3) then 4 M urea (W4) by centrifuging after each step and taking a sample of supernatant. Remaining inclusion body proteins were obtained by centrifugation (IB). Proteins were separated by SDS PAGE then visualised with Coomassie Brilliant blue and anti-PCV2d western blots.

Cells were cultured and processed using the standard cell growth and fractionation method, except for the differing growth temperatures post-induction during cell culturing. After separating the soluble and insoluble cell fractions, wash buffers 1 and 2 containing Triton X-100 were used to solubilise remnants of the cell membrane within the insoluble pellet, whilst wash buffers 3 and 4 containing a low and moderate concentration of urea were used to denature the inclusion body proteins. Interestingly, a small amount of soluble protein was observed in the soluble cell fraction of cells grown at 18 °C post-induction (Fig. 26a. Western blot, S) and some protein was also liberated from the inclusion body following washing in buffer containing 4 M urea (Fig. 26a. lower panel, W4). However, the majority of full length protein in the 18 °C condition, and all protein in the 22 °C and 30 °C conditions remained completely insoluble.

Despite the discovery that cell culture at a lower temperature post-induction could potentially yield some soluble full-length protein, the overarching conclusion was that mild solubilisation methods would not be sufficient to denature the inclusion bodies formed by the PCV2d-PCV3 chimera protein. It seemed that a much harsher approach would be required.

A protocol was therefore devised to apply harsh conditions to the inclusion bodies by using a highly concentrated denaturing solution containing 8 M urea, testing a range of pH solutions with the aim to reduce the tendency of protein-protein interactions. Each solution also contained DTT in the event that disulphide bonding that may be promoting an inclusion body structure.

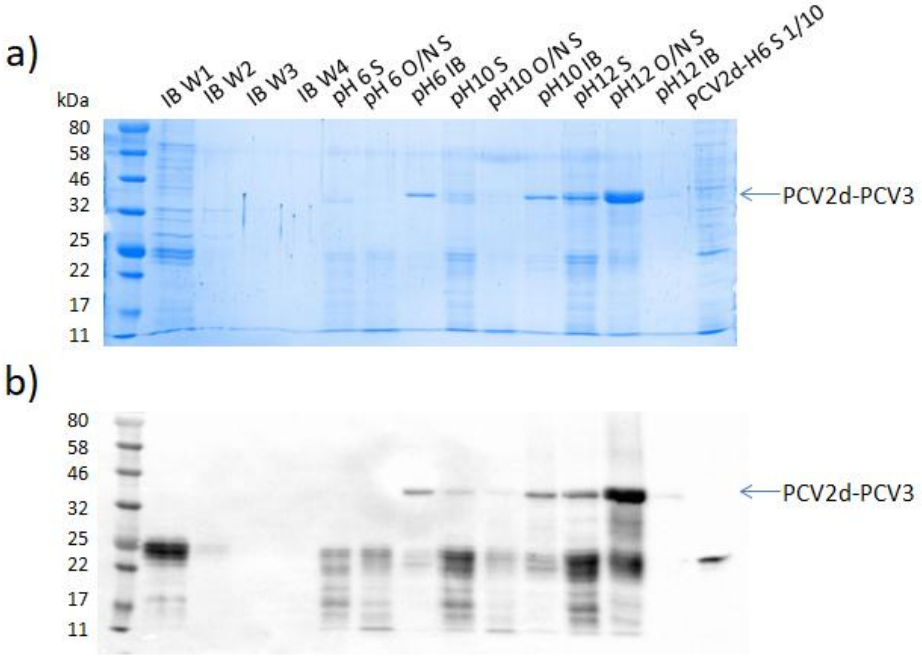

Figure 27. Isolation of PCV2d-ΔMetPCV3 inclusion bodies from W3110 cells grown at shake flask. Cells were harvested following 21 hours post-induction in LB media at 30 °C, lysed and the insoluble cell fraction isolated. Inclusion bodies were washed three times in buffer containing 1 % Triton X-100 and 4 M urea (IB W1 – IB W3) then washed in dH_2O (IB W4) before resuspending in buffer containing 8 M urea at pH 6.0, pH 10.0 or pH 12.0. A sample of soluble protein was obtained immediately following resuspension (S) and then again after 16 hours (O/N S). Remaining inclusion bodies after 16 hours incubation were isolated (IB). Proteins were separated by SDS PAGE then visualised by a) Coomassie Brilliant blue and b) anti-PCV2d western blot. A positive control of soluble PCV2d protein was used for both SDS PAGE and western blot (PCV2d-H6 S 1/10).

As before, cells were cultured and processed using the standard cell growth and fractionation method. From the previous experiment, it was determined that a wash buffer containing a low concentration of Triton X-100 (1 %) and a moderate concentration of urea (4 M) was sufficient to clean up cellular proteins from the insoluble pellet without denaturing any of the inclusion bodies. When treating the inclusion body proteins with a harsh denaturing buffer at pH 6.0, it was observed that all full length protein remained insoluble, but only a minimal proportion of protein remained following 16 hour incubation, suggesting protein degradation was occurring in this buffer. When treated with a pH 10.0 buffer, a small amount of the protein began to solubilise immediately after resuspension, with a similar effect following overnight incubation with the buffer. However, the majority of the chimera protein still remained insoluble. Finally, when

treated with a pH 12.0 buffer, virtually all of the full length chimera protein was able to be solubilised after incubation overnight.

Now that an effective method had been developed to obtain soluble, denatured PCV2d-PCV3 protein in its full length form, the intention was to prepare a purified sample of the solubilised protein that could be immunised into rabbits to raise specific antibodies against PCV3, which had so far proved very difficult to visualise by immunoblotting due to low expression and suspected susceptibility to proteolytic degradation. This required some optimisation to the protocol, as it was advised that for rabbit immunisation, the injected solution should not contain a concentration more than 6 M urea or risk adverse reaction in the animal.

To find a suitable buffer for this application, an alternate approach was taken by this time keeping the pH of the denaturing buffer consistent at pH 12.0 and instead varying the urea concentration from 0 M up to 8 M.

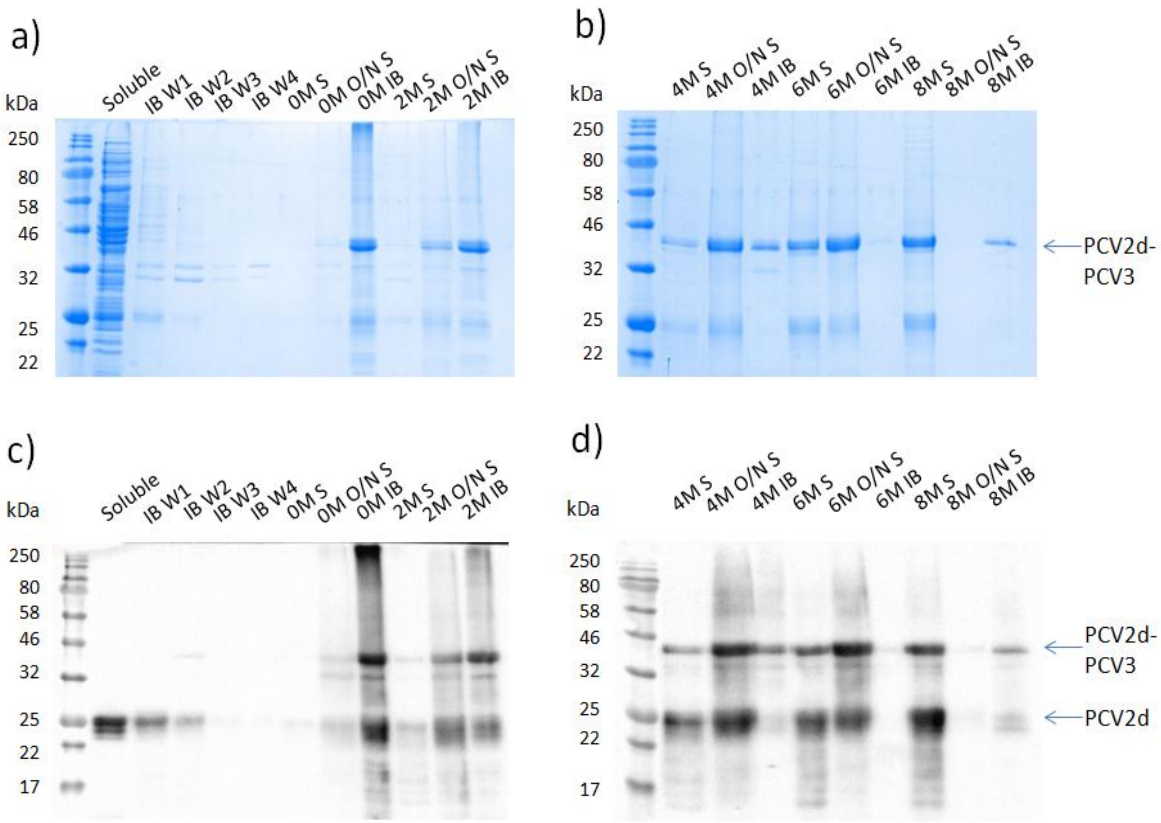

Figure 28. Isolation of PCV2d-ΔMetPCV3 inclusion bodies from W3110 cells grown at shake flask. Cells were harvested following 21 hours post-induction in LB media at 30 °C, lysed and the insoluble cell fraction isolated. Inclusion bodies were washed three times in buffer containing 1 % Triton X-100 and 4 M urea (IB W1 – IB W3) then washed in dH_2O (IB W4) before resuspending in pH 12.0 buffer containing 0, 2, 4, 6 or 8 M urea. A sample of soluble protein was taken

immediately following resuspension (S) and then again after 16 hours (O/N S). Remaining inclusion bodies after 16 hours incubation were isolated (IB). Proteins were separated by SDS PAGE then visualised by a-b) Coomassie Brilliant blue and c-d) anti-PCV2d western blot.

While incubation in 0 M or 2 M urea buffer left the majority of inclusion body proteins unaffected, the data showed that 6 M urea was sufficient to completely solubilise the PCV2d-PCV3 chimera after 16 hours (Fig. 28d). Curiously, it was also apparent that a significant proportion of the proteins visualised by immunoblotting were lower molecular weight, including peptides of cleaved PCV2d around 25 kDa. These peptides were present at almost every step but were of particular note in the inclusion body sample remaining after incubation in pH 12.0 buffer containing 0 M urea which had proved to be insufficiently denaturing to disrupt the inclusion body. This indicated that PCV2d cleaved peptides may also be associating as part of the inclusion body. The Coomassie stained gel further demonstrated high purity of the inclusion bodies and associated PCV2d peptides had already been achieved simply by utilising the four washing steps (Fig. 28a. IB W1 - W4). This data showed 6 M urea was sufficient to effectively solubilise the PCV2d-PCV3 chimera protein inclusion bodies in a buffer at pH 12.0 and therefore may be suitable for rabbit immunization subject to some further processing.

4.2.3 Solubilisation of chimeric proteins at fed-batch fermentation scale

Cultures expressing the PCV2d-PCV3 chimera protein were grown in fed-batch fermentation experiments using 1.5 L Minifors 2 bioreactors containing 500 mL SM6 media under standard conditions as detailed in Chapter 2.

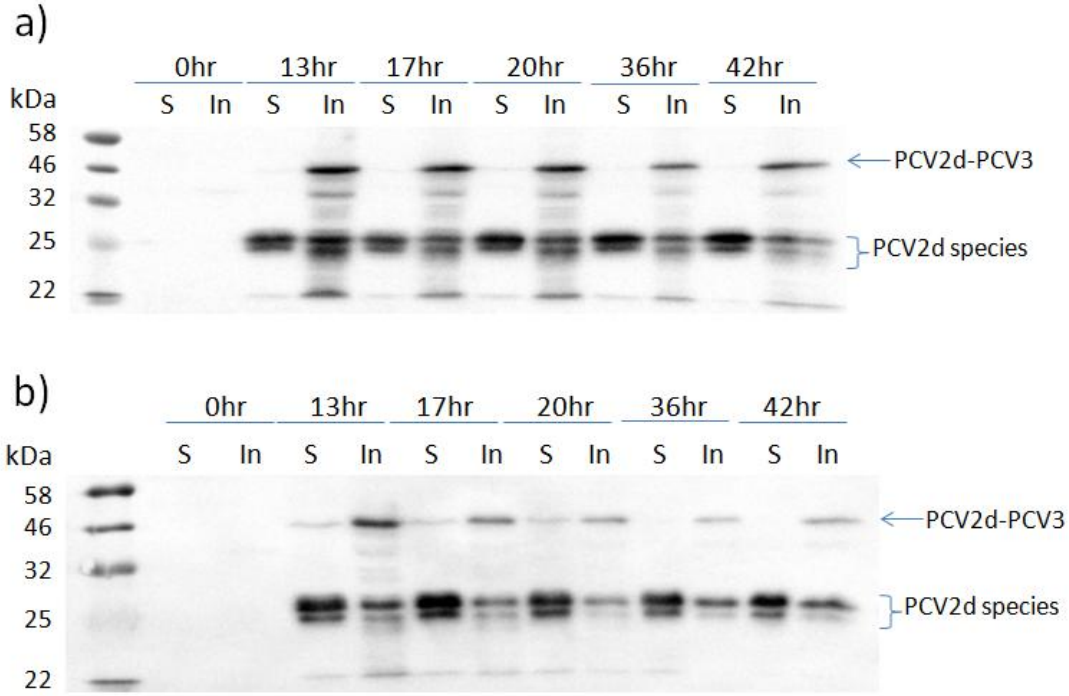

Figure 29. Anti-PCV2d western blot of cell extracts from W3110 cells expressing PCV2d-ΔMetPCV3 at fed-batch fermentation. Cells were grown at a temperature of a) 25 °C for the induction period or b) 20 °C for the induction period. Parameters used: 40 % pO_2 target; glycerol feed rate at 0.7 % of pump capacity (80 % w/v glycerol). Cell samples were taken at time points following addition of IPTG and separated into insoluble and soluble fractions (In: Insoluble; S: Soluble) then separated by SDS PAGE before transferring to western blot.

While the proportion of degraded peptides visualised by western blotting was comparatively lower in the cells grown at 20 °C than 25 °C, cells grown at 25 °C showed a large variety of cleaved peptide species and almost all full length chimera protein was in the insoluble cell fraction. Aside from the dominant doublet of PCV2d cleaved species around 27 kDa which was present in both conditions, there was no apparent improvement in solubility of the full length chimera protein. The overall yield of full length protein at the time of harvest was also much lower in cells grown at 20 °C and all visible protein was in the insoluble cell fraction.

A sample of cells harvested following 42 hours expression in fed-batch fermentation at 25 °C was lysed and separated into soluble and insoluble cell fractions using the standard cell fractionation protocol. As described previously, the same washing and solubilisation procedure was then used to treat inclusion bodies harvested from fed-batch fermentation, testing a range of urea concentrations from 0 – 8 M urea in pH 12.0 buffers.

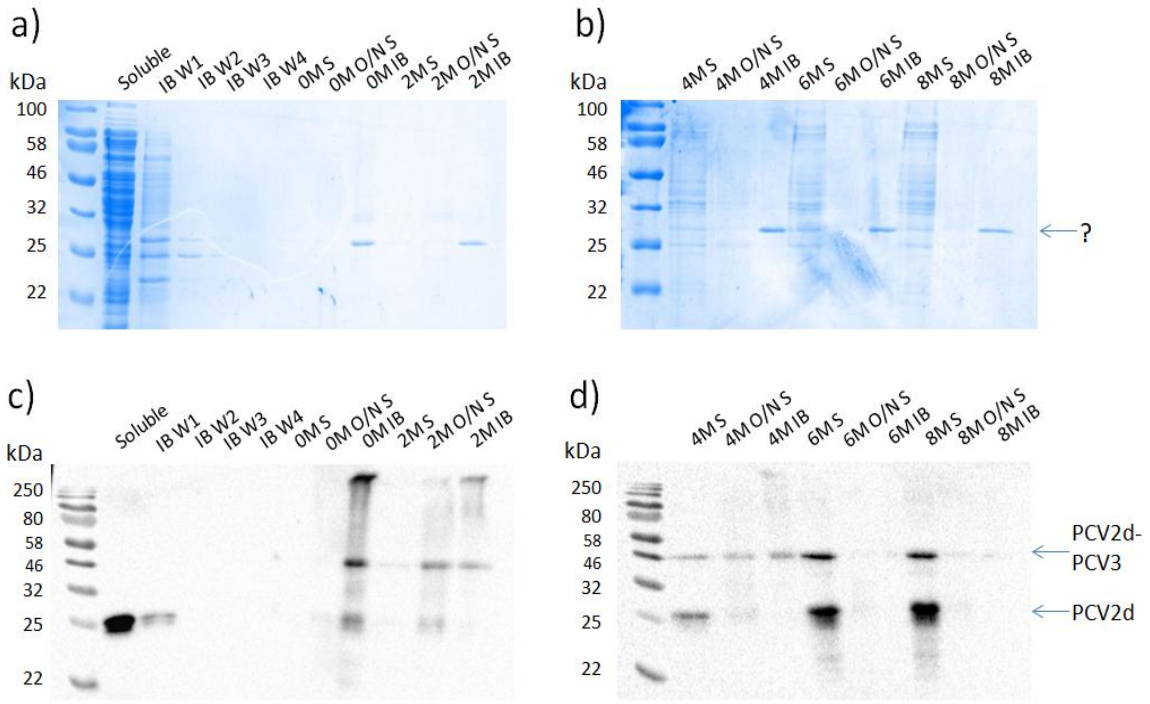

Figure 30. Isolation of PCV2d-ΔMetPCV3 inclusion bodies from W3110 cells grown at fed-batch fermentation at 25 °C. Cells were harvested following 42 hours growth post-induction at 25 °C, and the insoluble cell fraction isolated. Inclusion bodies were washed three times in buffer containing 1 % Triton X-100 and 4 M urea (IB W1 – IB W3) then washed in dH_2O (IB W4) before resuspending in pH 12.0 buffer containing 0, 2, 4, 6 or 8 M urea. A sample of soluble protein was taken immediately following resuspension (S) and then again after 16 hours (O/N S). Remaining inclusion bodies after 16 hours incubation were isolated (IB). Proteins were separated by SDS PAGE then visualised by a-b) Coomassie Brilliant blue and c-d) anti-PCV2d western blot.

The Coomassie stained gels showed most notably a visible band around 27 kDa, which only appeared in the inclusion body fraction after 16 hours incubation in pH 12.0 buffers (Fig. 30a, b), which was assumed to be a PCV2d cleaved peptide. However, the same band did not appear equivalently when immunoblotted (Fig. 30c, d); while even 2 M urea was able to solubilise a small amount of inclusion body protein, 6 M urea was the lowest concentration sufficient to solubilise all inclusion body proteins from cells grown at 25 °C in fed-batch fermentation – reflecting the results seen in shake flask experiments.

It was clear that a significant portion of the proteins visible following urea treatment appeared to be cleaved PCV2d peptides and the amount of total protein on the gels after processing was considerably lower compared to fractions obtained from shake flask cultures. Cells grown at 20 °C in fed-batch fermentation were also tested in solubilisation trials, and although these inclusion

bodies showed slightly improved solubility at lower urea concentrations, the overall protein yields were similarly low. This suggested the inclusion body proteins isolated from cells harvested from fed-batch fermentation were more susceptible to degradation during processing.

4.2.4 IMAC purification of chimera proteins under denaturing conditions

With the development of a sufficiently denaturing, lower urea buffer suitable for rabbit immunisation, the final stage of inclusion body processing was to remove the residual PCV2d peptides that seemed to be associating with the full length PCV2d-ΔMetPCV3 chimera, as the aim was to maximise the number of anti-PCV3 antibodies raised by the animal. Immobilised metal affinity chromatography using nickel-sepharose resin was chosen to purify the full length chimera protein by way of its HIS tag. This resin is able to withstand the harsh conditions of the denaturing buffer developed in the previous experiments, so a large shake flask preparation of the solubilised inclusion bodies was prepared for purification. The basis of the experiment was to bind the full length, HIS-tagged inclusion body proteins to the IMAC column under denaturing conditions, so that the cleaved PCV2d peptides containing no HIS-tag could be washed through the column and removed.

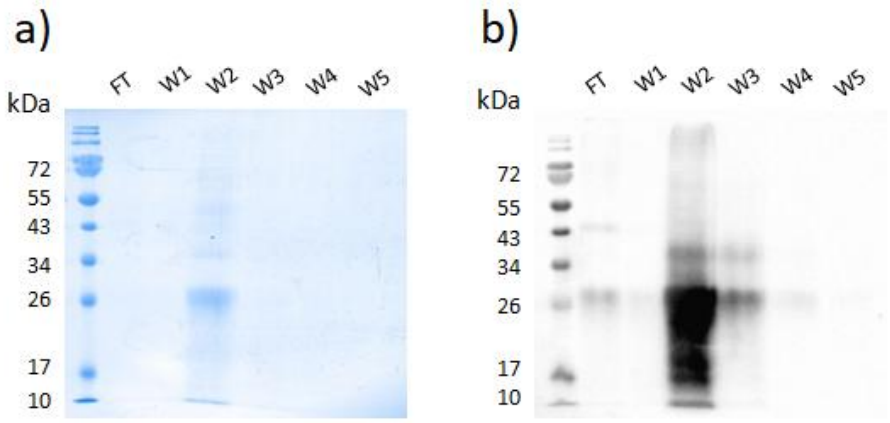

Figure 31. Purification of PCV2d-ΔMetPCV3 inclusion bodies by IMAC. Inclusion bodies were generated in shake flask culture. Following protein denaturation in pH 12.0 buffer containing 6 M urea, solubilised inclusion body proteins were isolated by centrifugation, the supernatant applied to a 5 mL HisTrap™ column and the flow through collected (FT). The column was washed five times with denaturing buffer containing 20 mM imidazole (W1, W2, W3, W4, W5) to remove residual PCV2d cleaved peptides. Proteins were separated by SDS PAGE then visualised by a) Coomassie Brilliant blue and b) anti-PCV2d western blot.

After removal of cleaved PCV2d peptides by washing steps using a low concentration of imidazole, a high concentration of imidazole was applied to the column to elute the purified, full length PCV2d-ΔMetPCV3 chimera proteins.

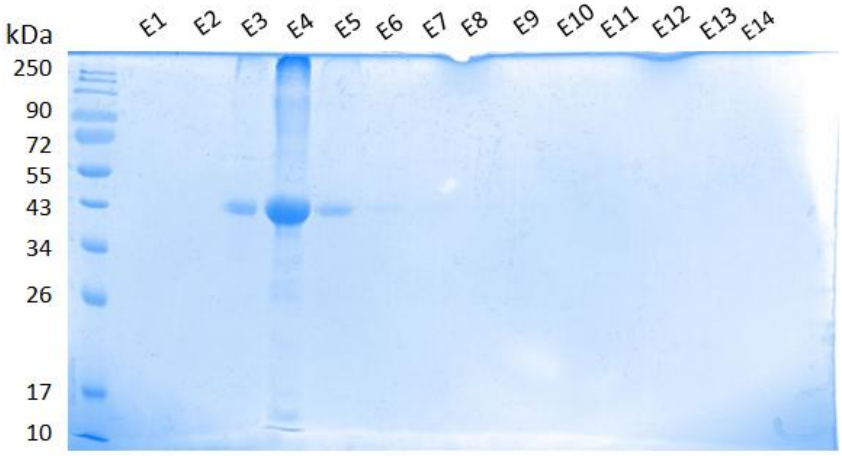

	E3	E4	E5	E6	E7	E8	E9
Conc. mg/ml	0.232	1.859	0.220	0.129	0.115	0.111	0.108

Figure 32. Purification of PCV2d-ΔMetPCV3 inclusion bodies by IMAC. Inclusion bodies were generated in shake flask culture. Following protein denaturation in pH 12.0 buffer containing 6 M urea, solubilised inclusion body proteins were isolated by centrifugation and the supernatant applied to a 5 mL HisTrap™ column. After washing, the full length chimera proteins were eluted by applying denaturing buffer containing 500 mM imidazole then collected in fourteen 2 mL fractions (E1 - E14). Proteins were separated by SDS PAGE then visualised by Coomassie Brilliant blue. Protein concentrations of selected elution fractions quantified by Bradford Assay are shown.

SDS PAGE analysis showed that after applying the solubilised inclusion body proteins to the IMAC column, no impurities were visible in the flow through on either Coomassie stained gel or western blot, indicating the cell fractionation and washing process had been very effective in removing cellular proteins even without purification. The majority of the cleaved PCV2d peptides among others were successfully eluted in the second wash using a low concentration of imidazole (W2) and by the fifth wash step (W5), all cleaved peptides appeared to have been eliminated. The full length PCV2d-ΔMetPCV3 chimera proteins were eluted using a high concentration imidazole buffer with the aim to elute into a small volume, which proved effective as the eluted proteins were collected almost entirely in a single peak fraction (E4) containing 1.859 mg/mL protein, as quantified by Bradford Assay. The peak fraction was clear on a Coomassie stained gel to contain very little to no impurities or cleaved peptides. In order to immunise into rabbits without adverse reaction, the solubilised protein sample was adjusted to pH 8.0 and remained soluble at this pH.

4.2.5 Generation of a specific PCV3 antibody

A preparation of the IMAC purified, denatured PCV2d-ΔMetPCV3 adjusted to neutral pH was transferred to Cambridge Research Biochemicals in order to raise a specific antibody. To achieve this, two rabbits, K52 and K53, were each immunized with 0.1 mg of the PCV2d antigen at weeks 1, 3, 5, 7 and 9. Blood samples were taken at weeks 4, 6 and 8 (test bleeds 1, 2 and 3 respectively) and the final harvest bleed was obtained at week 10. Samples of test bleeds were transferred periodically for antibody specificity testing by western blotting using a range of test samples and controls, and all sera were used at a 1 in 10,000 dilution in PBST for immunoblotting.

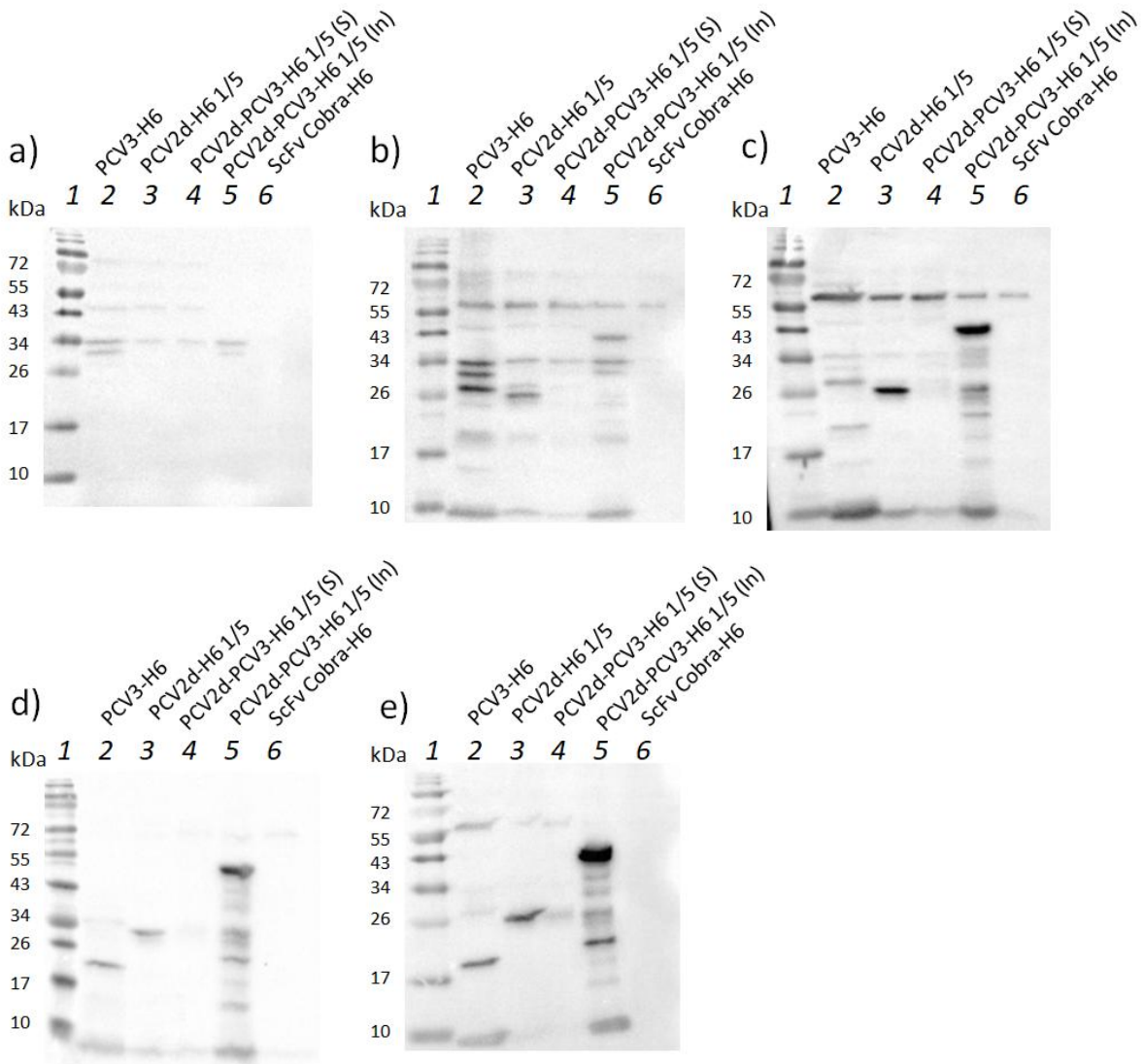

Figure 33. Western blots using test serum from K52 rabbit immunized with PCV2d-ΔMetPCV3 protein. After blocking in 5 % milk with PBS tween, blots were incubated in a) pre-immune serum; b) test bleed 1; c) test bleed 2; d) test bleed 3; e) harvest bleed. Following this, blots were incubated in anti-rabbit secondary antibody. Lane 1: Protein marker; lane 2: Soluble fraction from *E. coli* cells expressing PCV3-H6, undiluted; lane 3: Soluble fraction from *E. coli* cells expressing PCV2d-H6, 1/5 dilution; lane 4: Soluble fraction from *E. coli* cells expressing PCV2d-PCV3-H6, 1/5 dilution; lane 5: Insoluble fraction from *E. coli* cells expressing PCV2d-PCV3-H6, 1/5 dilution; lane 6: Periplasmic fraction from *E. coli* cells expressing ScFv-Cobra-H6, undiluted (negative control).

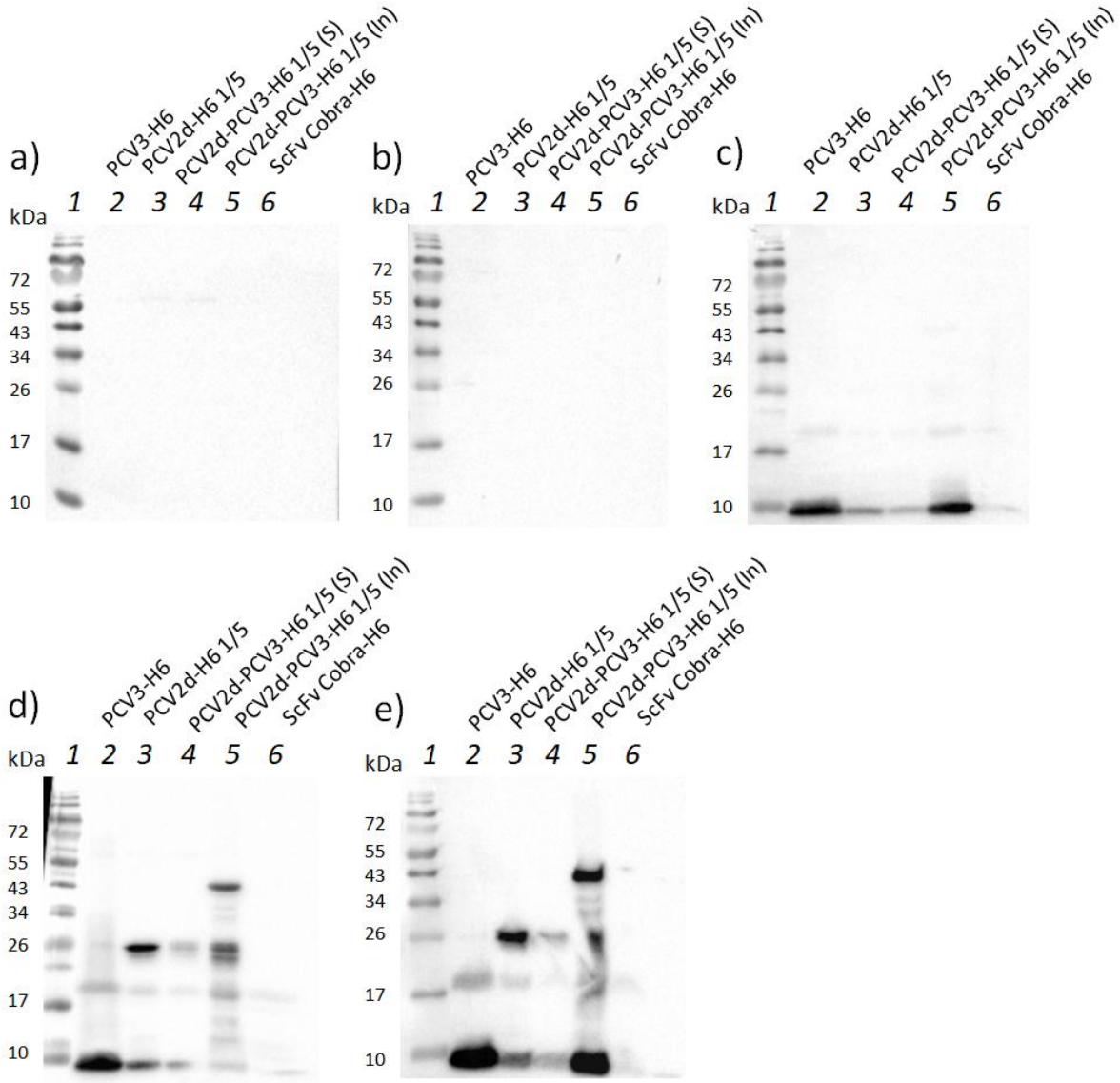

Figure 34. Western blots using test serum from K53 rabbit immunized with PCV2d-ΔMetPCV3 protein. After blocking in 5 % milk with PBS tween, blots were incubated in a) pre-immune serum; b) test bleed 1; c) test bleed 2; d) test bleed 3; e) harvest bleed. Following this, blots were incubated in anti-rabbit secondary antibody. Lane 1: Protein marker; lane 2: Soluble fraction from *E. coli* cells expressing PCV3-H6, undiluted; lane 3: Soluble fraction from *E. coli* cells expressing PCV2d-H6, 1/5 dilution; lane 4: Soluble fraction from *E. coli* cells expressing PCV2d-PCV3-H6, 1/5 dilution; lane 5: Insoluble fraction from *E. coli* cells expressing PCV2d-PCV3-H6, 1/5 dilution; lane 6: Periplasmic fraction from *E. coli* cells expressing ScFv-Cobra-H6, undiluted (negative control).

None of the test bleed sera from K52 or K53 rabbits showed any non-specific binding to an unrelated HIS-tagged protein, ScFv-Cobra. However other than this, from the pre-immune bleed and test bleed 1, K52 and K53 rabbits showed quite different detection profiles, with K52 rabbit serum surprisingly detecting a large number of proteins when used to probe an immunoblot

containing test samples. That said, test bleed 2 serum from K52 rabbit began to show clear detection of PCV2d (Fig. 33c. Lane 3; 23.4 kDa) and PCV2d-PCV3 chimeric proteins (Fig 33c. Lane 5; 42.3 kDa) which increased in specificity with further immunisations with the antigen. By test bleed 3, the serum was also displaying clear specificity for PCV3 protein (Fig. 33d. Lane 2; 19.4 kDa). On the other hand, while K53 rabbit sera showed higher specificity for PCV proteins in general when used for immunoblotting, when probing test samples containing PCV3 protein the sera appeared to show preferential detection of lower molecular weight proteins around 10 kDa, presumed to be cleaved peptides from PCV3, to a greater degree than the uncleaved PCV3 protein at 19.4 kDa (Fig. 34e. Lane 2). For this reason, the K52 rabbit harvest bleed serum was taken forward for purification.

A PCV2d-coupled NHS-activated sepharose affinity column was used to separate polyclonal antibodies specific to PCV2d epitopes from the K52 rabbit harvest bleed serum through selective binding of PCV2d-specific antibodies in the serum to the PCV2d protein-coupled sepharose resin. Following application of the serum to the column, the flow through containing PCV3-specific antibodies was collected and this was then used to probe an immunoblot containing the same test samples used previously.

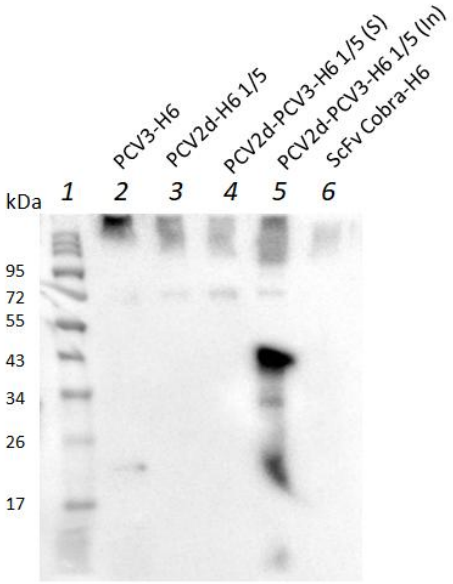

Figure 35. Western blot using purified anti-PCV3 antibodies. After blocking in 5 % milk with PBS tween, the blot was incubated in purified K52 rabbit serum containing PCV3 antibodies then incubated in anti-rabbit secondary antibody. Lane 1: Protein marker; lane 2: Soluble fraction from *E. coli* cells expressing PCV3-H6, undiluted; lane 3: Soluble fraction from *E. coli* cells expressing PCV2d-H6, 1/5 dilution; lane 4: Soluble fraction from *E. coli* cells expressing PCV2d-PCV3-H6, 1/5 dilution; lane 5: Insoluble fraction from *E. coli* cells expressing PCV2d-PCV3-H6, 1/5 dilution; lane 6: Periplasmic fraction from *E. coli* cells expressing ScFv-Cobra-H6, undiluted (negative control).

After PCV2d-coupled NHS-activated sepharose affinity chromatography, the purified anti-PCV3 serum showed no detection of PCV2d-H6 protein at the concentration used (Fig. 35. Lane 3). The purified serum detected some proteins between 17 - 26 kDa in a PCV2d-PCV3 sample (Fig. 35. Lane 5) corresponding to approximately PCV3 molecular weight (19.4 kDa) and only a single band in a sample from cells expressing PCV3 was visible (Fig. 35. Lane 2), showing potentially good specificity for PCV3; however, this band appeared very faint so a higher concentration of serum would be required for immunoblotting in order to make a reliable conclusion.

4.3 Conclusions

Altering growth temperature of cells expressing PCV2d-PCV3 proteins did not show any obvious improvement in soluble production of the chimeric protein and the majority of the recombinant protein formed inclusion bodies. Although, inclusion bodies isolated from cells expressing at lower temperatures were able to liberate a larger amount of solubilised protein when treated with mild denaturing conditions compared to those expressing at higher growth temperatures. This effect was observable when processing inclusion body proteins isolated from cells grown at small shake flask scale and also at fed-batch fermentation scale. In both circumstances, buffer pH was a major factor in effective denaturation. An effective and efficient method was developed to achieve high purity PCV2d-PCV3 inclusion body proteins. A centrifugation step was employed based on the higher density of the inclusion bodies compared to other *E.coli* cellular components, followed by a washing procedure to remove bacterial cell components utilising the reducing agent DTT, Triton X-100 as a surfactant to disrupt the lipid membrane, along with low concentrations of urea to remove cellular proteins. It was discovered that a strongly alkaline pH was most effective at solubilising PCV2d-PCV3 inclusion body proteins; in the presence of 6M urea, a pH 6.0 environment yielded virtually no soluble protein in comparison to a pH 12.0 environment which was able to solubilise the entire inclusion body. The harsh denaturing pH 12.0 was able to solubilise inclusion body proteins even in buffers containing as little as 2 M urea. A large proportion of the solubilised inclusion body proteins were found to be PCV2d cleaved peptides, which could be swiftly removed by a single step of immobilised metal affinity chromatography performed under denaturing conditions in buffers containing 6 M urea and 5 mM DTT at pH 12.0. Using this method, a preparation of denatured, solubilised PCV2d-PCV3 antigen was sent for rabbit immunisation which resulted in a PCV3 antibody being successfully raised and isolated. Serum harvested from the rabbits immunized with PCV2d-PCV3 antigen can in the future be used in viral neutralisation assay to test for neutralising antibody activity against a cultured PCV3 virus.

Chapter 5: PCV2d cysteine mutants

5.1 Introduction

PCV Cap proteins expressed by the ORF2 gene are responsible for formation of the spherical shell structure of porcine circoviruses, necessary for both packaging of the viral genome and mediating viral entry into host cells. In the absence of viral DNA as is the case in recombinant expression systems, when sixty copies of the capsid protein assemble into empty T=1 icosahedral VLPs, they are able to function as a major immunogen, carrying several epitopes (Nawagitgul et al., 2000). This makes VLPs a powerful scaffold for antigen presentation and therapeutic delivery strategies. Their success as immunogens can be attributed to their ability to mimic native viruses without containing a viral genome as their highly organized and repetitive antigen structure has shown effective cellular and humoral immune responses (Cervera et al., 2019). Virus-like particles can sometimes present viral antigens in a more authentic conformation than monomeric structural proteins. There are several licensed VLP-based vaccines currently on the market in human and animal therapeutics, such as Cervarix®, Gardasil®, Hecolin® or Porcilis PCV®. These VLP-based vaccines are commonly produced in baculovirus insect cell expression systems.

However, compared to single protein-based therapeutics, quality assessment requires a higher degree of refinement due to the organized structure of VLPs. Multiple recombinant microbial expression systems including *E. coli, L. lactis, S. cerevisiae* and *P. pastoris* have achieved expression of PCV2 Cap protein but presented challenges in self-assembly into VLPs (Trundova & Celer, 2007; Tu et al., 2013). In *S. cerevisiae*, the failure of PCV2 Cap protein production using the native coding sequence was reported. It was demonstrated that only a codon optimised gene allowed generation of PCV2 Cap VLPs in this system and still the generated VLPs were not homogeneous in size and shape (Bucarey et al., 2009). Quality assessment is of critical importance since the physicochemical and biological properties of the VLPs are essential in determining their clinical efficacy as a successful vaccine. The VLP's structural integrity must be preserved during all stages of vaccine manufacturing, storage and administration if their success is to be ensured (Jain et al., 2015). Transmission electron microscopy (TEM) is considered the gold standard technique for characterization of virus-like structures and uses a contrast medium for sample visualization, the most extended strategy being negative staining using a heavy metal solution containing a cationic or anionic salt. In TEM negative staining, a thin layer of the biological material is covered by a dried non-crystalline amorphous layer of a heavy metal salt, such as uranyl acetate. Differential electron scattering between the biological material and the surrounding staining layer enables visualization of the specimen (González-Domínguez et al., 2020).

It is for the reasons outlined here that this research aimed from the outset to produce a subunit vaccine design consisting monomeric PCV capsid proteins produced recombinantly, rather than a VLP-based vaccine; subunit vaccines are a highly popular modern vaccine design, with several commercially available PCV2 subunit vaccines on the market that are effective in protecting against concurrent and emerging PCV2 strains (Jeong et al., 2015; Seo et al., 2014).

Generally, it is considered from the literature that efficient production of recombinant PCV2 Cap protein requires modifications to the gene including removal of the N-terminal region containing the NLS (Zhou et al., 2005), supporting our findings in Chapter 3. That said, both full length and N-terminally truncated monomeric PCV2 Cap protein purified from *E.coli* have been shown to still successfully reassemble into VLPs in vitro (Khayat et al., 2011). Evidence suggests the NLS regions of adjacent capsid proteins interact to stabilize the VLP structure (Mo et al., 2019) while the unique cysteine 108 residue existing in PCV2 Cap proteins is thought to play an important role in the integrity of VLPs through disulphide bonding (Wu et al., 2012). In this chapter, modified versions of PCV2d Cap protein were generated by employing truncation of the NLS region and mutation of the unique cysteine residue, using multiple methods to investigate whether the modifications to recombinant PCV2d capsid proteins expressed in *E. coli* were able to prevent their oligomerisation into VLPs. Analysis was performed by biochemical methods such as non-reducing SDS PAGE, FPLC-based method gel filtration and imaging the conformation of the proteins by TEM.

5.2 Results

5.2.1 Design and expression of PCV2d and PCV2d-PCV3 chimera cysteine mutants

Nucleotide substitutions were introduced to the existing PCV2d genes by site-directed mutagenesis, using PCR to change the cysteine residue at position 108 to either a serine (C108S) or an alanine (C108A) residue in both the single PCV2d truncated construct and the PCV2d-PCV3 chimeric truncated construct. The new constructs were expressed in BL21 cell line and soluble protein contents analysed by reducing and non-reducing SDS PAGE for differences in oligomerisation.

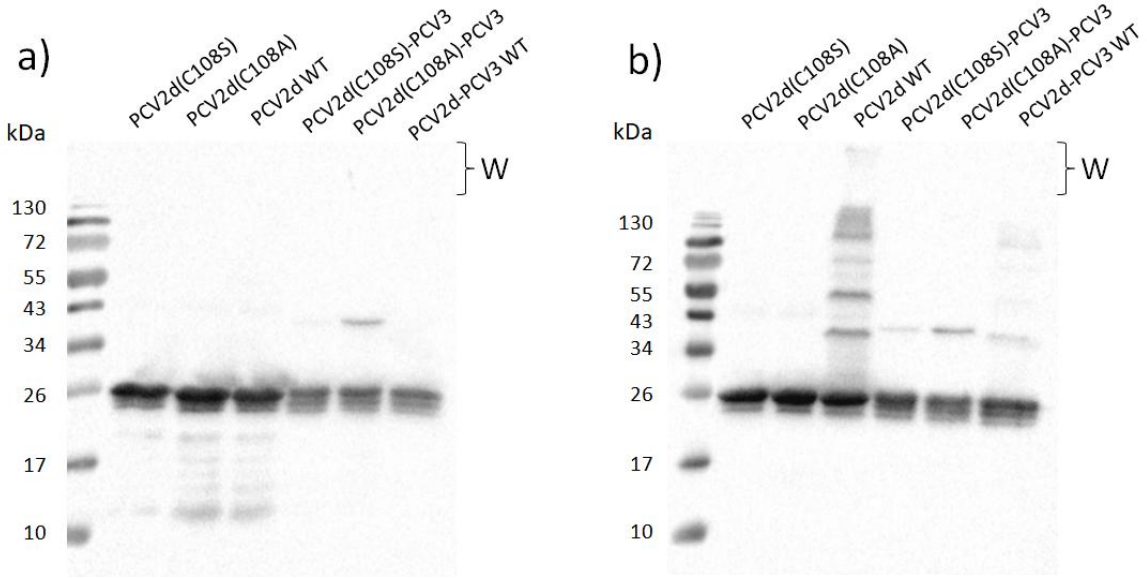

Figure 36. Anti-PCV2d western blots of cell extracts from BL21 cells expressing PCV WT and cysteine mutant constructs. Following 21 hours growth post-induction in LB media, soluble cell extracts were isolated then separated by a) SDS PAGE or b) non-reducing SDS PAGE then visualised by western blot. W: wells.

PCV2d species were detected around 23.4 kDa following both reducing SDS PAGE and non-reducing SDS PAGE appearing as a triplet of bands. Whilst not visualised by reducing SDS PAGE, a range of at least 8 higher molecular weight bands were detected in truncated PCV2d WT and soluble PCV2d derived from truncated PCV2d-PCV3 WT in non-reducing SDS PAGE; however these bands were not apparent in samples of truncated cysteine mutant proteins. A small amount of protein was also detected remaining within the wells of the gel in the PCV2d WT sample in non-reducing PAGE suggesting a large sized species. Overall, it was clear that while PCV2d WT protein was able to form oligomers, PCV2d-PCV3 WT soluble proteins showed a much lower tendency to do so and substitution of the cysteine residue in both proteins virtually abolished this tendency.

5.2.2 Gel filtration and TEM of PCV2d WT and cysteine mutant proteins for analysis of VLP formation

Separation of cellular proteins by non-reducing SDS PAGE had demonstrated a range of different sized species containing PCV2d when immunoblotting with the anti-PCV2d antibody, including at least one species of very high molecular weight. Further analysis was required to ascertain whether higher structures were being formed by truncated PCV2d WT in the single or chimeric proteins, or indeed whether cysteine mutation had an effect on this, and thus deduce by what mechanism these higher structures might be forming.

Gel filtration chromatography was performed using samples of PCV2d WT, PCV2d(C108S), PCV2d(C108A), PCV2d-PCV3 WT, PCV2d(C108S)-PCV3, PCV2d(C108A)-PCV3 proteins as derived

from expression of pARP25, pARP39, pARP40, pARP31, pARP41 and pARP42 constructs respectively. Prior to gel filtration, the proteins had been purified by CIEX without DTT. A calibration curve using protein standards was also performed.

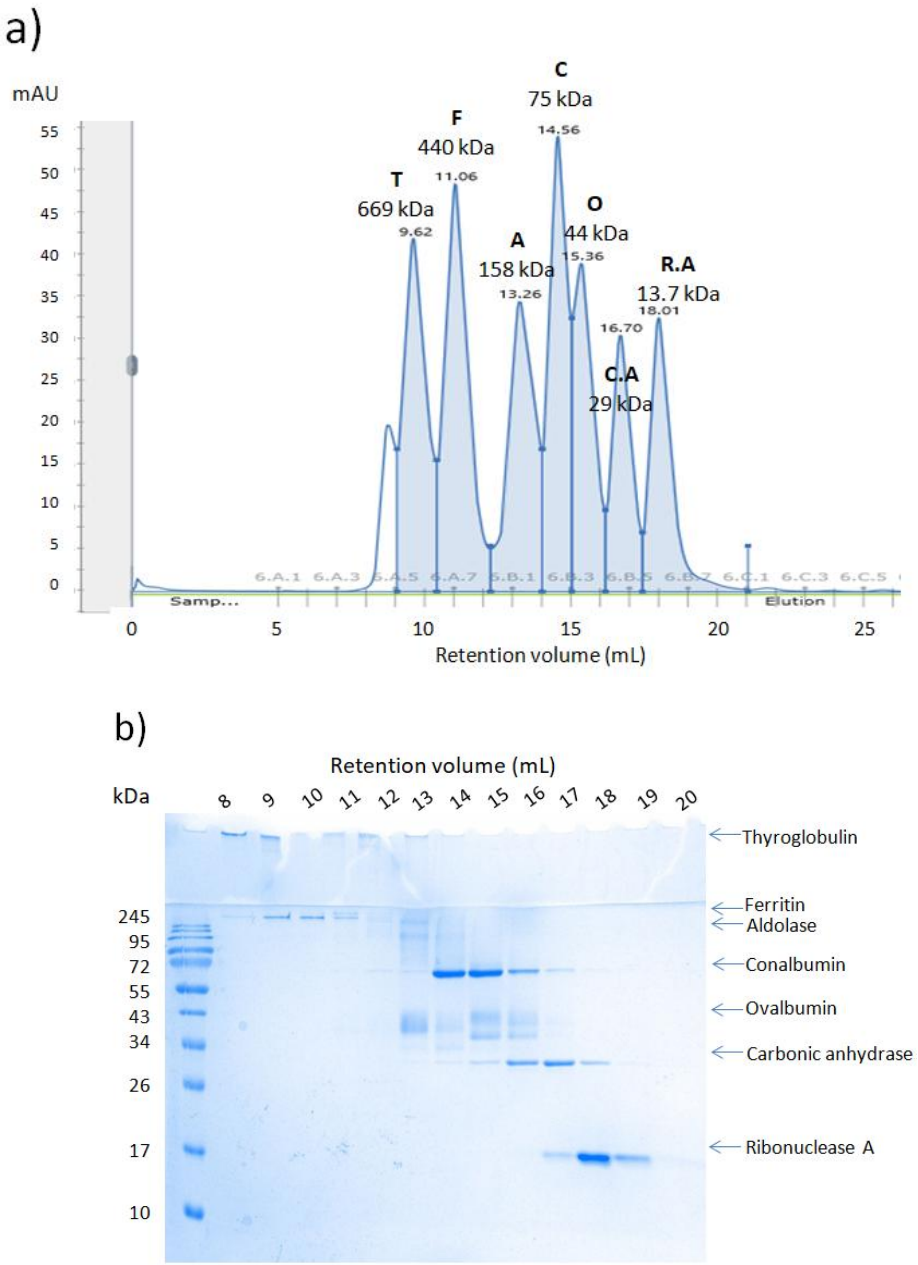

Figure 37. Gel filtration chromatography of protein standards for a calibration curve. A standardized concentration of protein standards were applied to a Superdex 200 Increase 10/300 column and separated based on size. a) Chromatogram of protein elution fractions by retention volume (mL) against peak intensity (mAU). b) Coomassie Blue-stained SDS PAGE gel of elution fractions containing protein standards. Peak retention volumes of standards: Thyroglobulin, 669 kDa, 9.62 mL; Ferritin, 440 kDa, 11.06 mL; Aldolase, 158 kDa, 13.26 mL; Conalbumin, 75 kDa, 14.56 mL; Ovalbumin, 44 kDa, 15.36 mL; Carbonic anhydrase, 29 kDa, 16.7 mL; Ribonuclease A, 13.7 kDa, 18.01 mL.

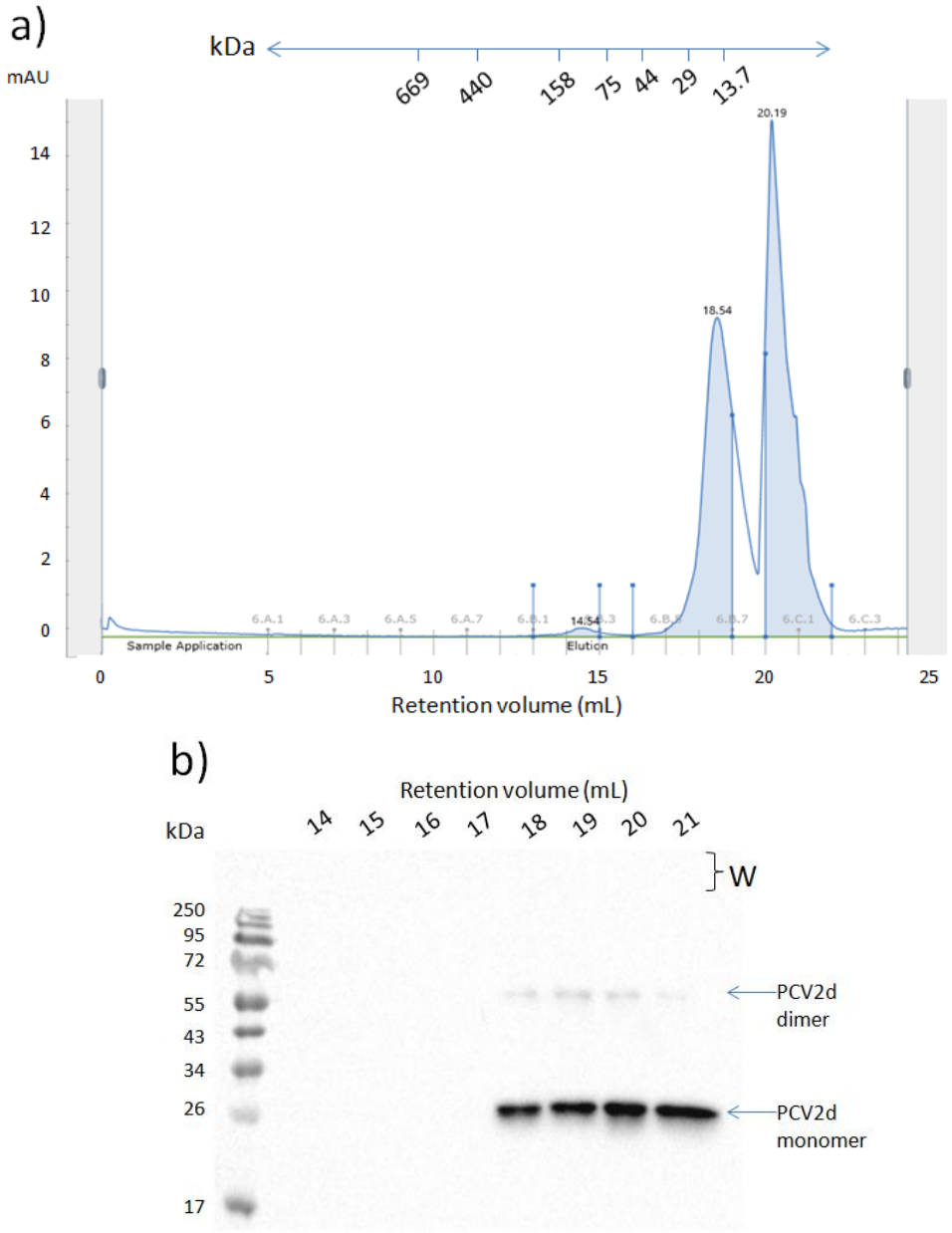

Figure 38. Gel filtration chromatography of PCV2d WT protein species. A preparation of soluble CIEX purified, PCV2d WT protein derived from pARP25 construct expression was applied to a Superdex 200 Increase 10/300 column and species separated based on size. a) Chromatogram of protein elution fractions by retention volume (mL) against peak intensity (mAU). b) Anti-PCV2d western blot following non-reducing SDS PAGE of peak elution fractions. Truncated PCV2d WT protein was detected in fractions corresponding to retention volume 18-21 mL, denoted by arrows. Bar denotes estimated molecular weights based on calibration curve.

The chromatogram trace produced from gel filtration of the truncated PCV2d WT protein showed a very small peak at a retention volume of 14.54 mL, indicating a protein between 44 – 75 kDa as predicted from the calibration data. Other than this, only two major peaks were observed

spanning five elution fractions corresponding to retention volumes between 17 – 22 mL. All elution fractions corresponding to any visible peak, which included all three of the mentioned peaks, were analysed by SDS PAGE separation followed by immunoblotting. The small peak corresponding to 14 mL retention volume did not show any visible PCV2d protein by immunoblotting, suggesting an impurity. The two major peaks eluting between 17-21 mL indicated the protein to be monomeric; the expected retention volume for monomeric PCV2d would be around 17 mL according to the calibration curve data, so the peak at 18.54 mL was assumed to be PCV2d, while the peak at 20.19 mL was thought to be an impurity as no lower molecular weight proteins were visualised by immunoblotting. Bands were visualised on western blot at a monomeric size of 23.4 kDa in addition to another set of bands around 60 kDa after separation by non-reducing SDS PAGE. This indicated that oligomerisation may have occurred following elution from the gel filtration column in the buffer conditions used during SDS PAGE sample preparation.

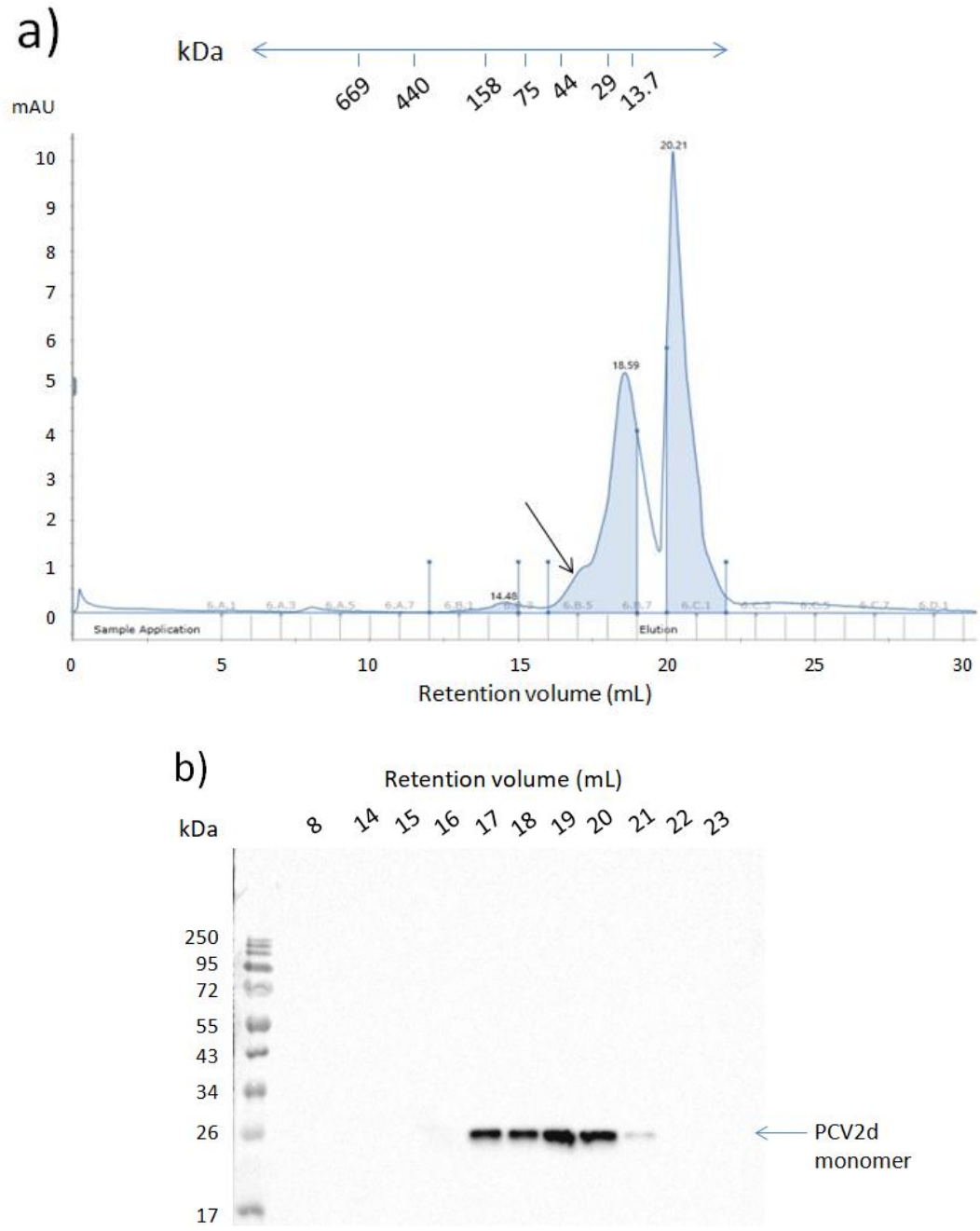

Figure 39. Gel filtration chromatography of PCV2d(C108S) protein species. A preparation of soluble CIEX purified, PCV2d(C108S) protein derived from pARP39 construct expression was applied to a Superdex 200 Increase 10/300 column and species separated based on size. a) Chromatogram of protein elution fractions by retention volume (mL) against peak intensity (mAU). Arrow indicates "shoulder" peak. b) Anti-PCV2d western blot following non-reducing SDS PAGE of peak elution fractions. Truncated PCV2d(C108S) protein was detected in fractions corresponding to retention volume 17-21 mL, denoted by arrow. Bar denotes estimated molecular weights based on calibration curve.

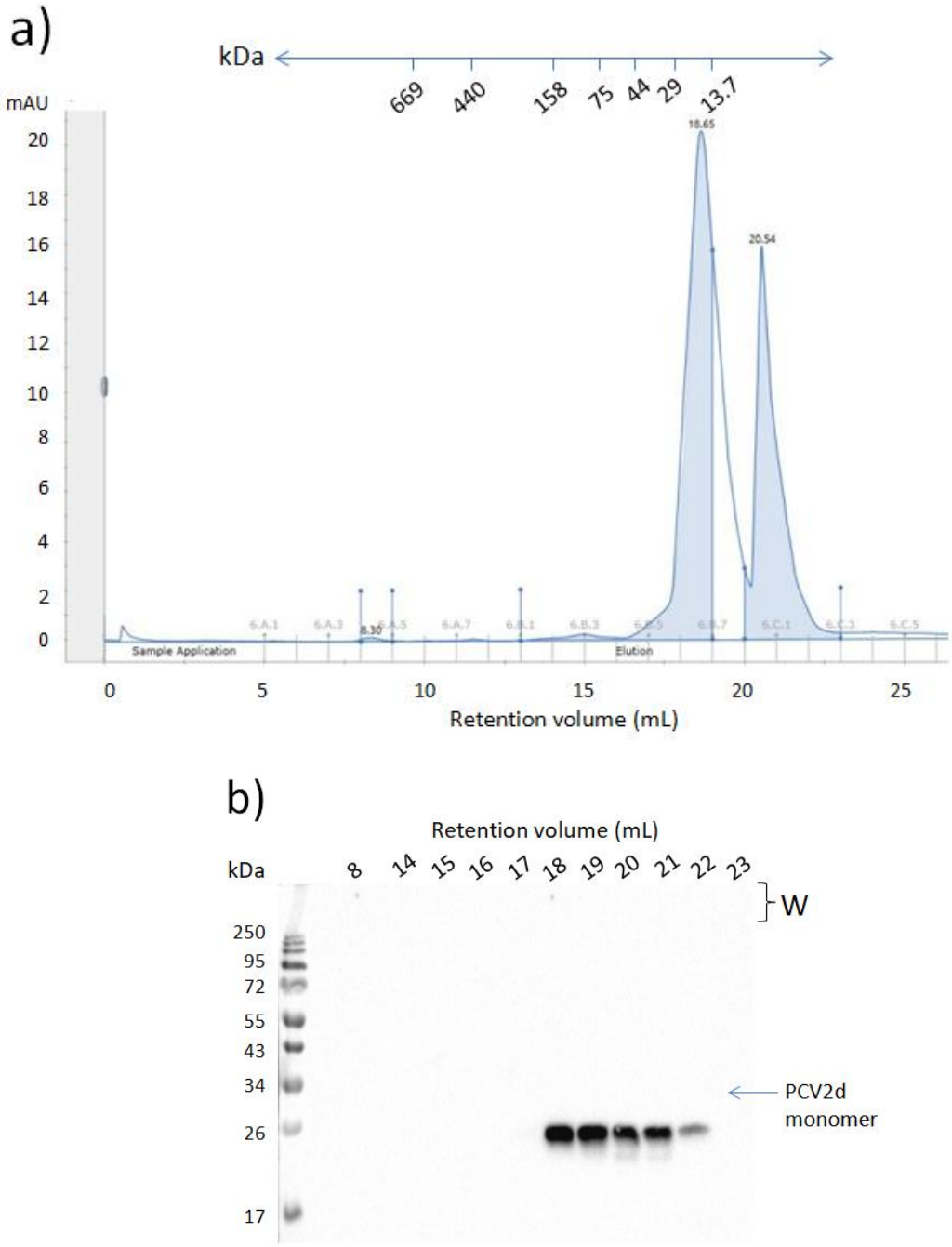

Figure 40. Gel filtration chromatography of PCV2d(C108A) protein species. A preparation of soluble CIEX purified, PCV2d(C108A) protein derived from pARP40 construct expression was applied to a Superdex 200 Increase 10/300 column and species separated based on size. a) Chromatogram of protein elution fractions by retention volume (mL) against peak intensity (mAU). b) Anti-PCV2d western blot following non-reducing SDS PAGE of peak elution fractions. Truncated PCV2d(C108A) protein was detected in fractions corresponding to retention volume 18-22 mL, denoted by arrow. Bar denotes estimated molecular weights based on calibration curve.

Gel filtration of both PCV2d(C108S) and PCV2d(C108A) mutants showed the two major peaks at 17 – 22 mL retention volume along with a smaller peak corresponding to approximately 14 mL retention volume, as seen in the chromatogram from PCV2d WT protein. Monomeric PCV2d protein in all experiments was consistently eluted from the column in a major peak appearing at around 18.5 mL whilst the second large peak around 20 mL appeared to be an impurity. The chromatogram of PCV2d(C108S) protein also showed a small "shoulder" peak to the left of the major PCV2d peak at 18.59 mL, which may be suggestive of heterogeneous protein species, although no mixed species were clearly identifiable from the immunoblot. Purification of both mutant proteins also indicated another very small peak appearing on the chromatogram around 8.3 mL retention volume not seen from the WT protein; analysis of the corresponding elution fractions by immunoblotting with PCV2d antibody however did not suggest this to be a PCV2d oligomer as no bands could be visualised and was concluded to be an impurity. Comparison of the immunoblots also showed that substitution of the cysteine residue in PCV2d eliminated dimerization potential during SDS PAGE sample preparation. Some doublet bands around expected PCV2d monomeric size were still observed in all iterations, indicative of HIS tag cleavage previously demonstrated in chapter 3.

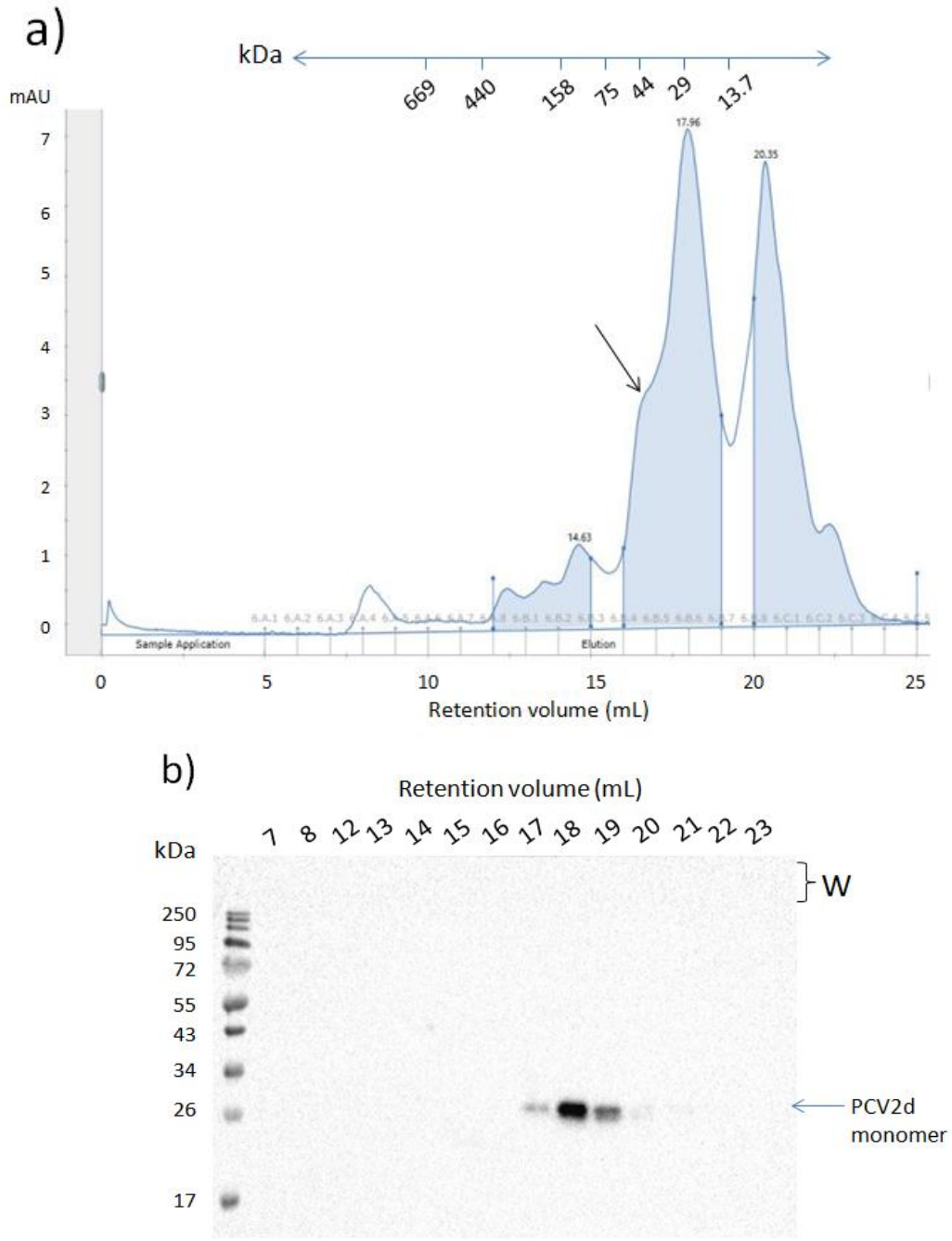

Figure 41. Gel filtration chromatography of PCV2d-PCV3 WT protein species. A preparation of soluble CIEX purified, PCV2d WT protein derived from pARP31 chimeric construct expression was applied to a Superdex 200 Increase 10/300 column and species separated based on size. a) Chromatogram of protein elution fractions by retention volume (mL) against peak intensity (mAU). Arrow indicates "shoulder" peak. b) Anti-PCV2d western blot following non-reducing SDS PAGE of peak elution fractions. Truncated PCV2d WT protein was detected in fractions corresponding to retention volume 17-21 mL, denoted by arrow. Bar denotes estimated molecular weights based on calibration curve.

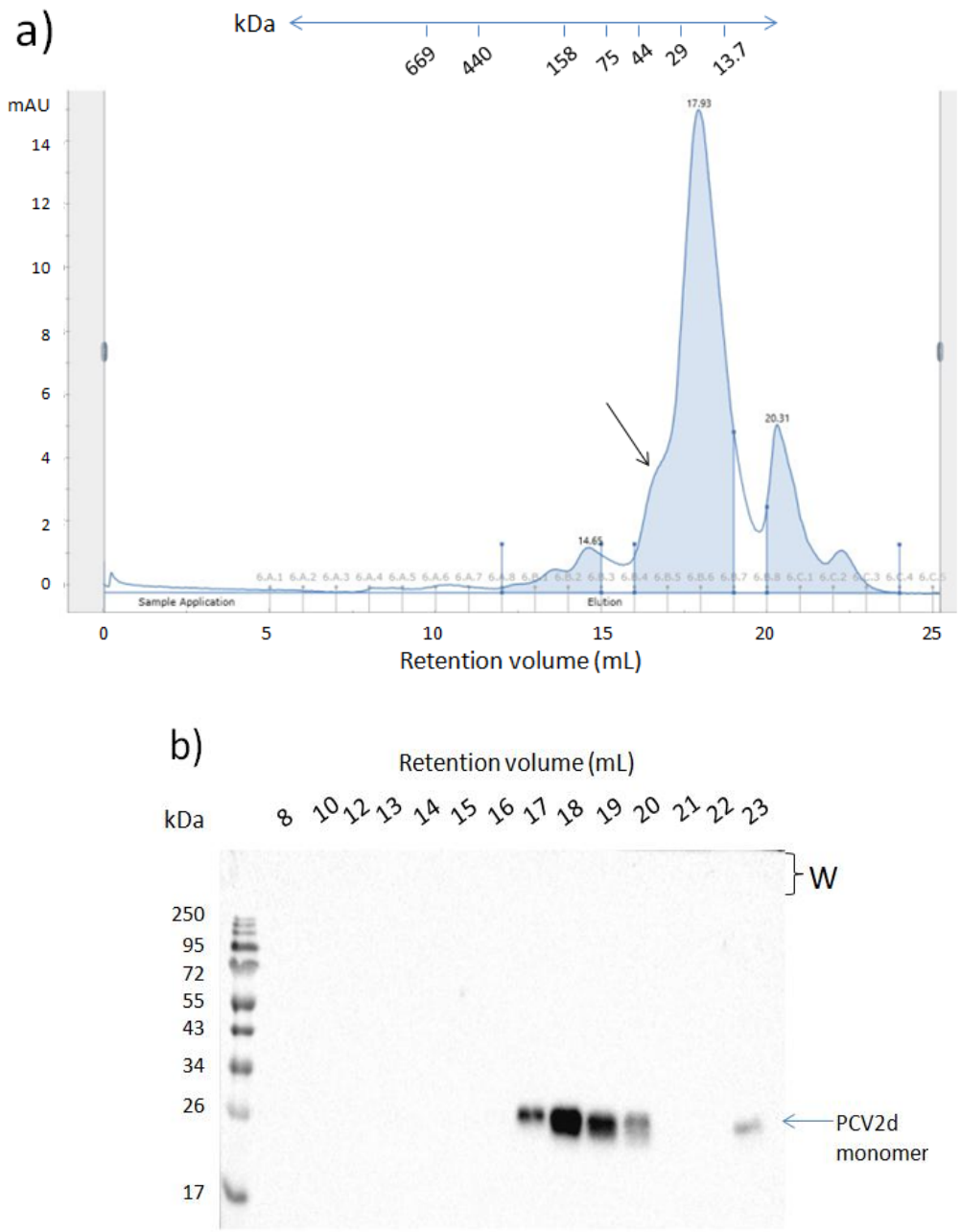

Figure 42. Gel filtration chromatography of PCV2d(C108S)-PCV3 protein species. A preparation of soluble CIEX purified, PCV2d(C108S) protein derived from pARP41 chimeric construct expression was applied to a Superdex 200 Increase 10/300 column and species separated based on size. a) Chromatogram of protein elution fractions by retention volume (mL) against peak intensity (mAU). Arrow indicates "shoulder" peak. b) Anti-PCV2d western blot following non-reducing SDS PAGE of peak elution fractions. Truncated PCV2d(C108S) protein was detected in fractions corresponding to retention volume 17-23 mL, denoted by arrow. Bar denotes estimated molecular weights based on calibration curve.

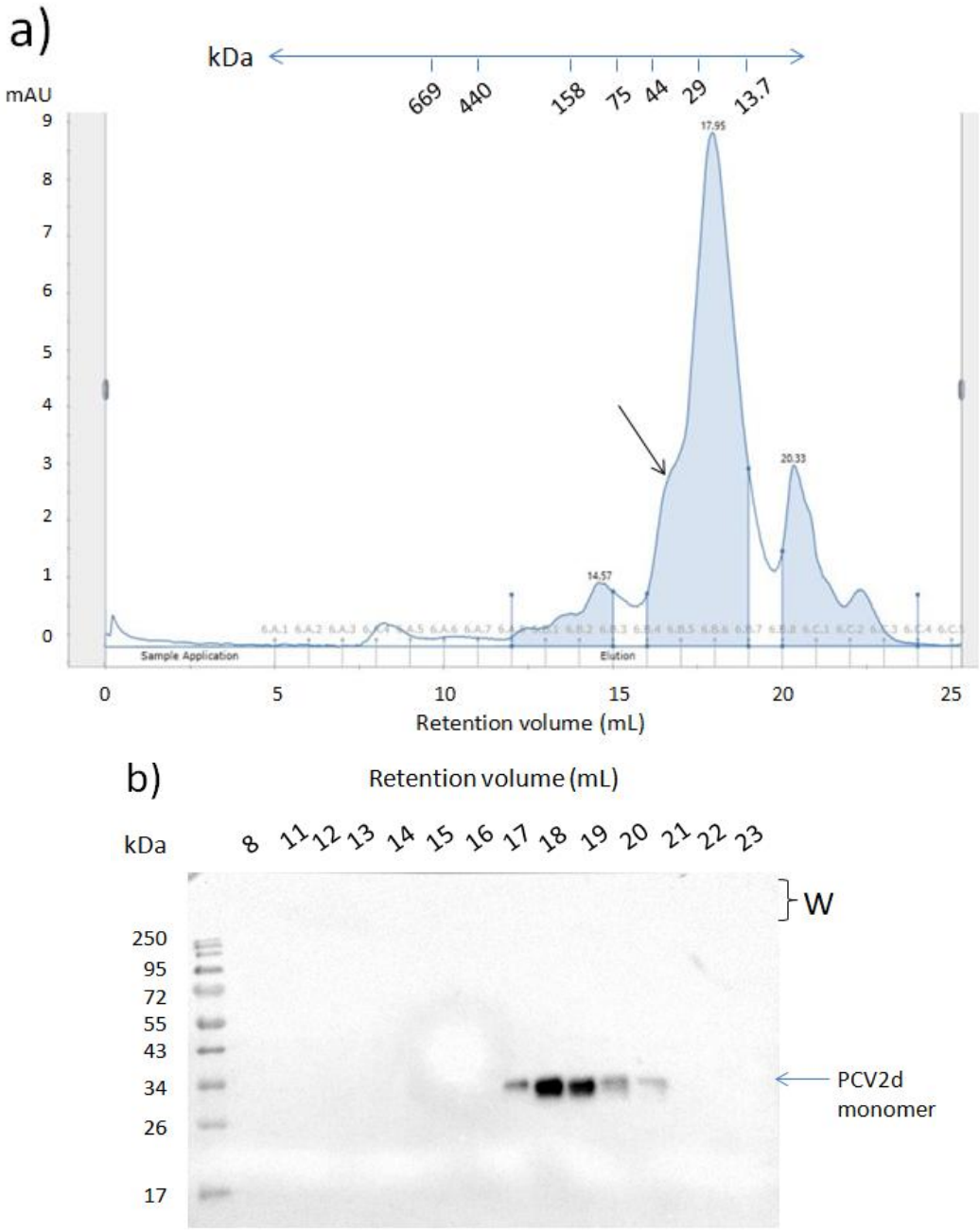

Figure 43. Gel filtration chromatography of PCV2d(C108A)-PCV3 protein species. A preparation of soluble CIEX purified, PCV2d(C108A) protein derived from pARP42 chimeric construct expression was applied to a Superdex 200 Increase 10/300 column and species separated based on size. a) Chromatogram of protein elution fractions by retention volume (mL) against peak intensity (mAU). Arrow indicates "shoulder" peak. b) Anti-PCV2d western blot following non-reducing SDS PAGE of peak elution fractions. Truncated PCV2d(C108A) protein was detected in fractions corresponding to retention volume 17-21 mL, denoted by arrow. Bar denotes estimated molecular weights based on calibration curve.

Gel filtration of soluble PCV2d as a degradation product from expression of the PCV2d-PCV3 chimeric protein showed rather a wider range of peaks in comparison to the PCV2d proteins that had been expressed alone, although none of them were detected by PCV2d antibody upon immunoblotting other than in the major two peaks corresponding to 17 – 21 mL retention volume. As with PCV2d derived from single constructs, the major peak at 17.95 mL contained monomeric PCV2d protein. All three chromatograms purifying PCV2d-PCV3 proteins whether WT or Cys mutants showed a clear "shoulder" peak to the left of the major PCV2d peak, indicating a slightly higher molecular weight species; it is hypothesised that this heterogeneous protein content could be indicative of multiple PCV2d species formed from proteolytic cleavage of the chimera protein at alternate sites. In addition, where dimerization was seen following SDS PAGE sample preparation for PCV2d WT protein expressed alone, PCV2d derived from PCV2d-PCV3 chimera did not show the same dimerization potential; this was the case in all derivatives of the chimeric protein, that being the wild type truncated PCV2d protein, PCV2d(C108S) or PCV2d (C108A).

For further confirmation that no VLP formation was occurring, samples of PCV2d WT, PCV2d(C108S), PCV2d(C108A) proteins purified by CIEX without DTT were prepared for visualization by transmission electron microscopy (TEM) by Ian Brown at the Microscopy Facility, University of Kent. Protein samples were supplied at a concentration of 0.05 - 0.1 mg/mL. Each of the samples were treated by negative staining alone; another set of samples were treated by immunogold-labelling, where proteins were probed using various dilutions of the PCV2d-specific antibodies generated from rabbits in Chapter 3, which had been tagged with gold particles 5 nm in diameter, followed by negative staining.

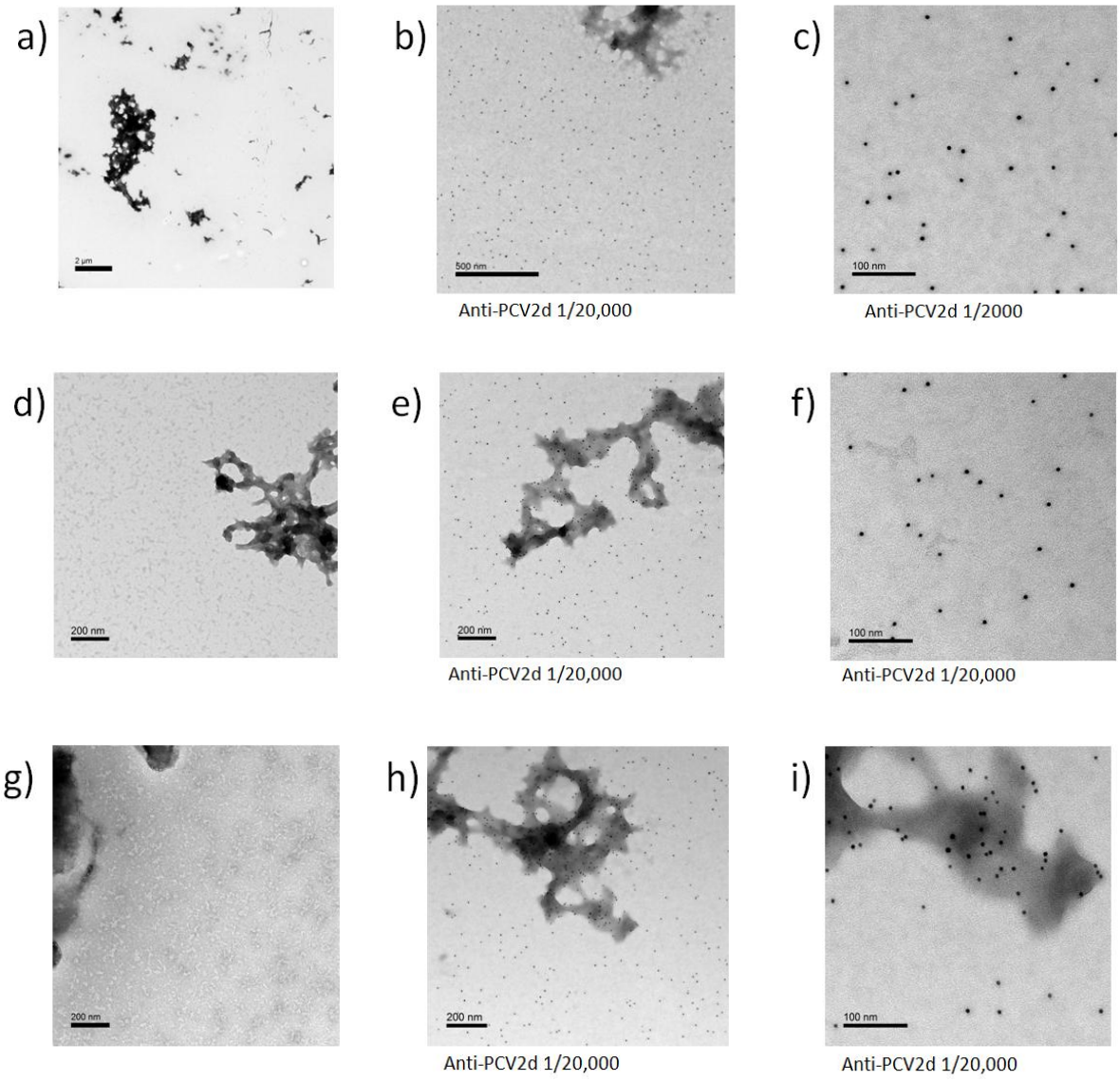

Figure 44. TEM imaging of purified PCV2d WT, PCV2d(C108S), PCV2d(C108A) proteins by negative staining and immunogold labelling. CIEX purified preparations of PCV2d WT and cysteine mutant proteins were fixed to carbon/formvar-coated mesh grids and subjected to negative staining only, or immunogold labelling using PCV2d-specific antibody tagged with 5 nm gold particles, followed by negative staining. a) Negative staining of PCV2d WT. b) Immunogold labelling of PCV2d WT using a 1/20,000 dilution of anti-PCV2d. c) Immunogold labelling of PCV2d WT using a 1/2000 dilution of anti-PCV2d (magnified). d) Negative staining of PCV2d(C108S). e) Immunogold labelling of PCV2d(C108S) using a 1/20,000 dilution of anti-PCV2d. f) Immunogold labelling of PCV2d (C108S) using a 1/20,000 dilution of anti-PCV2d (magnified). g) Negative staining of PCV2d(C108A). h) Immunogold labelling of PCV2d(C108A) using a 1/20,000 dilution of anti-PCV2d. i) Immunogold labelling of PCV2d(C108A) using a 1/20,000 dilution of anti-PCV2d (magnified).

Unfortunately, it was not possible to generate a positive control sample containing PCV2d VLPs for this experiment due to the difficulty of obtaining a sufficient yield of full length, correctly folded PCV2d WT protein in *E. coli.* As such, the samples were instead investigated simply for the presence of soluble protein clusters, which would be expected at around 18 – 20 nm in size if indicative of a VLP.

Many of the TEM images from all samples depicted irregular shaped dark patches which could indicate protein aggregates. Samples that had been negative stained only tended to show a fairly uniform appearance of "background noise" which can be attributed to monomers or small clumps of protein forming due to a high concentration, and the previously mentioned tendency of PCV2d protein to precipitate out of solution when concentrated. Immunogold labelling of PCV2d(C108A) protein indicated congregation of gold particles in dark regions, where a black dot indicates a single gold particle, further suggesting the presence of protein aggregates (Fig. 44i). Other than this, it was concluded that there was no indication of small soluble oligomers forming at the expected size of PCV2d VLPs. This was most clear in immunogold labelled samples which, other than aggregates, appeared to depict antibody binding to proteins at a relative distance from one another. It should be noted that the concentration of protein was quite high in the samples and was not saturated by antibody binding. Ideally a positive control containing visible VLPs would be used for a definitive conclusion to be made.

5.2.3 Preparation of PCV2d WT and PCV2d(C108S) mutant proteins for a mouse immunisation study

By this point in the research, a process for the production and purification of a large amount of high purity PCV2d protein had been developed; but a live animal trial was needed to test the efficacy of our PCV2d antigens in raising an immune response. In order to do this, a mouse immunisation study was planned and mice sourced. The PCV2d cysteine mutant proteins had presented a potentially promising method of producing recombinant PCV2d capsid protein for vaccination whilst avoiding undesirable dimerization or oligomerisation as may have posed an issue using the WT protein. Samples of CIEX purified PCV2d WT and PCV2d(C108S) proteins were prepared to compare their efficacy in mice.

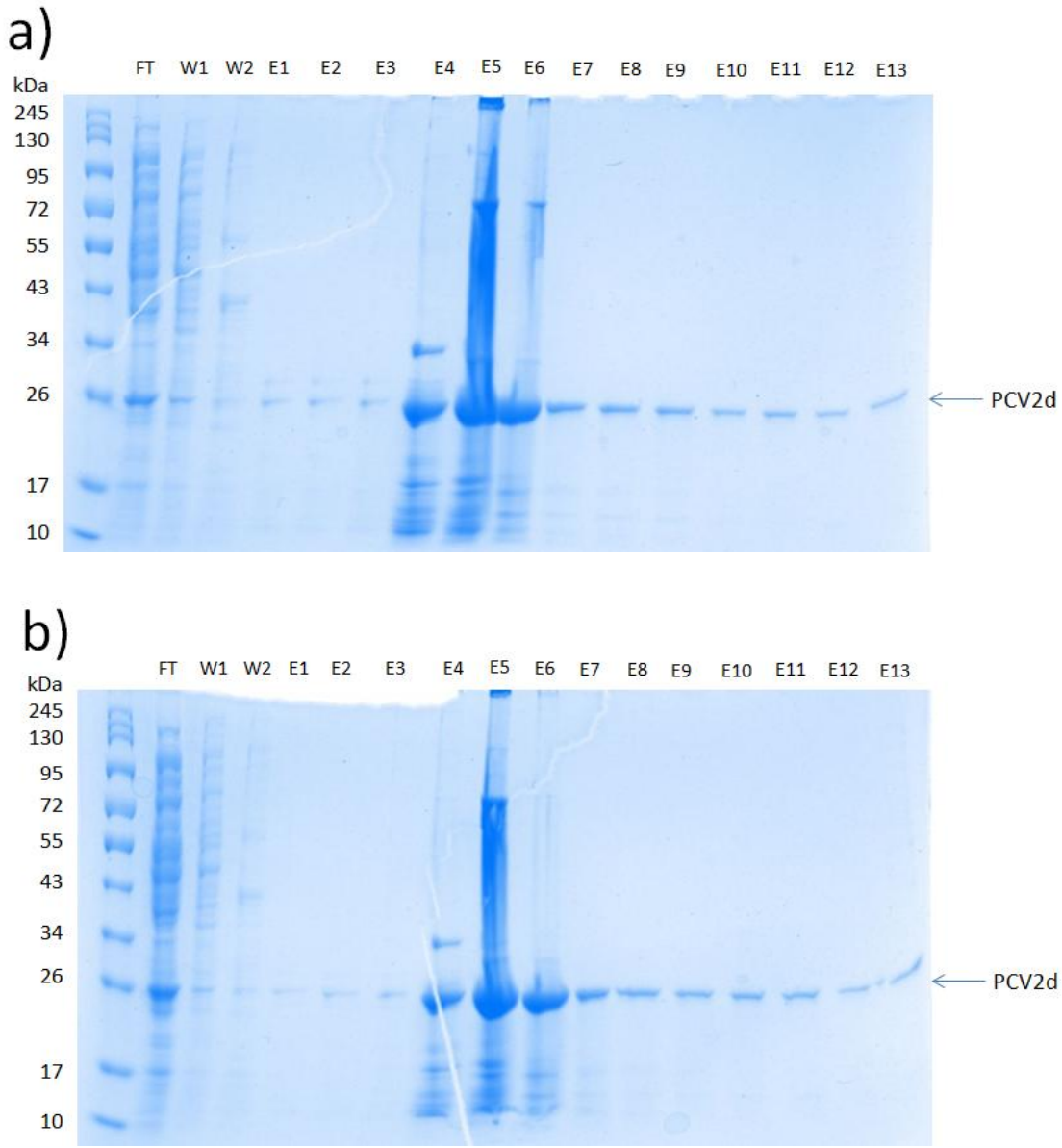

Figure 45. Purification of cell lysates from BL21 cells expressing PCV2d WT and C108S proteins at shake flask by CIEX. A 400 mL BL21 culture was grown in LB medium at shake flask and induced with 100 µM IPTG, then grown for a further 21 hours. Following cell harvest, soluble fractions from cells expressing a) PCV2d WT protein and b) PCV2d(C108S) protein were separated by centrifugation and the supernatant applied to a 5 mL HiTrap™ SP column and the flow through collected (FT). The column was washed with 50 mM Tris-HCl, pH 7.0 (W1), followed by 50 mM Tris-HCl, 450 mM NaCl, pH 7.0 (W2) then bound proteins were eluted using 50 mM Tris-HCl, 900 mM NaCl, pH 7.0 buffer (E1 – E13). Fractions were separated by SDS PAGE then visualised with Coomassie Brilliant Blue.

The majority of purified protein eluted between fractions E4 and E6, also showing some protein had not migrated from the wells of the gel and some smearing was observed in E5 lanes on both gels, likely due to high protein concentration. Multiple low molecular weight species of <26 kDa were detected in these fractions, along with an unidentified band around 72 kDa. A contaminating band was also visualised at around 34 kDa in E4. After CIEX purification, it was necessary to transfer the eluted proteins into an osmotically suitable buffer both for immunisation into mice and also to maintain the stability of the protein, so peak fractions E4 – E6 were dialysed into PBS, adjusted to pH 7.0.

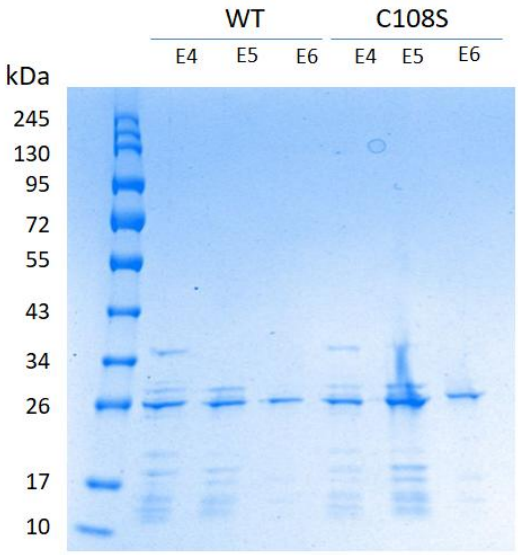

Figure 46. Purity of PCV2d WT protein and PCV2d(C108S) protein following dialysis. Peak fractions of soluble PCV2d WT protein and PCV2d(C108S) proteins from CIEX were dialysed into PBS pH 7.0. Following dialysis, samples were separated by SDS PAGE then visualised with Coomassie Brilliant Blue.

SDS PAGE analysis of protein samples following purification and dialysis showed all elutions to be relatively free from impurities and of similar protein concentrations. E4 elution fractions still showed the presence of a contaminating protein around 34 kDa in size. E5 fractions retained a sufficiently high concentration of protein whilst being relatively pure, thus E5 fractions were chosen for transfer to our collaborators at Biotec (Thailand) for mouse immunisation.

The mouse study consisted of four groups each containing 6 mice; two of the groups were immunised with either a sample of purified PCV2d WT antigen or PCV2d(C108S) antigen as generated in the previous experiment. One group was immunised with a sample of PCV2d WT protein that had been expressed in *Ogataea thermomethanolica* (OT), a species of thermo-tolerant yeast which is able to secrete heterologous proteins to the extracellular space for improved downstream processing. A control group of mice was immunised with PBS solution.

Samples of serum from the mice were taken at day 0 of the experiment immediately prior to immunisation and again and day 28 and 35 following immunisation. Efficacy of the raised antibodies was analysed by enzyme-linked immunosorbent assay (ELISA) in which serum samples were applied to ELISA plates coated with either recombinant PCV2d capsid protein or with live PCV2d virus particles, where viral titers were calculated as fluorescent focus units (FFU). Following incubation with mouse sera, plates were incubated with HRP-conjugated mouse-specific polyclonal antibodies for detection of antibody binding by absorbance at 450 nm in an ELISA plate reader.

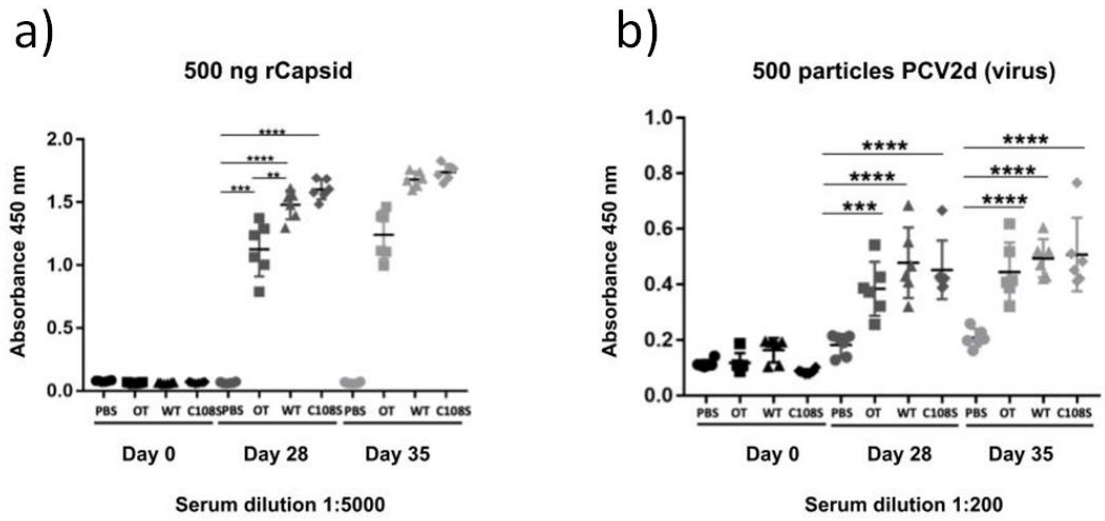

Figure 47. ELISA assay of serum taken from mice immunised with PCV2d antigen. a) ELISA plates were coated with 500 ng recombinant PCV2d capsid protein. Serum taken from immunised mice at day 0, 28 or 35 was added to the ELISA assay at a dilution of 1:5000. b) ELISA plates were coated with 500 FFU of PCV2d virus. Serum taken from immunised mice at day 0, 28 or 35 was added to the ELISA assay at a dilution of 1:200. Absorbances were measured at 450 nm. PBS: negative control; OT: PCV2d expressed in *Ogataea thermomethanolica* (OT); WT: *Δ2-40*PCV2d expressed in *E. coli*; C108S: *Δ2-40*PCV2d(C108S) mutant expressed in *E. coli.* Probability values: **, $p < 0.005$; ***, $p < 0.0005$; ****, $p < 0.0001$.

In the ELISA experiment using recombinant PCV2d capsid protein, none of the mice groups showed any reactivity at day 0 before immunisation. At timepoints after immunisation, serum from all mice immunised with a PCV2d antigen of any derivative showed binding to the recombinant PCV2d protein, while the PBS controls showed none. Mouse groups immunised with WT and C108S derivatives of PCV2d antigen from *E. coli* showed slightly higher recognition of the recombinant PCV2d protein in comparison to mice immunised with PCV2d antigen derived from

OT. The ELISA experiment using PCV2d virus particles showed somewhat less clear results. At day 0, all mice serum showed some, albeit low level of binding to virus particles. Serum samples taken from PBS control mice on day 28 or 35 maintained this low level of background signal. Serum samples from mice groups immunised with any derivatives of PCV2d antigen showed higher reactivity with the PCV2d virus, indicating induction of PCV2d virus-specific antibodies post-immunisation by relevant antigens.

The ELISA assay showed detection of PCV2d-specific binding antibodies in immunised serum samples only. To provide further evidence for induction of neutralising antibodies, the cell-based virus neutralisation assay was performed using antibodies from mouse serum taken at day 0, 28 and 35. As detailed in Chapter 2, DAPI stain was used to identify cell nuclei and the numbers of infected cells identified by concurrence of DAPI- and Alexa488-positive nuclei were scored on a high-content screening system. Undiluted serum produced some fluorescent background signal (green) but this did not coincide with DAPI staining (blue) so was not counted as infected cells. Using the scored number of infected cells, percent infection was plotted.

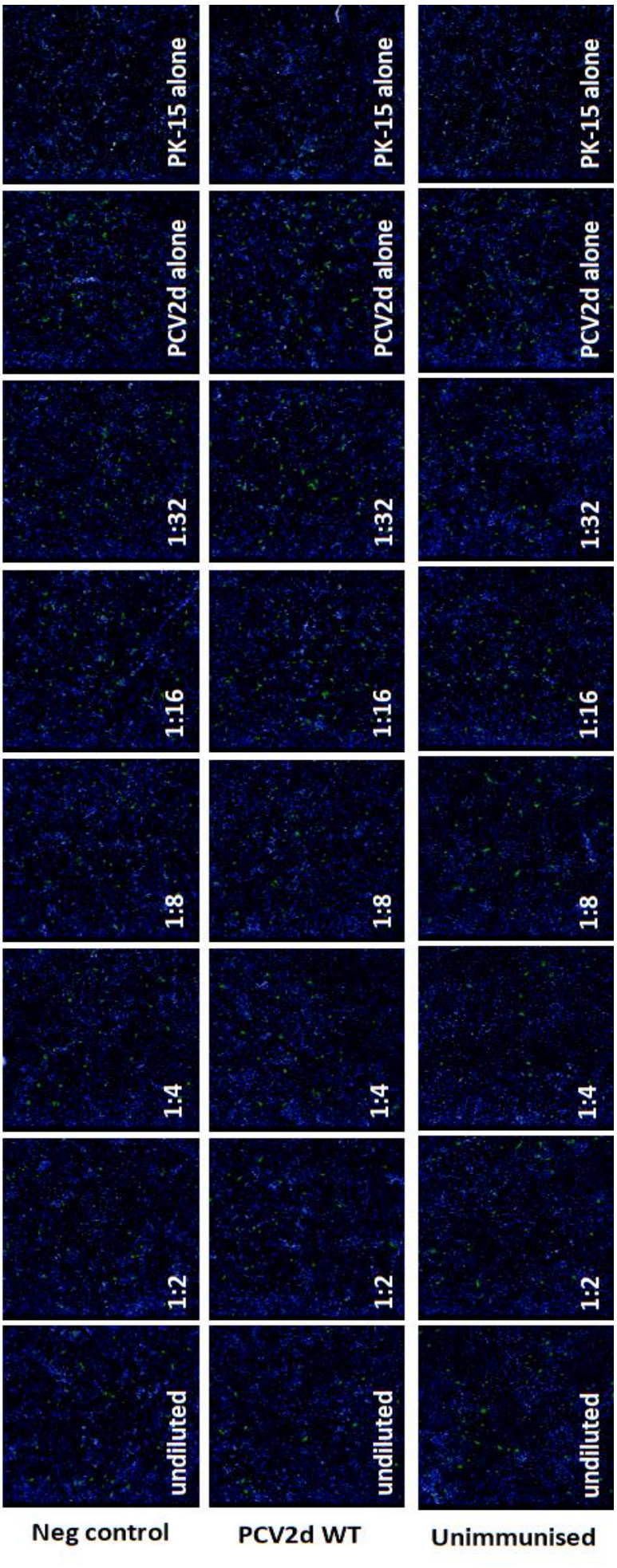

Figure 48. Immunofluorescence viral neutralisation assay using PK-15 cells with PCV2d-immunised mouse serum. Harvest bleed serum taken from mice immunised with PBS solution (Neg control), mice immunised with recombinant PCV2d WT capsid protein (PCV2d WT) or unimmunised mice (Unimmunised) was mixed with PCV2d virus particles, using undiluted serum or serum diluted to a ratio of 1:2, 1:4, 1:8, 1:16 or 1:32 then infected into PK-15 cells. Following incubation, PK-15 cell cultures were probed with immunofluorescent Alexa488-labelled anti-rabbit antibody to detect PCV2d infected cells indicated by green fluorescent foci. Controls were performed using uninfected PK-15 cells (PK-15 alone) and by infecting PK-15 cells with PCV2d virus particles not mixed with mouse serum (PCV2d alone).

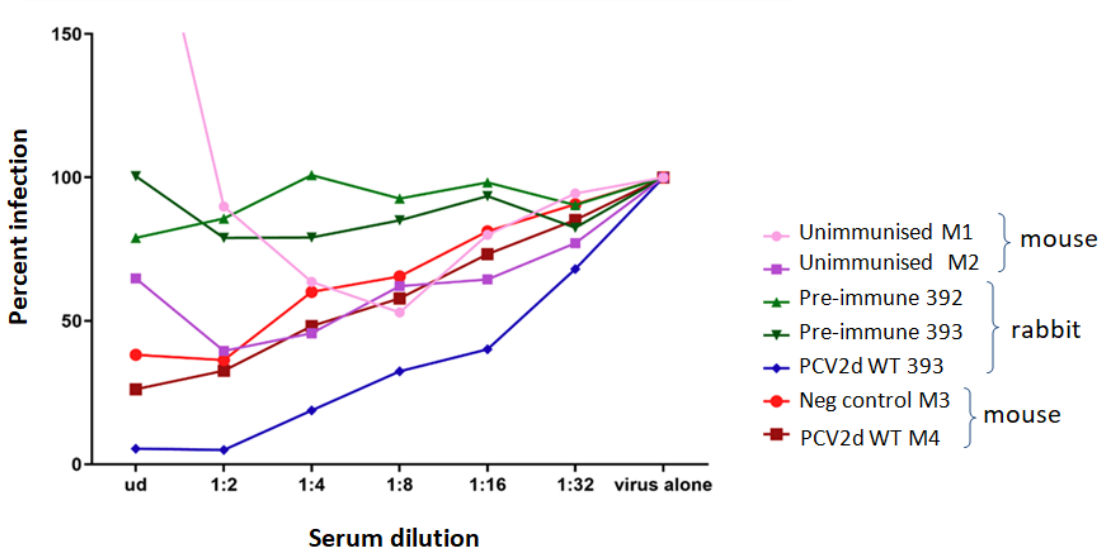

Figure 49. Percentage infection of PK-15 cells with PCV2d virus following incubation with mouse or rabbit serum. Immunofluorescence data from cell-based virus neutralisation assay was plotted. Serum samples used in generating this data were labeled as follows: Unimmunised M1: unimmunised mouse; Unimmunised M2: unimmunised mouse; Pre-immune 392: unimmunised rabbit CRB392; Pre-immune 393: unimmunised rabbit CRB393; PCV2d WT 393: test bleed from PCV2d-immunised rabbit, CRB393; Neg control M3: PBS control mouse; PCV2d WT M4: recombinant PCV2d-immunised mouse. Where PK-15 cells had been infected with PCV2d virus particles not mixed with mouse/rabbit serum (virus alone), this was used as the value for 100 % infection.

In order to compare between animal models, percent infection of PK-15 cells exposed to PCV2d virus particles mixed with rabbit serum as shown in neutralisation assays in Chapter 3, was also calculated and plotted for percentage infection (Fig. 48). Pre-immune sera from CRB392 and 393 rabbits both demonstrated little protection from viral infection, showing percentage infection of over 75 % at all serum dilutions as expected, while PCV2d WT 393 serum from CRB393 rabbit immunised with recombinant PCV2d capsid protein conferred the most protection to PK-15 cells against PCV2d viral infection, wherein only approximately 5 % of PK-15 cells showed infection with PCV2d virus following treatment of the cells with this serum undiluted or at 1:2 dilution. Infection percentage was strongly correlated to serum dilution for this serum. This data indicated that in rabbit serum samples, there was no non-specific inhibition of PCV2d infection.

On the other hand, control group unimmunised M1 mouse serum was able to protect against PCV2d viral infection, showing approximately 40 % infection of PK-15 cells when the unimmunised mouse serum was mixed at 1:2 dilution; as this sample was used as a negative control with no

PCV2d-specific antibodies, a percentage infection nearing 100 % would have been expected, comparable to the virus alone condition. Similarly, unimmunised M2 mouse serum was able to protect against infection, showing around 50 % infection of PK-15 cells when used at its optimal dilution of 1:8, in comparison to the virus alone. Neg control M3 serum taken from a mouse immunised with PBS showed comparable protection to PK-15 cells as unimmunised M2 when used at a 1:2 dilution. PCV2d WT M4 mouse immunised with recombinant PCV2d capsid protein showed only a slight reduction in PK-15 cell percentage infection with PCV2d virus compared to the three mouse control groups M1-3, and demonstrated that infection percentage was strongly correlated to serum dilution, where increased dilution of the serum lead to less protection against infection. However, this protection activity appears to be independent of PCV2d-specific antibodies, as the PBS-immunised mouse serum containing no PCV2d-specific antibody (from ELISA results) still displayed protection, the difference being almost indistinguishable when compared with mouse sera containing high levels of PCV2d-specific antibody. The cause of this interference is so far not understood. Heat inactivation, treatment with protease inhibitors, or changing cell types did not alleviate this problem. Notably, this is only specific to serum samples from mice.

Due to the results from the control mice groups indicating some level of pre-existing immunity to PCV2d virus that may already be present in their serum, it was determined the best course was to raise specific antibodies in rabbits to PCV2d(C108S) mutant protein and use this serum for analysis in a cell-based virus neutralisation assay instead, to accurately compare the neutralising activity of the mutant PCV2d protein to that of the wild type without confounding factors.

5.2.4 Generation of PCV2d Cys mutant antibody for neutralisation assay

A preparation of PCV2d(C108S) protein was generated in a large shake flask experiment followed by extraction and purification by CIEX. Peak elution fractions were transferred as previously to Cambridge Research Biochemicals where two rabbits, L92 and L93, were immunised with the protein. Again, each rabbit was immunised with 0.1 mg of the antigen at weeks 1, 3, 5, 7 and 9. Blood samples were taken at weeks 4, 6 and 8 (test bleeds 1, 2 and 3 respectively) and the final harvest bleed was obtained at week 10. Samples of test bleeds were testing by western blotting for specificity.

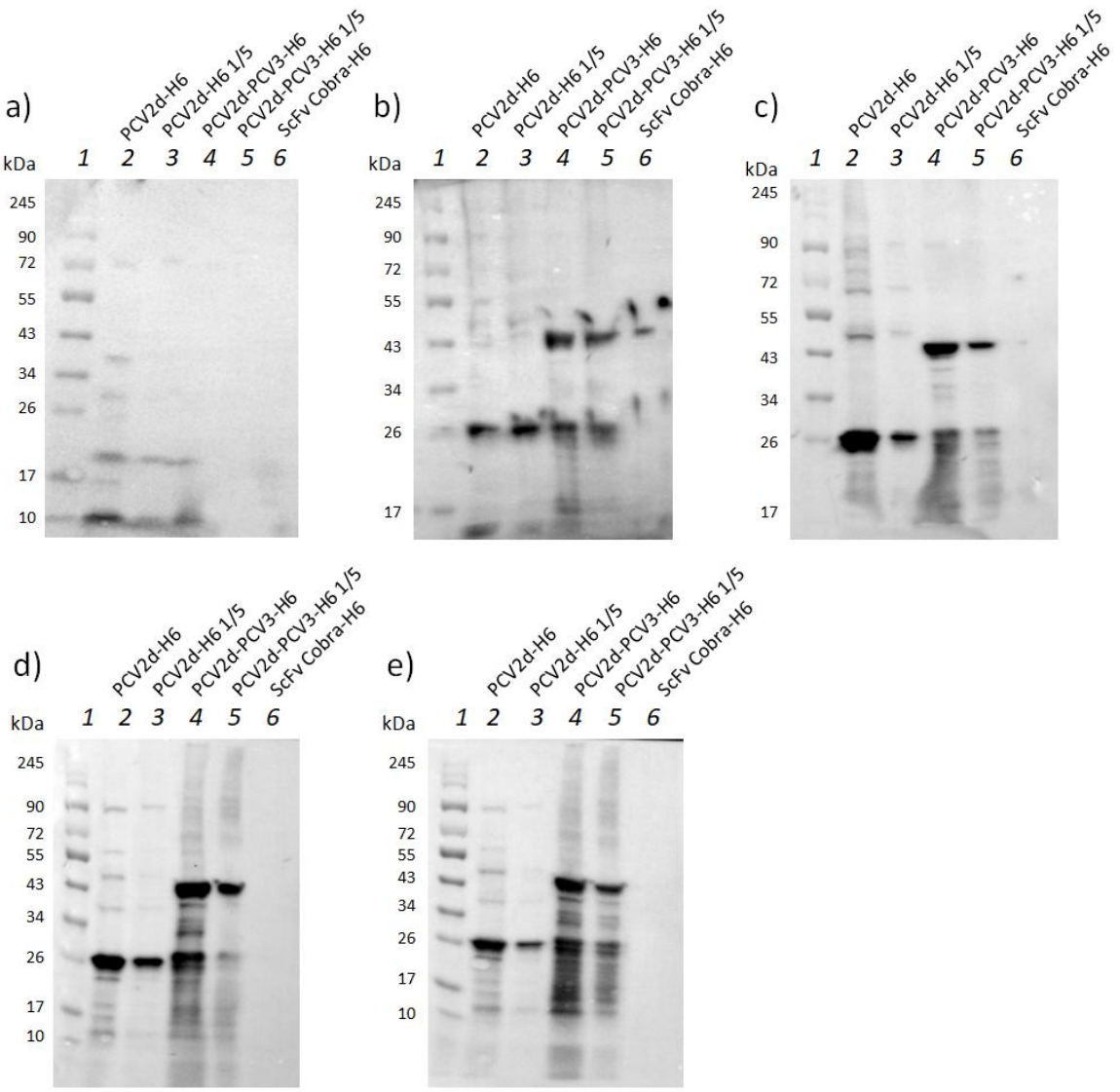

Figure 50. <u>Western blots using test serum from L92 rabbit immunised with PCV2d(C108S) protein.</u> After blocking in 5 % milk with PBS tween, blots were incubated in a) pre-immune serum; b) test bleed 1; c) test bleed 2; d) test bleed 3; e) harvest bleed. Following this, blots were incubated in anti-rabbit secondary antibody. Lane 1: Protein marker; lane 2: Soluble fraction from *E. coli* cells expressing PCV2d-H6; lane 3: As lane 2, 1/5 dilution; lane 4: Insoluble fraction from *E. coli* cells expressing PCV2d-PCV3-H6; lane 5: As lane 4, 1/5 dilution; lane 6: Periplasmic fraction from *E. coli* cells expressing ScFv-Cobra-H6 (negative control).

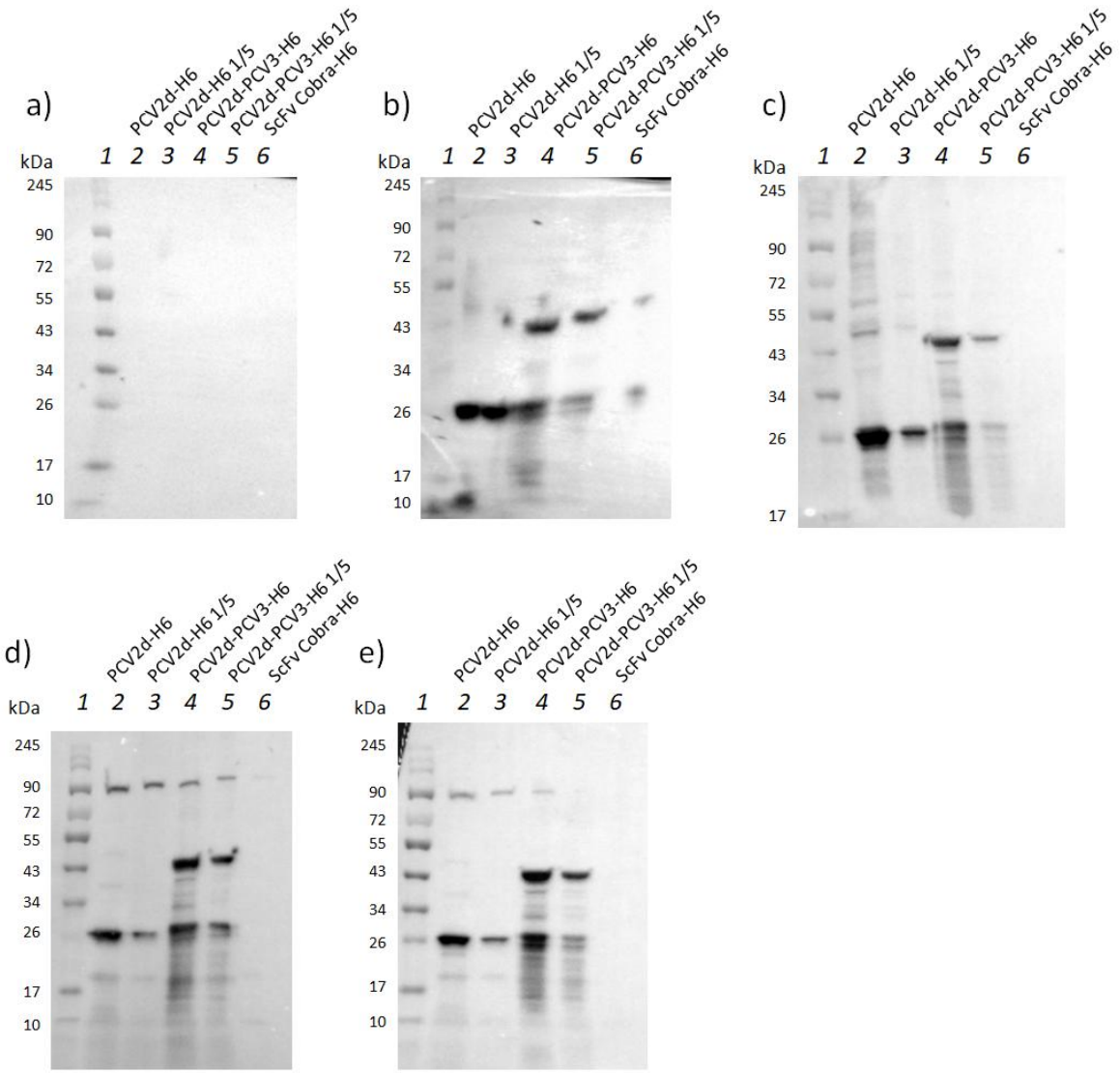

Figure 51. Western blots using test serum from L93 rabbit immunised with PCV2d(C108S) protein. After blocking in 5 % milk with PBS tween, blots were incubated in a) pre-immune serum; b) test bleed 1; c) test bleed 2; d) test bleed 3; e) harvest bleed. Following this, blots were incubated in anti-rabbit secondary antibody. Lane 1: Protein marker; lane 2: Soluble fraction from *E. coli* cells expressing PCV2d-H6; lane 3: As lane 2, 1/5 dilution; lane 4: Insoluble fraction from *E. coli* cells expressing PCV2d-PCV3-H6; lane 5: As lane 4, 1/5 dilution; lane 6: Periplasmic fraction from *E. coli* cells expressing ScFv-Cobra-H6 (negative control).

Other than some non-specific binding to what was assumed to be a native *E. coli* protein around 90 kDa when probing with rabbit L93 test bleed 3 and harvest sera, both L92 and L93 rabbit sera showed a high degree of specificity for PCV2d peptides by immunoblotting, indicating mutation of the cysteine residue in the immunised antigen had not interfered with the ability to raise antibodies recognizing WT PCV2d. The next step was to ensure that the mutant antigen retained

the capacity to raise a neutralising antibody response to PCV2d virus. To do this, serum from both rabbits was transferred to Biotec (Thailand) for a cell-based virus neutralisation assay.

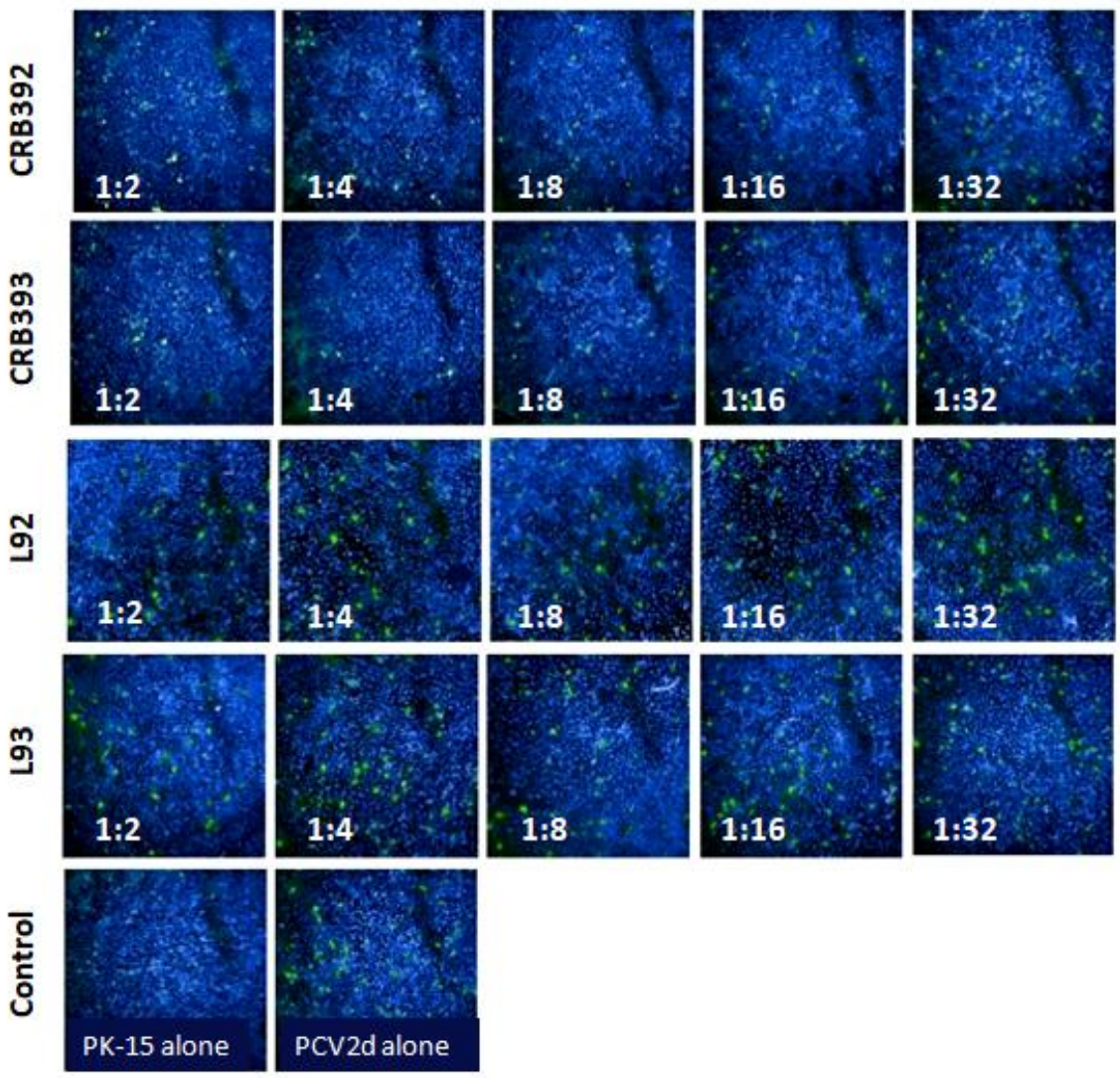

Figure 52. Immunofluorescence viral neutralisation assay using PK-15 cells with PCV2d WT versus PCV2d(C108S)-immunised rabbit serum. Serum taken from L92 and L93 rabbits immunised with PCV2d(C108S) antigen was mixed with PCV2d virus particles, using serum diluted to a ratio of 1:2, 1:4, 1:8, 1:16 and 1:32. The same was performed using serum taken from CRB392 and CRB393 rabbits immunised with PCV2d WT antigen. The virus particles were then infected into PK-15 cells. Following incubation, PK-15 cell cultures were probed with immunofluorescent Alexa488-labelled anti-rabbit antibody to detect PCV2d infected cells indicated by green fluorescent foci. Controls were performed using uninfected PK-15 cells (PK-15 alone) and by infecting PK-15 cells with PCV2d virus particles not mixed with rabbit serum (PCV2d alone).

PK-15 cell cultures infected with PCV2d virus that had been mixed with CRB392 or CRB939 rabbit serum at dilutions of 1:2 up to 1:16 showed a low number of foci indicating infected cells, with slightly more infected cells visible as foci when serum was mixed at 1:32 dilution. However, there were a significantly higher number of foci observed in cell cultures where they had been mixed with L92 or L93 serum from PCV2d(C108S) immunised rabbits at equivalent dilutions; although all serum samples demonstrated some viral neutralizing activity in comparison to the PCV2d virus alone control, immunisation with PCV2d(C108S) antigen was inferior in raising a neutralising antibody response compared to PCV2d WT.

5.3 Conclusions

Initial analysis of PCV2d oligomerisation by non-reducing SDS PAGE indicated PCV2d WT protein was forming a wide range of oligomerisation species when expressed alone. PCV2d WT derived from the chimera protein showed significantly less oligomerisation in comparison. All PCV2d Cys mutant derivatives showed little oligomerisation on non-reducing SDS PAGE, apart from a minor single band around the expected size of a dimer. In gel filtration, a similar trend was observed, wherein PCV2d WT protein expressed alone showed some dimer formation by non-reducing SDS PAGE following elution from the column, suggesting the biochemical environment may play an important role in the potential of the protein to oligomerise. However, under the conditions used for gel filtration, there was no indication that oligomers or dimers were prone to forming. There were also no peaks suggesting any VLP formation was occurring in any of the PCV2d WT or cysteine mutant proteins tested.

ELISA using mice-derived antibodies from unimmunised, control mice showed some reactivity with PCV2d virus particles suggesting the mice may have some innate immunity against PCV2d. This was further supported by neutralisation assay data where serum from unimmunised control mice and PBS-immunised control mice showed a similar level of virus neutralising activity to serum from mice that had been immunised with a PCV2d antigen. Because of this unexpected finding, rabbits, whose pre-immune serum had previously confirmed no innate virus neutralising activity, were immunised with the PCV2d(C108S) antigen. Harvested serum from these rabbits was found to generate a neutralising antibody response to PCV2d virus in a cell-based neutralisation assay but the activity of antibodies raised by PCV2d(C108S) immunisation did not appear to be as strong as that induced by immunisation with PCV2d WT antigen.

Chapter 6: Preparation of a PCV2d vaccine candidate

6.1 Introduction

In previous chapters, it was demonstrated how a highly pure preparation of PCV2d antigen had been obtained from *E. coli* using fed-batch fermentation and a single step cation exchange purification protocol, as analysed by mass spectrometry. The next step of the process development was to formulate this antigen into the first vaccine candidate of the study – and test this in a live animal host. To achieve this, a range of Montanide™ Vaccine Adjuvant Technology formulations were obtained from SEPPIC (Paris, France) to determine their compatibility, stability and effectiveness with the PCV2d antigen.

The adjuvant types obtained from SEPPIC were in particular their sodium polyacrylate gel and oil type immunostimulant adjuvants; many current swine vaccines on the market still contain aluminium adjuvants, the technology for which has not been updated for many years (Rijke, 1997). Since its first use in 1932, aluminium was the only adjuvant in use in licensed vaccines for approximately 70 years and despite its extensive use, the immune mechanism of action remains in question (Marrack et al., 2009). Another early adjuvant attempt containing mineral oil-in-water emulsion, Freund's incomplete adjuvant, is now considered too reactogenic for vaccine use. SEPPIC's Montanide Gel adjuvants contain a dispersion of highly stable gel particles of sodium polyacrylate in water, reporting significant enhancement of the immune response while retaining a safety profile equivalent to aluminium salts (Deville et al., 2012; Wangkaghart et al., 2021). The mechanism of action of these adjuvant types is to improve the recruitment of the innate immune system by the depot effect, achieving slow release of antigen due to the adsorption properties of the polymer (Vialle et al., 2010). They are suitable for use in a wide variety of livestock species and are recommended for inactivated or live vaccines and for parenteral or mucosal administration.

Montanide Water-in-Oil-in-Water (W/O/W) formulations meanwhile are double emulsions consisting a continuous aqueous phase, containing a secondary aqueous phase within droplets of mineral oil. These adjuvants are able to induce short and long-term protective immunity and field trials have demonstrated effective stimulation of both humoral and cell mediated immune responses (Dar et al., 2013; Ibrahim et al., 2015; Park et al., 2014). W/O/W adjuvants are considered most compatible for live inactivated vaccines as well as with recombinant antigens, in addition to being well tolerated and easy to administer in vaccinating cattle, swine and small ruminants via intramuscular injection. Finally, SEPPIC's Montanide Water-in-Oil (W/O)

formulations are continuous oil phase emulsions of non-mineral origin and have been shown to achieve a long-term protective immune response with field trials indicating stimulation of both humoral and cell mediated immune responses (Fox et al., 2012; Klimka et al., 2015). These adjuvants types are commonly used in swine, fish and poultry via intramuscular injection and are compatible with live inactivated and recombinant antigens.

Two types of gel adjuvants were trialled, gel 01 (PR 36067D) and its successor, gel 02 (PR 36084X). In addition, two types of W/O/W adjuvants were used, which were ISA 206 (VG 36022E) and its successor, ISA 201 (VG 36075M). A W/O adjuvant ISA 660 (VG 80274Q) was also tested.

To formulate the vaccine, an aqueous phase containing the desired antigen must be emulsified with the adjuvant under specific conditions and process which can vary widely depending on adjuvant type.

Adjuvant	Type	Ratio Adj/Aqu phase (v/v)	Mixing requirements
Montanide™ Gel 01 PR 36067D	Gel	55/45	Low shear agitation
Montanide™ Gel 02 PR 36084X	Gel	54/46	Low shear agitation
Montanide™ ISA 201 VG 36075M	W/O/W	55/45	Low shear agitation, highly temperature dependent
Montanide™ ISA 206 VG 36022E	W/O/W	54/46	Low shear agitation, highly temperature dependent
Montanide™ ISA 660 VG 80274Q	W/O	64/36	High shear energy and two step emulsification

Table 17. Preparation requirements of Montanide adjuvants for emulsification with an antigen. Adj/Aqu phase: Adjuvant to aqueous phase ratio by volume.

While analysing the stability and efficacy of a vaccine candidate using *in vitro* methods is an essential first step in optimisation and eventual commercialisation, *in vivo* animal studies using a live host organism provide a wealth of information in early stage vaccine development. Although results from the cell-based assay presented in Chapters 3 and 5 indicated that the PCV2d antigen was able to stimulate a strong neutralising antibody response, there are many factors that require optimisation for vaccination and these can only be elucidated in a live animal trial. Administration of a new vaccine candidate must be analysed for adverse reactions in the live animal, including undesirable side effects caused by the antigen or the adjuvant, such as localised reactions at the injection site or indeed systemic reactions. Reactivity at the injection site can be in part accounted for by the adjuvant used and its mechanism of immune stimulation and therefore can be minimized by choosing a highly refined adjuvant type. Choosing an appropriate antigen dosage

can meanwhile be a delicate balancing act between minimizing adverse reactivity and ensuring a sufficiently strong immune response; two of the main considerations which must be clarified by a live animal trial are the vaccine's potential to raise a specific antibody response against the antigen, which is analysed by serology, and the speed with which the host's immune system is able to activate this following challenge with the live virus – in large determined by the adjuvant's ability to stimulate an effective cell-mediated immune response upon vaccination. Further to this, analysing the effectiveness of the immune response on clearance of the virus is essential. Viral clearance in a live animal trial can be measured by quantifying the viral titer in circulation by serology, and also the titer of virus expelled via routes of transmission; both of these measures are indicative of the capability of the vaccine to raise a neutralising antibody response to facilitate rapid viral clearance and reduce transmissibility of the infection.

In this chapter, we present the development of an optimised PCV2d vaccine candidate for short and long term emulsion stability and analyse the vaccine's suitability in a live animal trial.

6.2 Results

6.2.1 Choosing an appropriate adjuvant for a PCV2d vaccine candidate

To determine a suitable adjuvant for formulation with purified PCV2d antigen obtained from *E. coli* expression, the five adjuvants obtained from SEPPIC were emulsified with the antigen at laboratory scale, to be stored and monitored for short and long term stability as an indicator of suitability and compatibility for the application and with the antigen. Stability analyses of the vaccine emulsions over time were classified by a combination of visual checks, and regular drop testing where applicable. A stable emulsion for all adjuvant types is classified by a uniform appearance without any separation of phases or distinction of layers. For gel emulsions, a non-critical defect was classified if any gel sedimentation was present, whereas a critical defect was characterized by the emulsion displaying increasing opacity over time, indicating incompatible interactions with the antigen. For emulsions formulated with W/O/W adjuvants, a non-critical defect was classified if any separation of phases was present providing they could be re-homogenized and any oil layer did not exceed 10 % of the total volume; alternatively, very small to small aqueous phase breakages appearing on the bottom of the vial were also classified as non-critical defects, although these cannot be re-homogenized, provided the breakage did not progress to a critical defect. A critical defect was characterized by complete separation of phases that could not be re-homogenized, such as aqueous phase breakages leading to a water layer of >1 % of the total volume or an oil layer >10 % of the total volume. A failed drop test was also indicative of a critical defect; the drop test was performed by dropping a small volume of the emulsion from a height into a beaker of water, observing the phase separation. For a successful

W/O/W drop test, the oil phase remains on the surface of the water while the aqueous phase should diffuse into the water. If either of these phase separations did not occur, the drop test was considered a failure. Similarly, for emulsions formulated for W/O adjuvants the visual checks determined separation of an oil layer or sedimentation to be non-critical defects, but provided any oil layer did not exceed 30 % of the total volume and could be re-homogenized; tiny aqueous phase breakages appearing on the bottom of the vial were also classified as non-critical defects but progression in the breakage would be determined a critical defect. Emulsions displaying critical defects cannot be salvaged. Drop testing was also used to determine stability of W/O emulsions, in which a successful drop test was classified by the drop remaining entirely on the surface of the water, with no diffusion observed. Wherein the drop diffused into the water, the drop test was considered a failure.

For the first trial, emulsions were generated at a small pilot scale of 4 mL with three repeats per condition. A set of control samples was created containing 50 mM Tris-HCl, 150 mM NaCl, pH 7.0 buffer as the aqueous phase, emulsified with the adjuvant phase, while experimental samples contained purified PCV2d antigen derived from expression of *Δ2-40* PCV2d pARP25 construct or soluble cleaved *Δ2-40* PCV2d protein from expression of pARP31 chimeric PCV2d-PCV3 construct as the aqueous phase, at a final concentration of 40 µg/mL. Gel 01 and gel 02 emulsions were formulated using low shear agitation to mix the two phases, while emulsification of W/O/W adjuvants ISA 206 and ISA 201 required low shear agitation to be performed specifically at 31 °C. W/O adjuvant ISA 660 on the other hand required high shear energy along with a two-step emulsification procedure for effective mixing. Emulsions were prepared on day 0 of the trial then left to settle without disturbing for at least one day before the first analysis was performed, storing at 4 °C. Findings are summarized in Table 18.

	Adjuvant/aqueous phases														
	Montanide™ Gel 01 PR 36067D			Montanide™ Gel 02 PR 36084X			Montanide™ ISA 201 VG 36075M			Montanide™ ISA 206 VG 36022E			Montanide™ ISA 660 VG 80274Q		
Day	C	pARP25	pARP31	C	pARP25	pARP31	C	pARP25	pARP31	C	pARP25	pARP31	C	pARP25	pARP31
2	✓	✓	-	✓	✓	✓	✓	✓	✓	✓	✓	✓	✓	✓	✓
7	✓	✓	-	✓	✓	✓	✓	✓	✓	✓	✓	✓	✓	✓	NCD 1/3
13	✓	✓	-	✓	✓	✓	✓	✓	✓	✓	✓	✓	NCD 1/3	✓	NCD 1/3
20	✓	✓	-	✓	✓	✓	✓	✓	✓	✓	✓	✓	NCD 1/3	✓	NCD 1/3
27	✓	✓	-	✓	✓	✓	✓	✓	✓	✓	✓	✓	NCD 1/3	✓	NCD 1/3
45	✓	✓	-	✓	✓	✓	✓	✓	✓	✓	✓	✓	NCD 1/3	✓	NCD 1/3
60	✓	✓	-	✓	✓	✓	✓	✓	✓	✓	✓	✓	NCD 3/3	NCD 3/3	NCD 3/3
76	✓	✓	-	✓	✓	✓	✓	✓	✓	✓	✓	✓	NCD 3/3	NCD 3/3	NCD 3/3
90	✓	✓	-	✓	✓	✓	✓	✓	✓	✓	✓	✓	NCD 3/3	NCD 3/3	NCD 3/3
118	✓	✓	-	✓	✓	✓	✓	✓	✓	✓	✓	✓	NCD 3/3	NCD 3/3	NCD 3/3
164	✓	✓	-	✓	✓	✓	✓	✓	✓	✓	✓	✓	NCD 3/3	NCD 3/3	NCD 3/3
206	✓	✓	-	✓	✓	✓	✓	✓	✓	✓	✓	✓	NCD 3/3	NCD 3/3	NCD 3/3

Table 18. Summary of PCV2d vaccine storage trial #1 with Montanide adjuvants. Gel 01, Gel 02, ISA 201, ISA 206 and ISA 660 adjuvants were tested for storage stability and compatibility with PCV2d antigens purified from *E. coli.* Samples were stored at 4 °C. C: Control containing buffer; pARP25: soluble PCV2d protein derived from expression of pARP25 PCV2d. pARP31: soluble PCV2d protein derived from expression of pARP31 PCV2d-ΔMetPCV3. Emulsion stability classification was performed on three technical repeats where a stable emulsion is indicated by ✓, and defective emulsions are classified as either NCD: Non-critical defect or CD: Critical defect. Number of repeats showing any defect is indicated out of three (/3).

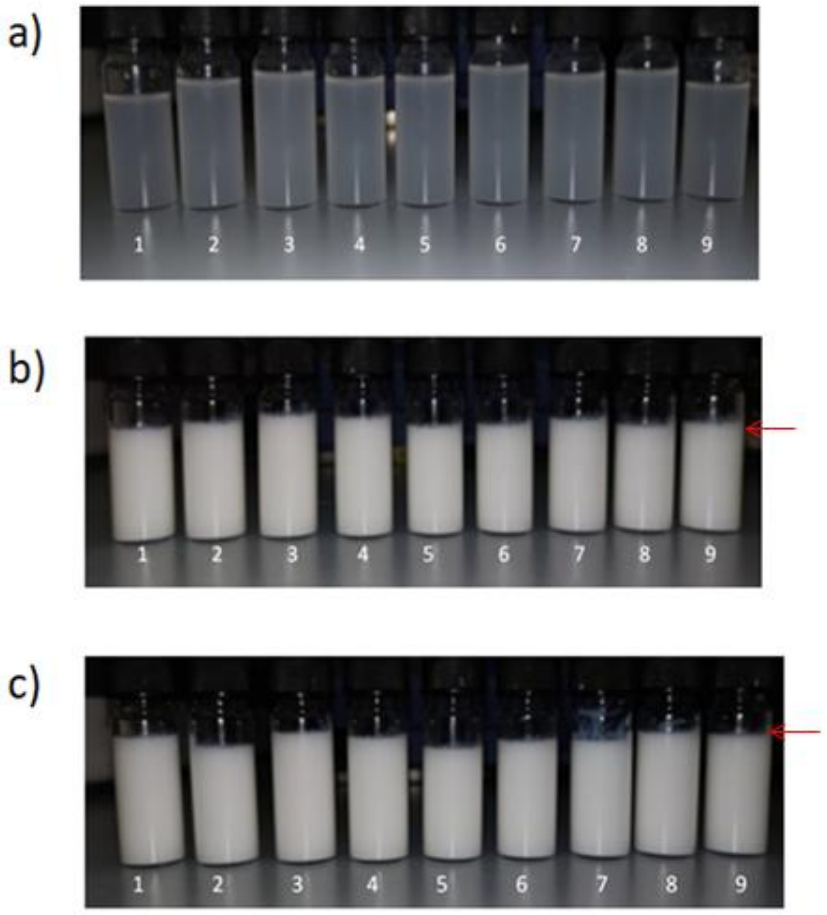

Figure 53. Visual checks for stability of gel 02, ISA 201 and ISA 206 emulsions at day 118 of trial #1. Emulsions formulated with adjuvants a) gel 02 b) ISA 201 and c) ISA 206 were observed for stability following 118 days storage at 4 °C. Samples are labelled as follows: Vials 1-3: Three technical repeats of control samples containing buffer; Vials 4-6: Three technical repeats of samples formulated with soluble PCV2d protein derived from expression of pARP25 PCV2d; Vials 7-9: Three technical repeats of samples formulated with soluble PCV2d protein derived from expression of pARP31 PCV2d-ΔMetPCV3. Arrows indicate small oily layer.

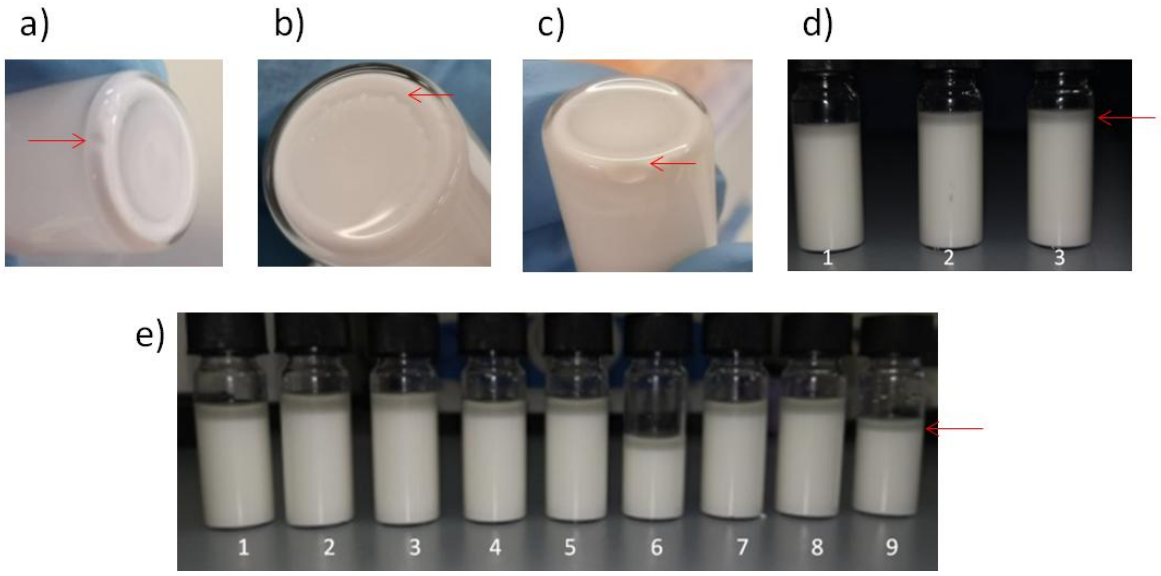

Figure 54. Visual checks for stability of ISA 660 emulsions throughout trial #1. Emulsions formulated with ISA 660 adjuvant were observed for stability at various timepoints throughout the trial period at 4 °C. Defects were noted in sample vials a) Control R2, day 13; small aqueous phase breakage. b) pARP31 R1, day 45; multiple small aqueous phase breakages. c) pARP31 R1, day 60; progressing aqueous phase breakage. d) Control R1-3, day 76; >5 % phase separation. e) Control, pARP25 and pARP31 all repeats, day 164; >10 % phase separation. Vials 1-3: Three technical repeats (R) of control samples containing buffer; Vials 4-6: Three technical repeats (R) of samples formulated with soluble PCV2d protein derived from expression of pARP25 PCV2d; Vials 7-9: Three technical repeats (R) of samples formulated with soluble PCV2d protein derived from expression of pARP31 PCV2d-ΔMetPCV3. Arrows indicate visible defects.

Visual checking throughout the storage time period demonstrated all gel 02, ISA 201 and ISA 206 emulsions were still highly stable at day 118 as shown in Figure 53. The gel 01 and gel 02 emulsions appeared uniformly translucent for the entirety of the trial (Fig. 53a), displaying no defects in either control or PCV2d antigen groups. Emulsions formulated with W/O/W adjuvants ISA 201 or ISA 206 also remained stable for the entirety of the trial, only displaying a very small oily layer forming at the top of the samples from day 45 onwards, which increased at a very slow rate until photographing at day 118 (Fig. 53 b, c).

However, emulsions formulated with W/O adjuvant ISA 660 began to display non-critical defects as early as day 7, where a very small aqueous phase breakage was observed in one of three samples containing PCV2d antigen derived from pARP31 expression. By day 13, one sample in the control group also displayed a similar defect (Fig. 54a). By day 45, some samples began showing multiple small aqueous phase breakages (Fig. 54b). Analysis at day 60 onwards demonstrated

some samples showed growing aqueous phase breakages (Fig. 54c) and all ISA 660 samples in all groups including controls presented an oily layer on the top of the sample, making up approximately 5-10 % of the total volume (Fig. 54d). While this layer could be re-homogenized, it required vigorous shaking by hand so was classified as a non-critical defect; when analysed at day 90 and onwards, this separation had evolved and the oily layer was making up approximately 15 % of the total sample volume (Fig. 54e). Despite this, the emulsions could still be re-homogenized by vigorous hand shaking and continued to pass the drop test, so remained classified as a non-critical defect. Defects such as these indicate a suboptimal emulsification process or incompatibility between the antigen and the adjuvant.

6.2.2 Storage and stability testing of a PCV2d vaccine candidate

For the second trial, the variables were narrowed down based on the findings from the first trial, closer to determining the best combination for vaccine preparation. Whilst both gels and both W/O/W adjuvant formulations tested had performed exceptionally well with no defects observed over the course of the trial, gel 02 and ISA 201 were chosen to proceed with for the second trial as both contained the "R" surfactant, which made them a better choice than their predecessors for predicted long-term stability. Emulsions formulated with the PCV2d antigen derived from expression of pARP25 construct appeared to show fewer defects in comparison to samples formulated using pARP31-derived PCV2d antigen, so for the second trial, only pARP25-derived antigen was used. Some optimisations were also made to the preparation protocols and this time, two temperatures were tested, 4 °C as previously or 22 °C to give an accelerated indication of any undesirable interactions between antigen and adjuvant. Emulsions were generated as in the first trial at a small laboratory scale of 4 mL with three repeats per condition, again including a set of control samples containing 50 mM Tris-HCl, 150 mM NaCl, pH 7.0 buffer as the aqueous phase. Experimental samples were formulated using *Δ2-40*PCV2d as the aqueous phase, to a final concentration of 40 µg/mL as previously. Both control and experimental samples were formulated with gel 02 or ISA 201 adjuvants and the emulsions were left to settle without disturbing for at least one day after preparation before the first analysis was performed, storing samples at either 4 °C or 22 °C. Findings are summarized in Table 19.

	Adjuvant/aqueous phases							
	Montanide™ Gel 02 PR 36084X				Montanide™ ISA 201 VG 36075M			
	4°C		22°C		4°C		22°C	
Day	C	pARP25	C	pARP25	C	pARP25	C	pARP25
2	✓	✓	✓	✓	✓	✓	✓	✓
8	✓	✓	✓	NCD 3/3	✓	✓	✓	✓
14	✓	✓	✓	✓	✓	NCD 1/3	✓	NCD 3/3
22	✓	✓	NCD 3/3	NCD 3/3	✓	✓	✓	NCD 3/3
29	✓	✓	NCD 3/3	NCD 3/3	✓	NCD 1/3	✓	NCD 3/3
45	NCD 3/3	NCD 3/3	NCD 3/3	NCD 3/3	✓	✓	✓	CD 3/3
59	NCD 3/3	NCD 3/3	NCD 3/3	NCD 3/3	✓	✓	✓	CD 3/3
78	NCD 3/3	NCD 3/3	NCD 3/3	NCD 3/3	✓	✓	NCD 3/3	CD 3/3
120	NCD 3/3	NCD 3/3	NCD 3/3	NCD 3/3	✓	✓	NCD 3/3	CD 3/3

Table 19. Summary of PCV2d vaccine storage trial #2 with Montanide adjuvants. Gel 02 and ISA 201 adjuvants were tested for storage stability and compatibility with PCV2d antigen purified from *E. coli.* Samples were stored at 4 °C or 22 °C. C: Control containing buffer; pARP25: soluble PCV2d protein derived from expression of pARP25 PCV2d. Emulsion stability classification was performed on three technical repeats where a stable emulsion is indicated by ✓, and defective emulsions are classified as either NCD: Non-critical defect or CD: Critical defect. Number of repeats showing any defect is indicated out of three (/3).

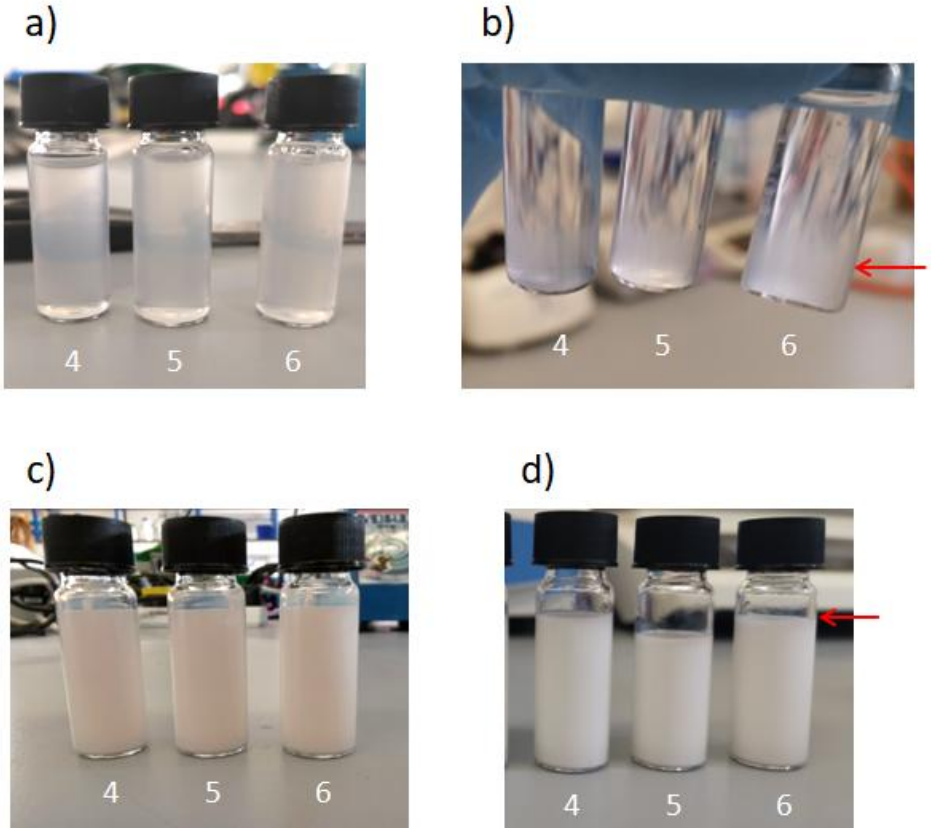

Figure 55. Visual checks for stability of gel 02 and ISA 201 emulsions throughout trial #2. Emulsions formulated with adjuvants gel 02 and ISA 201 were observed for stability during storage at 4 °C or 22 °C. Samples are labelled as follows: Vials 4-6: Three technical repeats (R) of samples formulated with soluble PCV2d protein derived from expression of pARP25 PCV2d. a) Gel 02 with pARP25 R1-3, 22 °C, day 1. b) Gel 02, pARP25, R3, 22 °C, day 120; gel sedimentation. c) ISA 201, pARP25, R1-3, 4 °C, day 1. d) ISA 201, pARP25, R1-3, 4 °C, day 190; very small oily layer. Arrows indicate defects.

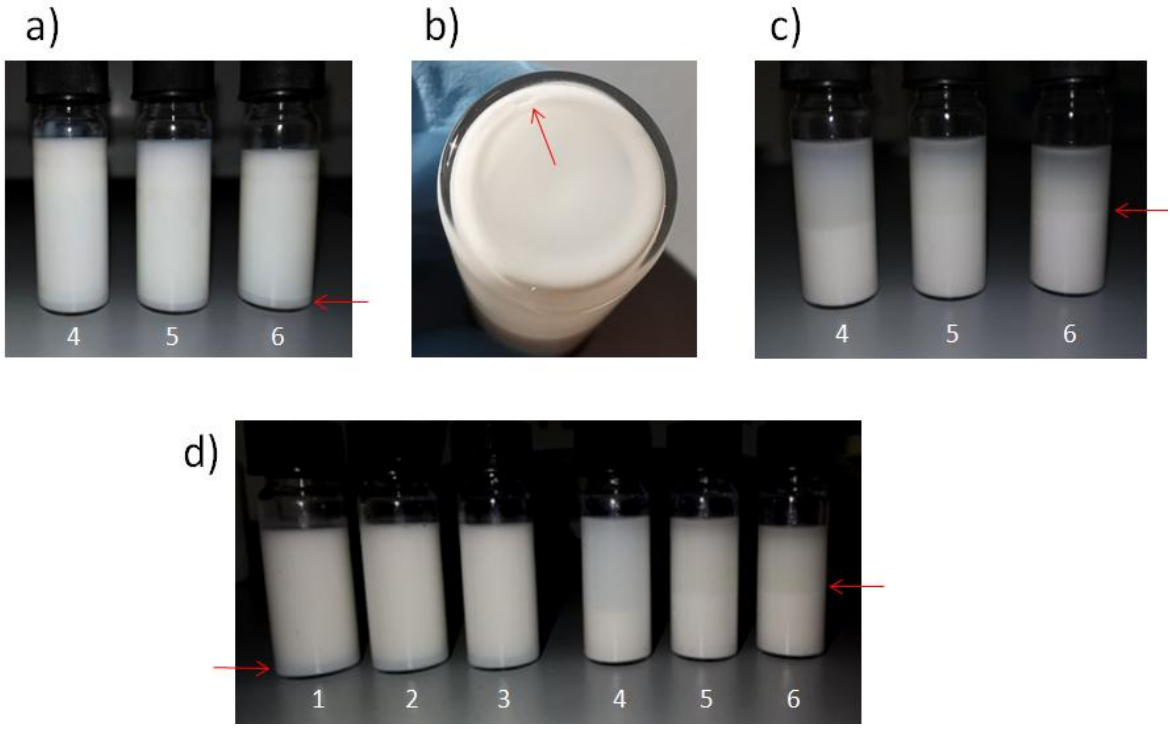

Figure 56. Visual checks for stability of ISA 201 emulsions at 22 °C in trial #2. Emulsions formulated with adjuvants gel 02 and ISA 201 were observed for stability during storage at 4 °C or 22 °C. Samples are labelled as follows: Vials 1-3: Three technical repeats (R) of control samples containing buffer; Vials 4-6: Three technical repeats (R) of samples formulated with soluble PCV2d protein derived from expression of pARP25 PCV2d. Defects were observed in samples a) pARP25, R1-3, day 22; <5 % phase separation. b) pARP25, R3, day 45; small aqueous phase breakage. c) pARP25 R1-3, day 120; 50 % phase separation. d) Control R1-3 (1-3), pARP25 R1-3 (4-6), day 78; phase separation in control (<5 %) versus PCV2d samples (30-40 %). Arrows indicate defects.

Gel 02 emulsions began to demonstrate non-critical defects as early as day 8 when formulated with PCV2d antigen and stored at 22 °C, whilst this was not observed in the control samples until day 22. These groups showed some sedimentation of gel settling towards the bottom of the vial, giving the appearance of two layers, the upper transparent while the lower was translucent (Fig. 55b); however this could be easily re-homogenized by inverting. Similarly, both gel 02 experimental and control samples stored at 4 °C began to demonstrate non-critical defects in the form of gel sedimentation, but this was not observed until day 45. Following on from the onset of gel sedimentation, the degree of contrast between transparent and translucent layers became more pronounced in all samples displaying the defect as time progressed in the trial, but remained able to re-homogenize easily, thus remained classified as a non-critical defect.

Of emulsions formulated with ISA 201 and stored at 4 °C, control samples remained stable for the entirety of the time period measured, while samples formulated with PCV2d antigen displayed only a few very minor non-critical defects in the form of a slight oily layer appearing on the top of the emulsion (Fig. 55d) or very small aqueous breakage. These samples could be re-homogenized by hand shaking. However, ISA 201 emulsions stored at 22 °C began to display non-critical defects in samples formulated with PCV2d antigen as early as day 14 in the form of minor aqueous phase separation on the bottom of the vials, although these could be re-homogenized (Fig. 56a). By day 45, all three PCV2d ISA 201 emulsions stored at 22 °C failed drop tests, wherein no aqueous phase could be observed diffusing into the water and thus were considered critically defective. By day 59, all samples had also formed two distinct phases: the top layer appeared to be translucent and slightly yellowish, while the bottom layer appeared creamy and opaque, and this bottom layer increased in proportion when measured in following time points; by day 120, the creamy bottom layer formed approximately 50 % of the total emulsion volume (Fig. 56c). On the other hand, ISA 201 emulsions in the control group at 22 °C did not start to demonstrate defects until day 78 when two distinct layers began to form, but these emulsions still performed successfully in drop tests.

Overall, it was determined that the most suitable adjuvant for the purpose of formulation with PCV2d antigen was ISA 201 W/O/W adjuvant due to its immunogenic properties and high level of stability provided emulsions were stored at 4 °C, thus a batch of this vaccine candidate was prepared to be used in animal challenge trial; vials were stored at 4°C until use in the challenge trial, with extra vials kept for monitoring.

Although from quality control analysis consisting regular visual checks and drop testing for signs of emulsion instability, it was still necessary to ascertain whether the antigen within the vaccine was retaining its integrity over the storage period, without showing signs of degradation. In order to clarify this, a sample of the ISA 201 emulsion with PCV2d antigen was taken from the prepared vaccine batch following 105 days storage at 4 °C and subjected to an acidification protocol using acetic acid to separate the antigen from the oil-based adjuvant.

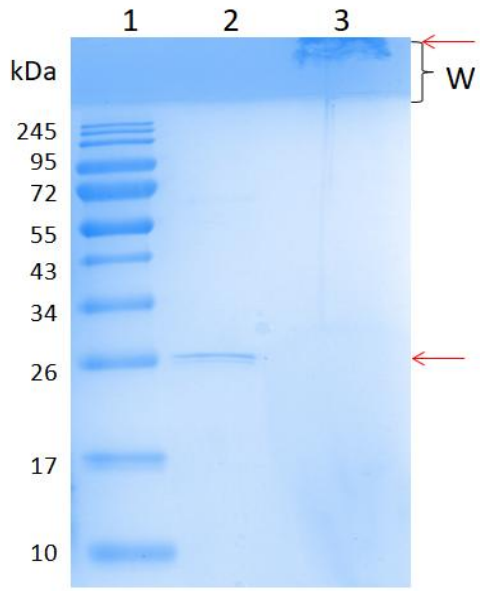

Figure 57. Extraction of PCV2d protein from W/O/W vaccine emulsion. Acetic acid acidification was utilised to extract PCV2d protein from an emulsion with ISA 201 adjuvant. Lane 1: Protein marker; Lane 2: 90 µg/mL sample of purified PCV2d protein stored in 50 mM Tris-HCl, 150 mM NaCl, pH 7.0 for 105 days at 4 °C (0.72 µg loaded). Lane 3: Sample of aqueous phase extracted from PCV2d vaccine preparation with ISA 201 adjuvant, stored for 105 days at 4 °C. W: wells. Arrows indicate presumed PCV2d species.

Although the acidification protocol proved the most effective at breaking the vaccine emulsion of all methods tested, it was not possible to remove all oily contaminants from the vaccine sample and as such, the sample once prepared for SDS PAGE was not able to migrate through the polyacrylamide matrix. Nevertheless, the extracted PCV2d antigen sample (Lane 3) showed only one visible band, indicative of the protein deposited within the stacking gel portion of the SDS PAGE gel. This suggested that the PCV2d protein was still intact within the vaccine sample although it was not clear whether the deposition of the protein within the stacking gel portion of the SDS PAGE gel was due to incomplete removal of oily contaminants that were hindering its migration, or whether the protein had formed an aggregate of large molecular weight.

6.2.3 Pig challenge trial using PCV2d vaccine candidate

The pig challenge trial was performed under instruction of Tanja Opriessnig at Iowa State University. A batch of ISA 201 PCV2d vaccine was prepared at the University of Kent then transferred to the livestock infectious disease isolation facility at Iowa State University for the live animal viral challenge trial to be performed. All pigs were tested on arrival at Iowa State University by enzyme-linked immunosorbent assay (ELISA) and confirmed free of PCV2 virus.

The study consisted of 40 pigs in total, with 4 groups of 10 pigs each, including a negative control group unchallenged with a live virus (NEG), a positive control group challenged with a live strain

of PCV2d virus (POS), and two vaccinated groups where one group was vaccinated with Ingelvac CircoFLEX® (Boehringer Ingelheim) commercial PCV2a vaccine (COM-VAC) and the other was vaccinated with the experimental ISA 201 PCV2d vaccine (EXP-VAC). Both vaccinated groups were also challenged with the live strain of PCV2d virus. Indications of disease and immune response were measured by observation of clinical signs of PCV2d infection including weight gain of the pigs, along with serology analysis for the presence of specific antibodies and viremia determined by viral titre. Nasal shedding of virus particles was measured and necropsy was also performed at the end of the trial for signs of disease.

6.2.3.1 Clinical signs and weight gain

Clinical signs of PCV2 infection, including respiratory disease, nasal discharge, coughing and effects of viral infection on weight gain, were monitored throughout the trial. All pigs in the study were female to standardize for weight gain. The weight of each pig was measured upon arrival at 3.5 weeks of age, then one day prior to challenge with the live PCV2d virus at 9 weeks of age, and finally 21 days following viral challenge at 12 weeks of age when the trial was ended.

a)

Group	Arrival to challenge	Challenge to necropsy	Arrival to necropsy
NEG CONTROL	353.8±14.4^{A}	592.3±24.4^{A}	441.3±16.8^{A}
POS CONTROL	350.3±15.1^{A}	574.2±17.3^{A}	432.4±14.8^{A}
EXP-VAC	351.1±12.6^{A}	549.7±32.6^{A}	423.9±14.5^{A}
COM-VAC	379.0±16.9^{A}	538.7±26.1^{A}	437.6±10.5^{A}
	P=0.473	P=0.459	P=0.842

b)

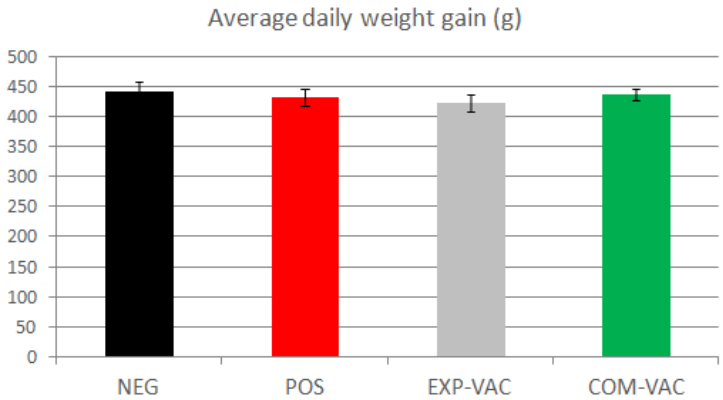

Figure 58. Average daily weight gain of pigs throughout the PCV2d challenge trial. a) Raw data of average daily weight increases of pigs in grams measured from the point of arrival to challenge, from challenge to necropsy and from arrival to necropsy, for each of the 10 pigs in each group. b) Graphical representation of average daily weight gain of pigs in each group, in grams, from arrival to necropsy.

Between the time of arrival and viral challenge, pigs in the unvaccinated, PCV2d-challenged positive control group gained slightly less weight per day compared to the other groups in the study, whereas the commercial vaccine group gained the most; between the time of viral challenge and necropsy, the negative control group which was not exposed to the PCV2d virus gained the most weight per day, as expected. However, both vaccinated groups gained less weight on average than the positive control group during this period. Overall, there were no other evident clinical signs of PCV2 infection observed and so it was determined that the differences in weight gain were not a significant side effect of vaccination. None of the animals showed any visible clinical signs of PCV2 infection suggesting asymptomatic, subclinical infection. Signs of adverse reaction to the vaccine were also monitored, such as swelling, redness, pain and rectal temperature. No adverse reactions were reported.

6.2.3.2 Serology

In order to measure the effectiveness of the experimental vaccine to stimulate a humoral immune response, serum samples were obtained from the animals at various timepoints in the study and analysed by ELISA assay for the presence of PCV2 antibodies. The relative amounts of antibodies in ELISA samples were calculated by referencing the absorbance to that of the positive control, to give a Sample to Positive Ratio (S/P) value; samples with an S/P ratio equal to or greater than the positive cut-off S/P were considered “positive” for PCV2 antibodies.

a)

Group	Arrival 3.5 w	Vaccination 1 5 w	Challenge 9 w	7 dpc 10 w	14 dpc 11 w	20 dpc 12 w
NEG CONTROL	10/10	5/10	2/10	0/10	0/10	0/10
POS CONTROL	10/10	6/10	0/10	0/10	0/10	6/10
EXP-VAC	9/10	4/10	2/10	1/10	9/10	10/10
COM-VAC	9/10	5/10	10/10	10/10	10/10	10/10

b)

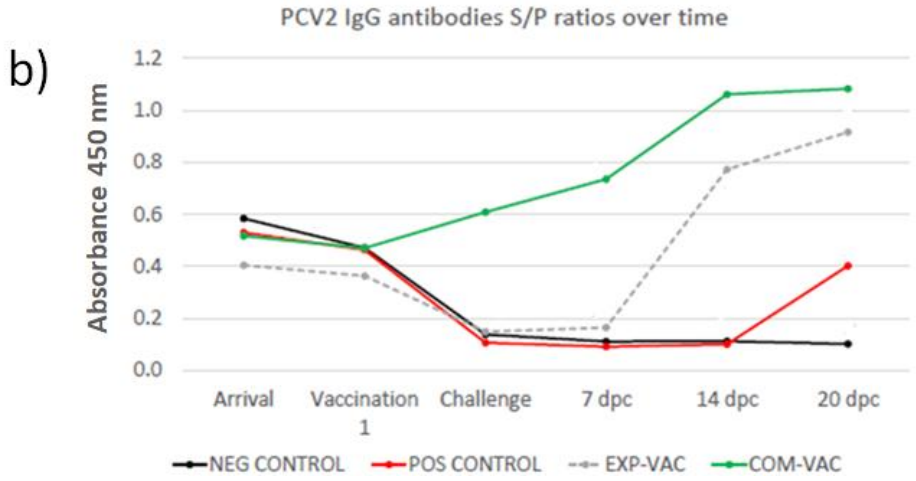

Figure 59. Serological analysis for the presence of PCV2-specific antibodies throughout the PCV2d challenge trial. a) Number of pigs in each group deemed "positive" for PCV2-specific antibodies determined by S/P ratio, as deemed by ELISA at each timepoint of days post-challenge (dpc) with PCV2d virus. b) Graphical representation of PCV2-specific antibody S/P ratio for each group in the study over time.

Serological analysis of blood serum by ELISA showed a moderate concentration of PCV2-specific antibodies were present in the animals upon arrival; these are considered to be maternally-derived antibodies as the pigs had been recently weaned. The negative control group demonstrates the natural decline of maternally-derived antibodies over the course of the study in the unvaccinated and unchallenged animals. In the positive control group, the first instance of significant PCV2-specific antibody generation did not occur until 20 days following challenge with the virus. In contrast, animals receiving the commercial vaccine demonstrated a PCV2-specific antibody response immediately upon viral challenge and the concentration of these antibodies rapidly increased for the next 14 days following exposure to the live virus. The animals receiving the experimental vaccine showed mixed results however; following viral challenge, there appeared to be a delayed specific immune response in comparison to the commercial vaccine, wherein there was not a significant PCV2-specific antibody response observed until 14 days following viral challenge. Although not to the level of the current commercial vaccine, the experimental vaccinated group was able to generate an antibody response to the virus 7 days

sooner than the unvaccinated positive control group, indicating some positive protective effect induced by the experimental vaccine.

6.2.3.3 Viremia

Samples of blood serum at various timepoints throughout the study were analysed for viremia, as classified by the presence of PCV2 viral DNA. This was performed by extraction of viral DNA from the serum using a MagMAX Pathogen RNA/DNA isolation kit, followed by amplification by PCR using a primer sequence probing for PCV2 ORF1.

a)

Group	Challenge 9 w	7 dpc 10 w	14 dpc 11 w	20 dpc 12 w
NEG CONTROL	0/10	0/10	0/10	0/10
POS CONTROL	0/10	2/10	9/10	6/10
EXP-VAC	0/10	9/10	9/10	10/10
COM-VAC	0/10	6/10	5/10	4/10

b)

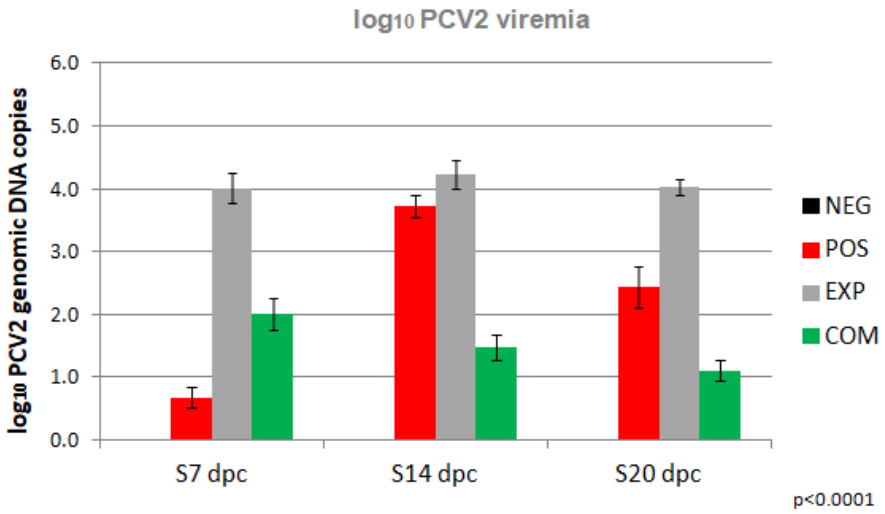

Figure 60. Viremia analysis for the presence of PCV2 viral DNA in serum following challenge with PCV2d virus. a) Number of pigs in each group containing PCV2 viral DNA in blood serum as determined by PCR at each timepoint of days post-challenge (dpc) with PCV2d virus. b) Graphical representation of viremia in the study over time (log_{10} number of viral genomic DNA copies). Probability value: $p<0.0001$.

Interestingly, the group showing the highest viremia in the first timepoint following viral challenge (7 dpc) was the experimental vaccine group. Both commercial and experimental vaccinated groups showed an increased number of pigs demonstrating viremia than the positive control group at 7 days following challenge, at 9/10 and 6/10 respectively; however this trend changed as the time following challenge went on. By 14 days following challenge, the positive control group contained 9/10 pigs positive for viremia, equal to the number of positive cases in the

experimental vaccine group. Nevertheless, by 20 days following challenge, the number of viremic pigs had decreased in the positive control group to 6/10 pigs, viremia had only increased in the experimental vaccine group to the point that all pigs in the group were viremic. This appears in contrast to the commercial vaccine group, where the number of pigs demonstrating viremia steadily decreased in each timepoint following viral challenge. These results suggest that vaccination with the experimental PCV2d vaccine correlated with high viremia, which manifested at an accelerated rate compared to when no vaccine was administered.

6.2.3.4 Nasal shedding

Whilst viremia is an effective measure of viral titre within infected animals, nasal shedding of viral particles was used to determine the transmissibility of the viral infection, an important factor in the rate of viral spread within the field. Nasal shedding was determined by nasal swab then subsequent extraction of viral DNA from the swab samples. The presence of PCV2 viral DNA using MagMAX Pathogen RNA/DNA isolation kit and PCR amplification using a primer sequence probing for PCV2 ORF1 as previously.

a)

Group	Challenge 9 w	7 dpc 10 w	14 dpc 11 w	20 dpc 12 w
NEG CONTROL	0/10	0/10	0/10	0/10
POS CONTROL	0/10	10/10	8/10	5/10
EXP-VAC	0/10	10/10	8/10	7/10
COM-VAC	0/10	10/10	5/10	1/10

b)

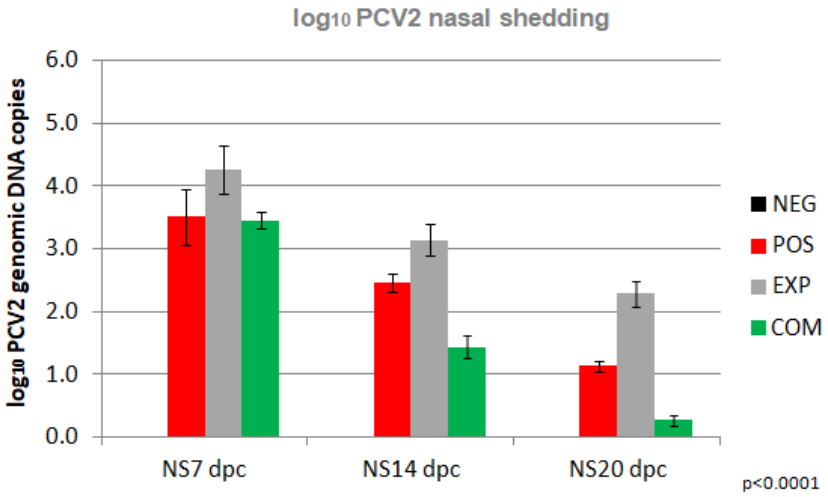

Figure 61. Nasal shedding analysis for the presence of PCV2 viral DNA in nasal mucus following challenge with PCV2d virus. a) Number of pigs in each group containing PCV2 viral DNA in nasal mucus as determined by PCR at each timepoint of days post-challenge (dpc) with PCV2d virus. b) Graphical representation of nasal shedding in the study over time (log10 number of viral genomic DNA copies). Probability value: $p<0.0001$.

Following viral challenge, all infected animals showed a high level of viral shedding after 7 days. Positive control and experimental vaccine groups showed at least 50 % of animals in the group displaying significant viral shedding at all timepoints measured in the trial, whereas the majority of animals in the commercial vaccine group were no longer infectious by the final timepoint of the trial at 20 days post challenge.

While it had been demonstrated that viremia in the experimental vaccine group was high at all timepoints measured following viral challenge, nasal shedding data indicated a trend that viral shedding in these animals did in fact decrease over time, although shedding remained highest in this group compared to both the positive control and commercial vaccinated groups. These data together may suggest that although the experimental vaccine appears to facilitate and in fact promote viral replication by some mechanism, it is also able to generate a successful, specific immune response.

6.3 Conclusions

In both adjuvant storage trials, all gel adjuvant formulations showed a high level of stability in terms of uniformity of their appearance, yet analysis was limited by the inability to separate the antigen following formulation to visualise remaining protein in the sample or any degradation that may be occurring during the time in storage. The second adjuvant storage trial demonstrated that there were some undesirable interactions occurring between ISA 201 adjuvant and PCV2d antigen which manifested as critical breakage defects and failure in drop tests when emulsions were stored at 22 °C, whereas samples formulated with buffer only continued to perform successfully in drop tests under the same conditions. That said, both storage trials suggested that formulation of ISA 201 with PCV2d antigen was highly stable for at least 7 months if stored at 4 °C, with very few defects occurring. Extraction of the PCV2d antigen from the oil-based emulsion also demonstrated that the protein was still present following 3.5 months storage at 4 °C, so this could be a promising candidate for our novel vaccine.

Once transferred for vaccination in a live animal trial, the presence of PCV2-specific antibodies in piglets upon arrival was observed. Due to the widespread reach of PCV2 infection, the piglets were assumed to have maternally derived antibodies against PCV2, which are intended to remain for a short period of time to confer immune protection to the piglet prior to raising its own immune response to pathogens. It was clear that by the point of viral challenge in unvaccinated piglets, they retained a negligible titre of maternally derived antibodies so this was not determined to have interfered with the accuracy of the data. Pigs vaccinated with the experimental ISA 201 PCV2d subunit vaccine appeared to elicit immunological memory, resulting in accelerated humoral immune response upon exposure to the live virus, depicted by a rapid

increase in PCV2d-specific antibodies as classified by serology data, in comparison to the unvaccinated control group. However, pigs in the experimental vaccine group suffered a high level of viremia and subsequent nasal shedding of virus particles, essential for continued transmission of the virus. This was a surprising finding and the reason behind this phenomenon was not at all understood, although other variables in the study had been suitably controlled such that it did not appear to be a confounding or anomalous result. It was clear the vaccine design required investigation and optimisations.

Chapter 7: Discussion

For centuries, vaccination technology in the form of immunoprophylaxis has existed as a method to protect livestock from disease (Hendriksen, 1996). However, approved, adjuvanted subunit vaccines have only been in use for just under 100 years since the discovery of aluminium salts as an immunostimulant. Since then, vaccination has become one of the most successful public health interventions ever to exist, and continues to have vast impacts in preventing disease and death due to infectious disease worldwide (Pasquale et al., 2015).

In this research, we aimed to develop a recombinant bacterial expression system using *E. coli* to contribute towards protection against PCV2d and PCV3 disease spread in low-middle income countries including Thailand and others in South East Asia. These countries have suffered from high rates of PCV2 infection and limitations in availability of vaccines due to the costs of import. Within the research presented here into the development of new recombinant PCV vaccine candidates generated in *E. coli* and processed using a simple, low cost production system, Chapter 3 focused on the optimisation of expression capacity of PCV proteins in *E. coli* strains, and maximising protein yield. The quality of the generated protein products was also investigated for their efficacy as potential vaccine candidates. Building on these expression findings, Chapter 4 aimed to combat issues with protein insolubility and aggregation in a PCV2d-PCV3 chimeric protein which was intended for use in a dual vaccine. The data presented in Chapter 5 focused on minimising potential problems with dimerisation and oligomerisation of the recombinant PCV2d protein by modifying protein disulphide bonding capabilities and testing the efficacy of these alternative designs. Chapter 6 finally presented the development of an adjuvanted PCV2d vaccine and a live animal trial in pigs as the recipients of our experimental vaccine.

7.1 Expression of PCV2d and PCV2d-PCV3 chimera

7.1.1 NLS truncation improves expression of PCV2d protein

The primary goal of this work was to develop an expression system for high yield production of soluble PCV2d capsid protein. Two types of expression vector backbones were tested during the construct optimisation phase as further gene designs were developed; the IPTG-inducible pET23/ptac vector and the arabinose-inducible pBAD24 vector. Through gene optimisation informed by growth and expression trialling, it was discovered that truncations to the PCV2d capsid protein were able to facilitate significant improvements in expression level and solubility. Ultimately, a single, optimal design was chosen to take forward to the next stage of experiments.

The chosen expression vector, a modified pET23 vector, generates a medium copy number of approximately 40 copies per cell and features a ptac promoter sequence in place of the traditional T7 promoter to enable more tightly controlled gene expression. Initially, expression of the full length protein with an OmpA signal peptide showed some visible expression when cell extracts were analysed by western blot. Analysis by native PAGE however indicated the protein to be forming a species of very high molecular weight, potentially indicating oligomerisation into VLP. Removal of the OmpA signal peptide eliminated the visible oligomer in native PAGE, suggesting this signal peptide may have aided protein stability. Multiple previous studies have reported that truncation of the PCV2 NLS region is able to increase expression, suggesting the NLS region is rich in rare arginine residues that may lead to premature termination of proteosynthesis in *E. coli* (Trundova & Celer, 2007) or target the protein for degradation by proteases (Gottesman et al., 1997). Codon optimisation of the gene for *E. coli* expression did not appear to improve the expression level and ultimately, truncation of the residues 2-40 was necessary to significantly improve the level of PCV2d expression. Nevertheless, this was advantageous in this study as it has been reported that removal of the PCV2 NLS region eliminates its ability to oligomerise into VLPs (P. Wu et al., 2012). This is supported by our finding that the high molecular weight oligomer indicative of a VLP was no longer visible when the NLS truncated PCV2d protein was analysed by native PAGE; however other lower molecular weight oligomerisation species along with an apparent dimer still appeared to form.

Ultimately, we found that using this pET23/ptac vector design in tandem with optimisation to the PCV2d Cap gene by truncation was able to achieve a high level of PCV2d Cap over-expression that was tolerable to the cell without causing a detrimental effect on growth rate or inducing cell lysis.

7.1.2 Dual truncation improves expression of PCV3 protein

PCV3 has been demonstrated as an emerging disease threat in Thailand and South East Asian swine farming. Thus, we also intended to investigate the potential of *E. coli* to be used as a recombinant expression host for generating a PCV3 subunit vaccine, in the same way that was being developed for PCV2d. The PCV3 Cap protein was less well characterised than PCV2d Cap due to the relatively recent discovery of this new species.

Initial expression of the full length PCV3 Cap protein proved more difficult than PCV2d, demonstrating no visible expression whatsoever. Sequence alignment of PCV2d and PCV3 Cap from the strains used demonstrated only 46 % homology and epitopes identified in PCV2d generally did not appear to be conserved in PCV3. That said, the N-terminal region of PCV3 was one such region that did show a high level of conservation with PCV2d sequence, also containing a

high concentration of arginine residues. Based on this alignment, truncation of the predicted PCV3 NLS region between residues 2-34 was employed but did not improve expression to a level detectable by immunoblot. It was not until a further truncation to the C-terminus of the PCV3 Cap protein was made that the first expression was detected; based on the sequence alignment with PCV2d, the equivalent PCV3 C-terminal region was slightly shorter in length and did not appear to contain a conserved epitope. Truncation was able to achieve soluble expression of PCV3, suggesting the presence of this region may have been important in targeting the protein for degradation; previous research has proposed that a high concentration of non-polar amino acids at the C-terminus of a protein can lead to rapid degradation in *E. coli* (Gottesman et al., 1997), which may explain this phenomenon as the last 12 residues of the C-terminal regions contained 6 out of 12 (50 %) non-polar amino acids in the original PCV3 Cap sequence, compared to only 4 (33.3%) in the truncated version. Despite this improvement and using the optimisation techniques tested, it was not possible to achieve a sufficient expression level of PCV3 alone for it to be feasible in the development of a PCV3 vaccine candidate.

7.1.3 Expression of a PCV2d-PCV3 chimeric gene significantly increases the expression level of PCV3

The design of PCV2d-PCV3 chimeras were conceived as a method of generating a dual vaccine candidate to protect against two porcine circoviruses of current relevance in the Thai swine farming industry. Due to the success in producing PCV2d Cap protein in a bacterial expression system, and the difficulties in achieving high enough expression of PCV3 Cap protein alone, the two were combined so that PCV2d may act as a fusion carrier for PCV3 expression. The chimeric proteins used in this study were essentially a fusion protein design, wherein upon testing the expression of the chimeric designs, it became apparent that the highly soluble PCV2d Cap protein appeared to be functioning as a fusion partner with a beneficial effect on the expression, stability and potentially folding of its passenger protein, PCV3 Cap when it was used as an N-terminal fusion tag. Research shows that the location of the fusion tag plays an important role, where N-terminal tags are usually advantageous over C-terminal tags in enhancing the solubility of their partner proteins – although the reason behind this is unclear.

At a translational level, one hypothesized mechanism is that a stable N-terminal fusion tag is able to provide a reliable starting point for efficient translation initiation; studies find that mRNA sequences containing fewer G or C nucleotides in their 5’ regions thus exhibiting reduced secondary structure correlate with a longer mRNA half-life in *E. coli,* thought to be through a protective effect mediated by RNA-binding proteins, such as RNA chaperones (Lenz et al., 2011). When looking at the composition of the PCV2d and PCV3 proteins used in this research, the

truncated N-terminal region of highly expressed PCV2d gene currently contains 20 % G and C nucleotides within the first 20 base pairs of its DNA sequence, in comparison to the N-terminus created by truncation of residues 2-34 of the PCV3 gene, which contains 45 % GC; this could suggest a chimeric protein using PCV2d as an N-terminal fusion tag could be aiding expression of PCV3 by this mechanism.

Another possible explanation is that during translation of a protein that does not express well in *E. coli* alone, such as PCV3 Cap, when the nascent protein emerges from the ribosome an incorrect, irreversible, folding pathway is initiated leading to the misfolded protein being tagged for rapid degradation, resulting in lower total expression levels; in *E.coli*, this is mediated by C-terminal fusion of the ssrA peptide to direct proteins to the endogenous ClpXP and ClpAP proteases through the transfer-messenger RNA system. For proteins that are difficult to translate and may cause translational arrest by the ribosome, this mechanism ensures rapid degradation of potentially deleterious truncated polypeptides (Janssen & Hayes, 2012). This scenario is more likely when expressing mammalian proteins in a bacterial system which lacks specific eukaryotic chaperones to facilitate correct protein folding, or potentially when expressing a viral protein that would ordinarily replicate in a mammalian host. However, when a soluble protein such as PCV2d Cap is fused at the N-terminus, this would be translated first and may increase the solubility of the downstream protein domain folding intermediates, increasing their half lives prior to irreversible aggregation and increase the probability that the protein would eventually reach the lowest free energy native conformation (Dyson et al., 2004)

At a protein level there are a number of mechanisms by which addition of a soluble fusion partner such as PCV2d Cap may facilitate production of its passenger protein. Fusion tags may enhance the solubility of their passenger proteins by forming a protective, micelle-like structure where soluble protein domains face outward while unfolded or misfolded regions are sequestered inside (Nallamsetty & Waugh, 2007). The choice of fusion protein linker is also important in this case, wherein an appropriate degree of conformational flexibility is required to facilitate interaction between the two proteins, a consideration that was also investigated for PCV2d-PCV3 chimera proteins although ultimately the ideal functional properties for its linker was not elucidated. Meanwhile, some commonly used fusion partners such as maltose binding protein (MPB) and N-utilization substance (NusA) have been shown to attract chaperones when expressed in *E. coli,* promoting their fusion partner to go through a chaperone-mediated folding pathway (Douette et al., 2005; Huang & Chuang, 1999). Further to this, some fusion partners exhibit intrinsic chaperone-like activity wherein hydrophobic regions of the fusion protein can interact with the partially folded passenger protein to assist proper folding and prevent self-aggregation

(Nallamsetty & Waugh, 2006; Waugh, 2005) and this beneficial activity is more efficient when the soluble fusion tag is located on the N-terminus of the passenger protein (Sachdev & Chirgwin, 2000). Similar evidence suggests a positive correlation between increasing numbers of contiguous hydrophobic amino acids and soluble expression, when utilized as an N-terminal tag (Dyson et al., 2004); PCV2 VLPs are known to contain an internalized, hydrophobic core (Khayat et al., 2019) suggesting the presence of hydrophobic regions of PCV2 Cap protein which may contribute to its efficiency as a fusion tag via this mechanism.

The design of PCV2d-PCV3 chimeras and subsequent process optimisation was able to produce a stable protein containing peptides of both PCV2d and PCV3 Cap proteins. However, the proteins consistently proved to be highly insoluble when expressed in *E. coli.* At the current level of development, the designs were not suitable for use as dual vaccine candidates.

7.1.4 High purity PCV2d protein can be obtained by a single step cation exchange method following fed-batch fermentation

A main aim in this project was to develop a low cost system to formulate a vaccine candidate, with minimal processing steps. In order to do this, an inexpensive purification method was required, with as few steps as possible – the ideal goal was to achieve sufficient purity in single step of purification. For ease of downstream processing, a high degree of target protein solubility would also be required. During this research, expression optimisation was performed in shake flask and in fed-batch fermentation, the behaviour of the PCV2d protein was characterized and its compatibility with various purification methods was assessed.

One major inconsistency between the expression of PCV2d in shake flask versus fed-batch fermentation was the proportion of soluble protein produced. Whilst in shake flask, virtually all PCV2d protein was expressed in soluble form, fed-batch fermentation growth led to cells expressing a large amount of the protein insolubly. However, this issue could likely be improved through optimisation of growth conditions such as temperature, media formulation and strength of induction (Lobstein et al., 2012). Initial purification attempts using IMAC proved not the ideal method for purification of this protein as it exhibited reduced binding to the nickel resin even when the HIS-tag was retained, as demonstrated in Chapter 3.2.5. It has been elucidated through the course of this research that the stability of the PCV2d protein is sensitive to buffer conditions, in particular salt concentration and pH; these factors also affect protein folding and may have contributed to a folding state which sequestered the HIS-tag from efficient interaction with the nickel resin. In addition, conductivity and the concentrations of monovalent cations in the purification buffer can alter the binding of proteins to the column (Yu et al., 2016). This

purification technique also eluted a number of contaminating *E. coli* proteins in peak fractions containing PCV2d protein, due to a similar affinity of these proteins to the nickel resin. This presents one of the main limitations of this technique, wherein proteins with highly similar affinities cannot be separated easily by altering the imidazole concentration of the elution buffer, so another step of purification such as size exclusion chromatography must be performed, requiring further resources (Sauer et al., 2019).

CIEX was chosen as an alternative purification technique due to the low cost resin and flexibility of the technique to be performed manually on the bench-top or using AKTA automated purification systems. CIEX using SP sepharose resin uses a strong cation exchanger composed of cross-linked agarose beads modified with sulphopropyl (SP). A suitable buffer for ion exchange can be chosen to ensure a known net charge for a target protein. Proteins with different pI values will have varying degrees of charge at a given pH and thereby have different affinities for the negatively charged surface groups on the cation exchange resin beads. Different proteins will bind to the resin with different strengths, facilitating their separation. Elution of proteins from CIEX resin simply requires an increasing salt gradient, a much cheaper reagent than imidazole used in IMAC. In this study, CIEX was deemed a particularly appropriate technique due to the unusual pI value of the PCV2d protein in comparison to most native *E. coli* proteins, with a pI of 9.43 for the truncated PCV2d-H6 protein. Distributions of *E. coli* K12 strain native proteins demonstrate the highest frequency of proteins have pIs between 4.5–7.0, with the next highest frequency occurring between approximately pI 8.5 – 9.5 while a very low frequency of proteins have pI values over 9.5 (Schwartz et al., 2001). For this reason, using pH 7.0 for CIEX with SP sepharose resin is able to achieve a high purity product by simply optimising the salt gradient of elution fractions. This technique is generally used as one of multiple purification steps (Coffman et al., 2002; He et al., 2017; Radli et al., 2017) and is rarely able to achieve such a high purity soluble, recombinant target protein from *E. coli* in a single step.

7.1.5 Recombinant PCV2d protein is capable of raising a neutralising antibody response in rabbits

It was an essential part of the analytics to test the immunological capabilities of our protein products as they were developed, before continuing to vaccine design. An *in vitro*, PK-15 cell-based virus neutralisation assay was used as an important preliminary analytical step. The cell-based neutralisation assay identifies the presence of neutralising antibodies in serum from rabbits immunised with PCV2d antigen, and quantifies the effectiveness of these antibodies to neutralise the live PCV2 virus i.e. prevent the virus from infecting and subsequently killing porcine kidney cells used in the assay, detected by immunofluorescence. In the cell-based assay using

serum from rabbits immunised with the first purified truncated PCV2d species purified by CIEX, a significant reduction of infected cells was observed using up to 1:8 anti-sera dilution. Quantitative analysis also demonstrated dose-dependent neutralising antibody titres for both rabbits. The data strongly indicate that PCV2d antigen produced by this process can induce generation of virus neutralising antibodies in test animals and suggest its potential use as a subunit vaccine.

Neutralising antibodies are an important specific defence against viral invaders. Neutralising antibodies not only to bind to a virus, they bind in a manner that blocks infection. A neutralising antibody might block interactions with the receptor, or might bind to a viral capsid in a manner that inhibits uncoating of the genome. Only a small subset of the many antibodies that bind a virus are capable of neutralisation, with the majority of other types having non-neutralising activity that is nevertheless important in dealing with an infection. Neutralising antibody protection relies on their ability to recognize neutralisation epitopes on the virus surface. Coating of virus particles by antibodies is necessary but not always sufficient for virus neutralisation. The effectiveness of virus neutralisation correlates with the rate of antibody binding to critical epitopes but occupancy of cell receptor binding sites on the virus surface might not be obligatory for neutralisation, as steric hindrance or induction of deleterious conformational changes may be sufficiently effective. Non-neutralising virus-surface-binding antibodies sometimes enhance the effectiveness of neutralising antibodies, limiting viral spread in the early phases of infection and contributing to its suppression (Neurath, 2008). The primary immune response is characterized by the appearance of neutralising antibodies of the IgM class, the earliest type of IgG to be generated, and can be detected between days 4 and 7 after exposure. After an infection, it can take some time for the host to produce highly effective neutralising antibodies and these are generally of IgG subclass, sometimes IgA or IgE depending on the type of pathogen and route of infection. However, these antibodies will persist for some months to protect against future encounters with the agent (Payne, 2017). In terms of measuring vaccine potency, the presence of neutralising antibodies provides the best evidence that protective immunity has been established, showing correlation with protection in biological assays (Hombach et al., 2005).

There are multiple important aspects that also must be considered in designing a vaccine with high efficacy; although the cell-based assay demonstrates effective virus neutralising antibody activity as a result of immunisation with the PCV2d antigen, it is not able to provide an indication of whether the antigen would generate immunological memory capable of inducing a long-term protective immunity as part of a secondary immune response. It is also not possible to know how a vaccine preparation may react upon administration to a live animal in terms of adverse

reactivity. It is for these reasons that it was essential to perform a live animal study using an adjuvant-formulated vaccine candidate.

7.2 Development of a dual-protective PCV2d-PCV3 vaccine candidate

7.2.1 Differing functional linkers do not improve solubility of PCV2d-PCV3 chimeric protein

The secondary goal of this project was to develop a system for production of a dual protecting PCV vaccine using the *E. coli* expression system. In Chapter 3.2.2, it was demonstrated that when expressing PCV2d-PCV3 Cap chimeric protein featuring N-terminal truncations to the NLS regions of both proteins, expression could be attained when utilizing a short glycine–serine linker (-GSGSG-). This linker design is theoretically appropriate for use with a protein such as PCV2d-PCV3 which has a tendency to form inclusion bodies which may be at risk of degradation by proteases, as linkers rich in glycine, serine and threonine are resistant to proteolysis (Eldridge et al., 2009). Interestingly, using a longer glycine-serine linker (-GSGSGSGSGS-) was not able to produce visible expression. Due to this finding, in Chapter 4.2.1 a range of functional linkers were tested for improvements in solubility, stability and aggregation potential of the PCV2-PCV3 Cap chimeric protein. We found a short, 80 % Gly glycine serine linker (-GGGGS-) with high flexibility did not improve expression of soluble chimeric protein nor show an increased yield of cleaved soluble PCV2d. Similarly, the properties of a short, rigid non-helical linker rich in proline residues (-EPEPEP-) neither improved nor diminished the overall solubility or stability of the PCV2d-PCV3 chimera. By use of a short rigid alpha helical linker (-EAAAK-) and a long alpha helical linker (-AEAAAKALEAEAAAKA-) between PCV2d and PCV3 Cap genes, neither demonstrated any impact on the propensity of the chimeric protein to form inclusion bodies. Although some research has found direct fusion of functional domains without a linker may lead to many undesirable outcomes, including misfolding, low protein yield or impaired bioactivity (Amet et al., 2008; Bai et al., 2005; Bai & Shen, 2006; Zhao et al., 2008), direct fusion of PCV2d to PCV3 Cap did not appear to have any impact on misfolding or protein yield compared to constructions including a linker region.

It should be noted that the constructions used in Chapter 4.2.1 all contained an additional C-terminal truncation to PCV3 Cap protein that was not tested using the long, glycine-serine linker (-GSGSGSGSGS-), and expression experiments in Chapter 3 demonstrated how significant removal of this region was in attaining overall expression of a chimeric PCV2d-PCV3 Cap protein. However, it appeared that the functional properties of the short glycine-serine linker were distinctly preferable for expression of the chimeric protein than the longer iteration. These results may suggest that the interaction of PCV2d Cap protein is a necessary element in facilitating expression

of PCV3 Cap in *E. coli.* However, despite the success of high level expression of PCV2d-PCV3 chimeric protein the fusion still remained, for all iterations tested, almost completely insoluble. This indicates the fusion was not of optimal design for solubility and could be an overriding factor over linker design. In general, a successful fusion tag is relatively small and has limited diversity in amino acid content in order to impose minimal metabolic burden on the host cell (Malhotra, 2009); this could be one explanation for the high level of inclusion bodies observed when expressing this proteins, as the PCV2d peptide acting as a fusion partner was still relatively long in length (195 amino acids) and consisting a diverse range of residues. As such, for design of a more soluble chimera, a smaller PCV2d peptide with low sequence diversity could be utilized as an N-terminal fusion tag for PCV3 to minimize metabolic burden, featuring a flexible linker region to facilitate interaction between the moieties necessary to achieve solubility.

7.2.2 PCV2d-PCV3 chimeric protein is highly susceptible to proteolysis but susceptibility can be reduced by improved folding

In Chapter 3, it was demonstrated that when the chimeric PCV2d-PCV3 protein was expressed in fed batch fermentation, the inclusion bodies formed by aggregation of the full length fusion protein appeared much more susceptible to proteolytic degradation compared to expression of the same protein at shake flask level. A higher proportion of breakdown products, including cleaved PCV2d protein and other PCV2d or PCV3 peptides could be observed following separation of the cellular contents by electrophoresis, suggesting significant differences in the nature of the inclusion body proteins formed from fed-batch fermentation versus shake flask expression. It is well understood from previous research that high level recombinant protein over-expression in *E.coli* done in order to achieve expression at a high translational rate often results in aggregation into inclusion bodies due to use of high expression temperatures, high inducer concentration and expression under strong promoter systems. Not only this, the conformation of inclusion bodies can be highly affected by the chemical and physical characteristics of the environment during formation and thus can have a significant impact on protein secondary structure (Przybycien et al., 1994); in the case of fermentation in particular, the combination of suboptimal chemical and physical environment for protein folding and the high translational rate can further overwhelm the bacterial protein quality control system (Carrió & Villaverde, 2005; A. Singh et al., 2015), which may have resulted in partially folded and misfolded PCV2d-PCV3 proteins that are not only prone to aggregation, but may also be conformationally more susceptible to proteolytic degradation.

This difference could well be explained by the cell lines used in culturing at shake flask versus fermentation. Shake flask experiments were carried out in BL21 cell line, a B strain of *E. coli* which

is deficient in Lon and OmpT proteases. On the other hand, K12 strains of *E. coli* such as the W3110 cell line used in this study for fed-batch fermentation experiments, retain these proteases. W3110 cell line was deemed more suitable for fed-batch fermentation due to its growth profile, in comparison to BL21 cell line which demonstrated a high oxygen consumption rate leading to cell death, and causing culture growth to be unsustainable over an extended period. It was noted from mass spectrometry data that the three cleavage sites within PCV3 amino acid sequence, giving rise to peptides A, B and C, all contained a K residue immediately before the cleavage site, while peptides B and C both contained a K residue immediately after the cleavage site. This pattern is suggestive of cleavage by OmpT, a membrane protease present on the surface of wild-type *E. coli* K12 strains that is known to cleave peptides preferentially at dibasic sites (-K-K-, -K-R-, -R-K-, and –R-R-) (Dekker et al., 2001; Kramer et al., 2000). In addition to the issue of proteolysis, some literature has shown that expression of recombinant proteins in the W3110 cell line resulted in increased aggregation compared to expression in BL21 cell line under certain conditions (Ratelade et al., 2009), which may also account for the difference in solubility observed between PCV2d-PCV3 proteins expressed in shake flask and fermentation experiments using the different cell lines.

Cell lines aside, in Chapter 3.2.4 we saw that a small proportion of soluble PCV2d-PCV3 expression could be achieved in shake flask culture when growing at 30 °C; this was mirrored by the expression of PCV2d-PCV3 in fed-batch fermentation which achieved a higher proportion of soluble, full length protein when expressed at 20 °C compared to at 25 °C, and expression at a lower temperature also gave rise to a smaller proportion of proteolytic cleavage peptides. This suggested that the misfolded, inclusion body conformations of PCV2d-PCV3 are more susceptible to proteolytic degradation. This is likely by the action of heat shock proteases which function as an important protein quality control mechanism (Schmidt et al., 1999). It is also possible that the higher expression temperature causes inclusion bodies to be disintegrated by chaperones at an accelerated rate (Jürgen et al., 2010).

Overall, it was clear that reducing the susceptibility of PCV2d-PCV3 chimeric protein to proteolytic cleavage by way of both cell line optimisation to avoid the activity of proteases and by preventing protein misfolding during expression are essential considerations in the development of this design into a dual PCV vaccine candidate using a recombinant bacterial system.

7.2.3 A simple and efficient procedure to produce highly pure PCV2d-PCV3 chimeric protein from inclusion bodies by applying a high pH, chaotropic environment

It was demonstrated early on in Chapter 3 that expression of PCV2d-PCV3 chimeric proteins resulted in the generation of cytoplasmic aggregates. In Chapter 4, initial attempts to yield soluble, monomeric chimeric proteins using detergent proved almost completely ineffective, strongly suggesting the formation of inclusion bodies.

A common hurdle in recombinant bacterial expression systems, inclusion bodies are hypothesized to be formed by an unbalanced equilibrium between aggregated and soluble proteins and are thought to occur as a result of intracellular accumulation of partially folded expressed proteins which aggregate through non-covalent, hydrophobic or ionic interactions, or a combination (Przybycien et al., 1994). High level expression of a non-native protein, generally considered as greater than 2 % of total cellular protein expression, is considered more prone to accumulation as inclusion bodies in *E. coli* (Mitraki et al., 1991). This can occur when the internal cellular biochemistry of the expression host differs from that of the original source of the gene, and as mechanisms for protein folding may also be absent, hydrophobic residues that normally would remain buried may be exposed and available for undesirable interactions with one another.

In early solubilisation experiments, it was demonstrated that of PCV2d-PCV3 inclusion body proteins, some soluble protein could be yielded in the presence of 4 M urea when proteins had been expressed under low temperatures, promoting slower translation and folding. Studies on bacterial inclusion bodies have shown that if a lower intensity production process is used, a greater proportion of properly folded and biologically active recombinant proteins are formed inside inclusion bodies (García-Fruitós & Villaverde, 2010; Peternel et al., 2008). This suggested the presence of, or potential to generate, non-classical inclusion bodies, which could contain a large amount of correctly folded protein precursor (Jevševar et al., 2005). Although the planned method for generating the PCV2d-PCV3 dual vaccine candidate was through soluble expression, inclusion bodies can be a useful tool in biotechnology as they are often highly pure, where the over-expressed recombinant protein may represent up to 95 % of total inclusion body protein content (Villaverde & Carrió, 2003). Furthermore, non-classical inclusion bodies are highly attractive for downstream isolation of target proteins as they have been shown to have protein molecules in native-like conformation with some inclusion bodies having significant biological activity, and the majority of other proteins can be simply washed from inclusion bodies after their isolation from bacterial cells (Jevševar et al., 2005; Peternel et al., 2008), This suggested a promising mechanism to produce PCV2d-PCV3 protein could be possible with further optimisation. That said, in this research, it was not possible to achieve a sufficiently large amount

of non-classical inclusion bodies by altering growth conditions alone to move forward with processing in this way. Thus it was determined that the most appropriate method for processing these inclusion bodies for our application was by use of high concentration of chaotropes like urea and guanidine hydrochloride to achieve complete denaturation. As a result, we developed a simple centrifugation and washing procedure to efficiently remove bacterial cell components from PCV2d-PCV3 chimera inclusion body proteins, leaving it highly pure.

One of the starkest findings was the impact of pH on the solubility of the PCV2d-PCV3 inclusion body proteins; in the presence of urea, applying a pH 6.0 environment yielded virtually no soluble protein in comparison to a pH 12.0 environment which was able to solubilise the entire inclusion body. These data indicated that the combination of highly alkaline pH along with a slightly lower concentration of urea (6 M) was necessary for solubilisation of PCV2d-PCV3 inclusion body proteins and in fact was more effective than 8 M urea in any less alkaline environment. Similar solubilisation of inclusion body proteins at high pH along with a low concentration of a chaotrope such as urea has been reported in previous research (Panda, 2003; S. M. Singh et al., 2008), in which it was suggested that differential solubility of inclusion body proteins can be attributed to involvement of different forces causing aggregation during expression of recombinant proteins. It has been theorized that the combination of urea and high pH works synergistically to improve the solubilisation of inclusion body proteins, where high pH likely contributes by imparting negative charge to the partially folded protein intermediate, enabling urea to break hydrogen bonds among the aggregated molecules. Urea used along with alkaline pH is thought to disrupt the hydrophobic interaction between the inclusion body aggregates resulting in protein solubilisation (S. M. Singh et al., 2008).Apart from high pH, other non-denaturing conditions such as use of detergents like CTAB (Puri et al., 1992) and low concentration of L-arginine or guanidine hydrochloride (Raina et al., 2004; Umetsu et al., 2005) have been successfully used for solubilisation of protein aggregates, where in most cases such non-denaturing solubilisation resulted in improved recovery of bioactive protein (S. M. Singh et al., 2008). Solubilisation of PCV2d-PCV3 inclusion body proteins in detergent with lower, non-denaturing concentrations of chaotrope was attempted in order to protect the pre-existing native-like secondary structures of the proteins and enable folding, as has been previously demonstrated for recombinant proteins in *E. coli* (Khan et al., 1998) however in the case of PCV2d-PCV3, these approaches did not achieve a sufficient yield of solubilised protein. Here we conclude that where disulphide bonds are not critical for the downstream application, solubilisation in strong denaturing conditions combining highly alkaline pH, moderately high chaotrope concentration and a strong reducing agent can provide a highly efficient method for recovery of PCV2d-PCV3 chimera protein from inclusion

bodies. Using this information, it may be possible to investigate a method to refold these inclusion body proteins in order to obtain a sufficiently soluble material that could be used in a parenteral PCV2d-PCV3 dual protective vaccine.

7.3 PCV2d cysteine mutants

7.3.1 Cysteine mutation eliminates dimerization potential of PCV2d protein and PCV2d derived from chimera protein also shows no dimerization potential (and neither form VLPs)

A consideration in designing the protein to be formulated into our PCV2d vaccine was its folding capability; whilst it was important to avoid secondary structure or monomer association for ease of downstream processing, it was also necessary to consider the effect of protein folding on the exposure of epitope regions to the host's immune system upon vaccination.

Each monomer of PCV2d Cap contains one cysteine residue. Disulphide bonds formed between cysteine residues are considered fundamental building blocks in molecular architecture. The formation of a disulphide bond by two side chain Sγ atoms of spatially proximal cysteines are most commonly formed intramolecularly. A disulphide bond constitutes a two-electron oxidation process, from reduced sulphydryl groups of cysteine residues (S-H) to the oxidized cysteine (S-S) residue. As mentioned in Chapter 5, studies have shown that the cysteine 108 residue in PCV2d capsid protein is important in stabilization of the VLP structure through disulphide bonding between adjacent proteins. To avoid this, it was advantageous to express these proteins cytoplasmically in *E. coli,* in a physiological environment that would not favour disulphide bonding. The cysteine 108 residue in mutant PCV2d proteins was substituted for either an alanine or a serine residue, chosen as they are both similarly small amino acids to cysteine but lacking the functional groups to form disulphide bonds. Our results also reflected the findings of previous research, where it was observed that while PCV2d WT protein expressed from the single gene construct formed a large range of oligomerisation species under certain conditions, mutation of the cysteine residue virtually eliminated this.

There were two cases where PCV2d WT protein formed oligomerisation species under different physiological conditions after cell lysis. The first phenomenon was observed in bacterial lysates containing soluble cell contents, wherein the PCV2d WT protein expressed from the single gene construct showed oligomerisation into at least 8 different species of various sizes between 23.4 and >250 kDa despite being expressed cytoplasmically in *E. coli.* Under physiological conditions, the *E. coli* cytoplasm is maintained in a reduced state that strongly disfavours the formation of stable disulphide bonds, maintained through glutathione- and thioredoxin-dependent reduction systems (Bessette et al., 1999) so disulphide bonding is limited to take place the periplasmic space

where it is facilitated by bacterial thiol disulfide oxidoreductase enzymes (Bardwell et al., 1991). Two disulphide pathways coexist in *E. coli,* the DsbA–DsbB oxidative pathway and the DsbC–DsbD isomerization pathway. Disulphide bonds are introduced into proteins by the highly oxidizing protein DsbA. As a redox-active member of the thioredoxin family, DsbA has a redox-active site that interconverts between disulphide and dithiol. After donating its disulphide to a substrate protein, DsbA is reoxidized to carry out further disulfide catalysis. This reoxidation step is catalyzed by the membrane-bound protein DsbB, using quinones as the electron acceptors that deliver the electrons ultimately to molecular oxygen. *E. coli* encodes two disulfide isomerases, DsbC and DsbG. Inner membrane redox-active protein DsbD maintains these and other disulphide reductases in their catalytically-active reduced form. The isomerization pathway plays a proof-reading role, where DsbC is thought to be important for rearranging incorrectly paired cysteines introduced by DsbA.

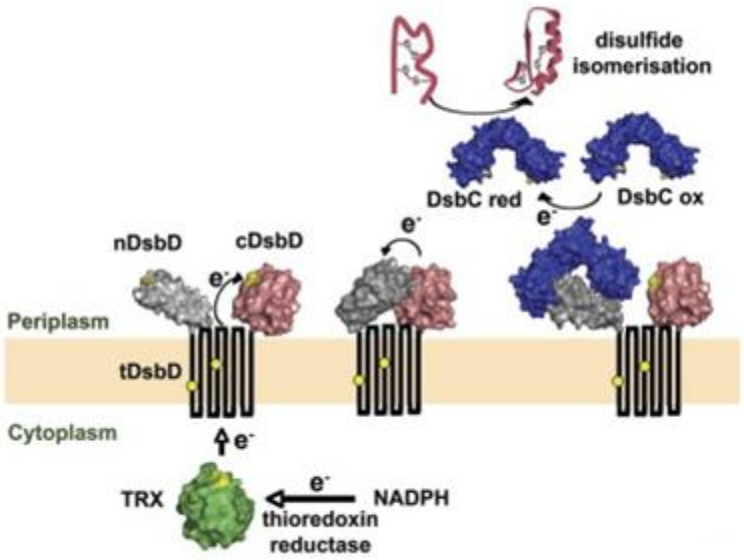

Figure 62. Disulphide shuffling in the bacterial periplasm. Membrane protein DsbD plays a central role in transferring electrons from the reducing cytoplasm to the oxidative environment of the periplasm. DsbD has an N-terminal domain nDsbD (grey), a transmembrane domain tDsbD, and a C-terminal thioredoxin-like domain cDsbD (pink). DsbD utilizes two electrons flow from NADPH via thioredoxin reductase and thioredoxin (TRX, shown in green) then transfers these to cDsbD and nDsbD (cDsbD–nDsbD complex, shown in grey and pink). Reduced nDsbD reduces substrates including the disulphide isomerases DsbC and DsbG (oxidized and reduced DsbC shown in dark blue; nDsbD–DsbC complex shown in grey and dark blue). The cysteines of tDsbD involved in

electron transfer are represented as yellow dots and the active site cysteines of the other proteins are shown in yellow (Heras et al., 2007).

In bacterial lysates showing oligomerisation species of PCV2d WT protein, it is possible that this occurred through residual catalytic activity by the periplasmic Dsb proteins after cell lysis, once the proteins were no longer separated by compartmentalization. DsbA in its oxidized form would have the capacity to catalyze disulphide bond formation between adjacent PCV2d WT proteins in solution, although its reoxidation by DsbB could be dependent on locality of the necessary components. Although oligomerisation can also occur through electrostatic bonds or Van der Waals forces, the PCV2d cysteine mutants did not show oligomerisation, indicating this was a disulphide bonding-mediated phenomenon. Interestingly, the PCV2d WT protein derived as a proteolytic cleavage product from the WT PCV2d-PCV3 chimera did not exhibit the same oligomerisation capability as PCV2d WT protein that had been expressed from the single gene construct.

The second phenomenon was observed when PCV2d WT proteins, purified to a high level by CIEX followed by gel filtration, were seen to form dimers only following sample preparation for non-reducing SDS PAGE. It is accepted that disulphide bonds can be formed spontaneously by molecular oxygen, albeit very slowly in comparison to the rate of an enzyme-catalyzed reaction. This has been shown to occur under aerobic conditions where a thin layer of cysteine is generated at the air–liquid interface when a cysteine solution is left exposed to air (Anfinsen & Haber, 1961). Disulphides typically function to stabilize the tertiary structure of a protein and a protein whose cysteines are linked via disulphide bonds can take on many fewer conformations than a protein whose cysteines remain free. The decrease in chain entropy makes a disulphide bonded protein energetically favourable over the unfolded form of the protein (Pace et al., 1988; Schellman, 1987).

These results are nevertheless reflective of the truncated PCV2d Cap proteins' capacity to form disulphide bonds. One of the main findings to emphasize is that no PCV2d WT oligomerisation species were detectable under the conditions used in gel filtration; the buffer used for gel filtration was very similar in composition to PBS, the aqueous component used in vaccine formulation (Results Chapter 6) and used as a control substance in animal trials (Results Chapters 5 & 6). These data confirm with high certainty that under the conditions used in vaccination, no iterations of PCV2d protein tested were able to form oligomers, while cysteine mutation of the truncated PCV2d protein eliminated all oligomerisation capacity.

7.3.2 PCV2d cysteine mutant shows reduced immunogenicity compared to PCV2d WT

Multiple studies have previously used mouse models to investigate the pathogenicity of PCV2 virus without complications (Du et al., 2019; J. Li et al., 2010; Ouyang et al., 2018), however in mouse trials conducted by our collaborators using PCV2d Cap proteins derived from micro-organisms *E. coli* and *O. Thermomethanolica* for immunisation, there were some unexpected immunological findings.

In the live animal trial, which was testing the capacity of recombinant PCV2d antigens to raise specific antibody responses in mice, we found that serum from control mice that had not been immunised with PCV2d antigen appeared to demonstrate the presence of specific neutralising antibodies when mixed with the live virus, protecting PK-15 cells from infection. The reason for this was unknown, but indicated the mice may have some level of pre-existing immunity against PCV2d virus. Retrospective phylogenetic analysis has suggested PCV3 virus originated from bat-associated circoviruses and evolved through inter-species transmission (Fu et al., 2018) raising the possibility that a similar mechanism may have been involved in PCV2 evolution or at least that inter-species transmissibility is common in circoviruses. Analysis has also shown 92 % sequence identity between circoviruses of two different bird species (L. Li et al., 2011), indicating there may be a high level of sequence conservation between circoviruses in general, even between species. One hypothesis is that the mice used in our PCV2d viral challenge trial may have already been exposed to a similar circovirus species and were able to generate antibodies with some reactivity against PCV2d.

Furthermore, neutralising antibody data from the cell-based assay indicated PCV2d WT antigen was able to generate a greater neutralising antibody response than PCV2d(C108S) antigen. Although the reason for this is purely speculative, a previous study mapping the crystal structure of PCV2 capsid protein predicted the region of residues 106-115 could be an epitope for antibody binding (Wang et al., 2016) wherein substitution of the cysteine residue may alter antibody binding interactions. Alternatively, as discussed earlier in Chapter 5, VLP based vaccines have been shown to generate more effective cellular and humoral immune responses than monomeric subunit vaccines (Cervera et al., 2019). A hypothesis is that PCV2d dimers or higher oligomers may also raise a greater immune response compared to monomeric proteins. Although our data suggests the truncated PCV2d WT proteins are unable to form VLPs under the conditions used for vaccination, they do retain the capacity to form dimers or higher oligomers which may confer greater immunogenicity than the entirely monomeric preparation of PCV2d(C108S) protein.

7.4 Preparation of a PCV2d vaccine candidate

7.4.1 Vaccination with experimental water-oil-water PCV2d vaccine is able to generate immunological memory

Through months of storage trials testing the temperature and emulsion stability of a range of vaccine candidates in the laboratory, an optimal formulation was chosen. The live pig trial detailed in Chapter 6 was the first opportunity to truly assess the efficacy of our experimental vaccine formulation.

From storage trials, our experimental ISA 201 PCV2d vaccine demonstrated high stability in at 4 °C for up to 9 months, with very few defects and no signs of adverse interaction between the adjuvant and the antigen, although there had been challenges in extracting the antigen for anaylsis once emulsified with the adjuvant. When this formulation was transferred to a live animal challenge trial in swine, it gave important immunological insights: serological data showed some positive effects as a result of administration of our experimental vaccine. A major difference between the serological data generated from pigs in the experimental PCV2d vaccine group versus the commercial vaccine group was that the commercial vaccine was able to raise PCV2-specific antibodies from the point of vaccination, with this response further increasing in all timepoints following viral challenge. In contrast, from the point of receiving the first dose of experimental vaccine up until the point of viral challenge, there was no observable protective effect. From this alone, the conclusion may be drawn that the experimental vaccine was unable to raise a sufficient immune response to confer protection; however, the experimental vaccine was able to generate an accelerated adaptive immune response when challenged with the virus compared to in the unvaccinated control, suggestive of immunological memory which is characterized by *"*the pre-existence of a clonally expanded population of antigen-specific lymphocytes" (Janeway et al., 2001).

Immunologic memory is dependent on clonal selection. When encountering an antigen, B cells recognize it through membrane antibodies, known as surface immunoglobulins, which bind to the antigen. This activates the B-cells to expand rapidly in population, creating progeny clones that differentiate into plasma cells and memory B cells with the same antigen specificity. Plasma cells secrete a large number of antibodies to neutralize the antigens, but die quickly after clearing the antigens due to a short lifespan. Memory cells on the other hand have a long lifespan and can remain in the body for many years. They do not produce antibodies, unless re-exposure to the antigen drives their differentiation into antibody-secreting plasma cells. This reactivation is a rapid process, such that booster responses are characterized by the rapid increase in antibodies to

higher titers that have a higher affinity for the antigen than antibodies generated during primary responses. The immune memory provides an efficient strategy to defend against pathogens after a second intrusion or in the case of a vaccinated individual, on exposure to the live pathogen (Siegrist, 2008; Tao & Xu, 2016).

Despite this positive finding suggesting immunological memory had been generated, it was observed that the speed at which a protective antibody response was raised by the experimental vaccine was comparatively slower than the commercial vaccine; this suggests the initial immune response raised upon administration of the vaccine was lower in the experimental vaccine group. The commercial vaccine used in this study, Ingelvac CircoFLEX®, is a VLP based-vaccine; evidence shows VLP-based vaccines are highly immunogenic and can stimulate robust cellular and humoral immune responses due to their highly repetitive display of antigenic epitopes (Grgacic & Anderson, 2006), to a greater degree than monomeric subunit vaccines such as our experimental vaccine candidate. In a livestock population, the ability of a vaccine to generate a rapid specific antibody response upon encountering the live virus is essential as a delayed response would allow propagation of the virus to higher titres and facilitate increased transmissibility of the virus. There are a number of ways in which the initial recruitment of immune cells could be improved upon vaccine administration, such as by altering the adjuvant used to one that is more immune reactive, using an adjuvant type that exhibits slow localized antigen release or increasing the antigen dosage.

Although numerous studies have attempted to use *E. coli* as an expression system for a PCV2 Cap vaccine in the past, but none have been successful enough for commercialization and these designs have mostly relied on self-assembly of the capsid protein into a VLP (P. C. Wu et al., 2016; Yin et al., 2010). Current PCV2 vaccines on the market consist of live attenuated PCV, killed whole PCV or baculovirus vector subunit vaccines. Due to the comparatively lower immunogenicity of subunit vaccines compared to whole organism vaccines, they are often adjuvanted with oil of mineral or non-mineral origin as oil-adjuvanted vaccines are known to significantly increase humoral immunity and have superior antibody formation (M. E. Park et al., 2014), including PCV2 subunit vaccines Porcilis® PCV (Schering-Plough/Merck) and Circumvent® (Intervet/Merck). Dosage information for PCV subunit vaccines is limited to those using the baculovirus expression system. Circumvent® patent states that at least 20 μg of PCV2 Cap protein per dose is capable of eliciting a protective immune response against PCV2 infection, where 80 μg per dose is the most preferable dosage. The patent also presents an antigenic mass up to 275 μg per dose could be used without eliciting local reactions at the injection site (Wo et al., 2007). Meanwhile, the patent for Ingelvac CircoFLEX® (Boehringer Ingelheim) presents a dosage less than 20 μg per dose was

preferable for protection of young pigs against PCV2 (Hernandez et al., 2017) while another using a similar system also suggested administering at least 20 µg per dose (Roerink & Woensel, 2009). Alternative designs generating PCV2 VLPs in *E. coli* expression systems have been patented for potential diagnostic use, but have not been successful in generating usable vaccine. One such design could not achieve statistically significant decrease in viral load in swine by administration of either one or two doses of 150 µg of the VLP vaccine (Almeida et al., 2016).

Overall, the experimental vaccine does present some promising findings in terms of its ability to generate immunological memory and potentially the desired protective effect. Due to the relative novelty of using an *E. coli* expression system to produce a PCV2 subunit vaccine in a monomeric form, further challenge trials using the experimental vaccine in swine and testing a range of alternative adjuvant types and dosages is the best way to efficiently optimise the design.

7.4.2 Vaccination with experimental PCV2d vaccine results in increased viremia

Whist it had been clear from serology data that vaccination using the experimental ISA 201 PCV2d vaccine formulated in this study was able to generate an antibody response, and cell-based virus neutralisation assay data using serum from rabbits immunised with the PCV2d antigen demonstrated neutralising antibody activity on the live virus, the formulated vaccine appeared to be causing some unexpected phenomena. The live pig trial showed significantly increased levels of viremia and nasal shedding in the experimental vaccine group comparison to any other, including the unvaccinated, virus challenged positive control group. Nasal shedding is a factor of particular importance in PCV2 viral transmission and is an essential measure in testing the vaccine's suitability in an animal population-dense, livestock environment.

It was hypothesised that the unexpected effect on viremia and nasal shedding may be due to the adjuvant used in the experimental vaccine. Previous studies have shown different classes of adjuvants result in different immune response profiles. In one study investigating adjuvants used in vaccine formulations with a *Mycobacterium bovis* BCG antigen, a pathogen known to cause bovine tuberculosis, it was demonstrated that a water-oil emulsion induced both an effector cell and a central memory T cell response while a cationic-liposome adjuvant only induced a central memory response. Furthermore, induction of these immune phenotypes in cattle were not reported when the same vaccines were tested in mice, demonstrating the importance of testing adjuvant formulations directly in the target species, and of measuring different types of immune response (Vordermeier et al., 2009).

In general, newer adjuvant formulations contain a vehicle, which carries antigens to antigen-presenting cells. Some adjuvants also contain immunomodulators, which augment cytokine

production. In a primary cascade of cytokine production at the site of injection, TNF-α promotes the migration of dendritic cells to lymphoid tissues while GM-CSF accelerates differentiation of dendritic cells into antigen presenting cells. These adjuvants can also function to upregulate a secondary cytokine cascade in lymphoid tissues in response to antigenic stimulation wherein IL-12 promotes production of IFN-γ for generation of protective antibodies. They can also stimulate follicular dendritic cells and B cells, important in generation of B-cell memory, which is a highly important factor for vaccination (Allison, 1997). ISA 201 is designed to improve the cell-mediated immune response yet avoid inflammatory reactions at the injection site as commonly seen with other mineral-oil based adjuvants. Research shows that vaccination with ISA 201 adjuvant increases Th1 cell-mediated immune response by upregulating transcription of cytokines IL-2, IL-10, IL-17A, and most notably IFN-γ. ISA 201 is also able to successfully enhance production of specific antibodies (Jang et al., 2010).

However, further investigation poses a major incompatibility for the use of ISA 201 adjuvant in PCV2 vaccination. It has been shown that treatment of PCV2-infected cells with INF-γ or IFN-α increases PCV2 replication in vitro, thought to be due to an interferon-stimulated response element (ISRE) sequence identified within the promoter region of the Rep gene (A Mankertz et al., 1997; Annette Mankertz et al., 2003, 2004), a defensive mechanism evolved by the virus. Studies have found that in PK-15 cells infected with PCV2 mutant viruses containing altered ISRE sequences, diminished viral replication-enhancing activity was observed when the cells were treated with porcine IFN-γ or IFN-α (Gu et al., 2009; S. Ramamoorthy et al., 2009). By adding IFN-γ to PK-15 or porcine monocytic (3D4/31) cell cultures increased the number of PCV2-infected cells by 691% in PK-15 cells and 423% in 3D4/31 cells, while IFN-α addition enhanced PCV2 infection by 529% in PK-15 cells and by 308% in 3D4/31 cells. Overall, treatment of PK-15 cultures with IFN-γ resulted in 20 times higher production of progeny virus, achieved by increased internalization of PCV2 VLPs, it was concluded (Meerts et al., 2005). It is also important to note that cytokine profiles of pigs infected with PCV2 show high levels of proinflamatory cytokines including IFN-α, and it is suspected that co-infecting pathogens exacerbate disease by increasing the circulating levels of interferons and proinflamatory cytokines (Kim et al., 2006; Ramamoorthy & Meng, 2009), highlighting the need for early and effective vaccination against PCV2.

These findings made clear that an alternative choice of adjuvant would be needed to move forward with the PCV2d vaccine candidate. ISA 201 consists of an enriched light mineral oil with a highly refined emulsifier derived from mannitol and purified oleic acid, but studies show differences in immune response are observed amongst different types of Montanide mineral oil adjuvants (Vordermeier et al., 2009). In studies in sheep, vaccination with formulations containing

ISA 201 has shown an increased antigen-specific IFN-γ response, while SEPPIC's Montanide Gel 01 did not stimulate an antigen-specific IFN-γ response after vaccination. That said, Gel 01 has been reported to stimulate a lower level of antigen-specific antibodies and a higher incidence of lesions (Begg et al., 2019). Although some research claims that gel vaccines are not suitable for pigs due to their short duration of immunity (J-H. Park, 2013), some serotypes of inactivated FMD vaccines are currently produced using gel adjuvants, while Ingelvac CircoFLEX®, one of the baculovirus-expressed PCV2 subunit vaccines on the market, is also formulated using a similar water-based polymer adjuvant, ImpranFLEX®. Formulation with a gel adjuvant will require further investigation to determine the appropriate antigen dosages needed for a sufficient immune response and to minimize adverse reactions, but gel adjuvants could be a promising option for development of our PCV2d vaccine candidate.

7.5 Future perspectives

One of the main aims of this research to continue work on in the future is to generate a recombinant protein containing PCV3 peptides for use in a novel subunit vaccine. PCV3 amino acid structure proved difficult for expression in *E coli*. Based on the literature, one potential improvement to increase expression of PCV3 Cap protein may be further truncation of PCV3 between amino acid residues 2-37 to provide a more long-lasting mRNA transcript for protein production based on the low content of G and C nucleotides within its DNA sequence. As discussed in Chapter 7, the truncated N-terminal region of highly expressed PCV2d protein currently contains 20 % G and C nucleotides within the first 20 base pairs of its DNA sequence. With the additional 9 nucleotide truncation from the current PCV3 gene design to the proposed PCV3 gene design, the new N-terminal region would contain only 20 % GC in comparison to the previous N-terminus created by truncation of residues 2-34, which contained 45 % GC. This could be a useful tool in expressing PCV3 alone, as well as improving soluble expression of a soluble chimeric PCV2d-PCV3 protein for a dual protective vaccine.

In addition to this, there is a wide scope of optimisations that can be done in fed-batch fermentation design to increase the yield of soluble protein and reduce the issue of protein insolubility due to sub-optimal growth conditions; these are likely down to limited oxygen availability leading to insufficient distribution to cells and a suboptimal feeding strategy or nutrient availability. More investigations into this could have the potential of improving expression of PCV3 alone or improving the solubility of a dual PCV2d-PCV3 chimera protein once a modified gene design has been obtained.

A further design that may promote solubility of difficult proteins could be to use a soluble protein such as PCV2d as a backbone for implanting epitopes from PCV3 for use in a dual vaccine. Such a strategy could also be utilised for other dual vaccine designs using structural protein epitopes from other livestock disease-causing organisms of significance, such as foot and mouth disease (FMD) virus. The ability to perform a single step of purification to obtain highly pure PCV2d protein means as long as a sufficient proportion of the PCV2d protein backbone is retained, this simple process could be extended to dual vaccine candidates.

Finally, we have discovered a recombinant, *E. coli*-produced PCV2d subunit vaccine is able to stimulate an immune response in pigs – more trials will be required to determine the best choice of adjuvant for this vaccine.

Overall, we have made small steps towards making vaccine production capabilities and protection of livestock economy accessible for those who need it, and a contribution to benefitting economic development and reducing poverty in Thailand, South East Asia and beyond.

References

Afolabi, K. O., Iweriebor, B. C., Okoh, A. I. & Obi, L. C. (2017). Global status of porcine circovirus type 2 and its associated diseases in Sub-Saharan Africa. Advances in Virology, 2017, 1–16. https://doi.org/10.1155/2017/6807964

Allison, A. C. (1997). Immunological adjuvants and their modes of action. Archivum Immunologiae et Therapiae Experimentalis, 45(2–3), 141–147.

Almeida, M. R. D. E., Junior, A. S., Fietto, J. L. R., Bressan, G. C., Salgado, R. L., Onofre, T. S., Fausto, M. C., Vidigal, P. M. P., Kalks, S. P., Crispim, J. S., Amaziles Silva Leite, R., Andrade Teixeria, J. de, Fialho Gonzaga, N., Jaquel Zilch, T., Lino De Souza, L. F., De Cruz Souza, A. M., & De Morais, Montiero, A. (2016). Recombinant antigens of porcine circovirus 2 (PCV-2) for vaccine formulations, diagnostic kit and use thereof. US20160000897A1.

Alving, C. R. (1995). Liposomal vaccines: clinical status and immunological presentation for humoral and cellular immunity. Annals of the New York Academy of Sciences, 754(1), 143–152. https://doi.org/10.1111/J.1749-6632.1995.TB44447.X

Amet, N., Lee, H.-F. & Shen, W.-C. (2008). Insertion of the designed helical linker led to increased expression of Tf-based fusion proteins. Pharmaceutical Research, 26(3), 523–528. https://doi.org/10.1007/S11095-008-9767-0

Anfinsen, C. B. & Haber, E. (1961). Studies on the reduction and re-formation of protein disulfide bonds. Journal of Biological Chemistry, 236(5), 1361–1363. https://doi.org/10.1016/S0021-9258(18)64177-8

Arai, R., Ueda, H., Kitayama, A., Kamiya, N. & Nagamune, T. (2001). Design of the linkers which effectively separate domains of a bifunctional fusion protein. Protein Engineering, 14(8), 529–532. https://doi.org/10.1093/PROTEIN/14.8.529

Argos, P. (1990). An investigation of oligopeptides linking domains in protein tertiary structures and possible candidates for general gene fusion. Journal of Molecular Biology, 211(4), 943–958. https://doi.org/10.1016/0022-2836(90)90085-Z

Bai, Y., Ann, D. K. & Shen, W.-C. (2005). Recombinant granulocyte colony-stimulating factor-transferrin fusion protein as an oral myelopoietic agent. Proceedings of the National Academy of Sciences, 102(20), 7292–7296. https://doi.org/10.1073/PNAS.0500062102

Bai, Y. & Shen, W.-C. (2006). Improving the oral efficacy of recombinant granulocyte colony-stimulating factor and transferrin fusion protein by spacer optimization. Pharmaceutical Research, 23(9), 2116–2121. https://doi.org/10.1007/S11095-006-9059-5

Balasundaram, B., Harrison, S. & Bracewell, D. G. (2009). Advances in product release strategies and impact on bioprocess design. Trends in Biotechnology, 27(8), 477–485. https://doi.org/10.1016/J.TIBTECH.2009.04.004

Bao, F., Mi, S., Luo, Q., Guo, H., Tu, C., Zhu, G. & Gong, W. (2018). Retrospective study of porcine circovirus type 2 infection reveals a novel genotype PCV2f. Transboundary and Emerging Diseases, 65(2), 432–440. https://doi.org/10.1111/TBED.12721

Bardwell, J. C. A., McGovern, K. & Beckwith, J. (1991). Identification of a protein required for disulfide bond formation in vivo. Cell, 67(3), 581–589. https://doi.org/10.1016/0092-8674(91)90532-4

Bastola, R., Seo, J. E., Keum, T., Noh, G., Choi, J. W., Shin, J. Il, Kim, J. H. & Lee, S. (2019). Preparation of squalene oil-based emulsion adjuvants employing a self-emulsifying drug delivery system and assessment of *Mycoplasma hyopneumoniae*-specific antibody titers in BALB/c mice. Pharmaceutics, 11(12), 667. https://doi.org/10.3390/pharmaceutics11120667

Begg, D. J., Dhungyel, O., Naddi, A., Dhand, N. K., Plain, K. M., de Silva, K., Purdie, A. C. & Whittington, R. J. (2019). The immunogenicity and tissue reactivity of *Mycobacterium avium* subsp. *paratuberculosis* inactivated whole cell vaccine is dependent on the adjuvant used. Heliyon, 5(6), e01911. https://doi.org/10.1016/J.HELIYON.2019.E01911

Bessette, P. H., Åslund, F., Beckwith, J. & Georgiou, G. (1999). Efficient folding of proteins with multiple disulfide bonds in the *Escherichia coli* cytoplasm. Proceedings of the National Academy of Sciences, 96(24), 13703–13708. https://doi.org/10.1073/PNAS.96.24.13703

Boer, H. A. de, Comstock, L. J. & Vasser, M. (1983). The tac promoter: a functional hybrid derived from the trp and lac promoters. Proceedings of the National Academy of Sciences, 80(1), 21–25. https://doi.org/10.1073/PNAS.80.1.21

Bornhorst, J. A., & Falke, J. J. (2000). Purification of proteins using polyhistidine affinity tags. Methods in Enzymology, 326, 245–254. https://doi.org/10.1016/S0076-6879(00)26058-8

Bucarey, S., Noriega, J., Reyes, P., Tapia, C., Sáenz, L., Zuñiga, A. & Tobar, J. (2009). The optimized capsid gene of porcine circovirus type 2 expressed in yeast forms virus-like particles and elicits antibody responses in mice fed with recombinant yeast extracts. Vaccine, 27(42), 5781–5790. https://doi.org/10.1016/J.VACCINE.2009.07.061

Carrió, M. M. & Villaverde, A. (2005). Localization of chaperones DnaK and GroEL in bacterial inclusion bodies. Journal of Bacteriology, 187(10), 3599–3601. https://doi.org/10.1128/JB.187.10.3599-3601.2005

Cervera, L., Gòdia, F., Tarrés-Freixas, F., Aguilar-Gurrieri, C., Carrillo, J., Blanco, J. & Gutiérrez-Granados, S. (2019). Production of HIV-1-based virus-like particles for vaccination: achievements and limits. Applied Microbiology and Biotechnology, 103(18), 7367–7384. https://doi.org/10.1007/S00253-019-10038-3

Cheung, A. K., Lager, K. M., Kohutyuk, O. I., Vincent, A. L., Henry, S. C., Baker, R. B., Rowland, R. R. & Dunham, A. G. (2007). Detection of two porcine circovirus type 2 genotypic groups in United States swine herds. Archives of Virology, 152(5), 1035–1044. https://doi.org/10.1007/S00705-006-0909-6

Coffman, J. D., Zhu, J., Roach, J. M., Bavari, S., Ulrich, R. G. & Giardina, S. L. (2002). Production and purification of a recombinant staphylococcal enterotoxin B vaccine candidate expressed in *Escherichia coli*. Protein Expression and Purification, 24(2), 302–312. https://doi.org/10.1006/PREP.2001.1556

Constans, M., Ssemadaali, M., Kolyvushko, O. & Ramamoorthy, S. (2015). Antigenic determinants of possible vaccine escape by porcine circovirus subtype 2b viruses. Bioinformatics and Biology Insights, 9, 1–12. https://doi.org/10.4137/bbi.s30226

Cox, J. & Coulter, A. (1997). Adjuvants--a classification and review of their modes of action. Vaccine, 15(3), 248–256. https://doi.org/10.1016/S0264-410X(96)00183-1

Danielsson, R. & Eriksson, H. (2021). Aluminium adjuvants in vaccines – a way to modulate the immune response. Seminars in Cell and Developmental Biology, 115, 3–9. https://doi.org/10.1016/j.semcdb.2020.12.008

Dar, P., Kalaivanan, R., Sied, N., Mamo, B., Kishore, S., Suryanarayana, V. V. S. & Kondabattula, G. (2013). Montanide ISATM 201 adjuvanted FMD vaccine induces improved immune responses and protection in cattle. Vaccine, 31(33), 3327–3332. https://doi.org/10.1016/J.VACCINE.2013.05.078

Dekker, N., Cox, R., Kramer, R. & Egmond, M. (2001). Substrate specificity of the integral membrane protease OmpT determined by spatially addressed peptide libraries. Biochemistry, 40(6), 1694–1701. https://doi.org/10.1021/BI0014195

Demain, A. & Vaishnav, P. (2009). Production of recombinant proteins by microbes and higher organisms. Biotechnology Advances, 27(3), 297–306. https://doi.org/10.1016/J.BIOTECHADV.2009.01.008

Demento, S. L., Siefert, A. L., Bandyopadhyay, A., Sharp, F. A. & Fahmy, T. M. (2011). Pathogen-associated molecular patterns on biomaterials: a paradigm for engineering new vaccines. Trends in Biotechnology, 29(6), 294–306. https://doi.org/10.1016/J.TIBTECH.2011.02.004

Deng, J., Li, X., Zheng, D., Wang, Y., Chen, L., Song, H., Wang, T., Huang, Y., Pang, W. & Tian, K. (2017). Establishment and application of an indirect ELISA for porcine circovirus 3. Archives of Virology, 163(2), 479–482. https://doi.org/10.1007/S00705-017-3607-7

Deville, S., Arous, J. Ben, Ionkoff, G., Kukushkin, F. B. S., Baybikov, T., Borisov, V. & Dupuis, L. (2012). Load reduction in live PRRS vaccines using oil and polymer adjuvants. Procedia in Vaccinology, 6, 134–140. https://doi.org/10.1016/J.PROVAC.2012.04.018

Didierlaurent, A. M., Morel, S., Lockman, L., Giannini, S. L., Bisteau, M., Carlsen, H., Kielland, A., Vosters, O., Vanderheyde, N., Schiavetti, F., Larocque, D., Van Mechelen, M. & Garçon, N. (2009). AS04, an aluminum salt- and TLR4 agonist-based adjuvant system, induces a transient localized innate immune response leading to enhanced adaptive immunity. The Journal of Immunology, 183(10), 6186–6197. https://doi.org/10.4049/jimmunol.0901474

Douette, P., Navet, R., Gerkens, P., Galleni, M., Lévy, D. & Sluse, F, E. (2005). *Escherichia coli* fusion carrier proteins act as solubilizing agents for recombinant uncoupling protein 1 through interactions with GroEL. Biochemical and Biophysical Research Communications, 333(3), 686–693. https://doi.org/10.1016/J.BBRC.2005.05.164

Du, Q., Zhang, H., He, M., Zhao, X., He, J., Cui, B., Yang, X., Tong, D. & Huang, Y. (2019). Interleukin-10 promotes porcine circovirus type 2 persistent infection in mice and aggravates the tissue lesions by suppression of T cell infiltration. Frontiers in Microbiology, 10, 2050. https://doi.org/10.3389/FMICB.2019.02050

Dutton, R., Boyd, D., Berkmen, M. & Beckwith, J. (2008). Bacterial species exhibit diversity in their mechanisms and capacity for protein disulfide bond formation. Proceedings of the National Academy of Sciences of the United States of America, 105(33), 11933–11938. https://doi.org/10.1073/PNAS.0804621105

Dyson, M. R., Shadbolt, S. P., Vincent, K. J., Perera, R. L. & McCafferty, J. (2004). Production of soluble mammalian proteins in *Escherichia coli*: identification of protein features that correlate with successful expression. BMC Biotechnology, 4, 32. https://doi.org/10.1186/1472-6750-4-32

Eichmeyer, M. A., Johnson, W., Vaughn, E., Roof, M. B. & Hayes, P. W. (2018). Development of ingelvac provenza: a new tool against IAV-S. 49th Annual Meeting of the American Association of Swine Veterinarians, San Diego, CA.

Eldridge, B., Cooley, R., Odegrip, R., McGregor, D., Fitzgerald, K. & Ullman, C. (2009). An in vitro selection strategy for conferring protease resistance to ligand binding peptides. Protein Engineering, Design & Selection: PEDS, 22(11), 691–698. https://doi.org/10.1093/PROTEIN/GZP052

Fabre, M. L., Arrías, P. N., Masson, T., Pidre, M. L. & Romanowski, V. (2020). Baculovirus-derived vectors for immunization and therapeutic applications. Emerging and Reemerging Viral Pathogens, 2, 197-224. https://doi.org/10.1016/B978-0-12-814966-9.00011-1

Ferrer, M., Chernikova, T. N., Yakimov, M. M., Golyshin, P. N. & Timmis, K. N. (2003). Chaperonins govern growth of *Escherichia coli* at low temperatures. Nature Biotechnology, 21(11), 1266–1267. https://doi.org/10.1038/nbt1103-1266

Fox, C. B., Baldwin, S. L., Vedvick, T. S., Angov, E. & Reed, S. G. (2012). Effects on immunogenicity by formulations of emulsion-based adjuvants for malaria vaccines. Clinical and Vaccine Immunology: CVI, 19(10), 1633. https://doi.org/10.1128/CVI.00235-12

Franzo, G., Grassi, L., Tucciarone, C. M., Drigo, M., Martini, M., Pasotto, D., Mondin, A. & Menandro, M. L. (2019). A wild circulation: high presence of porcine circovirus 3 in different mammalian wild hosts and ticks. Transboundary and Emerging Diseases, 66(4), 1548–1557. https://doi.org/10.1111/TBED.13180

Freudl, R. (2018). Signal peptides for recombinant protein secretion in bacterial expression systems. Microbial Cell Factories, 17(1), 1–10. https://doi.org/10.1186/S12934-018-0901-3

Fu, X., Fang, B., Ma, J., Liu, Y., Bu, D., Zhou, P., Wang, H., Jia, K. & Zhang, G. (2018). Insights into the epidemic characteristics and evolutionary history of the novel porcine circovirus type 3 in southern China. Transboundary and Emerging Diseases, 65(2), e296–e303. https://doi.org/10.1111/TBED.12752

García-Fruitós, E. & Villaverde, A. (2010). Friendly production of bacterial inclusion bodies. Korean Journal of Chemical Engineering, 27(2), 385–389. https://doi.org/10.1007/S11814-010-0161-3

Gava, D., Serrão, V. H. B., Fernandes, L. T., Cantão, M. E., Ciacci-Zanella, J. R., Morés, N. & Schaefer, R. (2018). Structure analysis of capsid protein of porcine circovirus type 2 from pigs with systemic disease. Brazilian Journal of Microbiology, 49(2), 351–357. https://doi.org/10.1016/j.bjm.2017.08.007

Genzow, M., Schwartz, K., Gonzalez, G., Anderson, G. & Chittick, W. (2009). The effect of vaccination against porcine reproductive and respiratory syndrome virus (PRRSV) on the porcine

circovirus-2 (PCV-2) load in porcine circovirus associated disease (PCVAD) affected pigs. Canadian Journal of Veterinary Research, 73(2), 87–90.

George, R. A. & Heringa, J. (2002). An analysis of protein domain linkers: their classification and role in protein folding. Protein Engineering, Design and Selection, 15(11), 871–879. https://doi.org/10.1093/PROTEIN/15.11.871

Gherardi, R. K., Crépeaux, G. & Authier, F. J. (2019). Myalgia and chronic fatigue syndrome following immunization: macrophagic myofasciitis and animal studies support linkage to aluminum adjuvant persistency and diffusion in the immune system. Autoimmunity Reviews, 18(7), 691–705. https://doi.org/10.1016/J.AUTREV.2019.05.006

González-Domínguez, I., Puente-Massaguer, E., Cervera, L. & Gòdia, F. (2020). Quality assessment of virus-like particles at single particle level: a comparative study. Viruses, 12(2), 223. https://doi.org/10.3390/V12020223

Gottesman, S., Wickner, S. & Maurizi, M. R. (1997). Protein quality control: triage by chaperones and proteases. Genes & Development, 11, 815–823.

Grgacic, E. V. L & Anderson, D. A. (2006). Virus-like particles: passport to immune recognition. Methods, 40(1), 60-65. https://pubmed.ncbi.nlm.nih.gov/16997714/

Gu, J., Cao, R., Zhang, Y. & Chen, P. (2009). Biological character of porcine circovirus type 2 with site mutation at interferon stimulation reaction element (ISRE) like region in Rep gene promoter. Acta Microbiologica Sinica, 49(9), 1217–1222. https://pubmed.ncbi.nlm.nih.gov/20030061/

Gu, J., Zhang, Y., Lian, X., Sun, H., Wang, J., Liu, W., Meng, G., Li, P., Zhu, D., Jin, Y. & Cao, R. (2012). Functional analysis of the interferon-stimulated response element of porcine circovirus type 2 and its role during viral replication in vitro and in vivo. Virology Journal, 9, 152. https://doi.org/10.1186/1743-422X-9-152

Guo, L. J., Lu, Y. H., Wei, Y. W., Huang, L. P. & Liu, C. M. (2010). Porcine circovirus type 2 (PCV2): genetic variation and newly emerging genotypes in China. Virology Journal, 7(1), 273. https://doi.org/10.1186/1743-422X-7-273

Guo, L., Fu, Y., Wang, Y., Lu, Y., Wei, Y., Tang, Q., Fan, P., Liu, J., Zhang, L., Zhang, F., Huang, L., Liu, D., Li, S., Wu, H. & Liu, C. (2012). A porcine circovirus type 2 (PCV2) mutant with 234 amino acids in Capsid protein showed more virulence in vivo, compared with classical PCV2a/b strain. PLoS ONE, 7(7), e41463. https://doi.org/10.1371/journal.pone.0041463

Guzman, L. M., Belin, D., Carson, M. J. & Beckwith, J. (1995). Tight regulation, modulation, and high-level expression by vectors containing the arabinose P(BAD) promoter. Journal of Bacteriology, 177(14), 4121–4130. https://doi.org/10.1128/JB.177.14.4121-4130.1995

Hamel, A. L., Lin, L. L. & Nayar, G. P. S. (1998). Nucleotide sequence of porcine circovirus associated with postweaning multisystemic wasting syndrome in pigs. Journal of Virology, 72(6), 5262–5267.

He, W., Shu, J., Zhang, J., Liu, Z., Xu, J., Jin, X. & Wang, X. (2017). Expression, purification, and renaturation of a recombinant peptide-based HIV vaccine in *Escherichia coli*. Canadian Journal of Microbiology, 63(6), 493–501. https://doi.org/10.1139/CJM-2016-0528

Helke, K. L., Ezell, P. C., Duran-Struuck, R. & Swindl, M. M. (2015). Chapter 16. Biology and Diseases of Swine. In Laboratory Animal Medicine, Third Edition, 695.

Hendriksen, C. F. (1996). A short history of the use of animals in vaccine development and quality control. Developments in Biological Standardization, 86, 3–10.

Heras, B., Kurz, M., Shouldice, S. R. & Martin, J. L. (2007). The name's bond……disulfide bond. Current Opinion in Structural Biology, 17(6), 691–698. https://doi.org/10.1016/J.SBI.2007.08.009

Hernandez, L. A., Muehlenthaler, C. M., Vaughn, E. M. & Haiwick, G. (2017). PCV2 ORF2 protein variant and virus like particles composed thereof. US 2017/0029471 A1.

HHS Food and Drug Association. (2012). Guidance for industry on evaluating the effectiveness of anticoccidial drugs in food-producing animals; availability. Notice. Federal Register, 77, 69634–69635. http://www.fda.gov/

Hombach, J., Solomon, T., Kurane, I., Jacobson, J. & Wood, D. (2005). Report on a WHO consultation on immunological endpoints for evaluation of new Japanese encephalitis vaccines, WHO, Geneva, 2–3 September, 2004. Vaccine, 23(45), 5205–5211. https://doi.org/10.1016/J.VACCINE.2005.07.002

Huang, C.-J., Lin, H. & Yang, X. (2012). Industrial production of recombinant therapeutics in *Escherichia coli* and its recent advancements. Journal of Industrial Microbiology and Biotechnology, 39(3), 383–399. https://doi.org/10.1007/S10295-011-1082-9

Huang, L. P., Lu, Y. H., Wei, Y. W., Guo, L. J. & Liu, C. M. (2011). Identification of one critical amino acid that determines a conformational neutralizing epitope in the capsid protein of porcine circovirus type 2. BMC Microbiology, 11(188), 1–10. https://doi.org/10.1186/1471-2180-11-188

Huang, X., Wang, X., Zhang, J., Xia, N. & Zhao, Q. (2017). *Escherichia coli*-derived virus-like particles in vaccine development. NPJ Vaccines, 2(1), 1–8. https://doi.org/10.1038/s41541-017-0006-8

Huang, Y. & Chuang, D. . (1999). Mechanisms for GroEL/GroES-mediated folding of a large 86-kDa fusion polypeptide in vitro. The Journal of Biological Chemistry, 274(15), 10405–10412. https://doi.org/10.1074/JBC.274.15.10405

Huynh, T. M. L., Nguyen, B. H., Nguyen, V. G., Dang, H. A., Mai, T. N., Tran, T. H. G., Ngo, M. H., Le, V. T., Vu, T. N., Ta, T. K. C., Vo, V. H., Kim, H. K. & Park, B. K. (2014). Phylogenetic and phylogeographic analyses of porcine circovirus type 2 among pig farms in Vietnam. Transboundary and Emerging Diseases, 61(6), e25–e34. https://doi.org/10.1111/TBED.12066

Ibrahim, E. E.-S., Gamal, W. M., Hassan, A. I., Mahdy, S. E.-D., Hegazy, A. Z. & Abdel-Atty, M. M. (2015). Comparative study on the immunopotentiator effect of ISA 201, ISA 61, ISA 50, ISA 206 used in trivalent foot and mouth disease vaccine. Veterinary World, 8(10), 1189. https://doi.org/10.14202/VETWORLD.2015.1189-1198

Iyer, A. V., Ghosh, S., Singh, S. N. & Deshmukh, R. A. (2001). Evaluation of three “ready to formulate” oil adjuvants for foot-and-mouth disease vaccine production. Vaccine, 19(9–10), 1097–1105. https://doi.org/10.1016/S0264-410X(00)00337-6

Jain, N., Sahni, N., Kumru, O., Joshi, S., Volkin, D. & Russell Middaugh, C. (2015). Formulation and stabilization of recombinant protein based virus-like particle vaccines. Advanced Drug Delivery Reviews, 93, 42–55. https://doi.org/10.1016/J.ADDR.2014.10.023

Janeway, C., Travers, P., Walport, M. & Shlomchik, M. (2001). Immunobiology: the immune system in health and disease. 5th edition. Garland Science. https://www.ncbi.nlm.nih.gov/books/NBK27158/

Jang, S. I., Lillehoj, H. S., Lee, S. H., Lee, K. W., Park, S., Bauchan, G. R., Lillehoj, E. P., Ois Bertrand, F., Dupuis, L. & Deville, S. (2010). Immunoenhancing effects of Montanide TM ISA oil-based adjuvants on recombinant coccidia antigen vaccination against Eimeria acervulina infection. Veterinary Parasitology, 172, 221–228. https://doi.org/10.1016/j.vetpar.2010.04.042

Janssen, B. D. & Hayes, C. S. (2012). The tmRNA ribosome-rescue system. Advances in Protein Chemistry and Structural Biology, 86, 151–191. https://doi.org/10.1016/B978-0-12-386497-0.00005-0

Jeong, J., Park, C., Choi, K. & Chae, C. (2015). Comparison of three commercial one-dose porcine circovirus type 2 (PCV2) vaccines in a herd with concurrent circulation of PCV2b and mutant PCV2b. Veterinary Microbiology, 177(1–2), 43–52. https://doi.org/10.1016/J.VETMIC.2015.02.027

Jevševar, S., Gaberc-Porekar, V., Fonda, I., Podobnik, B., Grdadolnik, J. & Menart, V. (2005). Production of nonclassical inclusion bodies from which correctly folded protein can be extracted. Biotechnology Progress, 21(2), 632–639. https://doi.org/10.1021/BP0497839

Jiang, M., Guo, J., Zhang, G., Jin, Q., Liu, Y., Jia, R. & Wang, A. (2020). Fine mapping of linear B cell epitopes on capsid protein of porcine circovirus 3. Applied Microbiology and Biotechnology, 104(14), 6223–6234. https://doi.org/10.1007/S00253-020-10664-2

Jiang, S., Zhou, N., Li, Y., An, J. & Chang, T. (2019). Detection and sequencing of porcine circovirus 3 in commercially sourced laboratory mice. Veterinary Medicine and Science, 5(2), 176–181. https://doi.org/10.1002/VMS3.144

Jin, J., Park, C., Cho, S, H. & Chung, J. (2018). The level of decoy epitope in PCV2 vaccine affects the neutralizing activity of sera in the immunized animals. Biochemical and Biophysical Research Communications, 496(3), 846–851. https://doi.org/10.1016/J.BBRC.2018.01.141

Jürgen, B., Breitenstein, A., Urlacher, V., Büttner, K., Lin, H., Hecker, M., Schweder, T. & Neubauer, P. (2010). Quality control of inclusion bodies in *Escherichia coli*. Microbial Cell Factories, 9(1), 1–13. https://doi.org/10.1186/1475-2859-9-41

Kamionka, M. (2011). Engineering of therapeutic proteins production in *Escherichia coli*. Current Pharmaceutical Biotechnology, 12(2), 268–274. https://doi.org/10.2174/138920111794295693

Kaslow, D. & Biernaux, S. (2015). RTS,S: Toward a first landmark on the malaria vaccine technology roadmap. Vaccine, 33(52), 7425–7432. https://doi.org/10.1016/J.VACCINE.2015.09.061

Kensil, C. R., Patel, U., Lennick, M. & Marciani, D. (1991). Separation and characterization of saponins with adjuvant activity from *Quillaja saponaria* Molina cortex. The Journal of Immunology, 146(2), 431–437.

Khan, R. H., Rao, K. B. C. A., Eshwari, A. N. S., Totey, S. M. & Panda, A. K. (1998). Solubilization of recombinant ovine growth hormone with retention of native-like secondary structure and its refolding from the inclusion bodies of *Escherichia coli*. Biotechnology Progress, 14(5), 722–728. https://doi.org/10.1021/BP980071Q

Khayat, R., Brunn, N., Speir, J. A., Hardham, J. M., Ankenbauer, R. G., Schneemann, A. & Johnson, J. E. (2011). The 2.3-angstrom structure of porcine circovirus 2. Journal of Virology, 85(15), 7856–7862. https://doi.org/10.1128/JVI.05863-11

Khayat, R., Wen, K., Alimova, A., Gavrilov, B., Katz, A., Galarza, J. & Gottlieb, P. (2019). Structural characterization of the PCV2d virus-like particle at 3.3 Å resolution reveals differences to PCV2a and PCV2b capsids, a tetranucleotide, and an N-terminus near the icosahedral 3-fold axes. Virology, 537, 186–197. https://doi.org/10.1016/J.VIROL.2019.09.001

Kim, J., Ha, Y. & Chae, C. (2006). Potentiation of porcine circovirus 2-induced postweaning multisystemic wasting syndrome by porcine parvovirus is associated with excessive production of tumor necrosis factor-α. Veterinary Pathology, 43(5), 718–725. https://doi.org/10.1354/VP.43-5-718

Kim, J. H. & Lyoo, Y. S. (2002). Genetic characterization of porcine circovirus-2 field isolates from PMWS pigs. In Journal of Veterinary Science, 3(1), 31–39. https://doi.org/10.4142/jvs.2002.3.1.31

Kimple, M. E., Brill, A. L. & Pasker, R. L. (2013). Overview of affinity tags for protein purification. Current Protocols in Protein Science, 73:9.9.1-9.9.23. https://doi.org/10.1002/0471140864.ps0909s73

Klaumann, F., Dias-Alves, A., Cabezón, O., Mentaberre, G., Castillo-Contreras, R., López-Béjar, M., Casas-Díaz, E., Sibila, M., Correa-Fiz, F. & Segalés, J. (2019). Porcine circovirus 3 is highly prevalent in serum and tissues and may persistently infect wild boar (*Sus scrofa scrofa*). Transboundary and Emerging Diseases, 66(1), 91–101. https://doi.org/10.1111/TBED.12988

Klimka, A., Michels, L., Glowalla, E., Tosetti, B., Krönke, M. & Krut, O. (2015). Montanide ISA 71 VG is advantageous to Freund's adjuvant in immunization against *S. aureus* infection of mice. Scandinavian Journal of Immunology, 81(5), 291–297. https://doi.org/10.1111/SJI.12279

Kramer, R., Zandwijken, D., Egmond, M. & Dekker, N. (2000). In vitro folding, purification and characterization of *Escherichia coli* outer membrane protease ompT. European Journal of Biochemistry, 267(3), 885–893. https://doi.org/10.1046/J.1432-1327.2000.01073.X

Ku, X., Chen, F., Li, P., Wang, Y., Yu, X., Fan, S., Qian, P., Wu, M. & He, Q. (2017). Identification and genetic characterization of porcine circovirus type 3 in China. Transboundary and Emerging Diseases, 64(3), 703–708. https://doi.org/10.1111/TBED.12638

Kumar, S., Stecher, G. & Tamura, K. (2016). MEGA7: Molecular Evolutionary Genetics Analysis version 7.0 for bigger datasets. Molecular Biology and Evolution, 33(7), 1870–1874. https://doi.org/10.1093/MOLBEV/MSW054

Kuo, T.-Y., Hong, Z.-W., Tsai, C.-C., Yang, Y.-C. & Fu, H.-W. (2016). One-step negative chromatographic purification of *Helicobacter pylori* neutrophil-activating protein overexpressed in *Escherichia coli* in batch mode. Journal of Visualized Experiments: JoVE, 2016(112), 54043. https://doi.org/10.3791/54043

Kwon, T., Lee, D. U., Yoo, S. J., Je, S. H., Shin, J. Y. & Lyoo, Y. S. (2017). Genotypic diversity of porcine circovirus type 2 (PCV2) and genotype shift to PCV2d in Korean pig population. Virus Research, 228, 24–29. https://doi.org/10.1016/j.virusres.2016.11.015

Kwon, T., Yoo, S. J., Park, C. K. & Lyoo, Y. S. (2017). Prevalence of novel porcine circovirus 3 in Korean pig populations. Veterinary Microbiology, 207, 178–180. https://doi.org/10.1016/J.VETMIC.2017.06.013

Lekcharoensuk, P., Morozov, I., Paul, P. S., Thangthumniyom, N., Wajjawalku, W. & Meng, X. J. (2004). Epitope mapping of the major capsid protein of type 2 porcine circovirus (PCV2) by using chimeric PCV1 and PCV2. Journal of Virology, 78(15), 8135–8145. https://doi.org/10.1128/jvi.78.15.8135-8145.2004

Lenz, G., Doron-Faigenboim, A., Ron, E. Z., Tuller, T. & Gophna, U. (2011). Sequence features of *E. coli* mRNAs affect their degradation. PLoS ONE, 6(12), 28544. https://doi.org/10.1371/JOURNAL.PONE.0028544

Li, J., Yuan, X., Zhang, C., Miao, L., Wu, J., Shi, J., Xu, S., Cui, S., Wang, J. & Ai, H. (2010). A mouse model to study infection against porcine circovirus type 2: viral distribution and lesions in mouse. Virology Journal, 7, 158. https://doi.org/10.1186/1743-422X-7-158

Li, L., Kapoor, A., Slikas, B., Bamidele, O. S., Wang, C., Shaukat, S., Masroor, M. A., Wilson, M. L., Ndjango, J. N., Peeters, M., Gross-camp, N. D., Muller, M. N., Hahn, B. H., Wolfe, N. D., Triki, H., Bartkus, J., Zaidi, S. Z. & Delwart, E. (2010). Multiple diverse circoviruses infect farm animals and are commonly found in human and chimpanzee feces. Journal of Virology, 84(4), 1674–1682. https://doi.org/10.1128/JVI.02109-09

Li, L., Shan, T., Soji, O. B., Alam, M., Kunz, T. H., Zaidi, S. Z. & Delwart, E. (2011). Possible cross-species transmission of circoviruses and cycloviruses among farm animals. Journal of General Virology, 92, 768–772. https://doi.org/10.1099/vir.0.028704-0

Liu, B. Y., Gao, B., Liu, M. Z., Zhang, T. T., Liu, B. S. & Chen, Z. L. (2020). High repetitive arginine in the anterior of PCV3 capsid protein is a severe obstacle for its expression in *E. coli*. AMB Express, 10(1), 1–7. https://doi.org/10.1186/S13568-020-01163-8

Liu, J., Huang, L., Wei, Y., Tang, Q., Liu, D., Wang, Y., Li, S., Guo, L., Wu, H. & Liu, C. (2013). Amino acid mutations in the capsid protein produce novel porcine circovirus type 2 neutralizing epitopes. Veterinary Microbiology, 165(3–4), 260–267. https://doi.org/10.1016/j.vetmic.2013.03.013

Liu, J., Chen, I. & Kwang, J. (2005). Characterization of a previously unidentified viral protein in porcine circovirus type 2-infected cells and its role in virus-induced apoptosis. Journal of Virology, 79(13), 8262–8274. https://doi.org/10.1128/JVI.79.13.8262-8274.2005

Liu, Q., Tikoo, S. K. & Babiuk, L. A. (2001). Nuclear localization of the ORF2 protein encoded by porcine circovirus type 2. Virology, 285(1), 91–99. https://doi.org/10.1006/viro.2001.0922

Liu, X., Hu, W., An, Z., Bai, Z., Dai, X. & Yang, Y. (2016). Exploration of cell lysis in a bioreactor using *Escherichia coli* expressing single-chain variable-domain antibody fragments. Annals of Microbiology, 66(3), 1207–1215. https://doi.org/10.1007/S13213-016-1202-X

Lobstein, J., Emrich, C. A., Jeans, C., Faulkner, M., Riggs, P. & Berkmen, M. (2012). SHuffle, a novel *Escherichia coli* protein expression strain capable of correctly folding disulfide bonded proteins in its cytoplasm. Microbial Cell Factories, 11(1), 1–16. https://doi.org/10.1186/1475-2859-11-56

Lou, Z. Z., Li, Z. Y., Wang, G., Li, J. Q., Lan, X., Li, X. R., Yin, X. P., Liu, J. X. & Liu, S. D. (2010). Prokaryotic expression and potential application of the truncated PCV-2: capsid protein. Virologica Sinica, 25(2), 86–97. https://doi.org/10.1007/s12250-010-3111-7

Lu, H.-Y., Chen, Y.-H. & Liu, H.-J. (2012). Baculovirus as a vaccine vector. Bioengineered, 3(5), 271. https://doi.org/10.4161/BIOE.20679

Lunney, J. K., Ho, C. S., Wysocki, M. & Smith, D. M. (2009). Molecular genetics of the swine major histocompatibility complex, the SLA complex. Developmental & Comparative Immunology, 33(3), 362–374. https://doi.org/10.1016/J.DCI.2008.07.002

Lunney, J. K., Fang, Y., Ladinig, A., Chen, N., Li, Y., Rowland, B. & Renukaradhya, G. J. (2016). Porcine reproductive and respiratory syndrome virus (PRRSV): pathogenesis and interaction with the immune system. Annual Review of Animal Biosciences, 4, 129–154. https://doi.org/10.1146/annurev-animal-022114-111025

Mahé, D., Blanchard, P., Truong, C., Arnauld, C., Le Cann, P., Cariolet, R., Madec, F., Albina, E, & Jestin, A. (2000). Differential recognition of ORF2 protein from type 1 and type 2 porcine circoviruses and identification of immunorelevant epitopes. Journal of General Virology, 81(7), 1815–1824. https://doi.org/10.1099/0022-1317-81-7-1815

Malhotra, A. (2009). Chapter 16 Tagging for protein expression. Methods in Enzymology, 463, 239–258. https://doi.org/10.1016/S0076-6879(09)63016-0

Mankertz, A., Persson, F., Mankertz, J., Blaess, G. & Buhk, H. J. (1997). Mapping and characterization of the origin of DNA replication of porcine circovirus. Journal of Virology, 71(3), 2562–2566. https://doi.org/10.1128/JVI.71.3.2562-2566.1997

Mankertz, A., Çaliskan, R., Hattermann, K., Hillenbrand, B., Kurzendoerfer, P., Mueller, B., Schmitt, C., Steinfeldt, T. & Finsterbusch, T. (2004). Molecular biology of porcine circovirus: analyses of gene expression and viral replication. Veterinary Microbiology, 98(2), 81–88. https://doi.org/10.1016/J.VETMIC.2003.10.014

Mankertz, A. & Hillenbrand, B. (2001). Replication of porcine circovirus type 1 requires two proteins encoded by the viral rep gene. Virology, 279(2), 429–438. https://doi.org/10.1006/VIRO.2000.0730

Mankertz, A., Mueller, B., Steinfeldt, T., Schmitt, C. & Finsterbusch, T. (2003). New reporter gene-based replication assay reveals exchangeability of replication factors of porcine circovirus types 1 and 2. Journal of Virology, 77(18), 9885–9893. https://doi.org/10.1128/JVI.77.18.9885-9893.2003

Marrack, P., McKee, A. & Munks, M. (2009). Towards an understanding of the adjuvant action of aluminium. Nature Reviews. Immunology, 9(4), 287–293. https://doi.org/10.1038/NRI2510

Meerts, P., Misinzo, G. & Nauwynck, H. (2005). Enhancement of porcine circovirus 2 replication in porcine cell lines by IFN-gamma before and after treatment and by IFN-alpha after treatment. Journal of Interferon & Cytokine Research, 25(11), 684–693. https://doi.org/10.1089/JIR.2005.25.684

Meng, X. (2013). Porcine circovirus type 2 (PCV2): pathogenesis and interaction with the immune system. Annual Review of Animal Biosciences, 1, 43–64. https://doi.org/10.1146/annurev-animal-031412-103720

Mingfang, B., Xiangdong, L., Weifeng, Z., Bo, Y., Kegong, T. & Xiaobing, M. (2020). Structural insight into the type-specific epitope of porcine circovirus type 3. Bioscience Reports, 40(6), BSR20201109. https://doi.org/10.1042/BSR20201109

Misinzo, G., Delputte, P., Meerts, P., Lefebvre, D. & Nauwynck, H. (2006). Porcine circovirus 2 uses heparan sulfate and chondroitin sulfate B glycosaminoglycans as receptors for its attachment to host cells. Journal of Virology, 80(7), 3487–3494. https://doi.org/10.1128/JVI.80.7.3487-3494.2006

Mitraki, A., Fane, B., Haase-Pettingell, C., Sturtevant, J. & King, J. (1991). Global suppression of protein folding defects and inclusion body formation. Science, 253(5015), 54–58. https://doi.org/10.1126/SCIENCE.1648264

Mo, X., Li, X., Yin, B., Deng, J., Tian, K. & Yuan, A. (2019). Structural roles of PCV2 capsid protein N-terminus in PCV2 particle assembly and identification of PCV2 type-specific neutralizing epitope. PLoS Pathogens, 15(3):e1007562. https://doi.org/10.1371/JOURNAL.PPAT.1007562

Morein, B., Villacrés-Eriksson, M., Sjölander, A. & Bengtsson, K. L. (1996). Novel adjuvants and vaccine delivery systems. Veterinary Immunology and Immunopathology, 54(1–4), 373–384. https://doi.org/10.1016/S0165-2427(96)05697-8

Morgan-Kiss, R. M., Wadler, C. & Cronan, J. E. (2002). Long-term and homogeneous regulation of the *Escherichia coli* araBAD promoter by use of a lactose transporter of relaxed specificity. Proceedings of the National Academy of Sciences, 99(11), 7373–7377. https://doi.org/10.1073/PNAS.122227599

Müller-Hill, B. (1996). The lac operon: a short history of a genetic paradigm. In The lac operon: a short history of a genetic paradigm. De Gruyter.

Nainys, J., Lasickiene, R., Petraityte-Burneikiene, R., Dabrisius, J., Lelesius, R., Sereika, V., Zvirbliene, A., Sasnauskas, K. & Gedvilaite, A. (2014). Generation in yeast of recombinant virus-like particles of porcine circovirus type 2 capsid protein and their use for a serologic assay and development of monoclonal antibodies. BMC Biotechnology, 14(1), 100. https://doi.org/10.1186/S12896-014-0100-1

Nallamsetty, S. & Waugh, D. (2007). Mutations that alter the equilibrium between open and closed conformations of *Escherichia coli* maltose-binding protein impede its ability to enhance the solubility of passenger proteins. Biochemical and Biophysical Research Communications, 364(3), 639–644. https://doi.org/10.1016/J.BBRC.2007.10.060

Nallamsetty, S. & Waugh, D. (2006). Solubility-enhancing proteins MBP and NusA play a passive role in the folding of their fusion partners. Protein Expression and Purification, 45(1), 175–182. https://doi.org/10.1016/J.PEP.2005.06.012

Nawagitgul, P., Morozov, I., Bolin, S. ., Harms, P. ., Sorden, S. & Paul, P. (2000). Open reading frame 2 of porcine circovirus type 2 encodes a major capsid protein. Journal of General Virology, 81(Pt 9), 2281–2287. https://doi.org/10.1099/0022-1317-81-9-2281

Neefjes, J., Jongsma, M. L. M., Paul, P. & Bakke, O. (2011). Towards a systems understanding of MHC class I and MHC class II antigen presentation. Nature Reviews Immunology, 11(12), 823–836. https://doi.org/10.1038/nri3084

Neurath, A. R. (2008). Immune Response to Viruses: Antibody-Mediated Immunity. Encyclopedia of Virology, 56-70. https://doi.org/10.1016/B978-012374410-4.00591-4

Opriessnig, T., Karuppannan, A. K., Castro, A. M. M. G. & Xiao, C. T. (2020). Porcine circoviruses: current status, knowledge gaps and challenges. Virus Research, 286, 198044. https://doi.org/10.1016/J.VIRUSRES.2020.198044

Opriessnig, T., Xiao, C. T., Gerber, P. F., Halbur, P. G., Matzinger, S. R. & Meng, X. J. (2014). Mutant USA strain of porcine circovirus type 2 (mPCV2) exhibits similar virulence to the classical PCV2a and PCV2b strains in caesarean-derived, colostrum-deprived pigs. Journal of General Virology, 95(Pt 11), 2495–2503. https://doi.org/10.1099/vir.0.066423-0

Ouyang, T., Liu, X., Ouyang, H. & Ren, L. (2018). Mouse models of porcine circovirus 2 infection. Animal Models and Experimental Medicine, 1, 23–28. https://doi.org/10.1002/AME2.12009

Ouyang, T., Niu, G., Liu, X., Zhang, X., Zhang, Y. & Ren, L. (2019). Recent progress on porcine circovirus type 3. Infection, Genetics and Evolution, 73, 227–233. https://doi.org/10.1016/J.MEEGID.2019.05.009

Pace, C. N., Grimsley, G. R., Thomson, J. A. & Barnett, B. J. (1988). Conformational stability and activity of ribonuclease T1 with zero, one, and two intact disulfide bonds. Journal of Biological Chemistry, 263(24), 11820–11825. https://doi.org/10.1016/S0021-9258(18)37859-1

Pacheco, B., Crombet, L., Loppnau, P. & Cossar, D. (2012). A screening strategy for heterologous protein expression in *Escherichia coli* with the highest return of investment. Protein Expression and Purification, 81(1), 33–41. https://doi.org/10.1016/J.PEP.2011.08.030

Palinski, R., Piñeyro, P., Shang, P., Yuan, F., Guo, R., Fang, Y., Byers, E. & Ben, H. (2017). A novel porcine circovirus distantly related to known circoviruses is associated with porcine dermatitis and nephropathy syndrome and reproductive failure. Journal of Virology, 91(1), 1–13.

Panda, A. (2003). Bioprocessing of therapeutic proteins from the inclusion bodies of *Escherichia coli*. Advances in Biochemical Engineering/Biotechnology, 85, 43–93. https://doi.org/10.1007/3-540-36466-8_3

Park, J.-H. (2013). Requirements for improved vaccines against foot-and-mouth disease epidemics. Clinical and Experimental Vaccine Research, 2(1), 8–18. https://doi.org/10.7774/CEVR.2013.2.1.8

Park, M. E., Lee, S. Y., Kim, R. H., Ko, M. K., Lee, K. N., Kim, S. M., Kim, B. K., Lee, J. S., Kim, B. & Park, J. H. (2014). Enhanced immune responses of foot-and-mouth disease vaccine using new oil/gel adjuvant mixtures in pigs and goats. Vaccine, 32(40), 5221–5227. https://doi.org/10.1016/J.VACCINE.2014.07.040

Park, M. E., Lee, S. Y., Kim, R. H., Ko, M. K., Park, J. N., Lee, K. N., Kim, S. M., Choi, J. H., You, S. H., Kim, B., Lee, J. S. & Park, J. H. (2016). Altered adjuvant of foot-and-mouth disease vaccine improves immune response and protection from virus challenge. Trials in Vaccinology, 5, 97–104. https://doi.org/10.1016/J.TRIVAC.2016.04.006

Parsy, C., Chapman, C., Barnes, A., Robertson, J. & Murray, A. (2007). Two-step method to isolate target recombinant protein from co-purified bacterial contaminant SlyD after immobilised metal affinity chromatography. Journal of Chromatography, 853(1–2), 314–319. https://doi.org/10.1016/J.JCHROMB.2007.03.046

Pasquale, A. Di, Preiss, S., Silva, F. T. Da & Garçon, N. (2015). Vaccine Adjuvants: from 1920 to 2015 and Beyond. Vaccines, 3(2), 320. https://doi.org/10.3390/VACCINES3020320

Payne, S. (2017). Immunity and resistance to viruses. Viruses, 61-71. https://doi.org/10.1016/B978-0-12-803109-4.00006-4

Pedersen, C., Petaja, T., Strauss, G., Rumke, H. ., Poder, A., Richardus, J. ., Spiessens, B., Descamps, D., Hardt, K., Lehtinen, M. & Dubin, G. (2007). Immunization of early adolescent females with human papillomavirus type 16 and 18 L1 virus-like particle vaccine containing AS04 adjuvant. The Journal of Adolescent Health, 40(6), 564–571. https://doi.org/10.1016/J.JADOHEALTH.2007.02.015

Peternel, S., Grdadolnik, J., Gaberc-Porekar, V. & Komel, R. (2008). Engineering inclusion bodies for non denaturing extraction of functional proteins. Microbial Cell Factories, 7, 34. https://doi.org/10.1186/1475-2859-7-34

Peternel, Š., Bele, M., Gaberc-Porekar, V. & Menart, V. (2006). Nonclassical inclusion bodies in *Escherichia coli*. Microbial Cell Factories, 5(1), 1–2. https://doi.org/10.1186/1475-2859-5-S1-P23

Pollard, A. J. & Bijker, E. M. (2021). A guide to vaccinology: from basic principles to new developments. Nature Reviews Immunology, 21(2), 83–100. https://doi.org/10.1038/s41577-020-00479-7

Przybycien, T. M., Dunn, J. P., Valax, P. & Georglou, G. (1994). Secondary structure characterization of ß-lactamase inclusion bodies. Protein Engineering, Design and Selection, 7(1), 131–136. https://doi.org/10.1093/PROTEIN/7.1.131

Pulendran, B. & Ahmed, R. (2011). Immunological mechanisms of vaccination. Nature Immunology, 12(6), 509–517. NIH Public Access. https://doi.org/10.1038/ni.2039

Puri, N., Crivelli, E., Cardamone, M., Fiddes, R., Bertolini, J., Ninham, B. & Brandon, M. (1992). Solubilization of growth hormone and other recombinant proteins from *Escherichia coli* inclusion bodies by using a cationic surfactant. The Biochemical Journal, 285(Pt 3), 871–879. https://doi.org/10.1042/BJ2850871

Radli, M., Veprintsev, D. B. & Rüdiger, S. G. D. (2017). Production and purification of human Hsp90β in *Escherichia coli*. PLoS ONE, 12(6), e0180047. https://doi.org/10.1371/JOURNAL.PONE.0180047

Raina, K., Panda, A., Ali, M. & Talwar, G. (2004). Purification, refolding, and characterization of recombinant LHRH-T multimer. Protein Expression and Purification, 37(1), 8–17. https://doi.org/10.1016/J.PEP.2004.03.008

Ramamoorthy, S., Huang, F. F., Huang, Y. W. & Meng, X. J. (2009). Interferon-mediated enhancement of in vitro replication of porcine circovirus type 2 is influenced by an interferon-stimulated response element in the PCV2 genome. Virus Research, 145(2), 236–243. https://doi.org/10.1016/J.VIRUSRES.2009.07.009

Ramamoorthy, S., & Meng, X.-J. (2009). Porcine circoviruses: a minuscule yet mammoth paradox. Animal Health Research Reviews, 10(1), 1–20. https://doi.org/10.1017/S1466252308001461

Ratelade, J., Miot, M. C., Johnson, E., Betton, J. M., Mazodier, P. & Benaroudj, N. (2009). Production of recombinant proteins in the lon-deficient BL21(DE3) strain of *Escherichia coli* in the absence of the DnaK chaperone. Applied and Environmental Microbiology, 75(11), 3803–3807. https://doi.org/10.1128/AEM.00255-09

Renard, C., Hart, E., Sehra, H., Beasley, H., Coggill, P., Howe, K., Harrow, J., Gilbert, J., Sims, S., Rogers, J., Ando, A., Shigenari, A., Shiina, T., Inoko, H., Chardon, P. & Beck, S. (2006). The genomic sequence and analysis of the swine major histocompatibility complex. Genomics, 88(1), 96–110. https://doi.org/10.1016/J.YGENO.2006.01.004

Rijke, E. O. (1997). Adjuvant research for veterinary vaccines: suitability of a new vitamin E based formulation. In Forschung ohne Tierversuche 1996, 224-232. https://doi.org/10.1007/978-3-7091-6833-2_29

Robinson, C., Matos, C., Beck, D., Ren, C., Lawrence, J., Vasisht, N. & Mendel, S. (2011). Transport and proofreading of proteins by the twin-arginine translocation (Tat) system in bacteria. Biochimica et Biophysica Acta, 1808(3), 876–884. https://doi.org/10.1016/J.BBAMEM.2010.11.023

Rubin, L. G., Levin, M. J., Ljungman, P., Davies, E. G., Avery, R., Tomblyn, M., Bousvaros, A., Dhanireddy, S., Sung, L., Keyserling, H. & Kang, I. (2014). 2013 IDSA clinical practice guideline for vaccination of the immunocompromised host. Clinical Infectious Diseases, 58(3), e44-100. https://doi.org/10.1093/cid/cit684

Ryan, B. J., & Henehan, G. T. (2013). Overview of approaches to preventing and avoiding proteolysis during expression and purification of proteins. Current Protocols in Protein Science, 71(1), 5.25.1-5.25.7. https://doi.org/10.1002/0471140864.PS0525S71

Sachdev, D. & Chirgwin, J. (2000). Fusions to maltose-binding protein: control of folding and solubility in protein purification. Methods in Enzymology, 326, 312–321. https://doi.org/10.1016/S0076-6879(00)26062-X

Saha, D., Lefebvre, D. J., Ooms, K., Huang, L., Delputte, P. L., van Doorsselaere, J. & Nauwynck, H. J. (2012). Single amino acid mutations in the capsid switch the neutralization phenotype of porcine circovirus 2. Journal of General Virology, 93(7), 1548–1555. https://doi.org/10.1099/vir.0.042085-0

Saraiva, G. L., Vidigal, P. M. P., Fietto, J. L. R., Bressan, G. C., Júnior, A. S. & Almeida, M. R. de. (2018). Evolutionary analysis of Porcine circovirus 3 (PCV3) indicates an ancient origin for its current strains and a worldwide dispersion. Virus Genes, 54(3), 376–384. https://doi.org/10.1007/s11262-018-1545-4

Sauer, D. G., Mosor, M., Frank, A. C., Weiß, F., Christler, A., Walch, N., Jungbauer, A. & Dürauer, A. (2019). A two-step process for capture and purification of human basic fibroblast growth factor from *E. coli* homogenate: Yield versus endotoxin clearance. Protein Expression and Purification, 153, 70–82. https://doi.org/10.1016/J.PEP.2018.08.009

Schellman, J. A. (1987). The thermodynamic stability of proteins. Annual Review of Biophysics and Biophysical Chemistry, 16, 115–137. https://doi.org/10.1146/ANNUREV.BB.16.060187.000555

Schmidt, M., Viaplana, E., Hoffmann, F., Marten, S., Antonio, V. & Rinas, U. (1999). Secretion-dependent proteolysis of heterologous protein by recombinant *Escherichia coli* is connected to an increased activity of the energy-generating dissimilatory pathway. Biotechnology

& Bioengineering, 66, 61–67. https://onlinelibrary.wiley.com/doi/10.1002/(SICI)1097-0290(1999)66:1%3C61::AID-BIT6%3E3.0.CO;2-G

Schwartz, R., Ting, C. S. & King, J. (2001). Whole proteome pI values correlate with subcellular localizations of proteins for organisms within the three domains of life. Genome Research, 11(5), 703–709. https://doi.org/10.1101/GR.158701

Segalés, J. (2012). Porcine circovirus type 2 (PCV2) infections: clinical signs, pathology and laboratory diagnosis. Virus Research, 164(1–2), 10–19. https://doi.org/10.1016/j.virusres.2011.10.007

Seo, H., Han, K., Park, C. & Chae, C. (2014). Clinical, virological, immunological and pathological evaluation of four porcine circovirus type 2 vaccines. Veterinary Journal, 200(1), 65–70. https://doi.org/10.1016/J.TVJL.2014.02.002

Shang, S. B., Jin, Y. L., Jiang, X. T., Zhou, J. Y., Zhang, X., Xing, G., He, J. L. & Yan, Y. (2009). Fine mapping of antigenic epitopes on capsid proteins of porcine circovirus, and antigenic phenotype of porcine circovirus Type 2. Molecular Immunology, 46(3), 327–334. https://doi.org/10.1016/j.molimm.2008.10.028

Siegrist, C.-A. (2008). Vaccine immunology. In Vaccines (fifth edition), 17-36. https://doi.org/10.1016/B978-1-4160-3611-1.50006-4

Silva, J. G., Coimbra, E. C., Jesus, A. L. S., Mariz, F. C., Silva, K. M. G., Lobato, Z. I. P., Campos, A. C., Coutinho, L. C. A., Castro, R. S. & Freitas, A. C. (2014). Secretory expression of porcine circovirus Type 2 capsid protein in *Pichia pastoris*. Journal of Virological Methods, 207, 226–231. https://doi.org/10.1016/j.jviromet.2014.07.021

Singh, A., Upadhyay, V., Upadhyay, A. K., Singh, S. M. & Panda, A. K. (2015). Protein recovery from inclusion bodies of *Escherichia coli* using mild solubilization process. Microbial Cell Factories, 14(1), 1–10. https://doi.org/10.1186/S12934-015-0222-8

Singh, S. M., Upadhyay, A. K. & Panda, A. K. (2008). Solubilization at high pH results in improved recovery of proteins from inclusion bodies of *E. coli*. Journal of Chemical Technology & Biotechnology, 83(8), 1126–1134. https://doi.org/10.1002/JCTB.1945

Sipos, W., Duvigneau, J. C. & Pietschmann, P. (2005). Porcine dermatitis and nephropathy syndrome (PDNS) is associated with a systemic cytokine expression profile indicative of proinflammation and a Th1 bias. Veterinary Immunology and Immunopathology, 107(3–4), 303–313. https://doi.org/10.1016/j.vetimm.2005.05.003

Song, D., Moon, H. & Kang, B. (2015). Porcine epidemic diarrhea: a review of current epidemiology and available vaccines. Clinical and Experimental Vaccine Research, 4(2), 166–176. https://doi.org/10.7774/CEVR.2015.4.2.166

Sørensen, H. P. & Mortensen, K. K. (2005). Advanced genetic strategies for recombinant protein expression in *Escherichia coli*. Journal of Biotechnology, 115(2), 113–128. https://doi.org/10.1016/J.JBIOTEC.2004.08.004

Stadejek, T., Woźniak, A., Miłek, D. & Biernacka, K. (2017). First detection of porcine circovirus type 3 on commercial pig farms in Poland. Transboundary and Emerging Diseases, 64(5), 1350–1353. https://doi.org/10.1111/TBED.12672

Stiehm, E. R. (2012). Joseph A. Bellanti (ed) Immunology IV: clinical applications in health and disease. Journal of Clinical Immunology, 32(3), 647. https://doi.org/10.1007/S10875-012-9648-5

Sukumaran, L., McNeil, M. M., Moro, P. L., Lewis, P. W., Winiecki, S. K. & Shimabukuro, T. T. (2015). Adverse events following measles, mumps, and rubella vaccine in adults reported to the vaccine adverse event reporting system (VAERS), 2003–2013. Clinical Infectious Diseases, 60(10), e58. https://doi.org/10.1093/CID/CIV061

Sun, W., Du, Q., Han, Z., Bi, J., Lan, T., Wang, W., Zheng, M., Q, Du, Q., Han, Z., Bi, J., Lan, T., Wang, W. & Zheng, M. (2021). Detection and genetic characterization of porcine circovirus 4 (PCV4) in Guangxi, China. Gene, 773, 145384. https://doi.org/10.1016/J.GENE.2020.145384

Tao, X. & Xu, A. (2016). Basic knowledge of immunology. In Amphioxus Immunity: Tracing the Origins of Human Immunity. Academic Press, 15-42. https://doi.org/10.1016/B978-0-12-849903-0.00002-6

Terpe, K. (2006). Overview of bacterial expression systems for heterologous protein production: from molecular and biochemical fundamentals to commercial systems. Applied Microbiology and Biotechnology, 72(2), 211–222. https://doi.org/10.1007/S00253-006-0465-8

Thangthamniyom, N., Sangthong, P., Poolperm, P., Thanantong, N., Boonsoongnern, A., Hansoongnern, P., Semkum, P., Petcharat, N. & Lekcharoensuk, P. (2017). Genetic diversity of porcine circovirus type 2 (PCV2) in Thailand during 2009–2015. Veterinary Microbiology, 208, 239–246. https://doi.org/10.1016/j.vetmic.2017.08.006

Thornton, P. K. (2010). Livestock production: recent trends, future prospects. Royal Society, 365(1554), 2853–2867. https://doi.org/10.1098/rstb.2010.0134

Tochetto, C., Lima, D. A., Varela, A. P. M., Loiko, M. R., Paim, W. P., Scheffer, C. M., Herpich, J. I., Cerva, C., Schmitd, C., Cibulski, S. P., Santos, A. C., Mayer, F. Q. & Roehe, P. M. (2018). Full-genome sequence of porcine circovirus type 3 recovered from serum of sows with stillbirths in Brazil. Transboundary and Emerging Diseases, 65(1), 5–9. https://doi.org/10.1111/TBED.12735

Trible, B. R., Suddith, A. W., Kerrigan, M. A., Cino-Ozuna, A. G., Hesse, R. A. & Rowland, R. R. R. (2012). Recognition of the different structural forms of the capsid protein determines the outcome following infection with porcine circovirus type 2. Journal of Virology, 86(24), 13508–13514. https://doi.org/10.1128/jvi.01763-12

Trundova, M. & Celer, V. (2007). Expression of porcine circovirus 2 ORF2 gene requires codon optimized E. coli cells. Virus Genes, 34(2), 199–204. https://doi.org/10.1007/s11262-006-0043-2

Tu, Y., Wang, Y., Wang, G., Wu, J., Liu, Y., Wang, S., Jiang, C. & Cai, X. (2013). High-level expression and immunogenicity of a porcine circovirus type 2 capsid protein through codon optimization in *Pichia pastoris*. Applied Microbiology and Biotechnology, 97(7), 2867–2875. https://doi.org/10.1007/S00253-012-4540-Z

Umetsu, M., Tsumoto, K., Nitta, S., Adschiri, T., Ejima, D., Arakawa, T. & Kumagai, I. (2005). Nondenaturing solubilization of beta2 microglobulin from inclusion bodies by L-arginine. Biochemical and Biophysical Research Communications, 328(1), 189–197. https://doi.org/10.1016/J.BBRC.2004.12.156

Varela, A. P. M., Loiko, M. R., Da Silva Andrade, J., Tochetto, C., Cibulski, S. P., Lima, D. A., Weber, M. N., Roehe, P. M. & Mayer, F. Q. (2021). Complete genome characterization of porcine circovirus 3 recovered from wild boars in Southern Brazil. Transboundary and Emerging Diseases, 68(2), 240–247. https://doi.org/10.1111/TBED.13679

Vargas-Bermudez, D. S., Campos, F. S., Bonil, L., Mogollon, D. & Jaime, J. (2019). First detection of porcine circovirus type 3 in Colombia and the complete genome sequence demonstrates the circulation of PCV3a1 and PCV3a2. Veterinary Medicine and Science, 5(2), 182–188. https://doi.org/10.1002/VMS3.155

Vialle, R., Dupuis, L., Deville, S., Bertrand, F., Gaucheron, J. & Aucouturier, J. (2010). Microgel particulate adjuvant: characterisation and mechanisms of action. Procedia in Vaccinology, 2(1), 12–16. https://doi.org/10.1016/J.PROVAC.2010.03.003

Villaverde, A. & Carrió, M. (2003). Protein aggregation in recombinant bacteria: biological role of inclusion bodies. Biotechnology Letters, 25(17), 1385–1395. https://doi.org/10.1023/A:1025024104862

Vogel, F. R. (2000). Improving vaccine performance with adjuvants. Clinical Infectious Diseases: An Official Publication of the Infectious Diseases Society of America, 30 Suppl 3(SUPPL. 3), S266–S270. https://doi.org/10.1086/313883

Vordermeier, H. M., Dean, G. S., Rosenkrands, I., Agger, E. M., Andersen, P., Kaveh, D. A., Hewinson, R. G. & Hogarth, P. J. (2009). Adjuvants induce distinct immunological phenotypes in a bovine tuberculosis vaccine model. Clinical and Vaccine Immunology, 16(10), 1443–1448. https://doi.org/10.1128/CVI.00229-09

Walsh, G. (2014). Biopharmaceutical benchmarks 2014. Nature Biotechnology, 32(10), 992–1000. https://doi.org/10.1038/nbt.3040

Wang, D., Zhang, S., Zou, Y., Yu, W., Jiang, Y., Zhan, Y., Wang, N., Dong, Y. & Yang, Y. (2018). Structure-based design of porcine circovirus type 2 chimeric VLPs (cVLPs) displays foreign peptides on the capsid surface. Frontiers in Cellular and Infection Microbiology, 8, 232. https://doi.org/10.3389/FCIMB.2018.00232

Wang, F., Guo, X., Ge, X., Wang, Z., Chen, Y., Cha, Z. & Yang, H. (2009). Genetic variation analysis of Chinese strains of porcine circovirus type 2. Virus Research, 145, 151–156. https://doi.org/10.1016/j.virusres.2009.05.015

Wang, N., Zhan, Y., Wang, A., Zhang, L., Khayat, R. & Yang, Y. (2016). *In silico* analysis of surface structure variation of PCV2 capsid resulting from loop mutations of its capsid protein (Cap). Journal of General Virology, 97, 3331–3344. https://doi.org/10.1099/jgv.0.000634

Wang, W., Sun, W., Cao, L., Zheng, M., Zhu, Y., Li, W., Liu, C., Zhuang, X., Xing, J., Lu, H., Luo, T. & Jin, N. (2019). An epidemiological investigation of porcine circovirus 3 infection in cattle in Shandong province, China. BMC Veterinary Research, 15(1), 60. https://doi.org/10.1186/S12917-019-1793-0

Wangkaghart, E., Deville, S., Wang, B., Srisapoome, P., Wang, T. & Secombes, C. J. (2021). Immune response and protective efficacy of two new adjuvants, Montanide™ ISA 763B VG and Montanide™ GEL02, administered with a *Streptococcus agalactiae* ghost vaccine in Nile tilapia (*Oreochromis niloticus*). Fish & Shellfish Immunology, 116, 19–29. https://doi.org/10.1016/J.FSI.2021.06.014

Waugh, D. (2005). Making the most of affinity tags. Trends in Biotechnology, 23(6), 316–320. https://doi.org/10.1016/J.TIBTECH.2005.03.012

Wei, R., Xie, J., Theuns, S. & Nauwynck, H. J. (2019). Changes on the viral capsid surface during the evolution of porcine circovirus type 2 (PCV2) from 2009 till 2018 may lead to a better receptor binding. Virus Evolution, 5(2), vez026. https://doi.org/10.1093/VE/VEZ026

Wilkins, A. L., Kazmin, D., Napolitani, G., Clutterbuck, E. A., Pulendran, B., Siegrist, C. A. & Pollard, A. J. (2017). AS03- and MF59-adjuvanted influenza vaccines in children. Frontiers in Immunology, 8, 1760. https://doi.org/10.3389/FIMMU.2017.01760

Williamson, M. P. (1994). The structure and function of proline-rich regions in proteins. Biochemical Journal, 297(Pt 2), 249. https://doi.org/10.1042/BJ2970249

Wittrup, A., Zhang, S.-H. & Belting, M. (2011). Studies of Proteoglycan Involvement in CPP-Mediated Delivery. Methods in Molecular Biology, 683, 99–115. https://doi.org/10.1007/978-1-60761-919-2_8

Wo, A., Roerink, F. & Woensel, P. V. (2007). Pcv2 vaccine. WO 2007028823

Worsfold, C., Dardari, R., Law, S., Eschbaumer, M., Nourozieh, N., Marshall, F. & Czub, M. (2015). Assessment of neutralizing and non-neutralizing antibody responses against porcine circovirus 2 in vaccinated and non-vaccinated farmed pigs. The Journal of General Virology, 96(9), 2743–2748. https://doi.org/10.1099/VIR.0.000206

Wu, P. C., Chen, T. Y., Chi, J. N., Chien, M. S. & Huang, C. (2016). Efficient expression and purification of porcine circovirus type 2 virus-like particles in *Escherichia coli*. Journal of Biotechnology, 220, 78–85. https://doi.org/10.1016/J.JBIOTEC.2016.01.017

Wu, P., Lin, W., Wu, C., Chi, J.-N., Chien, M.-S. & Huang, C. (2012). Characterization of porcine circovirus type 2 (PCV2) capsid particle assembly and its application to virus-like particle vaccine development. Applied Microbiology and Biotechnology, 95(6), 1501–1507. https://doi.org/10.1007/s00253-012-4015-2

Xiao, C. T., Harmon, K. M., Halbur, P. G. & Opriessnig, T. (2016). PCV2d-2 is the predominant type of PCV2 DNA in pig samples collected in the U.S. during 2014–2016. Veterinary Microbiology, 197, 72–77. https://doi.org/10.1016/j.vetmic.2016.11.009

Xiao, C.-T., Halbur, P. G. & Opriessnig, T. (2015). Global molecular genetic analysis of porcine circovirus type 2 (PCV2) sequences confirms the presence of four main PCV2 genotypes and reveals a rapid increase of PCV2d. Journal of General Virology, 96(7), 1830–1841. https://doi.org/10.1099/VIR.0.000100

Xiao, C., Halbur, P. G. & Opriessnig, T. (2012). Complete genome sequence of a novel porcine circovirus type 2b variant present in cases of vaccine failures in the United States. Journal of Virology, 86(22), 12469. https://doi.org/10.1128/JVI.02345-12

Xiao, Y., Zhao, P., Du, J., Li, X., Lu, W., Hao, X., Dong, B., Yu, Y. & Wang, L. (2018). High-level expression and immunogenicity of porcine circovirus type 2b capsid protein without nuclear localization signal expressed in *Hansenula polymorpha*. Biologicals, 51, 18–24. https://doi.org/10.1016/j.biologicals.2017.11.003

Yang, X., Lian, K., Meng, T., Liu, X., Miao, J., Tan, Y., Yuan, H. & Hu, F. (2018). Immune adjuvant targeting micelles allow efficient dendritic cell migration to lymph nodes for enhanced cellular immunity. ACS Applied Materials & Interfaces, 10(39), 33532–33544. https://doi.org/10.1021/ACSAMI.8B10081

Yang, Z., Sugawara, M., Ponath, P. D., Wessendorf, L., Banerji, J., Li, Y. & Strominger, J. L. (1990). Interferon gamma response region in the promoter of the human DPA gene. Proceedings of the National Academy of Sciences, 87(23), 9226–9230. https://doi.org/10.1073/PNAS.87.23.9226

Yin, S., Sun, S., Yang, S., Shang, Y., Cai, X. & Liu, X. (2010). Self-assembly of virus-like particles of porcine circovirus type 2 capsid protein expressed from *Escherichia coli*. Virology Journal, 7(1), 1–5. https://doi.org/10.1186/1743-422X-7-166

Yu, C., Tan, H. Y., Choi, M., Stanenas, A. J., Byrd, A. K., Raney, K. D., Cohan, C. S. & Bianco, P. R. (2016). SSB binds to the RecG and PriA helicases in vivo in the absence of DNA. Genes to Cells, 21(2), 163–184. https://doi.org/10.1111/GTC.12334

Zhan, Y., Wang, N., Zhu, Z., Wang, Z., Wang, A., Deng, Z. & Yang, Y. (2016). *In silico* analyses of antigenicity and surface structure variation of an emerging porcine circovirus genotype 2b mutant, prevalent in Southern China from 2013 to 2015. Journal of General Virology, 97(4), 922–933. https://doi.org/10.1099/jgv.0.000398

Zhang, H.-H. H., Hu, W.-Q. Q., Li, J.-Y. Y., Liu, T.-N. N., Zhou, J.-Y. Y., Opriessnig, T. & Xiao, C.-T. T. (2020). Novel circovirus species identified in farmed pigs designated as porcine circovirus 4, Hunan province, China. Transboundary and Emerging Diseases, 67(3), 1057–1061. https://doi.org/10.1111/TBED.13446

Zhang, J., Liu, Z., Zou, Y., Zhang, N., Wang, D., Tu, D., Yang, L., Deng, Z., Yang, Y., Jiang, P. & Wang, N. (2018). First molecular detection of porcine circovirus type 3 in dogs in China. Virus Genes, 54(1), 140–144. https://doi.org/10.1007/S11262-017-1509-0

Zhao, H. L., Yao, X. Q., Xue, C., Wang, Y., Xiong, X. H. & Liu, Z. M. (2008). Increasing the homogeneity, stability and activity of human serum albumin and interferon-α2b fusion protein by linker engineering. Protein Expression and Purification, 61(1), 73–77. https://doi.org/10.1016/J.PEP.2008.04.013

Zhou, J., Shang, S., Gong, H., Chen, Q., Wu, J., Shen, H., Chen, T. & Guo, J. (2005). *In vitro* expression, monoclonal antibody and bioactivity for capsid protein of porcine circovirus type II without nuclear localization signal. Journal of Biotechnology, 118(2), 201–211. https://doi.org/10.1016/J.JBIOTEC.2005.02.017